Revealing the light-harvesting properties of Photosystem I

Wientjes, Ina Emilia

Revealing the light-harvesting properties of Photosystem I

from single antenna to supercomplex

Emilie Wientjes

Printed by Ipskamp Drukkers, Enschede.

This Ph.D. study was carried out at the Groningen Biomolecular Sciences and Biotechnology Institute. Faculty of Mathematics and Natural Sciences, University of Groningen.

ISBN: 978-90-367-5221-3

RIJKSUNIVERSITEIT GRONINGEN

Revealing the light-harvesting properties of Photosystem I

from single antenna to supercomplex

Proefschrift

ter verkrijging van het doctoraat in de
Wiskunde en Natuurwetenschappen
aan de Rijksuniversiteit Groningen
op gezag van de
Rector Magnificus, dr. E. Sterken,
in het openbaar te verdedigen op
vrijdag 20 januari 2012
om 16.15 uur

door

Ina Emilia Wientjes

geboren op 2 maart 1984
te Driebergen-Rijsenburg

Promotor:	Prof. dr. R. Croce
Beoordelingscomissie:	Prof. dr. H. van Amerongen
	Prof. dr. E.J. Boekema
	Prof. dr. A.R. Holzwarth

Contents

	Abbreviations	
1	Introduction	7
2	The role of Lhca complexes in the supramolecular organization of higher plant Photosystem I	33
3	The light-harvesting complexes of higher plant photosystem I: Lhca1/4 and Lhca2/3 form two red-emitting heterodimers	51
4	Excitation energy transfer dynamics of higher plant photosystem I light-harvesting complexes	73
5	Conformational switching explains the intrinsic multi-functionality of plant light-harvesting complexes	91
6	From red to blue/far-red: how does the protein modulate the spectral properties of the pigments?	113
7	The role of the individual Lhcas in Photosystem I excitation energy trapping	129
8	PSM: Photosystem I electron donor of fluorescence quencher?	157
	Bibliography	169
	Summary	187
	Samenvatting	193
	Publications	200
	Dankjulliewel!	201

Abbreviations

ATP	adenosine triphosphate
Chl *a*	Chlorophyll *a*
Chl *b*	Chlorophyll *b*
Car	Carotenoid
CT	Charge Transfer
ETC	Electron transport chain
FNR	Ferredoxin-$NADP^+$ reductase
FWHM	Full width at half maximum
ISC	Intersystem crossing
Lhc	Light harvesting complex
Lhca	Lhc of PSI
Lhcb	Lhc of PSII
LHCI	Light-harvesting complex of PSI
LHCII	Major light-harvesting complex of PSII
LT	Low temperature
NADP	Nicotinamide Adenine Dinucleotide Phosphate
NPQ	Non photochemical quenching
PSI	Photosystem I
PSII	Photosystem II
RC	Reaction Centre

Chapter 1

Introduction

Abstract

The topic of this thesis is higher plant Photosystem I (PSI). PSI plays a major role in the light reactions of photosynthesis, a process which sustains almost all life on earth. In this chapter the light reactions of photosynthesis will be introduced first, followed by the role of PSI in these reactions. Next, I will focus on the structural and spectroscopic properties of PSI and its pigments. The effect of pigment-protein and pigment-pigment interactions on the spectroscopic behavior of these pigments will be discussed. Finally, the specific issues addressed in this thesis are introduced.

A concise history of light-harvesting in photosynthesis

Sunlight – Approximately 4.6 billion years ago our solar system was born (Manhes *et. al.* 1980; Bouvier and Wadhwa 2010), in which the Earth orbits the Sun together with 7 other planets. In the core of the sun nuclear fusion occurs, converting hydrogen into helium. During this reaction 0.7% of the fused mass is released as energy. This energy is the source of the sunlight we receive on Earth. Although, we receive only a small fraction of the radiation emitted from the sun, less than two hours of sunlight reaching the earth contains enough energy for one year of global energy consumption (e.g. Eisenberg and Nocera 2005). However, the energy of a photon (quantum of light) is not easy to store on earth, so to be stored the energy of light needs to be converted into a different form. In the process called photosynthesis this is exactly what happens: light energy is used to convert carbon dioxide into carbohydrates, thus storing light energy in stable chemical bonds. About 3.5 billion years ago the first organisms that could do photosynthesis evolved (Nisbet and Sleep 2001).

Big leaps in the understanding of photosynthesis – The nutrients that plants use to grow already interested Aristotle (384-322 BC) over 2000 years ago. He reasoned that plants gain their nutrients directly from earth and water. Johan Baptist van Helmont (1579-1644) investigated this theory by growing a willow tree in a pot. He found that after five years the mass of the tree had greatly increased, while the mass of the soil had only moderately decreased. Therefore, he concluded that the tree gained weight only from the water and not from the soil. In 1771 the Englishman Joseph Priestley showed that also gases in the air are involved in Photosynthesis. At the time people believed that a burning candle released a noxious substance, called *phlogiston*, in the air. When Priestley put a mouse and a burning candle in a closed container the mouse died after the flame extinguished.

However, when he added a sprig of mint the mouse survived. He concluded that the mint could remove the *phlogiston* from the air. Shortly after, a Dutch physician Jan Ingen-Housz (1730-1799) demonstrated that plants could only *dephlogistate* the air in the presence of sunlight. Antoine Lavoisier (1743-1794) discovered that a burning candle does not release *phlogiston*, but instead, consumes a gas, which he named oxygen. He also discovered that animals need oxygen for their respiration. This implied that the plants in Priestley's and Ingen-Housz's experiments produced oxygen when illuminated with light, a great breakthrough in photosynthesis research (Photosynthesis - History Of Research; Govindjee and Krogmann 2004).

Blackman and Mathaei investigated the effect of light, temperature and carbon dioxide concentrations on the rate of photosynthesis and published their findings in 1905. They developed the idea of light-limited and dark-limited photosynthesis, but it was not until 1924 that Warburg and Uyesugi explained this concept as a light and a dark reaction in photosynthesis. Emerson and Arnold showed in 1932 that only one out of several hundred chlorophylls (the main light-harvesting pigment) was directly involved in photo-chemistry. This led to the concept of "photosynthetic unit". Emerson was also the discoverer of the enhancement effect in oxygenic photosynthesis: two combined light beams of different wavelengths resulted in a larger oxygen production, compared to the sum of the oxygen production of each beam alone. Further experiments by Kok (published in 1959) and Duysens, Amesz and Kamp (published in 1961) led to the concept that there should be two "photosynthetic units" performing two different light reactions (reviewed in Govindjee and Krogmann 2004).

Photosynthetic organisms and Reaction Centers

Light is used as energy source by eukaryotes, prokaryotes and archaea. In the archaeal type of photosynthesis light energy is used to drive an ion pump (Oesterhelt 1998). This is completely unrelated to photosynthesis in the other organisms. In all eukaryote and prokaryote photosynthetic organisms light energy is used for the translocation of electrons and the generation of a proton gradient over a charge-impermeable membrane. These reactions are driven by the photosynthetic apparatus (Heathcote *et. al.* 2002). The light energy is harvested by antenna pigment-proteins complexes, the pigments being carotenoids (Cars), chlorophylls (Chls) and/or bilins. Absorption of light by the pigments brings them in an electronic excited state. This excitation energy is transferred to the reaction centre (RC), where charge separation occurs. There are two types of RCs, their

classification is based on their terminal electron acceptors. In Type I RCs these are Fe_4S_4 clusters, and in Type II RCs (bacterio)pheophytins and quinones (Heathcote *et. al.* 2002). Anoxygenic photosynthetic bacteria have either a Type I RC (sulphur bacteria and heliobacteria), or a type II RC (purple bacteria and green filamentous bacteria) (e.g. Fyfe *et. al.* 2002). Oxygenic photosynthetic organisms: plants, algae and cyanobacteria, use both Type I and Type II RCs. The type I RC is located in the core of Photosystem I (PSI) and the type II RC is located in the core of Photosystem II (PSII). The PSI and PSII core complexes of plants, algae and cyanobacteria are highly conserved (Jordan *et. al.* 2001; Heathcote *et. al.* 2002; Vanselow *et. al.* 2009; Amunts *et. al.* 2010).

The light reactions of photosynthesis in higher plants

Linear electron flow – In higher plants the light reaction takes place in a specialized organelle, the chloroplast. Four large protein complexes: PSI, PSII, ATP syntase and cytochrome b_6f, are embedded in the thylakoid membranes of the chloroplasts. The thylakoid membrane forms a continuous network that separates the inner aqueous space, the lumen, from the outer aqueous phase, the stroma (fig 1, e.g. Dekker and Boekema 2005). During linear electron flow, the four complexes work together to form ATP (adenosine triphosphate) and NADPH (nicotinamide adenine dinucleotide phosphate). The energy needed for this reaction is coming from the light absorbed by PSI and PSII.

Both PSs consist of a core complex and an outer antenna system (e.g. Glazer 1983). The core complexes contain Chlorophyll *a* (Chl *a*) and β-carotenes as pigments and locate the RC and the electron-transport chain (ETC) (Jordan *et. al.* 2001; Umena *et. al.* 2011). The outer antenna systems of PSI and PSII are encoded by the Lhc gene family (Jansson 1999). The Lhca antennas of PSI are organized as heterodimers, called Lhca1/4 and Lhca2/3 (Knoetzel *et. al.* 1992; Croce *et. al.* 2002; Ben-Shem *et. al.* 2003; Wientjes and Croce 2011, Chapter 3). In addition Lhca5 and possibly Lhca6 can be present in sub-stoichiometric amounts (Jansson 1999; Ganeteg *et. al.* 2004). The light-harvesting complex of PSII is composed of the major trimeric light-harvesting complexes (LHCIIs) (encoded by *lhcb1-3* genes) and the minor monomeric light-harvesting complexes, called CP29, CP26 and CP24 (encoded by *lhcb4-6* respectively) (Jansson 1999). The Lhc complexes bind Chl *a,* Chl *b*, and the Cars violaxanthin and lutein (Bassi *et. al.* 1993). Some Lhca complexes can also coordinate β-carotene (Schmid *et. al.* 2002; Castelletti *et. al.* 2003), while most Lhcb complexes bind neoxanthin (Caffarri *et. al.* 2007). The function of the outer light-harvesting antenna is to increase the absorption cross

section, but at the same time they are believed to be involved in photoprotection under high light conditions (Horton *et. al.* 1996).

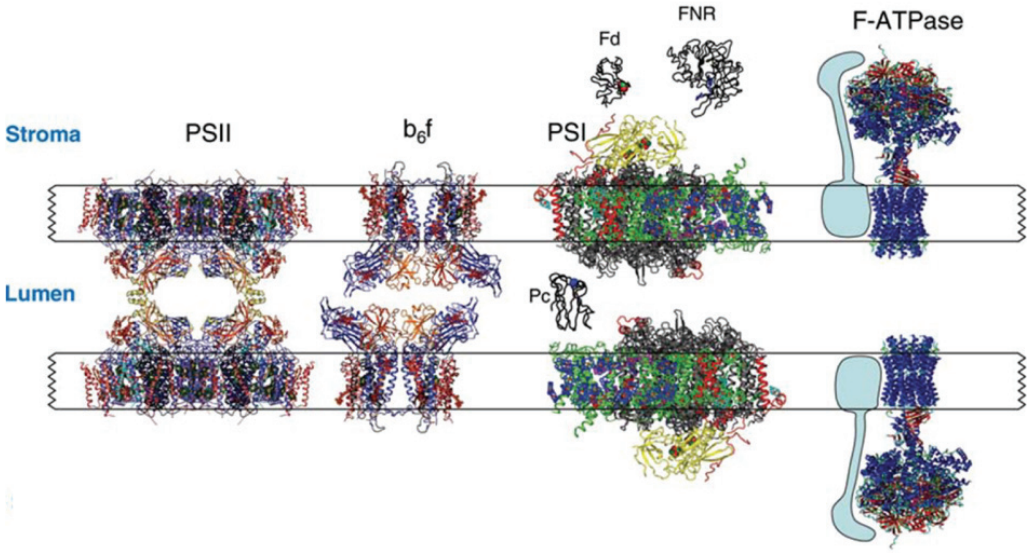

Figure 1 Thylakoid membrane complexes. The architecture of thylakoid membrane complexes and soluble proteins based on high resolution structures, taken from (Nelson and Yocum 2006).

The light energy harvested by the pigments in PSI and PSII is transferred to the RC, where charge separation occurs. For PSII it was recently suggested that accessory Chl *a* (Chl_{D1}) is the primary electron donor and pheophytin ($Pheo_{D1}$) the primary electron acceptor (Groot *et. al.* 2005; Holzwarth *et. al.* 2006b). Alternatively, it has been proposed that at least two pathways for primary charge separation coexist, either having Chl_{D1} or a Chl called P_{D1} as primary electron donor (Novoderezhkin *et. al.* 2007; Romero *et. al.* 2010). From Pheophytin the electron is transferred to plastoquinone Q_A and subsequently to Q_B at the stromal side of the PSII complex. After the second reduction by Q_A, Q_B takes two protons from the stroma and is released from its PSII binding site as plastoquinol. Before the second reduction step can take place $P680^+$ first needs to be reduced by a redox active tyrosine residue, called Y_Z, which in turn is reduced by the manganese (Mn_4CaO_5) cluster in the oxygen evolving complex (Umena *et. al.* 2011). When four electrons are removed the oxygen evolving complex can oxidize water to form molecular oxygen, protons and electrons. The electrons are used to neutralize the accumulated positive charges of the oxygen evolving complex, the protons and oxygen are released into the lumen (e.g. Blankenship 2002).

The plastoquinol diffuses from PSII through the thylakoid membrane to the cytochrome b_6f complex. This complex accepts the electrons and releases the protons into the lumen (inside) of the thylakoids. The electrons are used to reduce the copper-containing protein plastocyanin, which diffuses through the lumen to

PSI. Upon light absorption by PSI an electron is transported over the ETC to the iron-sulfur protein ferredoxin. The positive charge remains on the special Chl *a* dimer in the PSI RC called P700. Plastocyanin reduces $P700^+$ back to its neutral state. The electron accepted by ferredoxin is used by the enzyme ferredoxin-$NADP^+$ reductase (FNR) to reduce $NADP^+$ NADPH (e.g. Blankenship 2002).

The protons released in the lumen during the light reaction generate a proton motive force that drives the synthesis of ATP by ATP synthase. The ATP and NADPH molecules formed in the light dependent reaction are used in the light independent or dark reaction in the Calvin-Benson Cycle to form sugars out of CO_2 and H_2O (Bassham *et. al.* 1950).

Cyclic electron flow – Next to the linear electron flow, also cyclic electron flow around PSI can occur. During cyclic electron flow protons are transported over the thylakoid membrane into the lumen, generating a proton motive force which drives ATP synthase, which can balance the ATP:NADPH ratio and, by lowering the luminal pH, it might also help to induce non photochemical quenching, a process important to protect PSII in high light conditions (for a recent review see Johnson 2011). In higher plants there are (at least) two distinct pathways for cyclic electron flow, the protein gradient regulation 5 (PGR5) and the NAD(P)H dehydrogenase (NDH) dependent pathway. If both are impaired photosynthesis and plant growth are severely affected (Munekaga *et. al.* 2004). Interestingly, the NDH-dependent pathway involves a NDH-PSI super complex which can only be formed if Lhca5 and Lhca6 are present (Peng *et. al.* 2009).

Structure of higher plant Photosystem I

The PSI-LHCI structure – Higher plant PSI consists of two moieties: a core complex and an outer light-harvesting antenna system (LHCI, fig 2). The current PSI-LHCI structural data at 3.3Å resolution allowed assigning the position of 13 core proteins, PsaN, Lhca1-4, 173 Chls, 15 Carotenoids, 2 phyloquinones and 3 Fe_4S_4 clusters (Amunts *et. al.* 2010). In total 15 core proteins, PsaA-PsaP, are known (Table 1); however PsaO and PsaP could not be unambiguously traced in the structure while a possibly new unidentified polypeptide was modeled as polyalanine and named PsaR (Amunts *et. al.* 2010). About 100 Chls are bound to the core, the rest of the 173 Chls is bound to LHCI or located between LHCI and the core (Jordan *et. al.* 2001; Ben-Shem *et. al.* 2003; Amunts *et. al.* 2010).

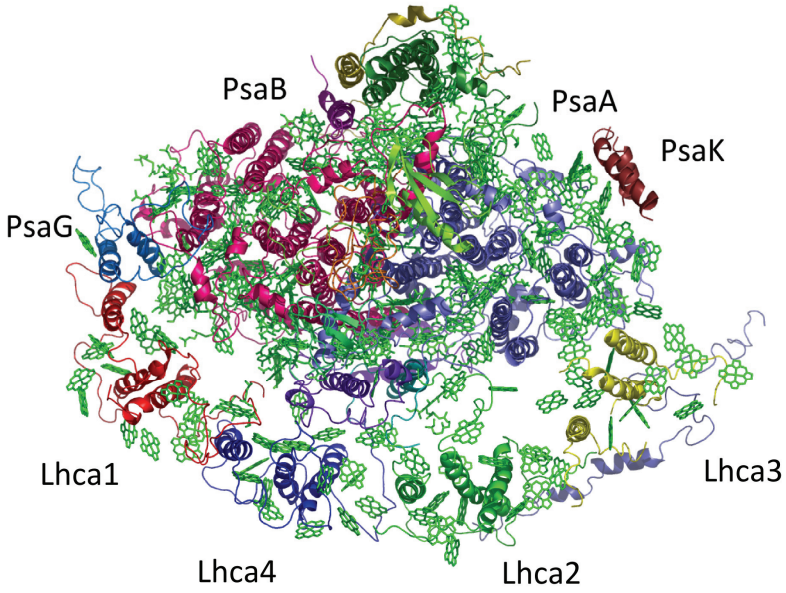

Figure 2 Model of PSI-LHCI structure. The structural model of plant PSI-LHCI proteins and Chls (Amunts *et. al.* 2007, PDB 2O01), with PsaA (light blue), PsaB (pink), Lhcas as indicated and Chls (green). The figure shows a top-view from the stromal side of the membrane, with PsaG at the left side and PsaK at the right side.

All 15 assigned β-carotenes were located in the core; the resolution in the LHCI part was not high enough to assign densities to Cars (Amunts *et. al.* 2010). The homologous proteins PsaA and PsaB comprise a large weight fraction of the core complex (fig 2) and coordinate most core Chls, including the RC Chls (Jordan *et. al.* 2001; Jensen *et. al.* 2007; Amunts *et. al.* 2010). The smaller core proteins are involved in the association of LHCI, plastocyanin, ferredoxin, FNR and, under specific light conditions, LHCII (reviewed in Jensen *et. al.* 2007).

Table 1 Molecular masses of higher plant PSI proteins. The predicted molecular masses for mature *A.thaliana* apo-proteins are reported. Data taken from (Jensen *et. al.* 2007) and [1](Khrouchtchova *et. al.* 2005).

Protein	Molecular mass (kDa)	Protein	Molecular mass (kDa)	Protein	Molecular mass (kDa)
PsaA	83.2	PsaH	10.4	PsaP	14[1]
PsaB	82.5	PsaI	4.1	Lhca1	21.5
PsaC	8.9	PsaJ	5.0	Lhca2	23.3
PsaD	17.9/17.7	PsaK	8.5	Lhca3	24.9
PsaE	10.4/10.5	PsaL	18.0	Lhca4	22.3
PsaF	17.3	PsaN	9.7	Lhca5	24.3
PsaG	11.0	PsaO	10.1	Lhca6	24.6

The structure of LHCI and Lhcs – LHCI forms a halve-moon-shaped belt coordinated at one side of the core (Boekema *et. al.* 2001; Ben-Shem *et. al.* 2003), organized as two heterodimers: Lhca1/4 and Lhca2/3 (fig 2). These complexes show a high degree of amino acid sequence similarity with the antenna complexes of PSII (Jansson 1999). Based on the structural models obtained by X-ray crystallography of LHCII (Kühlbrandt *et. al.* 1994; Liu *et. al.* 2004), CP29 (Pan *et. al.* 2011) and of PSI-LHCI (Ben-Shem *et. al.* 2003; Amunts *et. al.* 2010) it can be inferred that all Lhcs share a protein fold of three membrane spanning α-helices (fig 3) and have a similar Chl organization. The locations of the Lhca carotenoids, which could not be resolved, are also expected to be similar to those in LHCII and CP29. All Lhcs need to coordinate at least two carotenoids, forming a cross in the centre of the complex, to stabilize the complex (Plumley and Schmidt 1987; Paulsen *et. al.* 1990; Kühlbrandt *et. al.* 1994; Croce *et. al.* 1999). The Lut620 (L1) site (fig 2) is occupied by lutein, while the Lut621 (L2) site is occupied by lutein or violaxanthin, depending on the Lhc (Croce *et. al.* 1999). Neoxanthin is located at a peripheral site (Croce *et. al.* 1999; Caffarri *et. al.* 2007) and is present in LHCII, CP29 and CP26 (Bassi *et. al.* 1993).

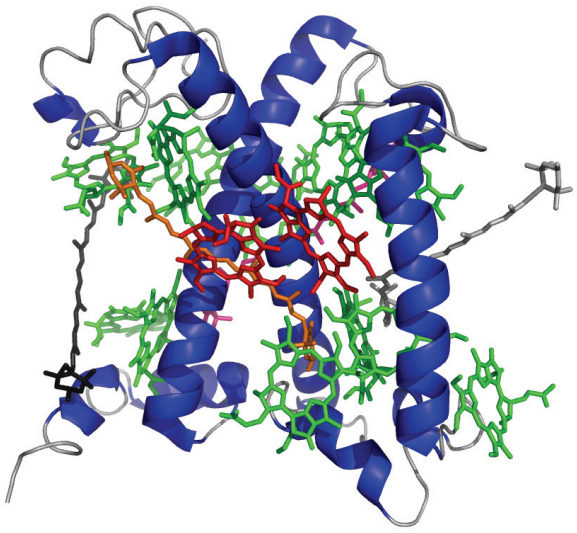

Figure 3 Lhc structure. Model of LHCII structure (Liu *et. al.* 2004, PDB 1RWT), with the protein (blue), Chls (green), Car in L1 site (pink), Car in L2 site (orange), Car in V1 site (dark gray) and Neoxanthin (light gray). Chls 603 and 609, which are important for the spectroscopic properties of Lhcas (see below), are depicted in red.

In LHCII an additional binding site (V1) is found at the periphery of the complex which coordinates violaxanthin (Ruban *et. al.* 1999; Caffarri *et. al.* 2001; Liu *et. al.* 2004). *In vitro* reconstitution of Lhca complexes indicates that Lhca1 and Lhca3 coordinate ~3 carotenoids, while Lhca2 and Lhca4 coordinate 2 (e.g. Croce *et. al.* 2007b). The third carotenoid might be present in the V1 site, but until now there is no evidence to support this suggestion. In purified LHCI 10-12 Chls are present per Lhca (Croce *et. al.* 2002; Wientjes and Croce 2011, Chapter 3). However, in the PSI-LHCI structure higher numbers (Lhca1: 15, Lhca2: 14, Lhca3: 17, and Lhca4: 15

(Amunts *et. al.* 2010) were found, suggesting that some Chls are lost during the purification. In addition, the low resolution in this part of the structure might have resulted in the over-estimation of the number of Chls coordinated by some Lhcas.

(Flexible) LHCI organization – In the past, the Lhca composition was believed to be flexible (Bailey *et. al.* 2001), however, recent biochemical evidence shows that the Lhca composition does not change under different light conditions (Ballottari *et. al.* 2007) and that each Lhca has a unique binding place which cannot be occupied by another Lhca (Klimmek *et. al.* 2005; Morosinotto *et. al.* 2005a; Wientjes *et. al.* 2009, Chapter 2). However, there is one exception: in a fraction of the PSI complexes from Lhca4 knock-out plants Lhca4 is replaced by Lhca5 (Wientjes *et. al.* 2009, Chapter 2).

From the first structure of PSI-LHCI (Ben-Shem *et. al.* 2003) it was suggested that LHCI is anchored to the core mainly through Lhca1 which strongly interacts with PsaG. However, the PsaG anti-sense plant still retained most of its Lhcas (Jensen *et. al.* 2002) and the Lhca1 knock-out plant retained a large part of Lhca2 and Lhca3 (Klimmek *et. al.* 2005; Wientjes *et. al.* 2009, Chapter 2). On the other hand, the weak association of Lhcas in the Lhca4 knock-out plant (Klimmek *et. al.* 2005; Morosinotto *et. al.* 2005a; Wientjes *et. al.* 2009, Chapter 2), suggests an important role for this sub-unit in LHCI anchoring.

The chlorophyll organization in the Photosystem I core – Figure 4 depicts the structural organization of the Chls and the ETC of the PSI core from cyanobacteria. The cyanobacterial PSI core is highly homologous to that of higher plants and algae (Jordan *et. al.* 2001; Ben-Shem *et. al.* 2003; Vanselow *et. al.* 2009), however, its structure has been resolved at higher resolution (2.5Å) which allows for a more detailed description of the complex (Jordan *et. al.* 2001). In the PSI core the light-harvesting Chls are distributed in an oval ring around the ETC Chls (Fig 4A). Most Chls on the ring have centre to centre distances between 7 and 16Å, allowing for fast and efficient excitation energy transfer (Jordan *et. al.* 2001). All but two linker Chls are well separated from the central Chls by more than 18Å. This organization allows many Chls to face the ETC Chls and transfer excitation energy to them (Gobets and van Grondelle 2001). The linker Chls are located only 10.9 and 12.8Å from the ETC. It has been suggested that they function as an energy transfer route from the antenna Chls to the ETC (Schubert *et. al.* 1997), although, structural simulations indicate that this is not the case (Gobets and van Grondelle 2001).

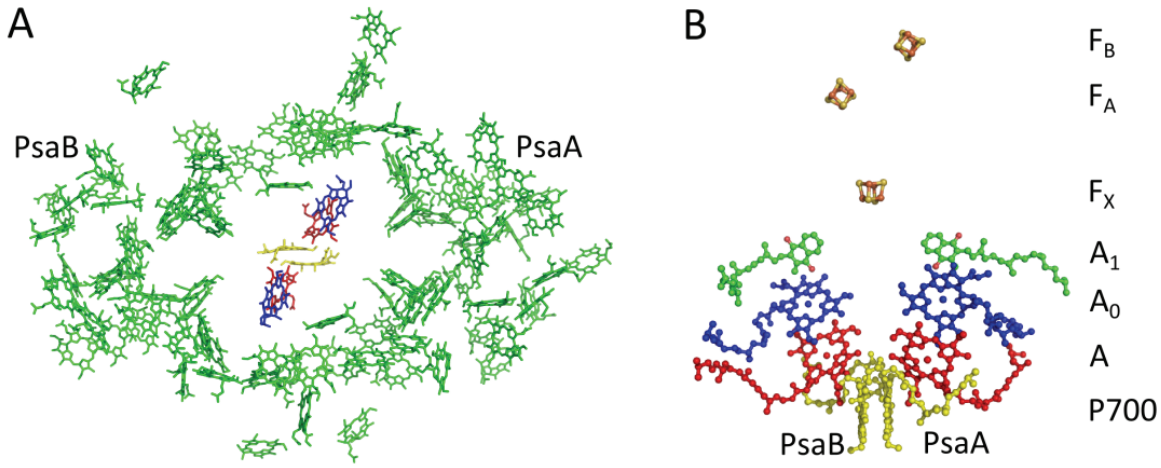

Figure 4 The arrangement of the PSI core Chls and electron transport chain. A: The arrangement of the PSI core Chls as seen from the stromal side. The bulk Chls are shown in green and the RC Chls P700 in yellow, A in red and A_0 in blue. For clarity the phytol chains (C0-C20) are not shown. B: Side-view of ETC cofactors, names are indicated (Jordan *et. al.* 2001, PDB 1JB0).

The electron transport chain – Figure 4B shows the PSI ETC; it is composed of 6 Chls *a*, 2 phylloquinones and 3 Fe_4S_4 clusters (F_X, F_A and F_B). The primary charge separation is thought to occur at P700, named after its absorption maximum. P700 is located at the luminal side of the membrane and consists of an asymmetric Chl *a* dimer. One Chl *a* is bound to PsaB, and one $C13^2$ Chl *a* epimer is bound to PsaA. From here there are two electron transport branches (the A- and the B-branch), each consisting of two Chls *a* and 1 phylloquinone. The branches merge again at F_X at the other side of the membrane. The first spectroscopically resolvable electron acceptor is Chl A_0, but the accessory Chl A located between P700 and Chl A_0 probably functions as electron transfer intermediate (Jordan *et. al.* 2001; Heathcote *et. al.* 2003). Alternatively, it has recently been proposed, based on spectroscopic evidence, that Chl A is the primary electron donor and that P700 is oxidized in a secondary electron transfer step (Müller *et. al.* 2003; Holzwarth *et. al.* 2006a; Di Donato *et. al.* 2011). Once the electron is located on A_0, it is transferred to A_1 which is a phylloquinone and from there to the iron-sulfur clusters: from F_X to F_A and finally to F_B (Brettel 1997). F_A and F_B are coordinated by PsaC, while all other electron transport co-factors are coordinated by PsaA and PsaB (Jordan *et. al.* 2001; Heathcote *et. al.* 2003).

Absorption, fluorescence and excitation energy transfer in PSI-LHCI

Purification of PSI-LHCI, PSI core and LHCI – Bengis and Nelson were the first to publish (1975) a purification protocol and absorption spectrum of the PSI core from higher plants, which they called the PSI RC. In (1980) Mullet *et al.* published the purification of PSI with its light-harvesting complex structurally and functionally associated. They show that the 77K emission maximum of PSI-LHCI (then called: PSI-110) is extremely red-shifted with its maximum at 736nm. The purification of LHCI was published by Haworth et al (1983) and it was shown that the red emission is preserved in LHCI. Lam et al. (1984) also purified LHCI, but in this case instead of one main 77K emission band at 730nm, a second band at 680nm was observed. In a subsequent purification step, two fractions were obtained and named LHCI-680 and LHCI-730, after their emission maxima. It was found that the LHCI-680 fraction was mainly composed of monomeric Lhca2 and Lhca3, and LHCI-730 of the Lhca1/4 dimer (Knoetzel *et. al.* 1992; Schmid *et. al.* 2002). The spectroscopic properties of both fractions were studied extensively (Knoetzel *et. al.* 1992; Palsson *et. al.* 1995; Tjus *et. al.* 1995; Melkozernov *et. al.* 1998; Schmid *et. al.* 2002). However, in 2000 it was found that Lhca2 and Lhca3 could be purified in a dimeric state together with Lhca1 and Lhca4, this sample had an 77K emission maximum at 730nm (Ihalainen *et. al.* 2000; Croce *et. al.* 2002). This indicated that the complexes in the LHCI-680 fraction were somewhat denaturated, supporting a previous suggestion of Bassi and Simpson (1987). Due to the very similar biochemical properties of the LHCI dimers, it was only possible to partly separate the complexes (Croce *et. al.* 2002). However, with the use of Lhca lacking mutant plants the Lhca1/4 and Lhca2/3 dimer could be purified (Wientjes and Croce 2011, Chapter 3).

The role of red forms in PSI – The presence of red forms, Chls with extremely red-shifted and broad absorption and emission spectra, is a general property of PSI in plants, algae and cyanobacteria (e.g. Mullet *et. al.* 1980; Gobets and van Grondelle 2001; Mozzo *et. al.* 2010). In higher plants and in the alga *Chlamydomonas reinhardtii* the red forms are mainly located in the antenna of PSI, while in cyanobacteria they are found in the PSI core (Haworth *et. al.* 1983; Gobets and van Grondelle 2001; Mozzo *et. al.* 2010). The function of the red forms is not completely clear. They might play a role in photoprotection (Karapetyan *et. al.* 1999), and likely, they are important for light harvesting in a dense vegetation system where light is enriched in the long wavelengths (Rivadossi *et. al.* 1999).

Lhca – So far it has not been possible to purify native Lhca complexes in their monomeric state, thus complicating the characterization of the individual complexes. However, it has been shown that Lhcs can fold spontaneously when the apo-protein and the pigments are combined (Plumley and Schmidt 1987; Paulsen *et. al.* 1990). The apoprotein can be obtained by overexpression of the protein in *E.coli* (Paulsen *et. al.* 1990) and the pigments can be purified from photosynthetic organisms. It has been demonstrated that this method, called *in vitro* reconstitution, provides complexes with identical properties as the native ones (Paulsen *et. al.* 1990; Giuffra *et. al.* 1996).

Analysis of reconstituted Lhca complexes provided information about their stability, pigment composition, and spectroscopic properties. The LT emission maxima of the Lhca complexes were found at 690nm (Lhca1), 702nm (Lhca2), 725nm (Lhca3), and 733nm (Lhca4) (Schmid *et. al.* 1997; Croce *et. al.* 2002; Castelletti *et. al.* 2003), all red-shifted compared to the maximum of Lhcb complexes at ~680nm. Also the absorption bands of the lowest energy Chls *a* (which are responsible for the LT emission) are red-shifted. This is most extreme for the red forms of Lhca3 and Lhca4, which have maxima at 705 and 708nm, respectively (Croce *et. al.* 2007a), at least 25nm red-shifted as compared to the maxima of bulk Chls *a* at 660-680nm (Hemelrijk *et. al.* 1992; Jennings *et. al.* 1993).

In vitro reconstitution has another advantage: it allows for an easy change of a specific amino acid of the apoprotein, which makes it possible, for instance, to substitute a Chl binding amino acid into an apolar one, which cannot coordinate the central Mg-ion of a Chl. In this way specific Chls can be “knocked-out” (Bassi *et. al.* 1999). Based on such mutation analysis, it was suggested that the red-shifted absorption of Lhcas arises from the lowest exciton state of the strongly coupled Chls *a* 603 and 609 (nomenclature as in (Liu *et. al.* 2004), red in figure 2) (Morosinotto *et. al.* 2002; Croce *et. al.* 2004; Morosinotto *et. al.* 2005b; Mozzo *et. al.* 2006), coupled to a charge-transfer (CT) state (Ihalainen *et. al.* 2003; Romero *et. al.* 2009). It was further shown that changing the ligand of Chl 603 in Lhca3 and Lhca4 from asparagine into histidine, the 603 ligand in all other Lhcs, induces a strong blue shift of the absorption band, which indicates the importance of this residue for the excitonic Chl 603-609 interaction (Morosinotto *et. al.* 2003).

Comparison of the properties of native and reconstituted Lhca1/4 shows that they are very similar. This is also true for the sum of reconstituted Lhca2 and Lhca3, compared to a mixture of the native complexes (Schmid *et. al.* 1997; Wientjes and Croce 2011, Chapter 3). Therefore, it can be concluded that the reconstituted complexes give valuable information about the native system. The spectroscopic properties of the purified Lhca1/4 and Lhca2/3 complexes are

described in (Wientjes and Croce 2011, Chapter 3) and (Wientjes *et. al.* 2011b, Chapter 4).

PSI-LHCI – The excited-state lifetime of isolated Lhcas is in the ns time range (Gobets *et. al.* 2001a; Ihalainen *et. al.* 2005a; Wientjes *et. al.* 2011b, Chapter 4). However, the lifetime of PSI is far shorter (tens of ps) due to trapping of the excitation energy in the RC (e.g. Gobets *et. al.* 2001b; van Oort *et. al.* 2008). The total trapping time is the sum of τ_{mig}, τ_{del} and τ_{trap}, where τ_{mig} is the average first passage time for the migration to approach the RC, τ_{del} is the extra time the excitation energy transfer to the relatively isolated RC takes (see fig 4A), τ_{trap} is charge separation time divided by the probability that the excitation is located on the RC. In case charge separation is reversible, also the secondary charge separation time and the drop in free energy on primary charge separation, should be taken into account (van Amerongen *et. al.* 2000; van Oort *et. al.* 2010). What the rate limiting step is in PSI energy trapping is discussed controversially in literature. Different groups find support for different models based on rather similar data. This is due to the high complexity of the system and to the fact that the measured optical signals are caused by a mixture of many energy and electron transfer steps; therefore extracting individual kinetic parameters is very complex (Savikhin 2006). Interestingly, even if charge separation already occurred and P700 is closed (positively charged), excitation energy can still be trapped with a similar efficiency as by open RCs (Nuijs *et. al.* 1986; Owens *et. al.* 1988; Savikhin *et. al.* 2000; Chapter 8).

The overall trapping time in the core of higher plants is ~20ps (Engelmann *et. al.* 2006; Slavov *et. al.* 2008; Wientjes *et. al.* 2011a, Chapter 7). This time is longer in PSI particles of cyanobacteria and is correlated with the number and energy levels of the red forms (Gobets *et. al.* 2001b). The trapping time is also increased when LHCI is associated to the PSI core of plants. This is partly due to the increased number of Chls, but mostly caused by the presence of red-forms in LHCI (e.g. Engelmann *et. al.* 2006; Slavov *et. al.* 2008). The energy levels of the red-forms in Lhca3 and Lhca4 are lower than the energy level of P700, so the excitation energy must be transferred “up-hill” to be used for charge separation, and, therefore it slows down the trapping rate (Jennings *et. al.* 2003). The routes and rates of excitation energy transfer between the individual Lhcas and the core are discussed controversially in literature (Ihalainen *et. al.* 2002; Ihalainen *et. al.* 2005b; Slavov *et. al.* 2008; van Oort *et. al.* 2008). The aim of chapter 7 (Wientjes *et. al.* 2011a) is to provide a clear picture of the excitation energy transfer in PSI-LHCI.

The pigments of Photosystem I

In photosynthesis light energy is harvested by photosynthetic pigments. In higher plants these are: Chl *a*, Chl *b*, lutein, violaxanthin, β-carotene, neoxanthin. Under high-light conditions part of the violaxanthin pool can be converted to antheraxanthin and zeaxanthin in the antenna of PSI and PSII (Demmig-Adams and Adams 1996; Wehner *et. al.* 2004).

Structure of the pigments – Figure 5 shows the schematic representation of the higher plant PSI pigments. Chlorophylls consist of a substituted porphyrin ring with a central magnesium ion, and a long phytol chain. The alternating single – double bonds in the porphyrin ring allow the π-electrons to delocalize over the molecule. This gives rise to strong electronic transitions in the visible region. Cars also make use of a large conjugated system, but in this case the backbone is a linear polyene chain. Cars without oxygen are called carotenes, while Cars with oxygen are called xanthophylls. The number of conjugated double bonds increases from Violaxanthin (*N* = 9), to Lutein (*N* = 10), to β-carotene (*N* = 11).

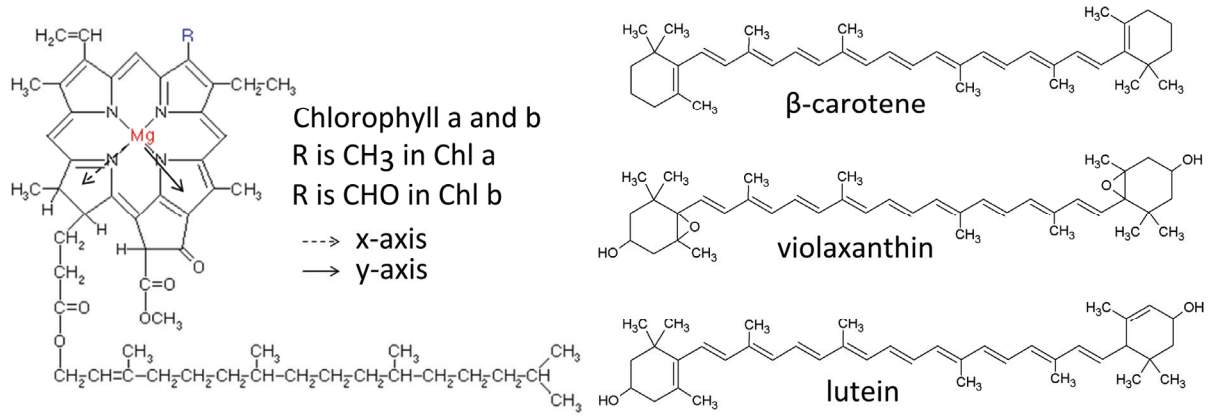

Figure 5 Molecular structures of PSI-LHCI pigments. Molecular structures of Chl *a*, Chl *b*, β-carotene, Violaxanthin and Lutein. The orientation of the x- and y-axis in Chl are indicated.

Spectra – Figure 6 shows the absorption spectra of the Cars and Chls, as well as the solar spectrum at sea level. The Cars predominantly absorb blue light and therefore appear orange. The Chls absorb blue and red light, but transmit the green part of the solar spectrum, therefore leaves appear green to us. The orange colors of the Cars are dominating in autumn when the Chls are degraded.

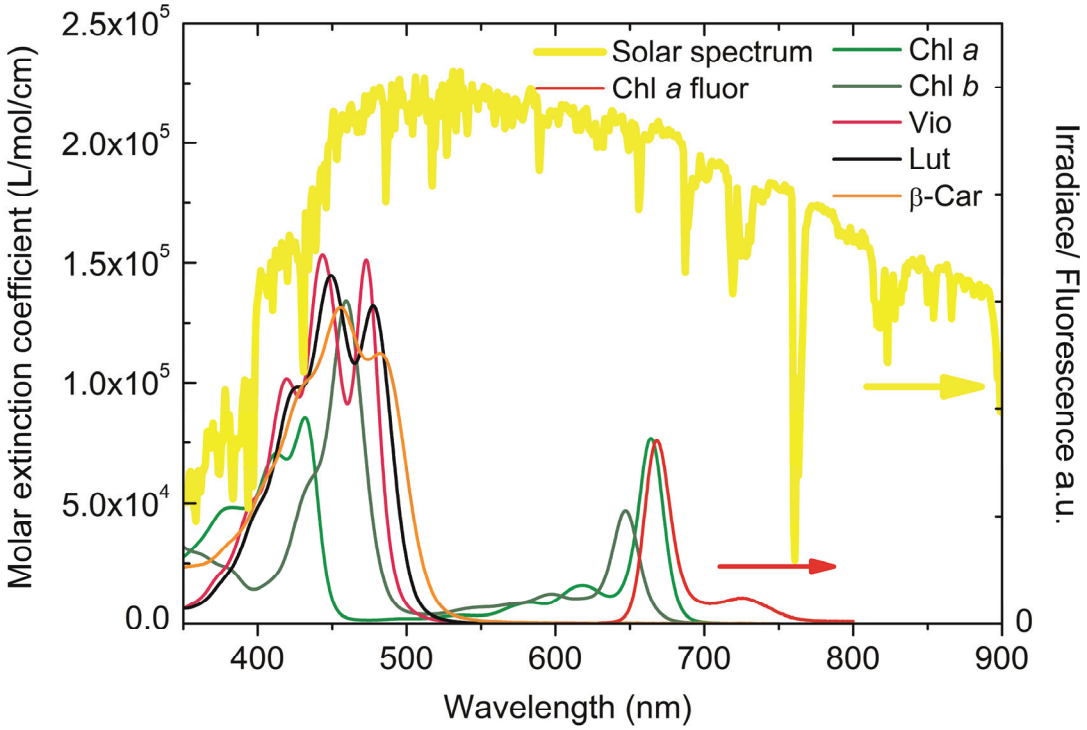

Figure 6 Spectra of pigments and sun. Figure shows absorption spectra of PSI-LHCI pigments in 80% aceton, emission spectrum of Chl *a* in 100% acetone and average terrestrial solar energy output spectrum for 48 contiguous states of the United States of America (ASTM).

Energy levels – In figure 7 the energy levels of the ground and excited states of Chl *a*, Chl *b*, and a Car are shown. Chls are porphyrin derivatives. It has been shown that the electronic transitions of such molecules can be explained by the 4-orbital model of Gouterman (Gouterman 1961). In this model only the two highest occupied molecular orbitals (HOMO's) and the two lowest unoccupied molecular orbitals (LUMO's) are considered. Linear combinations of one electron transitions from the HOMOs to the LUMOs give rise to four electronic transitions. The additive combination results in absorption bands in the ultra violet/blue spectral region, called B_X and B_Y with polarization along the x- and the y-axis, respectively (see fig 5). The difference gives rise to the absorption bands in the green/red/infra-red region that are called Q_X and Q_Y. In unsubstituted porphyrins the energy levels of the HOMO's and the LUMO's are degenerate, in this case only the B (also called Soret) transitions are allowed. Asymmetric substitutions, also present in Chls, break down the degeneracy of the energy levels and result in allowed Q transitions. As Chl *b* is more symmetric than Chl *a,* the Q transitions are weaker for Chl *b* than for Chl *a* (Gouterman 1961; van Amerongen *et. al.* 2000).

In Cars the transition to the first excited state (S_1) is forbidden for symmetry reasons, while the transition to S_2 is strongly allowed. The S_1 and S_2 energy levels decrease with increasing number of conjugated bonds (e.g. Polivka and Frank 2010). The energy levels of these states compared with those of Chls are important for energy transfer and pigment-pigment interactions.

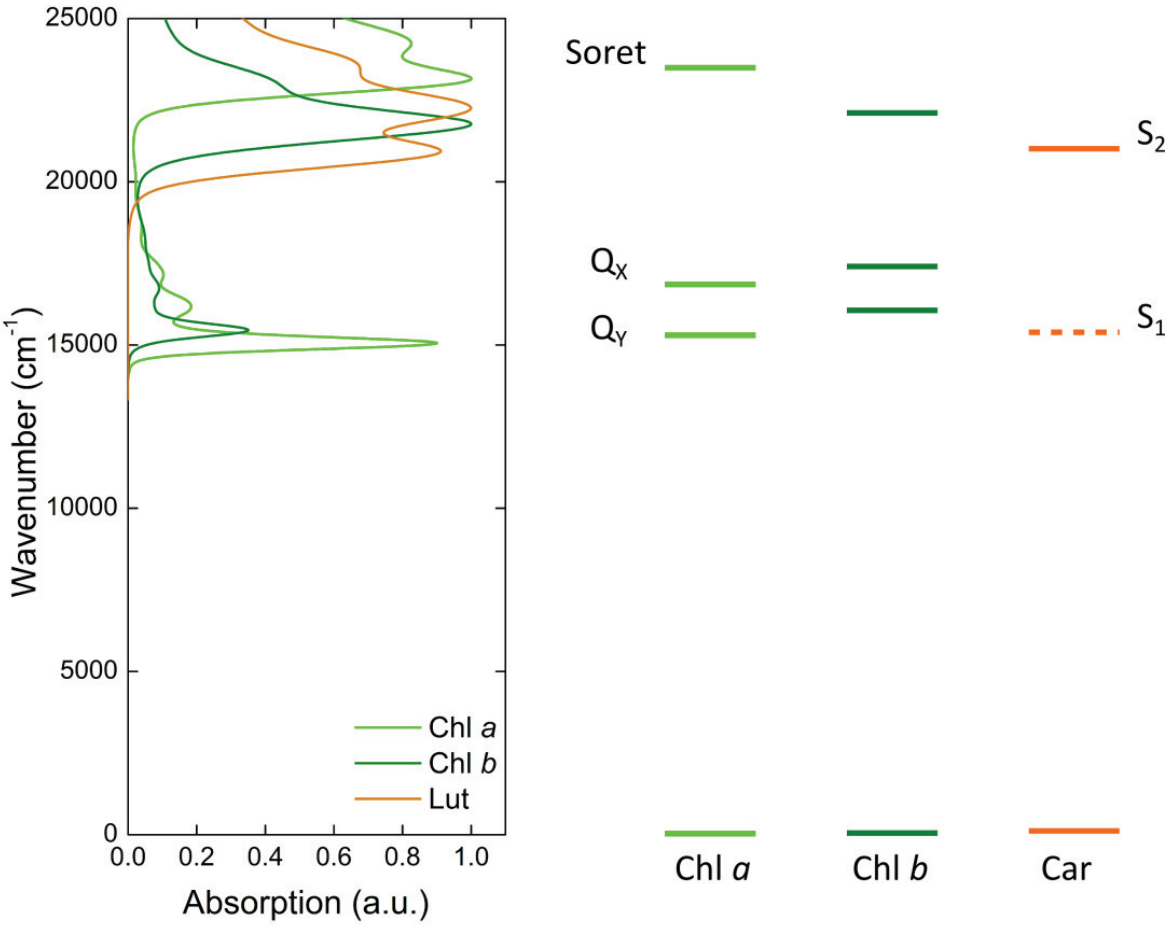

Figure 7 Energy level diagram of Chl and Car. Absorption spectra and energy level diagram of ground and excited states of Chl *a*, Chl *b* and carotenoids. The optical forbidden S_1 state of Cars is indicated as a dashed line. Absorption spectra are of pigments in 80% acetone. The figure is based on a figure on the homepage of P.J. Walla (Walla).

Electronic transitions – Figure 8 shows the electronic and vibrational energy levels of a pigment. When a pigment absorbs light of appropriate energy an electron is excited to a higher electronic state. Because the electron density distribution is different in the excited state than in the ground state, also the equilibrium position of the nuclei is different (fig 8B). As the nuclear geometry of a molecule does not change during the short time of an electronic transition we can imagine the transition as being up along the vertical line Figure 8B, and thus to occur from the vibrational ground state to a higher order vibrational level. According to the Franck-Condon principle the transition is more likely to occur if there is a stronger

overlap between the ground state and excited state vibrational wavefunctions. This means that the transition can occur to several vibrational levels, but with different intensity (e.g. Atkins 1992).

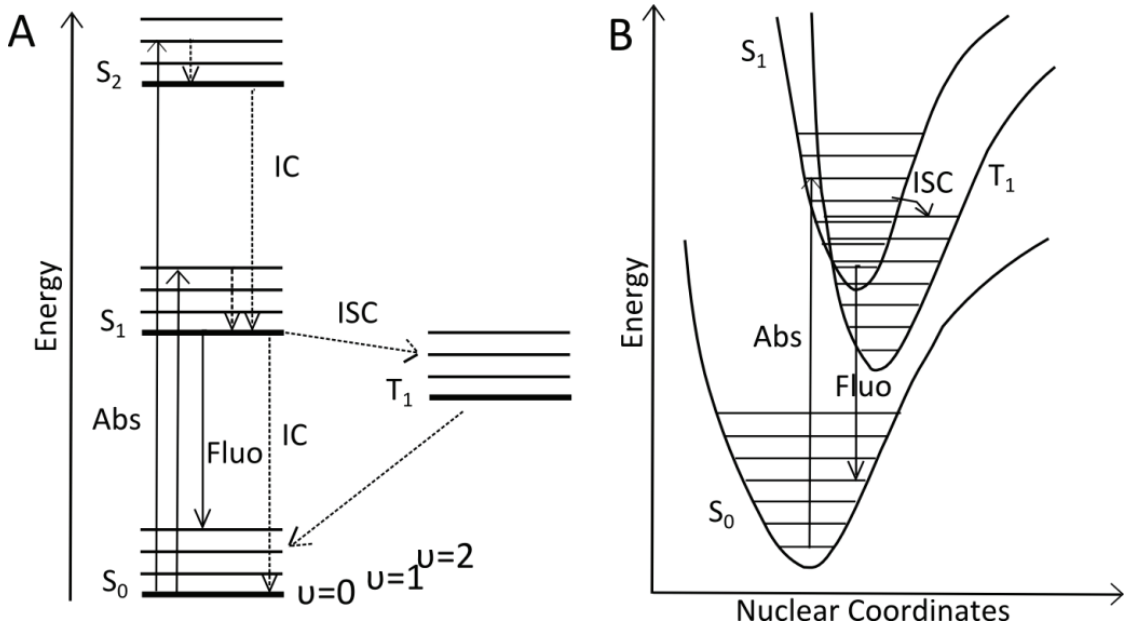

Figure 8 Energy levels and transitions in pigments. A: Jablonski diagram illustrating the energy levels of electronic states of a pigment and the transitions between them. The singlet ground state (S_0), first (S_1) and second (S_2) excited state, a triplet state (T_1) and vibrational energy levels (v = 0, 1, 2, ..) are indicated. Transitions are specified, Abs stands for Absorption, Fluo for Fluorescence, IC for Internal Conversion and ISC for Inter System Crossing. B: Franck-Condon principle energy diagram, as in A, but now as function of nuclear coordinates.

The pigment will rapidly relax to the lowest vibrational level of the first excited state (Q_Y or S_1 for Chl and Car) by internal conversion. From this state the pigment will go back to the ground state by either internal conversion, fluorescence or to the triplet state by intersystem crossing (ISC), which then decays to the ground state (fig 8). The internal conversion rate to the ground state is large for Cars, while it is small for Chls. Fluorescence is the emission of a photon while the pigment falls back from the singlet excited state to the ground state. As the S_1 to S_0 transition in Cars is optically forbidden, Cars can only fluorescence by borrowing dipole strength from the strongly allowed S_0 to S_2 transition; as a consequence the fluorescence emission is extremely weak (Gillbro and Cogdell 1989; Andersson *et. al.* 1995; van Amerongen *et. al.* 2000). On the contrary, the strongly allowed Q_y transitions of Chls are highly fluorescent. The fluorescence quantum yield of Chl *a* in acetone is 30% (Weber and Teale, 1957 cited in Palacios *et. al.* 2002). As the downward electronic transition also follows a vertical line (fig 8B), the electron is most likely to fall back in a higher vibronic state; therefore, the

fluorescence emission is red-shifted compared to the absorption (see fig 6 for Chl *a*).

In excited molecules the electronic spins are usually paired, that is the net-spin is zero and the molecule is in the singlet state. If a spin flips, in the process called Inter System Crossing the net spin is one, and the molecule is now in the triplet state. Chls in the triplet state are dangerous as they can react with molecular oxygen (which is naturally in the triplet state) to form singlet oxygen. Singlet oxygen is an extremely reactive and damaging species. Fortunately, if a Car is nearby it can quench the triplet Chl and scavenge singlet oxygen (reviewed in Krinsky 1979).

The sum of the different decay rates determines the excited state lifetime of the pigment. For Chl *a* in acetone this lifetime is 6 ns, (e.g. Palacios *et. al.* 2002), while it is only 5-35 ps for photosynthetic Cars of higher plants (reviewed in Polivka and Sundstrom 2004).

Interacting pigments

Pigment-protein interactions – The structure of a pigment is not the only determinant for its optical properties. The environment is also important. In Lhcs the pigments are coordinated to a protein. The protein scaffold keeps the pigments at specific distances and orientations with respect to each other and with respect to the protein itself. Hydrogen bonds between amino acids of the protein and Chls lead to red shifts in the absorption spectra. Also charged amino acids at close distance from the Chls will induce shifts (van Amerongen *et. al.* 2000). Furthermore, the bandwidth of the electronic transition of the pigments is strongly affected by coupling of the electronic transition to low frequency vibrations (phonons) of the protein (van Amerongen *et. al.* 2000).

Excitonic interactions – Next to the protein, the pigments also feel each other through excitonic interactions. For identical molecules the interaction energy (V_{12}) is given by:

$$V_{12} = C\frac{5.04kd}{R^3} \quad \text{with} \quad \kappa = \tilde{\mu}_1 \cdot \tilde{\mu}_2 - 3(\tilde{\mu}_1 \cdot \tilde{r}_{12})(\tilde{\mu}_2 \cdot \tilde{r}_{12})$$

Where V_{12} is the interaction energy in cm^{-1}, d is the dipole strength of a monomer transition in $debye^2$ and R is the inter-pigment distance in nm. κ is the dimensionless orientation factor, with $\tilde{\mu}_1$ and $\tilde{\mu}_2$ the normalized transition dipole moment vectors and $\tilde{r}_{12}$ the normalized vector between the centers of both pigments. The correction factor C depends on the refractive index of the medium, but is often taken to be 1 as it is in vacuum. From these formula it is clear that the

strength of an excitonic interaction strongly depends on the relative distance and orientation of the pigments (van Amerongen *et. al.* 2000).

Strong excitonic interactions – When V_{12} is very large compared to the difference in excited state energy of two pigments, the situation of identical molecules is approximated. In this case the excitations are delocalized over the two pigments and we speak of an excitonically coupled dimer. The excited-state energy levels are split by $2V_{12}$, and the average of these energy levels is often lowered, compared to the single molecules by the displacement energy, see figure 9. The distribution of the dipole strengths (*D*) between the two possible transitions depends on the angle (θ) between the transition dipole moments of the individual molecules. For isoenergetic molecules with identical dipole strength (*d*), the relation is: $D_{1,2} = d(1 \pm \cos \theta)$. In the most extreme case only one transition is allowed which gets a dipole strength of 2*d*, whereas the other transition is forbidden. When the transition dipole moments are parallel and in line the lowest energy transition is allowed, while the highest is forbidden. The opposite is true for the parallel sandwiched organization (fig 9) (van Amerongen *et. al.* 2000).

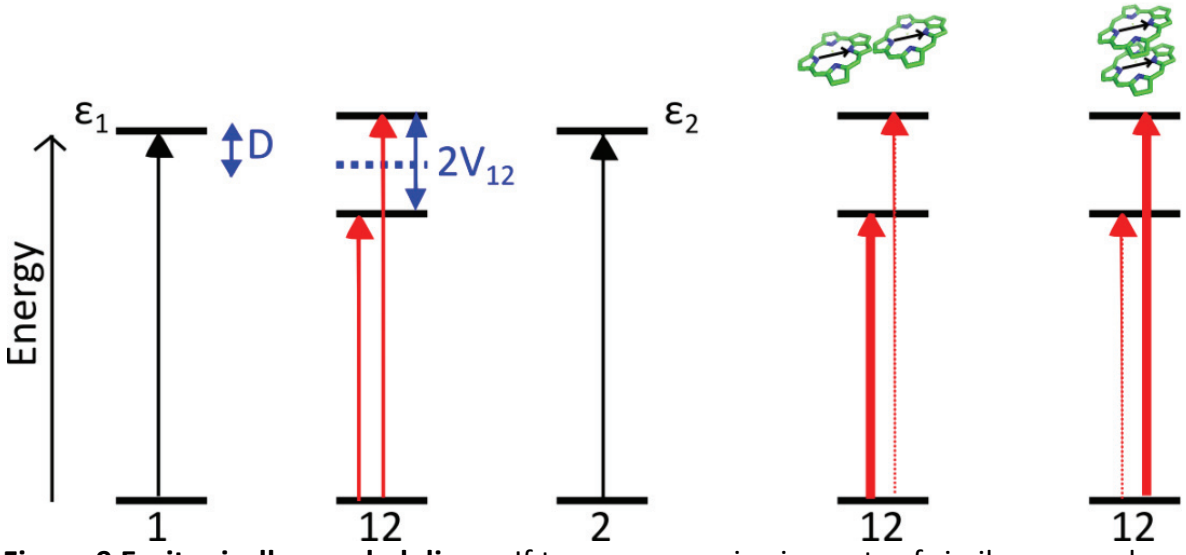

Figure 9 Excitonically coupled dimer. If two monomeric pigments of similar energy have a strong excitonic coupling ($V_{1,2}$) they form an excitonically coupled dimer. The average energy level is lowered by the displacement energy (D), and the energy levels are split by $2V_{12}$. The allowed electronic transitions for specific orientations of the transition dipole moments are shown.

In Lhcs strong pigment-pigment interactions, and therefore a high degree of delocalization of the excitons over the pigments, are common. This results in fast excitation energy transfer, which can be described by the modified Redfield theory (e.g. Novoderezhkin and van Grondelle 2010).

Weak excitonic interactions – In the case that the excitonic interaction between pigments is weak compared to the difference in energy, the excitations are essentially localized on one pigment. In this situation the rates of excitation energy transfer from the donor (*D*) pigment to the acceptor (*A*) pigment is given by the Förster Resonance Energy Transfer equation (Forster 1946, 1948; see e.g. Grondelle *et. al.* 1994):

$$k_{DA} = \frac{9*\ln 10}{128\pi^5}\frac{\kappa^2 c^4}{n^4 N \tau_{RD} R^6} J(\upsilon), \text{ with } J(\upsilon) = \int_0^\infty \frac{Fl_D(\upsilon)\varepsilon_A(\upsilon)}{\upsilon^4} d\upsilon$$

In these formula κ is the orientation factor (see above), *e* is the elementary charge, *n* is the refractive index of the pigments surrounding, *c* is the speed of light in vacuum, *N* is the number of Avogadro, τ_{RD} is the radiative lifetime of the donor, *R* is the distance between the pigments and *J* is the overlap integral of the normalized emission spectrum of the donor and absorption spectrum of the acceptor.

Chl to Chl energy transfer – The transfer rates between Chls *a* in the PSI core are expected to be very fast, as they are located at short distance (*R*) which respect to each other (fig 4) and there is a good overlap between the absorption and emission spectra (fig 5). Indeed, a very short depolarization time of ~160 fs has been reported (Du *et. al.* 1993; Kennis *et. al.* 2001) indicating extremely fast "hopping" of excitations.

Boltzmann distribution – Because fluorescence emission is red-shifted relative to absorption, the overlap integral will be smaller if the donor molecule absorbs at lower energy than the acceptor, compared to the opposite situation. Therefore, up-hill energy transfer is usually slower than down-hill transfer. In a system where the pigments transfer excitation energy to each other on a faster time scale than the excitation decays, a Boltzmann equilibrium will be reached in the excited state where the probability to find the excitation on a pigment will follow the Boltzmann distribution:

$$\frac{N_i}{N} = \frac{e^{-E_i/kT}}{\sum_i e^{-E_i/kT}}$$

Where *N* is the number of pigments, N_i/N the probability that the pigment with energy E_i is in the excited state, *k* the Boltzmann constant and *T* the absolute temperature. So the pigment with the lowest energy has the highest probability to be excited. This effect becomes stronger at lower temperature and therefore LT fluorescence is a direct method to obtain information about the low energy Chls.

Car to Chl energy transfer – In Lhcs energy is also transferred from Cars to Chls. This energy transfer occurs mostly from the S_2 state of Cars, but a contribution from the S_1 state has also been observed (Gradinaru *et. al.* 2000; Croce *et. al.* 2003). The overall transfer efficiency is 60-80% (Gradinaru *et. al.* 2000; Croce *et. al.* 2003; SI of Wientjes *et. al.* 2011a, Chapter 7). The S_2 state of Cars decays to the S_1 state in a few hundred fs (Polivka and Sundstrom 2004), therefore, the transfer from S_2 must be extremely fast to compete. This is achieved by optimized pigment-pigment orientations and distances (Polivka and Frank 2010).

Chl to Car energy transfer – Transfer in the opposite direction, from Chl to Car, has been proposed as a mechanism to shorten the excited state lifetime of Lhcs during non photochemical quenching (NPQ). NPQ is used by photosynthetic organism to dissipate excess absorbed light energy as heat, in sudden high-light conditions (Demmig-Adams and Adams 1996; Horton *et. al.* 1996). In plants NPQ can only develop to its full extent when part of the Violaxanthin pool gets converted into Zeaxanthin (Niyogi *et. al.* 1998). Based on measurements and calculations it was proposed that the S_1 state of Violaxanthin lies above that of Chl Q_Y, while that of Zeaxanthin (which has a longer conjugated π-system) lies below. This could explain the energy flow from Violaxanthin to Chls under normal light conditions and from Chls to Zeaxanthin under high light conditions (Frank *et. al.* 1994). As the excited state lifetime of Cars is far shorter than that of Chls, they can function as efficient energy quenchers. Instead of Chl to Zeaxanthin transfer Ruban et al. (2007) proposed, based on experimental evidence, that an energy transfer pathway from Chls to Lutein can be opened during NPQ due to a conformational change in LHCII.

Excitonic Car-Chl coupling – Another mechanism which can shorten the excited-state lifetime of Lhcs is excitonic Car-Chl coupling (van Amerongen and van Grondelle 2001). As the excited state lifetime of Cars is far shorter than of Chls a small degree of mixing of the Car S_1 state with the Chl Q_Y state will considerably decrease the excited state lifetime of the latter. Recently, it was experimentally shown that a strong correlation exists between the Chl-Car coupling strength and NPQ, indicating that this mechanism is indeed involved (Bode *et. al.* 2009). Excitonic Chl-Car coupling might also (partly) explain why the excited state lifetime of Chl *a* bound by LHCI (2.45ns (Wientjes *et. al.* 2011b, Chapter 4) or LHCII (~4ns, e.g. Palacios *et. al.* 2002) is shorter compared to that of Chl *a* in solution (~6ns, e.g. Palacios *et. al.* 2002) (van Amerongen and van Grondelle 2001).

Inter pigment charge transfer – A special type of pigment-pigment interaction is inter-pigment charge transfer. Such transfer lies at the heart of photosynthesis as it is the first electron transfer step in both PSI and PSII. Another example is the electron transfer from Zeaxanthin to Chl, which has also been correlated with NPQ and as such proposed as an NPQ mechanism (Holt *et. al.* 2005). Also charge transfer between Chls has been proposed to be involved in NPQ (Miloslavina *et. al.* 2008).

The red forms – Some Chls of PSI, called red forms, have very special spectroscopic properties; namely, strongly red-shifted absorption and emission spectra, a large Stokes' shift, broad absorption and emission bands and a large change of dipole moment between the ground and excited state (Haworth *et. al.* 1983; Ihalainen *et. al.* 2000; Croce *et. al.* 2007a; Romero *et. al.* 2009). It has been proposed that this can be explained by mixing of the lowest exciton state of a Chl dimer with a CT state (Ihalainen *et. al.* 2000). Generally a Chl-Chl CT state has a very low transition dipole moment from the ground state due to a poor overlap of the wavefunctions; furthermore, the energy level of the CT state is far higher than that of an excited Chl. However, when two Chls (or other pigments) come closer together the energy level of the CT state decreases (Hoffmann *et. al.* 2000; Dreuw *et. al.* 2003; Novoderezhkin *et. al.* 2007). In Lhcas two Chls are located closely together and apparently in this case the energy of the CT state is close enough to that of the lowest exciton state of the dimer, such that they can mix. The ground state is energetically too far away from the CT states and will be left unchanged. The now formed CT exciton state has still most of the dipole strength from the exciton dimer (Wientjes *et. al.* 2011b, Chapter 4), but also a large difference in dipole moment between the ground state and the excited state (Romero *et. al.* 2009). Due to the strong difference in electron distribution of the ground state and the excited state, also the nuclear equilibrium distances are likely to differ strongly. This will lead to a large contribution of optical transitions into higher vibronic sub-states (fig 8B). The degree of redistribution of the intensity between the zero-vibrational and higher vibrational sub-bands is determined by the Huang-Rhys factor. The Huang-Rhys factor of nearly three found for the red absorption region of LHCI is the largest for any photosynthetic antenna system (Ihalainen *et. al.* 2003). A Huang-Rhys factor of three means that the transitions into the second and third vibrational sub-band have the strongest intensity, while the zero-vibrational sub-band has only 5% of the intensity (van Amerongen *et. al.* 2000). The Stokes' shift will be very large, because fluorescence emission will likewise occur mostly into the higher vibrational subbands.

In Lhcs pigments are surrounded by the protein matrix. The low-frequency vibrations of the protein are called phonons. Coupling between the electronic transitions and the phonons results in homogeneous broadening (Γ_{hom}) of the absorption (and emission) spectra. In case of a large difference in dipole moment between the ground and excited state there will be a strong coupling between the electronic transition and the (polar) phonons of the protein and thus a large Γ_{hom} (van Amerongen *et. al.* 2000; Croce *et. al.* 2007a). Γ_{hom} is temperature dependent.

A protein can occur in many different conformations. As a result a pigment located at a specific position in a protein does not need to experience the same environment in each protein. This leads to inhomogeneous broadening of the absorption (and emission) band (Γ_{inhom}). As long as the distribution of protein conformations is not temperature dependent, Γ_{inhom} is not either. Excitonic interactions and CT states are strongly dependent on inter-pigment distances and orientations (see above) and therefore very sensitive to conformational variations (van Amerongen *et. al.* 2000).

The total broadening (Γ_{tot}) (or full width at half maximum) of the electronic transition is approximated by $\Gamma_{tot}^2 = \Gamma_{hom}^2 + \Gamma_{inhom}^2$. For the red-forms of LHCI both Γ_{hom} and Γ_{inhom} are very large: 200-360 cm^{-1} (Ihalainen *et. al.* 2003; Croce *et. al.* 2007a).

Scope of this thesis

In this thesis higher plant PSI-LHCI and its “building-blocks” are studied by (time-resolved) spectroscopy, biochemistry and electron microscopy. The aim is to improve the knowledge and understanding of the supra-molecular organization, spectroscopic properties and excitation energy transfer/trapping rates and routes of PSI-LHCI. The main problem in studying PSI-LHCI is that it is a large and complex system, which makes it difficult to obtain information about the properties, functions and roles of specific Lhcas. In this study the smaller PSI complexes of Lhca-lacking mutant *Arabidopsis thaliana* plants were used to overcome this problem. The remarkable spectroscopic properties of the red forms get special attention throughout the thesis.

In **chapter 2** the mild purification of PSI complexes with reduced antenna size from Lhca knock-out or anti-sense plants is described. The biochemical analysis of the antenna composition was combined with a single-particle electron microscopy study. This allowed answering questions, like: Is the binding of Lhcas to the core flexible? What is the position of each Lhca? Is the coordination of Lhcas to the core interdependent?

The Lhca1/4 and Lhca2/3 are biochemically very similar and for this reason full separation of the two was never successful. This especially hampered the investigation of the more fragile Lhca2/3 complex, which could not be obtained by other means. The PSI particles obtained from Lhca1 and Lhca2 lacking mutants coordinate only the intact Lhca2/3 or Lhca1/4 dimer, respectively. This allowed purification of Lhca2/3, the determination of its biochemical and spectroscopic properties, and the comparison of these properties with those of Lhca1/4, which is described in **chapter 3**.

In **chapter 4** the time-resolved emission properties of Lhca1/4 and Lhca2/3 were studied by Time Correlated Single Photon Counting and with a Synchroscan Streak camera. The average fluorescence lifetime in combination with the fluorescence quantum yield of the Lhca dimers allowed to investigate the (super)-radiativity of the dimers. Fitting the time-resolved fluorescence data to a compartmental model, in a procedure called target-analysis, allowed resolving of the inter-monomer transfer rates.

In chapter 4 heterogeneity in the decay associated spectra was observed for both dimers. This can be explained by presence of the dimers in different conformations with different spectroscopic properties or by heterogeneity in the sample. To investigate if a single Lhca complex can switch between states with different emission spectra, the complexes were studied by Single-Molecule fluorescence spectroscopy (**chapter 5**).

In chapter 5 it has been observed that Lhca complexes can display emission spectra similar to typical Lhcb complexes, while the opposite is true for Lhcb complexes. It was proposed that one protein can switch between different emission spectra by a conformational change. For Lhca complexes the equilibrium in general lies at the “red”-emitting site, while for Lhcb complexes it typically lies at the “blue”-emitting site. In **chapter 6** site-directed mutagenesis is used to investigate how large the change in inter-pigment distance/orientation must be to “convert” a typical Lhca complex into a typical Lhcb complex. Furthermore, it is investigated how the energy level of the red forms in Lhca4 can be tuned by changing the surrounding of these Chls.

The aim of **chapter 7** is to resolve the excitation energy transfer rates and routes in PSI-LHCI. To disentangle the contribution of the red forms and the individual Lhcas, PSI-LHCI as well as PSI particles with reduced antenna size or altered antenna composition were studied by time-resolved fluorescence spectroscopy.

Analysis and integration of this data with the information obtained on the isolated dimers gives new insights into the energy transfer in PSI-LHCI.

The electron donor phenazine methosulfate is often added during spectroscopic measurements on PSI in order to have the RCs in the open state. However, there are very few reports on the PSI RC re-opening rate for different phenazine methosulfate concentrations. This information is required to calculate what fraction of RCs is open under specific experimental excitation conditions. In **chapter 8** we measure these rates and compared these results with the data in literature. Furthermore, we show that phenazine methosulfate quenches the singlet excited state lifetime of Lhc complexes. Finally, we report the difference in fluorescence quantum yield of higher plant PSI with open and closed RCs.

Chapter 2

The role of Lhca complexes in the supramolecular organization of higher plant Photosystem I

Emilie Wientjes, Gert T. Oostergetel, Stefan Jansson, Egbert J. Boekema and Roberta Croce

This chapter is based on:

Journal of Biological Chemistry (2009) 284:7803-7810.

Abstract

In this work Photosystem I supercomplexes have been purified from Lhca-deficient lines of *Arabidopsis thaliana* using a mild detergent treatment which does not induce loss of outer antennas. The complexes have been studied integrating biochemical analysis with electron microscopy. This allows to directly correlate changes in the protein content with changes in the supramolecular structure of Photosystem I and to get information about the position of the individual Lhca subunits, the association of the antenna to the core and the influence of the individual subunits on the stability of the system. Photosystem I complexes with only two or three antenna complexes were purified showing that the binding of Lhca1/4 and Lhca2/3 dimers to the core is not interdependent, although the weak binding of Lhca2/3 to the core is stabilized by the presence of Lhca4. Moreover, it was found that Lhca2 and Lhca4 can be associated with the core in the absence of their "dimeric partners". It is shown that the structure of Photosystem I is very rigid and the absence of one antenna complex leaves a "hole" in the structure which cannot be filled by other Lhcas, clearly indicating that the docking sites for the individual subunits are highly specific. There is however an exception to the rule: Lhca5 can substitute for Lhca4, yielding highly stable PSI supercomplexes with a supramolecular organization identical to the WT.

Introduction

Photosystem I (PSI) operates in the light reactions of photosynthesis as a plastocyanin:ferredoxin oxidoreductase. In higher plants it is embedded in the thylakoid membranes of chloroplasts. It can be divided into two moieties (i) the core, harboring all the electron transport cofactors, 102 Chlorophyll *a* (Chl *a*) molecules and ~22 β-carotenes and (ii) the peripheral light harvesting complex (LHCI) (Fromme *et. al.* 2001; Jordan *et. al.* 2001; Amunts *et. al.* 2007). Under standard conditions LHCI is composed of four pigment-protein complexes (Lhca1-Lhca4), coordinating Chl *a*, Chl *b*, lutein, violaxanthin and β-carotene (Croce *et. al.* 2002b; Schmid *et. al.* 2002) arranged on one side of the core (Boekema *et. al.* 2001; Ben-Shem *et. al.* 2003). In the crystal structure of PSI from pea (Amunts *et. al.* 2007) the Lhca order was assigned starting at the G-pole, as Lhca1, Lhca4, Lhca2, Lhca3. These complexes are organized as dimers as shown by biochemical analysis (Croce *et. al.* 2002b). Studies of Lhca knock-out and anti-sense lines suggested that these subunits can only be associated with the core in their dimeric form (Morosinotto *et. al.* 2005a). One of the dimers, which has been purified from plants and refolded *in vitro* (Knoetzel *et. al.* 1992; Schmid *et. al.*

1997), is composed of Lhca1 and Lhca4. The second dimer is believed to be formed by Lhca2 and Lhca3, although the data are not conclusive due to the impossibility to purify it from plants and to refold it *in vitro*. Moreover, fluorescence data suggested that part of the Lhca2 and Lhca3 population can also form homodimers (Castelletti *et. al.* 2003).

A fifth pigment-protein complex, Lhca5, is present in non-stoichiometric amounts in WT plants. Its expression level is higher in mutant plants depleted in Lhca1 and Lhca4, however no corresponding polypeptide could be detected on SDS-PAGE, indicating that even in these mutants Lhca5 is not present in stoichiometric amount with the core (Ganeteg *et. al.* 2004a). Based on cross-linking studies Lhca5 has been suggested to form homodimers (Lucinski *et. al.* 2006), but *in vitro* reconstitution has shown that it can form heterodimers with Lhca1 (Storf *et. al.* 2004; Storf *et. al.* 2005).

Lhca proteins are encoded by nuclear genes belonging to the Lhc multi-gene family, which also encodes for the Lhcb proteins of Photosystem II (Jansson 1999). Judged from the crystal structure of PSI (Amunts *et. al.* 2007) and LHCII (Liu *et. al.* 2004) the Chl organization of the members of the family is rather similar, although their spectroscopic properties differ substantially. Lhca complexes absorb more to the red than Lhcb complexes and while Lhcb complexes have their low temperature fluorescence emission maxima at 680nm (Nussberger *et. al.* 1994), Lhca complexes have red-shifted maxima at 702nm (Lhca1 and Lhca2), 725nm (Lhca3) and 733nm (Lhca4) (Schmid *et. al.* 1997; Croce *et. al.* 2002b; Schmid *et. al.* 2002; Castelletti *et. al.* 2003). It was shown that Asn as a ligand for Chl A5 is required for the strong red-shifted absorption and emission of Lhca3 and Lhca4 (Morosinotto *et. al.* 2003). In Lhca5 the ligand for Chl A5 is a His, as in Lhca1 and Lhca2, and accordingly it does not contain low-energy Chls (Storf *et. al.* 2005).

The flexibility of the LHCI composition is a point of discussion. Ballottari *et al.* (Ballottari *et. al.* 2007) showed that the Lhca stoichiometry is not affected by growth conditions. Furthermore, studies on Lhca knock-out and anti-sense plants showed that the lack of one antenna subunit is not compensated by increased levels of other antenna subunits, thus suggesting a rigid LHCI organization (Ganeteg *et. al.* 2001; Klimmek *et. al.* 2005; Morosinotto *et. al.* 2005a). However, it has also been reported that the level of individual Lhcas can change, depending on the light condition (Bailey *et. al.* 2001; Tikkanen *et. al.* 2006).

To clarify this picture we combined biochemical analysis and electron microscopy (EM) single particle analysis to study PSI-LHCI complexes from Lhca-deficient lines (Δa) of *A. thaliana*. We show that the individual antennas (Lhca1-4) are not interchangeable, and that the absence of an antenna results in a “hole” in the PSI structure. There is one exception to this rule: Lhca4 can be replaced by

Lhca5 to yield PSI-LHCI particles with the same supramolecular organization as in WT plants.

Materials & Methods

Plant material – T-DNA knock-out (Δa1, Δa4) and anti-sense (Δa2 and Δa3) *Arabidopsis thaliana* (WT-col-0) plants (as described before, Ganeteg *et. al.* 2001; Ganeteg *et. al.* 2004b) were grown in a growing chamber at a day/night regime of 22 ^{o}C/19 ^{o}C, a photoperiod of 8h with a light intensity of 4000 lux and 70% relative humidity.

Isolation of PSI-LHCI – Thylakoids were isolated as described elsewhere (Croce *et. al.* 1996). PSI-LHCI isolation was modified from (Caffarri *et. al.* 2001). Thylakoid membranes were washed with 5 mM EDTA pH 8.0 and centrifuged for 10 min at 12000 *g*, 4 ^{o}C. The pellet was solubilized with 0.6% dodecyl-α-D-maltoside (α-DM) or dodecyl-β-D-maltoside (β-DM, see text), 10 mM tricine pH 7.8 at a final concentration of 0.5 mg Chl/ml and vortexed for 1 min. Unsolubilized material was removed by centrifugation at 12000 *g*, 10 min, 4 ^{o}C. The sample was loaded onto a 0.1-1 M sucrose gradient, and centrifuged for 22 h at 41000 rpm in a Beckman SW41 rotor. Fractions were harvested with a syringe, the lowest green band contained PSI-LHCI. This fraction was concentrated and diluted in a sucrose free buffer and loaded on a second gradient. The gradient was obtained by freezing and thawing a solution of 0.5 M sucrose, 0.06% α-DM and 10 mM tricine pH 7.8.

Electrophoresis and immunoblotting – A modified Laemmli SDS-PAGE system (Laemmli 1970) was used, as described in (Ballottari *et. al.* 2004). Non-denaturing Deriphat PAGE was modified from (Peter and Thornber 1991). The stacking gel contained 3.5% and the resolving gel 6% acrylamide (75:1 acrylamide/ bisacrylamide), polymerization was started by adding 0.03% ammonium persulphate and 0.1% TEMED, the running buffer contained 0.1% Deriphat-160. To investigate the stability of PSI-LHCI, the particles were solubilized prior to loading with 0.5% β-DM or 0.5% β-DM and 0.2% ZWITTERGENT 3-16 (ZG-16, Calbiochem) at a final Chl concentration of 0.2mg/ml, samples were vortexed for 1 min.

For immunoblot analysis, proteins were transferred to a nitrocellulose membrane (0.45μM, Millipore) using a Bio-Rad blot system. Primary antibodies against Lhca1-5 PsaD, PsbG and PsbK were from Agrisera (Sweden). The level of antibody binding was monitored with secondary goat anti-Rabbit IgG Alkaline Phosphatase antibody (Sigma-Aldrich) in combination with NBT/BCIP (AppliChem).

Electron Microscopy and Single Particle Analysis – Freshly prepared samples were dialyzed (Spectra/Por 12.000-14.000 MWCO dialysis membranes) for 2 to 4 h and negatively stained with 2% uranyl acetate on glow discharged carbon-coated copper grids. Electron microscopy was performed on a Philips CM120 electron microscope equipped with a LaB_6 tip, operated at 120 kV. Images were recorded with a Gatan 4000 SP 4K slow-scan CCD camera at 80000x magnification with a pixel size of 0.375 nm at the specimen level after binning the images. "GRACE" software was used for semi-automated specimen selection and data acquisition (Oostergetel *et. al.* 1998). Single-particles were selected with an 80x80 pixel frame and analyzed with the GRONINGEN IMAGE PROCESSING (GRIP) software package, with multi-reference procedures and multivariate statistical analysis and classification.

Pigment analysis – For pigment analysis a combined approach of HPLC and fitting the absorption spectra of the 80% acetone extract with the spectra of the individual pigments was used, as described before (Croce *et. al.* 2002a).

Absorption and Fluorescence Measurements – Absorption spectra were recorded at room temperature on a Varian Cary 4000 UV-Vis- spectrophotometer. Fluorescence spectra were recorded at 77K on a Fluorolog 3.22 spectrofluorimeter manufactured by Jobin Yvon-Spex. The bandwidth for excitation and emission was 3.5 nm. Spectra were corrected for wavelength-dependent sensitivity of the detector. Samples were diluted to OD 0.04 at the Q_y maximum in 66.7% (w/v) glycerol, 10mM tricine pH 7.8 and 0.03% α-DM.

Results

Purification of PSI-LHCI – In order to purify the PSI-LHCI complexes from Lhca-deficient plants, isolated thylakoids of WT and Δa1-Δa4 plants were mildly solubilized with 0.6% α-DM and subjected to sucrose density ultracentrifugation. Six pigment-containing bands were resolved (fig 1). The bands were identified by absorption spectroscopy and SDS-PAGE analysis (data not shown) as: free pigments (B1), monomeric light harvesting complexes (B2), trimeric LHCII (B3), LHCII-CP24-CP29 supercomplex (B4) and PSII core (B5). The lowest band (B6) was identified as PSI-LHCI with full (WT) or reduced (Δa1-Δa4) antenna size. In the gradient from Δa4 plants an additional band, identified as PSI core was present, in agreement with the reduced level of Lhca polypeptides in these plants (Ganeteg *et. al.* 2004a; Klimmek *et. al.* 2005).

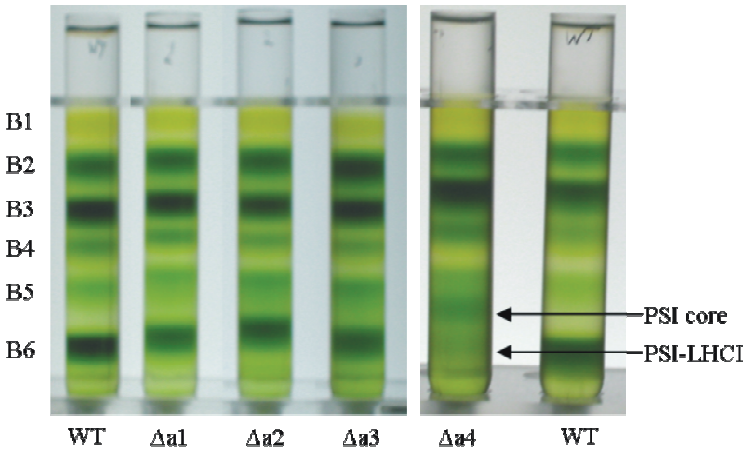

Figure 1: Sucrose gradient analysis of thylakoid membranes from WT, Δa1, Δa2, Δa3 and Δa4 plants solubilised with 0.6% α-DM. Six pigment containing bands were resolved, identified as: B1, free pigments, B2, Lhc monomers, B3, LHCII trimers, B4, supercomplex of LHCII trimer with CP24 and CP29, B5 PSII core and B6 PSI-LHCI. In the Δa4 gradient an additional band of PSI core was observed between PSII core and PSI-LHCI.

The PSI-LHCI fractions from all plants were slightly contaminated with PSII components, due to the presence of PSII supercomplexes resistant to the mild solubilization conditions. Therefore, the samples were concentrated and diluted in a sucrose-free buffer and loaded on a second gradient. This procedure resulted, for WT and Δa1-Δa3, in PSI preparations virtually free of PSII, only PSI-Δa4 remained slightly contaminated, due to the low abundance of PSI-LHCI compared to PSII.

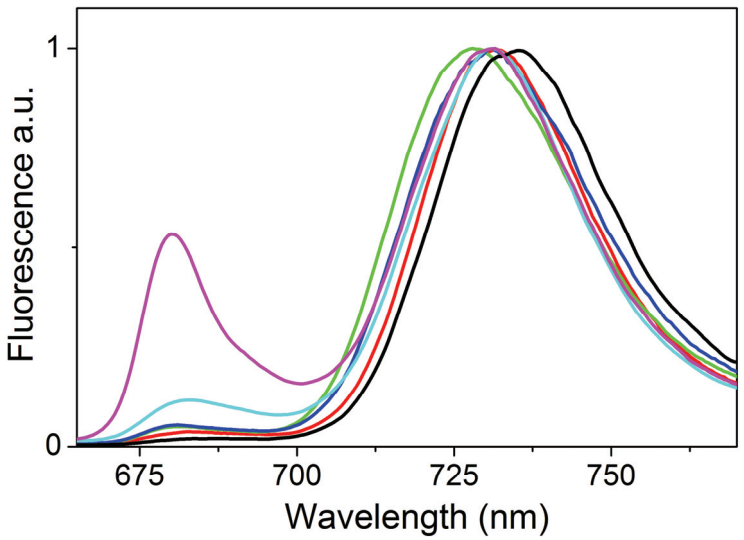

Figure 2: Low temperature fluorescence emission of PSI preparations. 77K emission spectra of PSI-LHCI from WT (black), Δa1 (red), Δa2 (green), Δa3 (blue) and Δa4 (magenta) plants. Excitation was at 475 nm, spectra are normalized to the red maximum. The fluorescence emission of PSI-Δa4 purified in β-DM is also reported (cyan).

To check the integrity of the preparations the fluorescence emission spectra were measured at 77K and they are reported in figure 2. PSI is characterized by the presence of low energy absorption forms, which act as an energy sink and are responsible for the red shifted fluorescence typical for the complex (Jennings *et. al.* 2003b). The absence in the complexes of significant fluorescence emission at

wavelengths shorter than 700 nm indicates that all Chls are connected to the red-forms, and thus that the complexes are functionally intact. Moreover, these data also confirm that the samples are not notably contaminated with PSII components, with the exception of PSI-Δa4, for which a relatively intense emission at 680 nm, typical for PSII, could be detected. After excitation at 475 nm the fluorescence emission maxima were at 735 nm for PSI-WT, 731.5 nm for Δa1, 728 nm for Δa2 and 731 nm for Δa3 and Δa4. For PSI-Δa1 and Δa2 the values are similar to those previously reported (Klimmek *et. al.* 2005), but for PSI-Δa3 and PSI-Δa4 the maxima are red-shifted by 4 and 11 nm respectively, indicating a higher amount of antennas associated to the core.

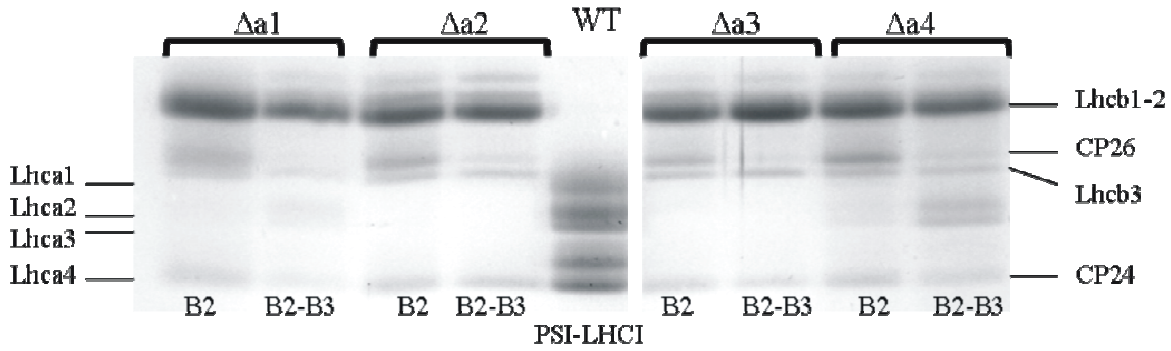

Figure 3: Analysis of B2 and B2-B3 from ΔLhca1-4 gradients. SDS-PAGE of monomeric antenna (B2) and the fraction between B2 and B3 (B2-B3) from the sucrose gradients of ΔLhca1-4 plants. The region of MW of Lhca and Lhcb antenna is shown. Identity of the bands is indicated.

Are Lhca antennas released upon thylakoid solubilization? – It was previously shown that in PSI of all Lhca–deficient lines the outer antenna is less strongly bound to the core as compared to the WT, resulting in the loss of Lhca complexes upon solubilization of the thylakoid membranes, whereas WT plants retained their antenna (Morosinotto *et. al.* 2005a). To investigate if a similar effect was also induced by our solubilization conditions, the gradient fractions in which monomeric (B2) and dimeric antenna complexes (B2-B3) are expected to migrate were analyzed. The presence of Lhca complexes in these fractions, strongly enriched in Lhcb antennas, was detected by absorption spectroscopy, taking advantage of the red absorption (above 700 nm) that characterizes the Lhca complexes and which is absent in Lhcb complexes (Croce *et. al.* 2002b). Increased absorption in the red as compared to WT, was observed for both fractions of the Δa4 lines and in small amount in the dimeric fraction of Δa1, indicating the presence of some Lhca complexes. This was confirmed by SDS-PAGE (fig 3), which reveals the presence of “free” Lhca2 and Lhca3. No traces of Lhca complexes could be detected in the WT and Δa2 and Δa3 fractions.

The results indicate that in our solubilization conditions, differently with respect to previous reports (Klimmek *et. al.* 2005; Morosinotto *et. al.* 2005a), PSI complexes from Δa2 and Δa3 lines and in first approximation from Δa1, can be purified without loss of external antenna components, as in the case of the WT. This allows to use these preparations to get quantitative data about the number of individual Lhca complexes present per PSI in the mutant plants.

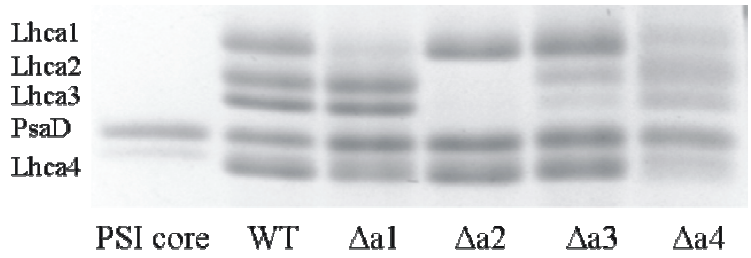

Figure 4: Analysis of Lhca content in PSI-LHCI of WT and ΔLhca1-4 plants. SDS-PAGE of PSI-LHCI purified from WT and ΔLhca1-4 plants, and PSI core. Region of the gel where Lhca1-4 and PsaD migrate is shown, the identity of the bands is from top to bottom: Lhca1, Lhca2, Lhca3, PsaD and Lhca4; note that one of the two isoforms of PsaD appears as a faint band at the level of Lhca4.

The release of Lhca2/3 from PSI of Δa4 plants indicates a weak association of these complexes in this mutant. However, the amount of "free" Lhca2 and Lhca3 in the Δa4 gradient is too low to explain the presence of the PSI core band in the gradient as the result of dissociation of PSI-LHCI. This clearly indicates that in the membranes of this mutant there is a population of PSI core complexes without antenna.

Lhca composition of PSI supercomplexes – To get quantitative information about the Lhca complexes coordinated to the core in the different PSI complexes, the samples were analyzed by SDS-PAGE (fig 4). In PSI from Δa1 plants (PSI-Δa1) a very small amount (<5%) of Lhca1 was still present, in agreement with the fact that the insertion is in the promotor region and not in the protein encoding region (Ganeteg *et. al.* 2004b). Lhca2 and Lhca3 were fully retained, while the amount of Lhca4 was reduced to ~60% of the WT level. Thus, in a substantial part of the PSI population Lhca4 is associated with the core in the absence of its partner, Lhca1. On the contrary, in Δa2 plants not only the level of Lhca2 (absent in this line as also assessed by western blotting), but also that of Lhca3 was reduced below the detection limits of Coomassie stain, suggesting that Lhca3 cannot be associated with the core in the absence of Lhca2. In this mutant the levels of Lhca1 and Lhca4 were not affected, indicating that the Lhca2/3 dimer is not necessary for the association of the Lhca1/4 dimer to the core. This result was confirmed by the analysis of PSI from Δa3 plants, in which the levels of Lhca1 and Lhca4 was also not affected. In these PSI particles there was some (<10%) residual amount of Lhca3 (probably due to re-expression in the anti-sense line used). However the level of

Lhca2 was about 35% of the WT level, thus indicating that, as it was the case of Lhca4, also Lhca2 can be bound to PSI without its partner. The analysis of PSI-LHCI from Δa4 plants was slightly complicated by the contamination of PSII components, due to similar migration behavior of Lhcb3 and Lhca1, and CP24 and Lhca4, and thus quantitative data could not be obtained (but see below). However, the SDS-PAGE shows the presence of Lhca2 and Lhca3 and of Lhca1, while Lhca4 was not detected (the faint band at the level of Lhca4 in the gel belongs to one of the isoforms of PsaD as assessed by western blotting). This is in line with the results of the western blotting on the thylakoids which shows the presence of Lhca1 in this mutant, although at levels lower than in the WT, and no traces of Lhca4 (data not shown).

We also checked the presence of PsaG and PsaK, which have been suggested to interact and stabilize the binding of dimer Lhca1/4 and Lhca2/3 respectively (Jensen *et. al.* 2000; Varotto *et. al.* 2002; Ben-Shem *et. al.* 2003). The immunoblotting shows that these two subunits are present at the same level as in the WT in the absence of their neighboring dimer (see supplementary information).

Supramolecular organisation of Lhca-deficient PSI particles – To reveal the supramolecular organization of the PSI complexes from WT and Δa1-Δa4 plants, electron microscopy was performed. Micrographs of negatively stained particles were recorded and PSI projections were selected. The obtained data-sets were analyzed by single particle analysis, including multi-reference alignments, multivariante statistical analysis and classification.

In figure 5 the projection views are presented with the same orientations and handedness as PSI in the PSI-LHCII complex, based on the correlation with the specific features of the PSI core, clearly visible in the projections as white features. In these projections PSI is viewed from the stromal side, and PsaK is located on the right side of the complex (Kouril *et. al.* 2005).

The top-view projection of WT PSI is in good agreement with the crystal structure (fig 5-A (Amunts *et. al.* 2007)). For PSI-Δa1 two types of particles could

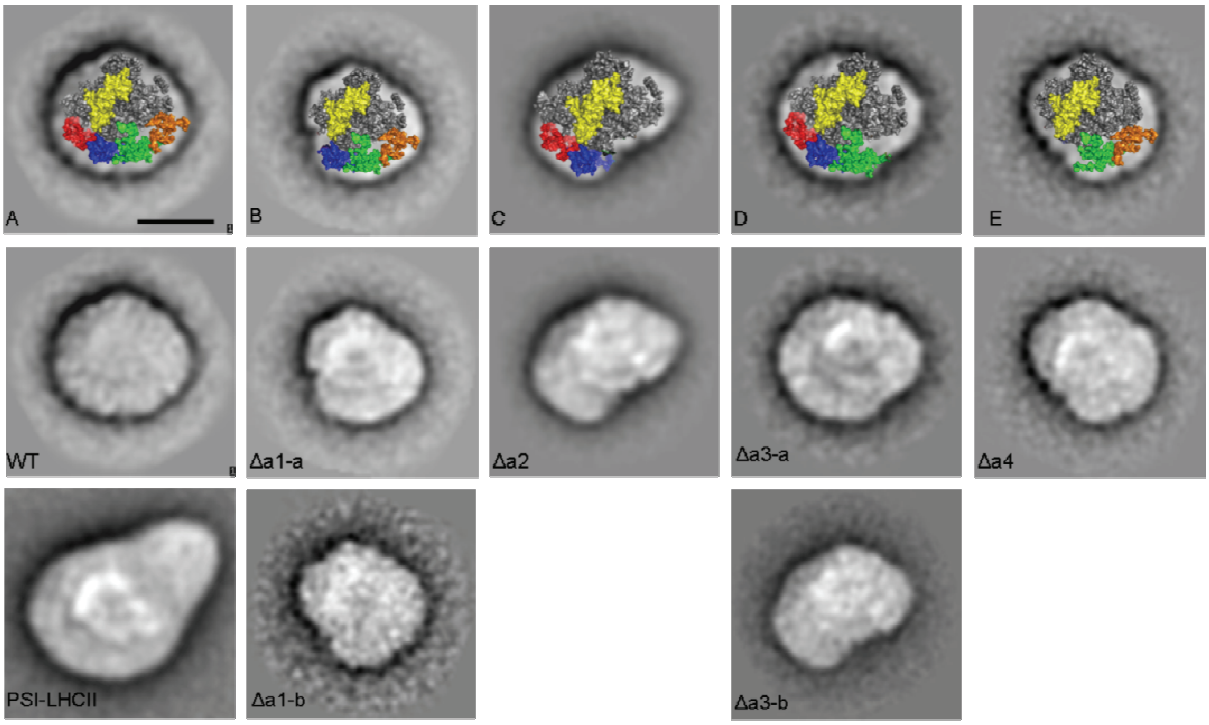

Figure 5: Electron microscopy analysis of PSI with different LHCI compositions. Figure A-E are top-views of the crystal structure (Amunts *et. al.* 2007) overlaying the projections of PSI-LHCI (A), PSI lacking Lhca1 (B), PSI lacking the Lhca2/3 dimer (C), PSI lacking Lhca3 (D), and PSI lacking the Lhca1/4 dimer (E). PsaC and PsaE are presented in yellow, Lhca1 in red, Lhca2 in green, Lhca3 in orange and Lhca4 in blue. All projections are viewed from the stromal side. Averaged images of PSI from WT, Δa1-Δa4 plants are presented, and, for comparison, a PSI-LHCII complex (Kouril *et. al.* 2005). Images are sums of 765 (WT), 768 (WT PSI-LHCII), 775 (Δa1-a), 64 (Δa1-b), 1317 (Δa2), 212 (Δa3-a), 217 (Δa3-b) and 648 (Δa4) aligned projections. The scale bar equals 10nm.

be observed: Δa1-a, which was the most abundant, and Δa1-b. In the former, absence of a protein density is observed on the left side of the complex, and it can account for the lack of Lhca1. The low abundance of Δa1-b particles resulted in a low-resolution image, but still it is clear that the loss of protein density is more severe in these particles, accounting for the lack of the Lhca1/4 dimer in agreement with the SDS-PAGE analysis, which revealed a decreased level of Lhca4 in this preparation.

The PSI-Δa2 particle shows a loss of density, with a size of two Lhca complexes, at the right side of the complex. For PSI from ΔLhca3 plants, two particles were found, with either three (Δa3-a) or two (Δa3-b) outer antenna complexes bound to the core. The density absent in both particles is assigned to Lhca3, in agreement with the SDS-PAGE, while the one only present in Δa3-a, is assigned to Lhca2. In the PSI-Δa4 preparation a particle identical to Δa1-b was observed, corresponding to PSI supercomplexes lacking the Lhca1/4 dimer. Taken together, these results show that the order of the outer antenna complexes,

starting from the G-pole, is Lhca1, Lhca4, Lhca2, Lhca3, confirming the assignment of Amunts et al. (2007), see also fig 5A-E. Furthermore, the EM image clearly shows the presence of Lhca2 and Lhca4 associated with the core in the absence of their dimeric partner, in agreement with the SDS PAGE results.

Stability of PSI-LHCI complexes with reduced antenna sizes – In order to compare the stability of PSI-LHCI from WT and Δa1-Δa4 lines and to assess the strength of the association to the core of the individual Lhca complexes, the particles were subjected to different detergent treatments and analyzed by non-denaturing PAGE (fig 6). Treatment of the PSI particles with β-DM had the smallest effect on the WT preparation: only a small band of PSI with reduced antenna size was observed, but no PSI core was detected, indicating only limited and partial loss of the external antenna. A band corresponding to the PSI core could be detected for all mutants. This band was faint for PSI-Δa3 and its intensity was slightly higher for PSI-Δa2, increased for PSI-Δa1, and even more for PSI-Δa4. This indicates that the stability of PSI-LHCI is mostly affected when Lhca4 is lacking, as previously suggested (Morosinotto *et. al.* 2005a). Under the strongest solubilization conditions (DM plus zwittergent) all PSI particles lost most of their antenna. However, the PSI-WT complex was slightly more resistant to the detergent treatment compared to the Lhca-deficient complexes. In summary, these results demonstrate that PSI-LHCI of Δa2 and Δa3 plants is almost as stable as that of the WT, while the stability of PSI from Δa1 plants is more affected by the detergent, the strongest destabilization is observed for PSI-Δa4. This indicates that the Lhca1/4 dimer has a stronger association with the core than the Lhca2/3 dimer, in agreement with the release of this dimer (in PSI-Δa1 and PSI-Δa4) after very mild solubilisation of the thylakoids.

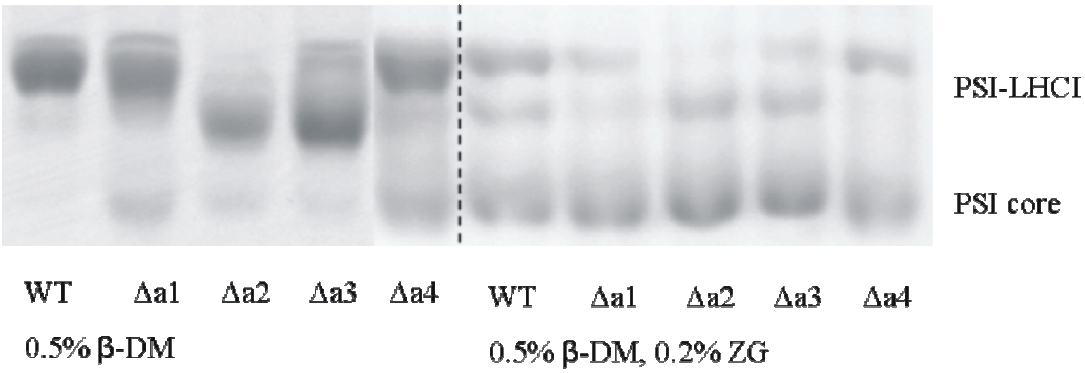

Figure 6: Stability analysis of PSI-LHCI from WT and ΔLhca1-4 plants. Non-denaturing Deriphat-PAGE of PSI from WT and ΔLhca1-4 plants under two conditions: (i) solubilised with 0.5% β-DM, or (ii) with 0.5% β-DM and 0.2% ZG-16 at a final Chl concentration of 0.2mg/ml. Section of gel where PSI migrates is shown. Position of PSI with antenna (PSI-LHCI) and PSI core are indicated.

Lhca5 is associated with PSI-LHCI in Δa4 plants – Surprisingly, after detergent treatment a green band with molecular weight similar to that of the WT complex was still present for PSI-Δa4 (fig 6), suggesting that part of the population of PSI-Δa4 is very resistant to detergent treatment.

To obtain a preparation enriched in these particles we repeated the PSI-LHCI purification from Δa4 plants with a modified procedure using β-DM instead of the milder α-DM. This had the additional advantage that the preparation was almost free of PSII contamination, as the analysis of the fluorescence emission spectrum confirms (fig 2), allowing to obtain quantitative data about the Lhca composition also of this mutant, see figure 7-A. The SDS page shows that Lhca2 and Lhca3 are retained and Lhca1 is present as for the preparation in α-DM, interestingly an additional band was observed in between Lhca1 and Lhca2. This band was identified by immunoblotting as Lhca5 (fig 7-B). The fact that Lhca5 was detectable on a gel, indicates that the β-DM PSI-Δa4 preparation is strongly enriched in this subunit. Further immunoblotting analysis showed that the level of Lhca5 in this preparation and in PSI-Δa1 is ~200 and 10 times higher respectively compared to PSI-WT (see supplementery information).

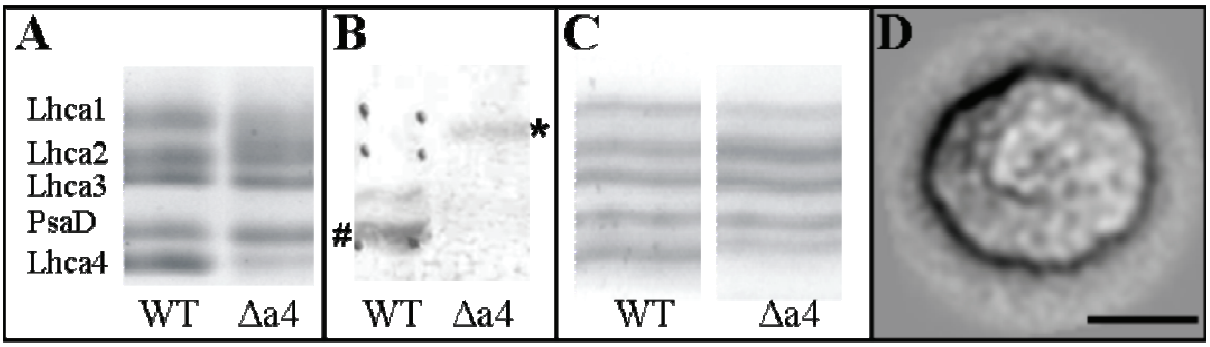

Figure 7: Analysis of PSI-LHCI from Δa4 plants, isolated using β-DM. A and C: SDS-PAGE analysis of Lhca composition of PSI-LHCI from WT and Δa4 plants. B: Immunoblot detection of PsaD (#) and Lhca5 (*) in PSI-LHCI of WT and Δa4 plants, respectively 7 and 0.32 µg Chl was loaded. D: Top-view projection of PSI-LHCI particle from Δa4 plants, the image is the sum of 2783 aligned projections.

Small variations in the gel preparation resulted in slight changes in the Lhca migration behavior. Figure 7-C shows the Lhca region of a second gel. Here Lhca5 overlaps with Lhca2, but Lhca1 is fully separated and can be quantified showing that it is almost completely (>90%) retained in this preparation.

To determine the location of the Lhca5 complex, the β-DM PSI-Δa4 particles were analyzed by EM. The analysis revealed that the preparation was highly homogeneous and was composed of particles practically identical to those of PSI-WT (fig 5-WT) revealing that four Lhca antenna subunits were present. The total absence of Lhca4 in this line (as assessed by western blotting) and the presence of

high levels of Lhca1 and of Lhca5 in this preparation suggest that Lhca5 substitutes Lhca4 in these complexes and forms a heterodimer with Lhca1.

Pigments composition – The pigment composition of the purified PSI complexes was analyzed. The results are presented in table 1. It is known that the Lhca complexes coordinate xanthophylls, β-carotene, Chl *a* and Chl *b* (Croce *et. al.* 2002b; Schmid *et. al.* 2002), while the PSI core coordinates only Chl *a* and β-carotene (Jordan *et. al.* 2001). In full agreement, the Lhca–depleted PSI complexes have decreased relative amounts of Chl *b* and xanthophylls, while the relative level of β-carotene is increased as compared to the WT. Note that the Chl *a/b* ratio of all Lhca-lacking PSI are lower than in a previous report (Klimmek *et. al.* 2005) indicating that the amount of antenna in our preparations is higher. The difference is particularly large for PSI-Δa4 which has a Chl *a/b* ratio of 10.8 in our preparation, while it was 18 and 32 in previous reports (Klimmek *et. al.* 2005; Morosinotto *et. al.* 2005a), indicating that these preparations contained mainly PSI core.

Table 1: Pigment analysis of PSI-LHCI complexes differing in antenna composition. For Δa4 the α-DM preparation is reported. The number of the carotenoids is normalized to 100 Chls. SD for four measurements is: Chl/Car < 0.1, Chl *a/b* < 0.4. SD in the Cars determined for two preparations is less than 0.3.

	Chl a/b	Chl/Car	n. Vio	n. Lut	n. β-car
WT	9.7	4.8	2.3	5.5	13.1
Δa1	10.8	5.0	1.6	4.8	13.6
Δa2	11.1	5.1	1.7	3.8	14.1
Δa3	11.1	5.0	2.0	4.3	13.7
Δa4	10.8	5.1	1.5	4.1	14.0

Discussion

In this work we analyze the PSI-LHCI from *A.thaliana* lines depleted in individual Lhca proteins in order to investigate the role of the subunits in the supramolecular organization of PSI. The new purification procedure used and the possibility to perform biochemical analysis and electron microscopy on the same preparations allows to relate variations in the protein composition to changes in the supramolecular organization and to obtain a comprehensive picture of the overall organization and stability of the PSI supercomplex.

Lhca1,2,3 and 4 have a fixed position in the PSI structure and are NOT interchangeable – It has been suggested that the level of Lhca complexes (Bailey

et. al. 2001) or at least of Lhca4 (Tikkanen *et. al.* 2006) changes depending on the growth conditions, although a more recent report shows that the level of the individual Lhca complexes is fixed to 1 per core in different light conditions (Ballottari *et. al.* 2007). A change in the antenna composition can occur in two ways: 1) extra dimers can be associated with the supercomplex; this is clearly not the case in our growing conditions, but we can not exclude the presence of extra dimers in other specific light conditions; 2) different subunits can occupy the same position in the structure. This is apparently not the case. The EM analysis clearly shows that each Lhca complex (type 1-4) has a specific binding site. The absence of an antenna complex resulted in a "hole" in the structure of PSI at the position, which in the WT is occupied by this complex, while the supramolecular organization of the rest of the complex remained the same. This suggests a very rigid organization of LHCI, with specific interactions between the individual Lhca types and their partners in the core and in the antenna. This is unlike the situation in Photosystem II for which it has been shown that in the absence of the two main subunits of the LHCII trimer (Lhcb1 and Lhcb2), CP26, which is monomeric in WT plants, forms trimers which perfectly substitute the LHCII trimers, leading to an overall organization of the Photosystem II supercomplex which is virtually indistinguishable from that of the WT (Ruban *et. al.* 2003).

The results also suggest that Lhca complexes only form heterodimers. This was already clear for Lhca1/4 (Schmid *et. al.* 1997), but the impossibility to purify Lhca2 and Lhca3 to homogeneity (Croce *et. al.* 2002b) and to obtain dimers by *in vitro* reconstitution (Schmid *et. al.* 2002), had led to different suggestions about the organization of these two subunits (Castelletti *et. al.* 2003; Amunts *et. al.* 2007). In the case that Lhca2 and Lhca3 would be able to form homodimers, we would have expected to detect particles with the full antenna complement in Δa2 and Δa3 plants, while this was not the case.

…but Lhca5 can replace Lhca4 in the supercomplex – Although the results clearly show that the different Lhca types (Lhca1-4) are not interchangeable, an exception to this rule exists: in the Δa4 line, totally lacking Lhca4, we were able to purify a small population (around 1%, normalized to the amount of PSI core) of PSI supercomplexes with the full antenna complement. These particles comprise Lhca1, Lhca2, Lhca3 and Lhca5, most likely as Lhca1/5 and Lhca2/3 dimers. This is supported by a mass-spectrometry study where Lhca5 was detected in the LHCI-730 fraction, suggesting an interaction with Lhca1 or Lhca4 (Storf *et. al.* 2004) and by the *in vitro* reconstitution results, which showed that the Lhca1/5 dimer can be obtained (Storf *et. al.* 2005). This novel PSI-Lhca1/5-Lhca2/3 complex is as stable as the WT complex, indicating that Lhca5 is a perfect substitute for Lhca4 in the

assembly of the system. It is thus likely that Lhca5 can also replace Lhca4 in PSI-LHCI from WT plants. The sequence identity between Lhca5 and Lhca4 is very high (Jansson 1999), suggesting that the the regions necessary for the interaction with the core complex are conserved in these two proteins. Interestingly, Lhca5 does not contain red forms (Storf *et. al.* 2005), which are present in Lhca4. Therefore, the tuning of Lhca5 expression could be important for optimal light-harvesting in varying light conditions. Previous studies have addressed the effect of light intensity on Lhca levels (Bailey *et. al.* 2001; Ganeteg *et. al.* 2004a; Tikkanen *et. al.* 2006; Ballottari *et. al.* 2007). However, in light of the different absorption properties of Lhca4 and Lhca5 it would be interesting to study the effect of light quality on the *Lhca5* expression and protein levels.

Role of the individual Lhcas in the assembly and stability of the supercomplex – The analysis of the structure of PSI-LHCI suggests that the interactions of Lhca complexes with the core are stronger at the G-pole than at the K-pole and that Lhca1 acts as an anchor point for facilitating the binding of other Lhca subunits (Amunts and Nelson 2008). In contrast biochemical analysis of Lhca-depleted plants suggested that Lhca4 is the key unit for the assembly of the antenna system around the core (Klimmek *et. al.* 2005; Morosinotto *et. al.* 2005a). Indeed, PSI purified from Δa4 was shown to consist mainly of core complexes (Ihalainen *et. al.* 2005b; Klimmek *et. al.* 2005; Morosinotto *et. al.* 2005a). It has been proposed that the low level of the other Lhca proteins in this mutant is influenced by post-translational events and is related to the stability of the proteins (Ganeteg 2004; Klimmek *et. al.* 2005). Our analysis shows that PSI core particles depleted in their outer antenna are present in the membranes of the Δa4 mutant. However, in contrast to previous results (Klimmek *et. al.* 2005; Morosinotto *et. al.* 2005a), in addition to the core, two other PSI populations were observed: PSI-Lhca2/3 and PSI-Lhca1/5-Lhca2/3. Moreover, in the Δa1 mutant, the levels of Lhca2 and Lhca3 are identical to those in the WT with 1 to 1 ratio with the core, although in 40% of the complexes Lhca4 is absent. This means that Lhca4 is not strictly required for the assembly of Lhca2/3 onto the core. Therefore, it seems that the very low level of Lhcas in Δa4 plants is not only related to the lower stability of the complex, but also to alterations at the protein expression level.

The data clearly shows that the Lhca1/4 dimer is interacting with the core more strongly than the Lhca2/3 dimer. Moreover, in the Δa2 mutant the PSI population (PSI core-Lhca1/4) is highly homogeneous, indicating that Lhca1/4 does not need Lhca2/3 for the assembly. The same is true for the Lhca2/3 dimer, although in this case the presence of Lhca1/4 or at least of Lhca4 stabilizes the binding of Lhca2/3 to the core via interaction of Lhca2 with Lhca4. The same

interactions are probably at the origin of the fact that, in contrast to a previous proposal (Morosinotto *et. al.* 2005a), both these subunits (Lhca2 and 4) can be stably associated with the core in the absence of their "dimeric partners". It seems to be a general rule that the stable association of an antenna complex in the photosynthetic supercomplexes needs interactions with at least two partners (Caffarri *et. al.* 2009). This can explain why it is possible to observe particles with Lhca4 or Lhca2 in the absence of their dimeric partners, but never with Lhca1 and Lhca3, which are located at the periphery of the half ring and already in the WT interact only with the core and one Lhca subunit.

Functional organization of the Lhca complexes – It is known that in PSI there are at least three Chl clusters which emit in the red, two of them are associated with the outer antenna complexes, in particular to Lhca3 (725 nm), Lhca4 (733 nm) and one to the core complex (720 nm) (Schmid *et. al.* 1997; Croce *et. al.* 1998; Croce *et. al.* 2002b; Schmid *et. al.* 2002; Castelletti *et. al.* 2003).

The fluorescence emission of PSI-WT has its maximum at 735 nm. Excitations at 440 nm and 475 nm, which lead to a different initial distribution of the excitation energy in the core and in the outer antenna (van Oort *et. al.* 2008), show no difference, indicating that even at low temperature the red forms of the core are transferring energy to the antenna. The emission spectrum of PSI-Δa4, which is highly enriched in PSI-Lhca2/3 dimer, shows no dependence on the excitation wavelength, indicating that the red forms of the core are still able to transfer to the antenna. As already reported (Klimmek *et. al.* 2005), this is not the case for PSI-Δa2 which shows an emission maximum at 728 nm for 475 nm excitation and at 725 nm for 440 nm excitation. It was suggested that excited core pigments cannot efficiently transfer excitation energy to the red pigments of the antenna and thus that this spectrum is the sum of two contributions: the red forms of the core and the red-forms of Lhca4. Indeed, the fluorescence spectra can be decomposed in the spectra of the PSI core and WT PSI-LHCI (data not shown). Based on these observations it can be suggested that the red forms of the core can equilibrate with those of the Lhca2/3 dimer, but not with those of Lhca1/4. Considering (i) the large energetic distance between the red forms and the bulk Chls and (ii) at low temperature the thermal energy is not sufficient to drive the energy transfer from the red forms to the bulk, it is likely that the low energy forms of the core are located in close proximity to the red forms of Lhca3.

The analysis of PSI-Δa4 allows the determination of the emission maximum of native Lhca3 associated to the core. The emission maximum of PSI-Δa4 is at 731 nm and it can be ascribed to Lhca3, which is the red-most emitter in this complex. However, based on the data of reconstituted complexes, the emission of Lhca3 is

expected at 725 nm (Castelletti *et. al.* 2003). Hence, the emission of native Lhca3 in the PSI complex is about 6 nm more to the red than for the *in vitro* refolded monomeric complex. This is supported by the analysis of absorption spectra which suggest that the red forms of Lhca3 associated with PSI absorb more to the red than in the reconstituted sample (Klimmek *et. al.* 2005). Indeed, the red forms are generated by interaction between two Chls (Morosinotto *et. al.* 2003) and a small change in the structure can easily account for a large change in the energy of these forms. Probably the docking of Lhca3 onto the core is stabilizing the most-red conformation.

The steady-state LT fluorescence emission experiments provided us with information about the properties of the individual Lhca antenna in the complex. A thorough time-resolved fluorescence study on these highly pure and well-characterized PSI particles is promising to increase our understanding of the energy transfer processes taking place in PSI-LHCI.

Acknowledgments

We would like to thank Dr. W. Keegstra for excellent technical support. This work is supported by the Council for Earth and Life sciences of the Nederlandse Organisatie voor Wetenschappelijk Onderzoek via a VIDI grant to R.C.

Supplementary Information

SI 1. PsaG and PsaK levels in absence of the neighboring antenna complex. Immunoblot detection of PsaG and PsaK in PSI-Δa1 and PSI-Δa2, respectively, compared to PSI-WT. Amount of Chl loaded as indicated.

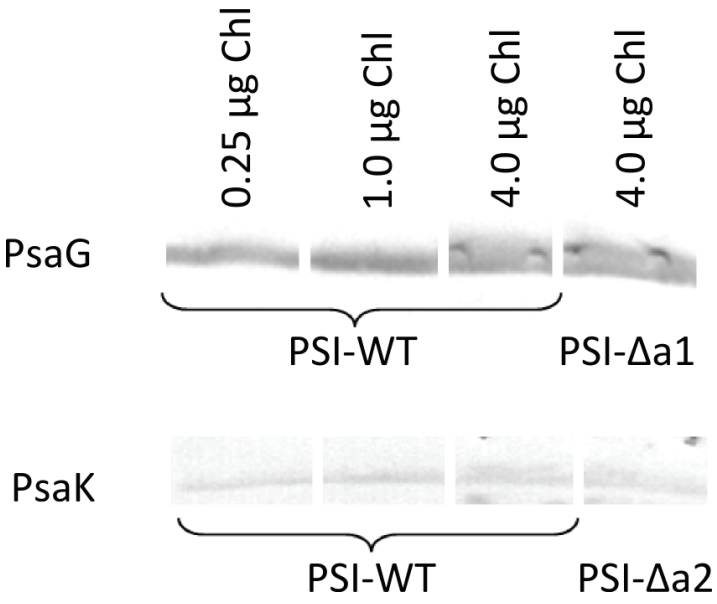

SI 2. Lhca5 levels in PSI-Δa1 and PSI-Δa4 compared to PSI-WT. Immunoblot detection of Lhca5 in PSI-Δa1, PSI-Δa4 and PSI-WT. Amount of Chl loaded as indicated.

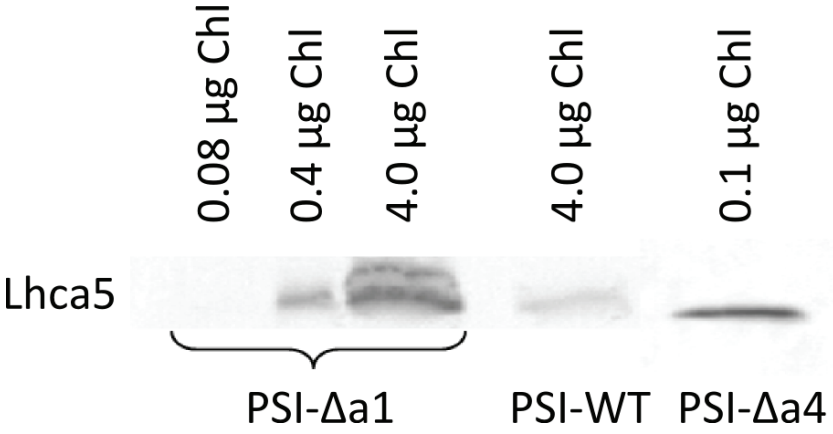

Chapter 3

The light-harvesting complexes of higher plants Photosystem I: Lhca1/4 and Lhca2/3 form two red-emitting heterodimers

Emilie Wientjes and Roberta Croce

This chapter is based on:

Biochemical Journal (2011) 433:477-485.

Abstract

The outer antenna of higher plants Photosystem I is composed of four complexes (Lhca1-4). Difficulties in their purification have so far prevented the determination of their properties. In this work we were able to purify the native complexes, showing that Lhca2/3 and Lhca1/4 form two functional heterodimers. Both dimers show red fluorescence emission with maxima around 730 nm, as in the intact PSI complex. This indicates that the dimers are in their native state and that LHCI-680, which was previously assumed to be part of the PSI antenna, does not represent the native state of the system. The data show that the light-harvesting properties of the two dimers are functionally identical, concerning the absorption, the long-wavelength emission and the fluorescence quantum yield, while they differ in their high light response. The properties of the native dimers were compared with those of the reconstituted complexes, showing that the latter represent excellent "replicas". Implications of the present results for the understanding of the energy transfer process in PSI are discussed.

Introduction

In the first steps of photosynthesis light energy is captured and converted into chemical energy. In higher plants and algae this process takes place in the thylakoid membrane, where

Photosystem II (PSII) and Photosystem I (PSI) work in concert with cytochrome b_6f and ATP-synthase to harvest the light and store its energy by generating ATP and NADPH.

Higher plant PSI is a multi-protein-pigment complex, composed of two moieties: the core and the peripheral light-harvesting antenna (LHCI). The core complex harbours the reaction centre (RC), all the electron transport cofactors, ~100 Chlorophylls (Chl) *a* and ~22 β-carotenes (Jordan *et. al.* 2001; Amunts *et. al.* 2007). LHCI coordinates Chl *a,* Chl *b,* and the carotenoids (Car) β-carotene, violaxanthin, and lutein (Croce and Bassi 1998). It is composed of four light-harvesting complexes (Lhc), called Lhca1-4. The Lhca proteins are encoded by the Lhc gene family, which also encoded the Lhcb antenna complexes of PSII. All Lhcs show high sequence conservation, with 43-55% sequence identity between the different Lhcas and up to 75% sequence homology (Jansson 1999). The Lhcas are located on one side of the core and are assembled into two dimers: Lhca1/4 and Lhca2/3 (Boekema *et. al.* 2001; Ben-Shem *et. al.* 2003). It has been suggested that under certain growth conditions Lhca2 and Lhca3 might be able to form homodimers (Amunts *et. al.* 2007). However, it has been shown that all four Lhca

proteins are present in a one to one ratio with the PSI core under standard (Ballottari *et. al.* 2004) and high- and low-light conditions (Ballottari *et. al.* 2007), in agreement with the exclusive presence of a heterodimeric Lhca2/3 complex.

The main function of LHCI is to harvest light and transfer the excitation energy to the RC, where it is used for charge separation. In addition, it has been shown that the LHCI moiety is the first target of high-light damage of PSI-LHCI, thereby protecting the core complex against photodamage (Hui *et. al.* 2000; Andreeva *et. al.* 2007; Alboresi *et. al.* 2009).

A peculiar feature of PSI is the presence of red forms: Chls that absorb at energy lower than that of the primary electron donor P700 and which have extremely broad and red-shifted fluorescence emission spectra (Gobets and van Grondelle 2001). They are conserved in plants, algae and bacteria. Still, their function is not fully understood. It has been suggested that they: (i) focus the energy to the primary electron donor, (ii) have a role in protection against light-stress, or (iii) absorb light efficiently in a dense vegetation system where light is enriched in wavelengths above 690 nm (Trissl 1993; Rivadossi *et. al.* 1999). It is shown that the red forms have an important effect on the excitation energy transfer of PSI (Gobets and van Grondelle 2001; Jennings *et. al.* 2003; Ihalainen *et. al.* 2005b). Being at low energy these Chls have a high probability to be populated (Croce *et. al.* 1996) and their excitation energy must be transferred energetically up-hill to P700, in order to be used for photochemistry (Jennings *et. al.* 2003). In higher plants the red forms are associated with LHCI. Although several studies have analysed the trapping kinetics in PSI, no general agreement has been reached (Ihalainen *et. al.* 2005b; Slavov *et. al.* 2008; van Oort *et. al.* 2008). This is mainly because PSI is a very large and complex system and little information is at present available about the properties of the individual PSI building blocks (e.g. Lhca dimers). This information is necessary to be able to disentangle the contribution of the individual complexes from the analysis of the whole system.

In the past, LHCI was often separated into two fractions upon isolation: LHCI-680 and LHCI-730, named after their low temperature at 77K (LT) fluorescence emission maxima (Lam *et. al.* 1984; Bassi and Simpson 1987; Knoetzel *et. al.* 1992; Tjus *et. al.* 1995; Schmid *et. al.* 2002). LHCI-680 lacks the red-shifted emission, and consists mainly of monomeric Lhca2 and Lhca3, while LHCI-730 is strongly enriched in the Lhca1/4 heterodimer (Knoetzel *et. al.* 1992; Tjus *et. al.* 1995; Schmid *et. al.* 2002). Based on these results it was assumed that only the Lhca1/4 dimer contains “red” Chls. However, the LT 680nm fluorescence was absent in preparations containing all four Lhca complexes in their native dimeric form (Croce *et. al.* 1998; Ihalainen *et. al.* 2000). Furthermore, dimeric fractions enriched in Lhca1/4 or Lhca2/3 both showed a red-absorption tail with similar

amplitude, indicating that red forms are also present in Lhca2/3 (Croce *et. al.* 2002b).

Due to the very similar properties of the two dimeric LHCI complexes, full separation has not been achieved yet and most of the available information on the individual Lhca complexes was obtained by *in vitro* reconstitution of monomeric Lhca1-4 and dimeric Lhca1/4 antenna complexes (Schmid *et. al.* 1997; Croce *et. al.* 2002b; Schmid *et. al.* 2002; Castelletti *et. al.* 2003). The LT fluorescence emission maxima were found at: 690nm (Lhca1), 702nm (Lhca2), 725nm (Lhca3), and 733nm (Lhca4) (Schmid *et. al.* 1997; Croce *et. al.* 2002b; Castelletti *et. al.* 2003). It has been shown that the red forms in the Lhca complexes originate from a strongly excitonically coupled Chl dimer, involving Chl603 and Chl609 (nomenclatur as in Liu *et. al.* 2004). It has also been demonstrated that an asparagines as ligand for Chl603, as it is in Lhca3 and Lhca4, is needed for this strong coupling. If this asparagine is mutated into a histidine, which is the ligand for Chl603 in all other Lhc family-members, than the red-forms are abolished (Morosinotto *et. al.* 2002; Morosinotto *et. al.* 2003; Croce *et. al.* 2004; Morosinotto *et. al.* 2005b; Mozzo *et. al.* 2006). To account for the extreme red-shift and the broad fluorescence emission spectra it was suggested that the lowest exciton state of the dimer mixes with a charge-transfer state (Ihalainen *et. al.* 2003; Ihalainen *et. al.* 2005a; Croce *et. al.* 2007a), which was recently demonstrated to be correct in the case of Lhca4 monomers (Romero *et. al.* 2009).

In this work we purified and fully characterized the Lhca2/3 and Lhca1/4 heterodimers, obtaining a complete picture of their biochemical, spectroscopic and functional properties, thus opening the way to a full understanding of the excitation energy transfer in PSI. We also show that LHCI-680 is not a native state of the antenna complexes of PSI. Finally, the availability of native purified complexes allows for a comparison with the recombinant antenna complexes.

Materials & Methods

Plant material – The WT, Lhca1 T-DNA knock-out (Δa1) and Lhca2 anti-sense (Δa2) *Arabidopsis thaliana* (WT-col-0) plants (described before in Ganeteg *et. al.* 2001; Ganeteg *et. al.* 2004) were grown at a day(8h)/night(16h) regime of 22 ^{o}C/19 ^{o}C, with a light intensity of 130μE m^2 s^{-1} and 70% relative humidity.

LHCI isolation and analysis – Thylakoids were isolated as described elsewhere (Bassi and Simpson 1987). PSI-LHCI isolation was as described in (Wientjes *et. al.* 2009). LHCI isolation was adapted from (Croce *et. al.* 1998). In short: PSI-LHCI with a Chl concentration of 0.3mg/ml was solubilised with 1% n-dodecyl-β,D-maltoside

(β-DM) and 0.5% Zwittergent-16. After 1 min of vortexing, the sample was loaded onto a 0.1-1M sucrose gradient, containing 10mM tricine, pH 7.8 and 0.03% β-DM and centrifuged at 41.000rpm for 22h in a Beckman SW41 rotor. The fractions were analysed by a modified Laemmli SDS-PAGE system and Coomassie staining, as described in (Ballottari *et. al.* 2004). Quantities loaded on a Chl basis were: 3µg PSI-LHCI, 1µg dimeric fraction of solubilised PSI-WT and 0.5µg for the dimeric fraction of PSI-Δa1 and Δa2. Quantification of Coomassie stain was done as described in (Ballottari *et. al.* 2004) after digitizing the gel with a Fujifilm LAS 3000 scanner. Immunoblot was done as described in (Wientjes *et. al.* 2009). Pigment analysis was done as in (Croce *et. al.* 2002a).

Steady-state spectroscopy – Absorption spectra were recorded on a Varian Cary 4000UV-Vis-spectrophotometer. For 77K measurements a home-built liquid N_2 cooled low-temperature device was used. Fluorescence spectra were recorded at 77K and 283K on a Fluorolog 3.22 spectrofluorimeter (Jobin Yvon-Spex). Samples were diluted to an OD of 0.04cm^{-1} at the Q_y maximum. Circular-dichroism (CD) spectra were recorded at 283K on an AVIV 62ADS spectropolarimeter. All measurements were performed in 10mM tricine pH 7.8, 0.03% α-DM and 0.5M sucrose (room temperature (RT) and 283K) or 67% (w/v) glycerol for 77K measurements.

Fluorescence quantum yield – Fluorescence quantum yields (Φ_{Fl}) at 283K were calculated by dividing the ratio of integrated fluorescence intensities on a wavenumber scale by the ratio of their total absorption factor (1- Transmission) for the spectral region around 630nm, where the sample was excited. The emission of Chl *a* in acetone, with Φ_{Fl} = 0.30 (Weber and Teale 1957) was used as a reference.

Photobleach assay – Lhca dimers were illuminated for 20 minutes in the presence of oxygen at RT with a Schott 200 cold white light source at stage 3, giving a light intensity of 5.5mE m^2 s^{-1}. Light was passed through a 1cm water filter. Samples in a 4x10mm cuvette, with an initial optical density at Q_y maximum of 0.3 in the light path of 4mm, were homogenized every 2 minutes. Control samples were kept at RT in the dark for 20 minutes. Samples were concentrated, loaded on a 0.1-1M sucrose gradient and centrifuged at 44.000rpm for 19h in a Beckman SW60 rotor.

Results

Isolation of the native LHCI dimers – LHCI of wild type (WT) plants is suggested to be composed of two dimers: Lhca2/3 and Lhca1/4 (Ben-Shem *et. al.* 2003). However, homogeneous purification of these dimers has never been achieved from PSI-WT because of the highly similar properties of the complexes (Croce *et. al.* 2002b). It has been shown recently (Wientjes *et. al.* 2009) that PSI complexes coordinating only Lhca2/3 or Lhca1/4 can be obtained from plants lacking either Lhca1 or Lhca2 (Δa1 and Δa2 *Arabidopsis* mutants). These preparations thus represent a good starting point for the homogeneous preparation of each dimer. PSI-Δa1, Δa2 and WT were solubilised and subjected to sucrose gradient density ultracentrifugation (fig 1A). Five pigment-containing fractions were obtained and identified by their mobility in the gradient, SDS-PAGE and absorption spectroscopy (data not shown) as: free pigments, dimeric Lhca, PSI core, and PSI supercomplexes with reduced (PSI-LHCI*) or with full (PSI-LHCI) antenna size. In the gradient of PSI-Δa1, which in addition to Lhca2 and 3 also retained part of the Lhca4 (Wientjes *et. al.* 2009), some monomeric Lhca4 was present between the free pigments and dimeric Lhca.

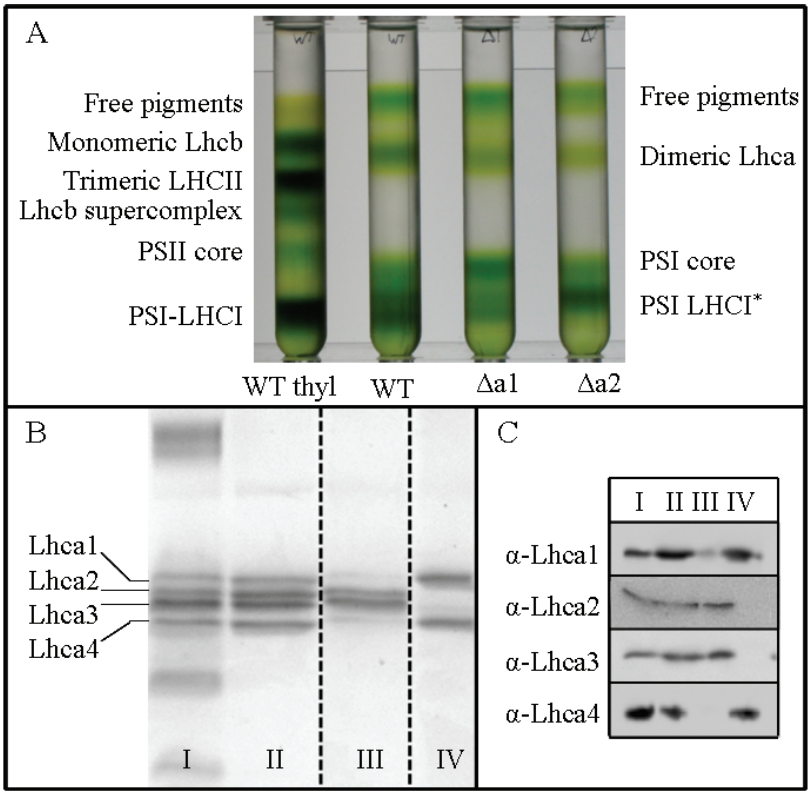

Figure 1: PSI solubilisation. Panel A: Sucrose gradients of solu-bilised PSI from WT, Δa1, and Δa2 plants. In addition a sucrose gradient of mildly solubilised WT thylakoids is presented, to show the migration behaviour of Lhc complexes in monomeric and trimeric aggregration state. Panel BC: SDS-PAGE (B) and immunoblot (C) of PSI-LHCI (I) and dimeric Lhca fraction of solubilised PSI from WT (II), Δa1 (III) and Δa2 (IV) plants. Note that in the case of PSI-LHCI, PsaD and Lhca3 overlap on this gel.

The SDS-PAGE and immunoblot analysis (fig 1BC) of the dimeric Lhca fraction purified from the Δa1, Δa2 and WT PSI preparations shows that they contain

respectively Lhca2/3, Lhca1/4 and a mixture of the two dimers (in the following named LHCI). The SDS-PAGE shows that the Lhca1/4 dimer is 100% clean, while the purity of the Lhca2/3 dimer is 95% (SI1 for details), the impurity being Lhca1/4, as expected because a small amount of Lhca1/4 dimer is present in the starting PSI preparation, as previously shown (Wientjes *et. al.* 2009). This is due to the fact that the T-DNA insertion of the Δa1 plants is located in the promoter region, and thus a small part of the PSI complexes in these plants retains Lhca1 (Klimmek *et. al.* 2005) and thus the Lhca1/4 dimer. The analysis of the gel (see SI1 for details) also showed that Lhca2 and Lhca3 are present in equal amounts, confirming that they are present as a heterodimer.

Pigment composition –The pigment composition of the Lhca1/4 and Lhca2/3 dimers is very similar (Table 1), both having a Chl *a/b* ratio of 3.7 and a Chl/Car ratio of 4.7-4.8. The main difference concerns the ratio between the Cars: the amount of β-carotene is higher in Lhca2/3 than in Lhca1/4, while the opposite is true for violaxanthin and lutein.

Table1 Pigment binding properties of Lhca dimers. The pigment compositions of LHCI, Lhca1/4, Lhca2/3 and the average of Lhca1/4 and Lhca2/3 are presented normalized to 100Chls. Values are averages of 3 measurements on independent preparations for Lhca1/4 and Lhca2/3 and of 2 repetitions for LHCI; standard deviations are indicated between brackets.

	Chl a/b	Chl/Car	Vio	Lut	β-car
LHCI	3.71 (0.01)	4.65 (0.01)	4.74 (0.04)	11.14 (0.02)	5.39 (0.03)
Lhca1/4	3.74 (0.09)	4.82 (0.04)	5.30 (0.05)	11.31 (0.13)	4.23 (0.13)
Lhca2/3	3.70 (0.12)	4.69 (0.07)	4.07 (0.15)	10.55 (0.35)	6.66 (0.46)
Average	3.72	4.77	4.69	10.9	5.45

LT absorption – The 77K absorption spectra (fig 2A) of the two dimers show clear differences reflecting the different environment in which the pigments are embedded as can be appreciated from the second derivative analysis of the spectra (fig 2BC). It is important to underline that in several regions in which the second derivative of Lhca1/4 shows a signal, no signal is present for Lhca2/3, indicating that the 5% impurity (Lhca1/4) in the latter preparation is below the detection sensitivity and does not influence our measurements.

The most peculiar feature of Lhca complexes is the presence of low-energy absorption forms. Interestingly, the absorption in the red tail is extremely similar for both dimers. In order to get more details about the red forms, the Q_y region of the spectra was described in terms of Gaussians (see SI2 for details). The red-most

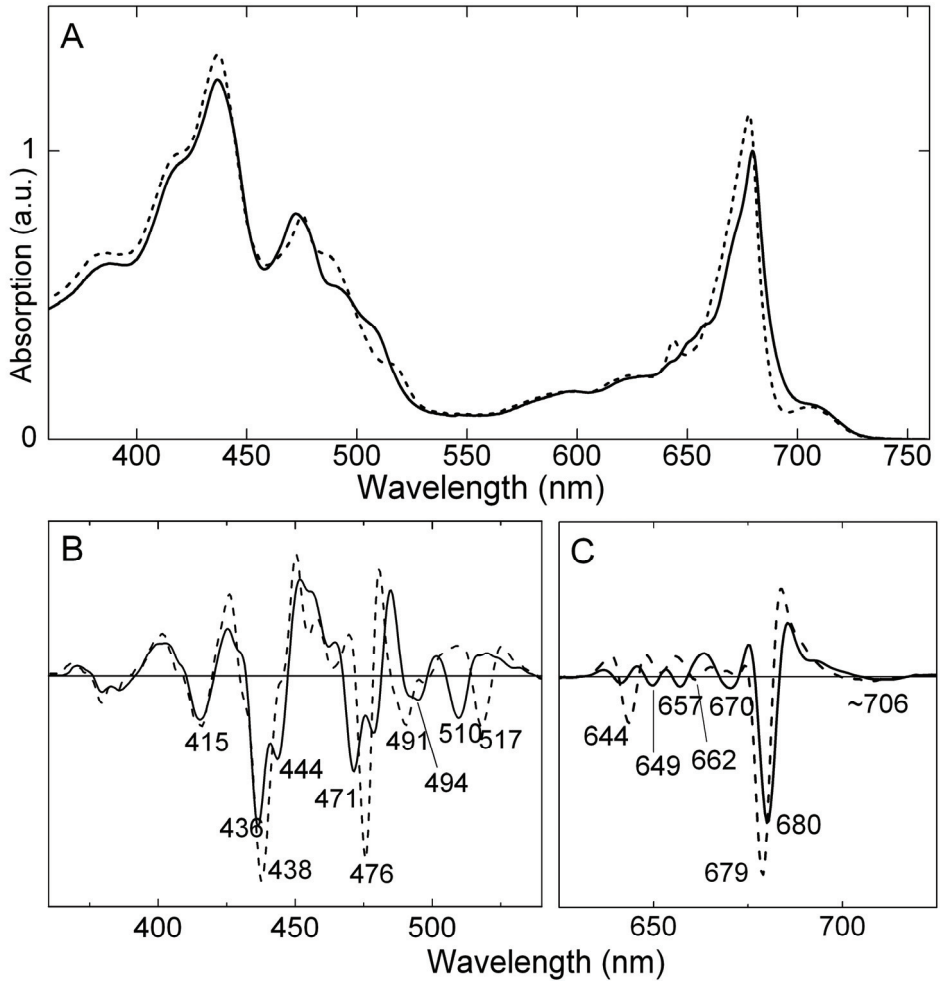

Figure 2: LT Absorption of Lhca1/Lhca4 and Lhca2/Lhca3. Panel A: 77K Absorption spectra of Lhca1/4 (dash) and Lhca2/3 (solid). Spectra are normalized to Chl content. Panel BC: Second derivatives of the absorption spectra in the Soret (B) and Q_y region (C).

bands show a maximum at 706-707nm and a FWHM of 25nm and they represent 8.5% and 8.9% of the total oscillator strength in the Q_y region (630-750nm) for Lhca1/4 and Lhca2/3, respectively. The high similarity of the absorption properties indicates that the organization of the Chls responsible for the red absorption is also very similar in the two dimers.

Circular Dichroism – In order to compare the pigment-pigment interactions in Lhca1/4 and Lhca2/3, the CD spectra were recorded (fig 3A). In the Q_y region, the main components of both dimers have the characteristic (-+-) signal like all other members of the Lhc family (Mozzo *et. al.* 2008), indicating a similar structural arrangement of the pigments. In the blue region the spectra are rather different, indicating specific pigment-pigment or pigment-protein interactions in the two dimers.

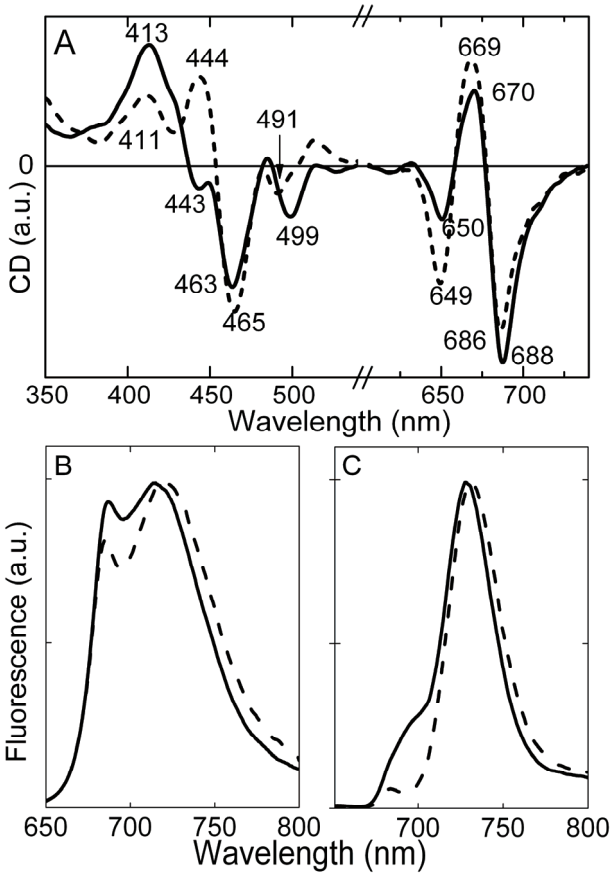

Figure 3: Circular dichroism and fluorescence of the dimeric Lhca complexes. A: CD spectra of Lhca1/4 (dash) and Lhca2/3 (solid) at 283K. Spectra are normalized to the Chl concentration. BC: Fluorescence emission spectra of Lhca1/4 (dash) and Lhca2/3 (solid) at 283K (B) and 77K (C). Excitation was at 475nm, spectra are normalized to the maxima.

Steady-State Fluorescence – The fluorescence emission spectra of the two dimers, recorded at 283K and 77K, are presented in figure 3BC. At 283K the Lhca1/4 spectrum has maxima at 685.5nm and 721nm. Lhca2/3 has a similar spectral shape with maxima at 687 and 713nm. Upon lowering the temperature to 77K the Lhca1/4 dimer loses nearly all 685.5nm emission, while the maximum shifts to 731.5nm. The maximum of Lhca2/3 also shifts to lower energies (728.5nm), however a shoulder remains around 697 nm. An emission band around 700nm was observed previously for an LHCI preparation containing both Lhca dimers (Croce *et. al.* 1998; Ihalainen *et. al.* 2000), and was assigned to Lhca2 (Castelletti *et. al.* 2003). This is puzzling, because for an equilibrated, intact Lhca2/3 dimer at 77K nearly all excitation energy is expected to be located on the lowest-energy form of Lhca3 (Castelletti *et. al.* 2003). A possible explanation for the observed emission could be that some dissociation of dimers has occurred, giving rise to Lhca2 that cannot transfer its energy to Lhca3. To investigate whether this is the case, the oligomeric state of the sample was analysed on a sucrose gradient. Only one band was observed (not shown), and its LT fluorescence spectrum was recorded directly after harvesting. The 697 nm emission was still present, indicating that it is an intrinsic property of the dimeric complex.

Previous data on recombinant complexes have shown that the fluorescence yield of Lhca complexes is far lower than that of LHCII, thus indicating that Lhca complexes are in a partially quenched state in solution (Ihalainen *et. al.* 2005a).

This is particularly interesting because a quenched conformation can be related to the mechanisms of energy dissipation in the antenna (for a review see Horton *et. al.* 1996), which protect the plants against high light damage. To check if this is also the case for native dimeric Lhca, the fluorescence yield (Φ_{Fl}) at 283K was calculated (for details see section: Experimental). Φ_{Fl} was 0.15 (+/- 0.01) for Lhca2/3 and 0.14 (+/- 0.01) for Lhca1/4. These values for the native dimers are significantly higher than the value of 0.063 reported for the reconstituted Lhca1/4 complex (Ihalainen *et. al.* 2005a), but lower than that of LHCII (Φ_{Fl} = 0.22 (Palacios *et. al.* 2002)), indicating that the Lhca dimers are indeed in a partially quenched state in solution.

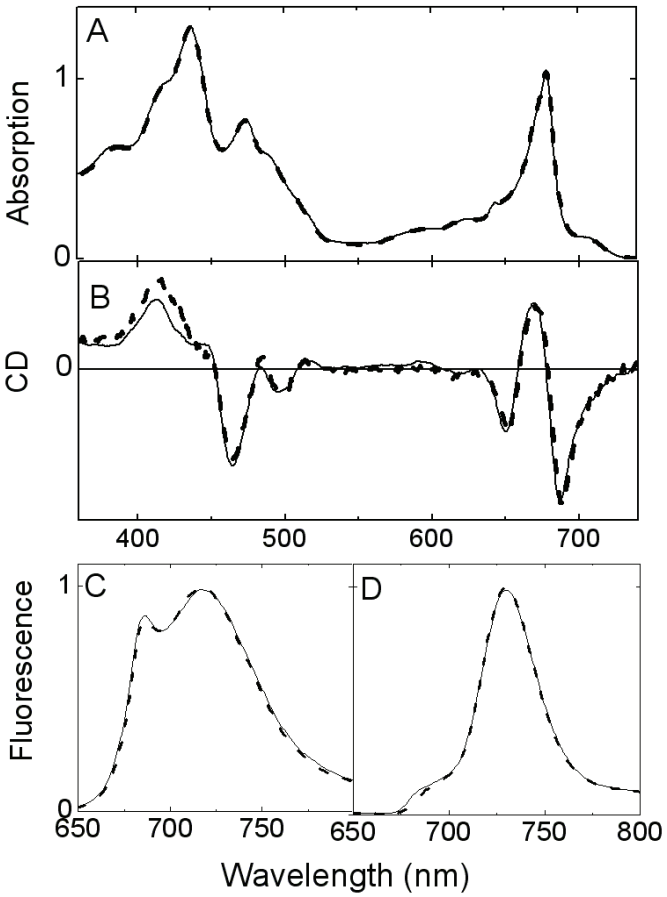

Figure 4: Comparison of the spectra of Lhca1/4 and Lhca2/3 with those of LHCI. A: Sum of LT absorption spectra of Lhca1/4 and Lhca2/3 (black solid), compared with LHCI (red dash). Spectra are normalized in the Q_y region to the number of Chls. B: Sum of CD spectra of Lhca1/4 and Lhca2/3 (black solid) compared to that of LHCI (red dash). C: 283K fluorescence emission spectra of average Lhca1/4 and Lhca2/3 (black solid) and LHCI (red dash). Spectra are normalized on an energy scale to their fluorescence quantum yield. For LHCI a value of 14.5% was used. D: LT fluorescence emission spectra of average from Lhca1/4 and Lhca2/3 (solid) and LHCI (dash). Spectra are normalized to the same fluorescence quantum yield.

Comparing the properties of Lhca1/4 and Lhca2/3 with the one of LHCI – The peripheral antenna complex of PSI (LHCI) is composed of equal amounts of Lhca1/4 and Lhca2/3 (Ballottari *et. al.* 2004). Therefore the normalized spectra of the purified Lhca1/4 and Lhca2/3 dimer should add up to the spectra of LHCI. Figure 4 shows the comparison of the sum of the absorption, CD and fluorescence spectra of the two dimers with the spectra of the LHCI fraction purified from WT plants. The excellent agreement shows that indeed the spectroscopic properties of LHCI can be explained by those of the two purified dimers.

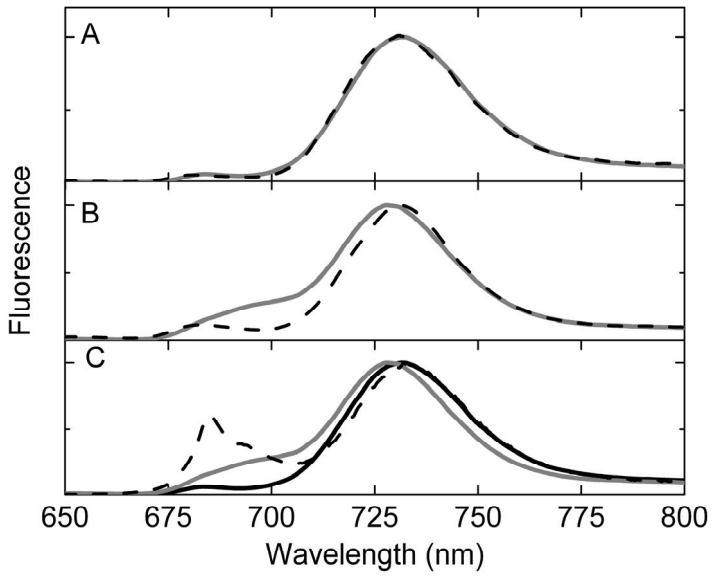

Figure 5: Fluorescence emission of Lhca dimers compared to PSI. LT emission spectra of Lhca1/4 (grey solid) and Δa3-PSI (black dash) (A), Lhca2/3 (grey solid) and Δa4-PSI (black dash) (B), and Lhca1/4 (black solid), Lhca2/3 (grey solid), and thylakoids (black dash) (C). Thylakoids were of Lhcb2 antisense plants which have a reduced LHCII antenna size and therefore the PSI emission is less obscured by PSII emission. Spectra are normalized to the maxima.

Comparing the dimers with the intact system – In order to investigate whether the properties of the dimers change during purification, their LT emission is compared to those in isolated PSI systems and PSI in the thylakoid membranes. In Δa3-PSI Lhca3 is completely lacking, therefore Lhca4 coordinates the lowest-energy Chls and is responsible for most of the LT emission. This allows comparison of the spectroscopic properties of the red forms of Lhca4 in PSI with those of Lhca1/4 (fig 5A). The properties of the red forms in Lhca3 (of Lhca2/3) can be compared with those of Δa4-PSI, where Lhca4 is replaced by Lhca5 (Wientjes *et. al.* 2009). In this complex Lhca3 is responsible for most of the LT emission (fig 5B). In both cases there is a good match between the compared spectra. This means that the properties of the red forms remained unchanged during the purification of the Lhca1/4 and Lhca2/3 dimer. This is further confirmed by the comparison of the spectra of the dimers with that of the thylakoid membrane (fig 5C). Also in this case there is a good overlap between the spectra of the dimers and the reddest peak of the thylakoid spectrum which originates from PSI. Because the red forms are very sensitive to changes in the environment of the corresponding pigments (van Amerongen *et. al.* 2000), the fact that LT emission does not change upon isolation indicates that the dimers are in their native state.

Photobleaching – It has been shown that the LHCI moiety is the first target of high-light damage in PSI-LHCI (Hui et. al. 2000; Andreeva et. al. 2007; Alboresi et. al. 2009). This was explained by the concentration of excitation energy on the red forms, thus giving rise to the highest probability of generating dangerous triplets on the corresponding Chls (Alboresi et. al. 2009), which are mainly located in LHCI

(Croce et. al. 1998). However, it has also been reported that triplets formed on the red forms are quenched with 100% efficiency by a nearby Car located in the 621 site (Carbonera et. al. 2005), which would provide excellent photoprotection to the whole system. Thus there is a discrepancy: on the one hand the red forms are proposed as a site of photodamage, on the other hand they were shown to be fully protected. To clarify this point we investigated the photodamage for isolated dimers.

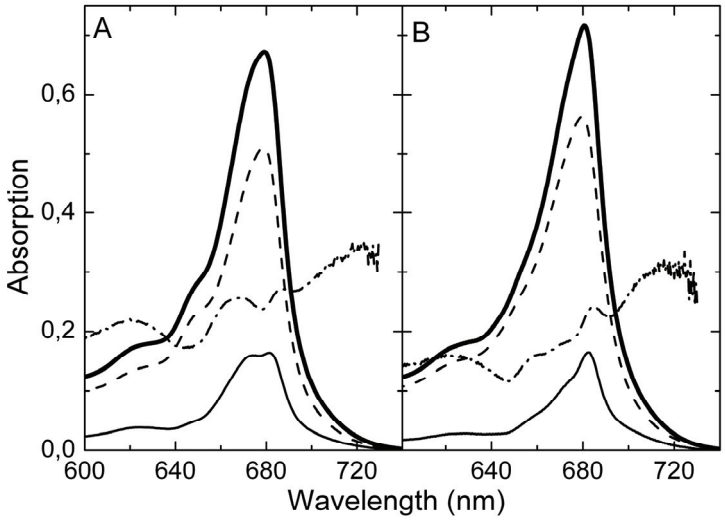

Figure 6: Photobleaching of native Lhca dimers. Absorption spectra of Lhca1/4 (A) and Lhca2/3 (B), control (solid bold), light-treated sample (dash), difference (solid thin), and the ratio difference /control (dash-dot).

Both dimers were subjected to high-light treatment. The absorption spectra of the treated and untreated samples are presented in figure 6. The total absorption in the Q_y region decreased demonstrating that photobleaching had occurred. The difference spectra untreated-treated of both dimers show a peak at 682nm, a shoulder at 672nm and a tail extending into the red, meaning that the red forms are not fully protected.

A light-induced trimer to monomer transition has been observed for the major light-harvesting complex of PSII (LHCII) (Garab *et. al.* 2002). Therefore, it was investigated whether light-induced monomerization also occurs in the Lhca dimers. The complexes were exposed to strong light followed by density-gradient centrifugation. Interestingly, light-induced monomerization was observed for Lhca2/3, but not for Lhca1/4 (fig 7).

Monomerization affects pigment organization – For recombinant Lhca1/4 it has been shown that dimerization affects the pigment interactions, as indicated by the fact that the CD spectrum of the dimer differs from the sum of the CD spectra of the monomers (Croce *et. al.* 2002b). The light induced monomerization of the Lhca2/3 dimer (fig 7) allows to investigate if a similar effect occurs in these complexes. Figure 8 shows that the CD spectra of the monomeric band, containing

Lhca2 and Lhca3, is rather different from the dimer. Therefore, it can be concluded that dimerization affects the pigment organization in both dimers and/or create new interactions between pigments of different monomers.

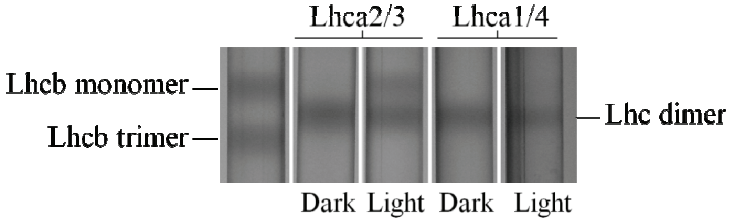

Figure 7: Analysis of oligomeric state of light-treated Lhca complexes. Sucrose density gradient loaded with Lhca2/3 and Lhca1/4, kept for 20 minutes at RT in the dark or in strong light. The left gradient was loaded with a mixture of monomeric and trimeric Lhcb complexes.

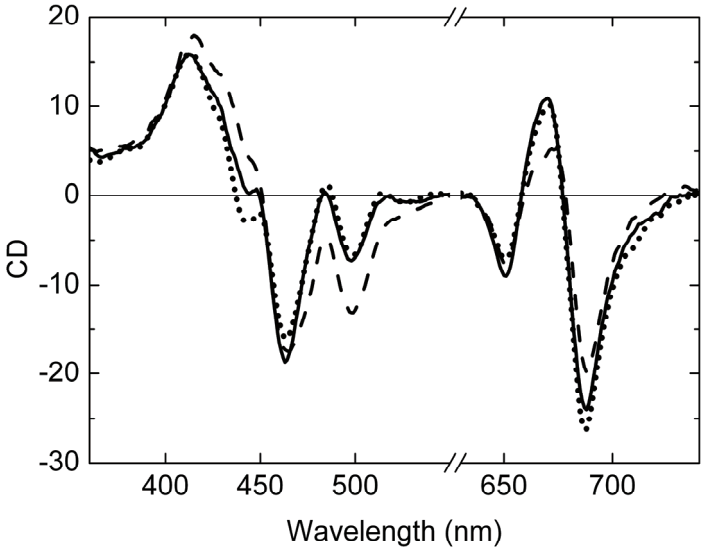

Figure 8: CD spectra of monomeric vs dimeric Lhca2/3. CD spectra of dimeric Lhca2/3 before (dot) and after (solid) light treatment, and a light induced mixture of monomeric Lhca2 and Lhca3 (dash). Spectra are normalized to the absorption in the Q_y region.

Reconstituted vs native Lhca complexes – The availability of native dimers and monomers Lhca allows for a comparison of their properties with those of the reconstituted complexes (SI3), which have been widely used for the study of the PSI antenna complexes.

Based on the pigment composition of the monomers, identical Chl *a*/*b* ratio and Chl/Car ratio's are expected in both dimers, as is indeed the case (table SI3). The Car composition of the sum of the monomers is similar to that of the dimer, indicating that the specificity for the Car binding is maintained in the reconstituted complexes. The only difference is the higher amount of β-carotene (at the cost of lutein) in the dimers. This was also observed for the reconstituted Lhca1/4 dimer, indicating that dimerization stabilises the coordination of β-carotene, or that the binding of β-carotene is required for dimerization, but that this difference is not due to the reconstitution procedure.

The data also show high similarity between the spectroscopic properties of the native and reconstituted Lhca1/4 dimer (figSI3.1). The properties of the red most bands are identical, although the reconstituted complex shows somewhat smaller intensity in the red.

So far it has not been possible to reconstitute the Lhca2/3 dimer (Schmid *et. al.* 2002), but the individual monomers were obtained (Schmid *et. al.* 2002; Castelletti *et. al.* 2003). In figure SI3.2 the sum of the reconstituted Lhca2 and Lhca3 spectra is compared with the mixture of native Lhca2 and Lhca3 obtained by light-induced monomerization. The striking similarity of the spectra shows that also in this case the pigment organization in the reconstituted complexes is virtually identical to that of the native ones.

Discussion

LHCI-680 is not a natural component of the PSI antenna complex – For a long time it has been thought that LHCI is composed of two fractions, one without red forms: LHCI-680 (enriched in Lhca2 and Lhca3) and one with red forms: LHCI-730 (enriched in Lhca1 and Lhca4). However, it was also shown that fractions containing all four Lhca complexes in dimeric state did not show emission at 680 nm at LT and it was inferred that the LHCI-680 fraction was composed of partially denatured complexes in a monomeric state (Croce *et. al.* 2002b; Croce *et. al.* 2006). Therefore, it was suggested that native LHCI is composed of dimeric complexes which all contain red forms (Croce *et. al.* 2002b). Unfortunately, these complexes could never be fully separated. Here, by using PSI complexes from mutant plants, we were able for the first time to purify these dimeric complexes: Lhca1/4 and Lhca2/3. The properties of these dimers can fully explain the pigment composition (Table1), CD, absorption and fluorescence spectra (fig 4) of LHCI. Moreover, both dimers show red emission forms with maxima around 730 nm, the same as in the PSI complex, implying that the purification does not alter the properties of the dimers. These results present the final proof that LHCI-680 is not a natural component of the PSI antenna complex.

Lhca2 and Lhca3 form a functional heterodimer – It is well established that Lhca1 and Lhca4 form a heterodimer, while the heterodimeric association state of Lhca2 and Lhca3 could not be confirmed by either reconstitution *in vitro* (Schmid *et. al.* 2002) or purification of the complex (Croce *et. al.* 2002b). Several results indicate that Lhca2 and Lhca3 are not associated to PSI core as a homodimer: (i) In Lhca2 anti-sense plants Lhca3 is completely lacking at the PSI level, while its mRNA is present (Ganeteg *et. al.* 2001; Klimmek *et. al.* 2005; Morosinotto *et. al.* 2005a;

Wientjes *et. al.* 2009), thus demonstrating that an Lhca3 homodimer is not being formed. (ii) In the Lhca3 anti-sense plants 35% of Lhca2 (as compared to the WT level) is still associated with the core, but exclusively in its monomeric form as is evident from both electron-microscopy and sucrose density ultracentrifugation, where Lhca2 was only found in the monomeric fraction (Wientjes *et. al.* 2009). In this study we were able to isolate Lhca2/3 and to show that it is a functional heterodimer in which energy-transfer between the monomers occurs (as apparent from the small intensity of "blue" fluorescence emission arising from Lhca1 and Lhca2, thus indicating that most of the excitation energy is transferred to Lhca4 and Lhca3 (Schmid *et. al.* 1997; Croce *et. al.* 2002b; Castelletti *et. al.* 2003), respectively).

Four different Lhca complexes form two nearly identical dimers –The four monomeric Lhcas obtained by *in vitro* reconstitution strongly differ from each other in their biochemical and spectroscopic properties (Ihalainen *et. al.* 2005a; Croce *et. al.* 2007b). However, it was noticed previously (Morosinotto *et. al.* 2005a) that the sum of the absorption spectra of reconstituted monomeric Lhca1 and Lhca4 was similar to the sum of Lhca2 and Lhca3, suggesting that the two dimers also have similar absorption properties. The analysis of the native complexes shows that this is indeed the case: the two dimers have identical Chl *a*/*b* ratio's and rather similar absorption spectra. What is surprising is that this similarity is not limited to the absorption, but it extends to most of the spectroscopic properties including long-wavelength emission and fluorescence quantum yield Φ_{Fl}. From a functional point of view this means that PSI has two identical antenna units.

Although light harvesting represents the main task of Lhca complexes, they are also involved in photoprotection: in high-light conditions they can act as a "fuse" and dissipate excess energy to minimize photodamage to the core complex (Alboresi *et. al.* 2009). In this respect, the data show a clear difference in functionality for the two dimers: light treatment leads to the monomerization of Lhca2/3 but not of Lhca1/4. In PSI-LHCI monomerization of Lhca2/3 might induce the dissociation of the dimer from the core complex. In this case Lhca2/3 cannot transfer its excitation energy to P700, which leads to an increase of the excited-state lifetime and thus to an increased probability to form Chl triplets. This can thus explain why Lhca2 and Lhca3 are the first antennas to be degraded upon light treatment of PSI-LHCI (Hui *et. al.* 2000; Wei *et. al.* 2001; Rajagopal *et. al.* 2005).

The domain harbouring the red forms is conserved in the two dimers – A peculiar feature of the antenna complexes of PSI is the presence of Chls that absorb above 700 nm and which are associated with Lhca3 and Lhca4 (Croce *et. al.* 2007a). The properties of these forms could be studied for native and functional dimers, allowing a direct comparison of Lhca2/3 with Lhca1/4 (SI4). The data show that the red forms have nearly identical spectroscopic properties in both dimers, indicating that their environment and organization must be very similar.

The two dimers have identical light-harvesting properties: implications for energy transfer in PSI-LHCI – The study of excitation energy transfer and trapping in PSI is extremely complex because the system is composed of 170 Chl molecules, making the modelling of the fluorescence kinetics very challenging. The system is usually described using compartment models in which the major building blocks (Lhca complexes, core complex, RC) are considered. Knowledge about the spectroscopic properties of the compartments is required for the evaluation of these models (Slavov *et. al.* 2008). Until now this information was not available. The newly obtained data for the dimers open the way to design and evaluate a model which truly describes the energy trapping and transfer in PSI.

The reconstituted complexes are good replicas of the native system – In this study the biochemical and spectroscopic properties of native and reconstituted complexes were compared. The data clearly demonstrate that all the major properties of the monomeric Lhcas are perfectly reproduced in the *in vitro* systems, testifying once more that the reconstituted complexes are valuable "replicas" of the native systems.

Acknowledgements

We thank Stefan Jansson for kindly providing the seeds and Herbert van Amerongen for helpful discussion. This work was supported by ''De Nederlandse Organisatie voor Wetenschappelijk Onderzoek (NWO), Earth and Life Science (ALW)'', through a Vidi grant (to R.C.).

Supplementary information

SI1 Composition of dimeric Lhca complexes

All samples used in this work were analysed by SDS-PAGE (Fig SI1). The dimers obtained by solubilising PSI from Δa2 plants, were composed of Lhca1 and Lhca4. The dimeric fraction obtained after solubilisation of PSI-Δa1 consisted mostly of Lhca2 and Lhca3, however Lhca1 and Lhca4 were also present. Densitometric analysis of the gel (table SI1) showed that the amount of Lhca1/4 was 5.3±2.7%.

To evaluate the Lhca2/Lhca3 ratio in the dimer obtained after PSI-Δa1 solubilisation, the amount of Coomassie bound to the two polypeptides in the gel was compared. The staining was 1.48±0.26 higher for Lhca3 than for Lhca2. Ballottari *et al.* 2004 found that the affinity of Coomassie binding is ~1.4 times higher for Lhca3 than for Lhca2. This indicates that Lhca2 and Lhca3 are present in equal amounts, in agreement with a heterodimeric Lhca2/3 complex.

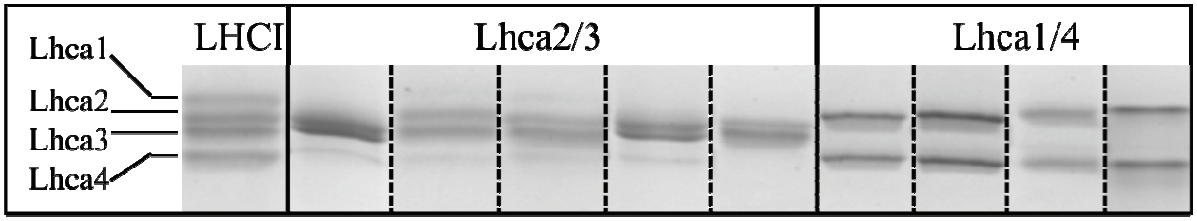

Fig SI1 SDS-PAGE analysis of dimeric Lhca complexes, obtained after solubilisation of PSI-WT (LHCI), PSI-ΔLhca1 (Lhca2/3) and PSI-ΔLhca2 (Lhca1/4). Five different purifications of Lhca2/3 dimer and four of Lhca1/4 dimer are shown.

Table SI1. Quantification of Coomassie bound to Lhca polypeptides in the five preparations of Lhca2/3 presented in figure SI1. Amount of Coomassie bound determined by integrating the optical density (IOD) of each Lhca band, values are normalized to IOD of Lhca2. Contamination of Lhca1/4 is determined by the IOD of Lhca4 in the Lhca2/3 dimers to that of LHCI.

Sample	LHCI	Lhca2/3	Lhca2/3	Lhca2/3	Lhca2/3	Lhca2/3
Lhca1	0.80	0.05	0.06	0.04	0.07	0.00
Lhca2	1	1	1	1	1	1
Lhca3	1.28	1.40	1.33	1.54	1.25	1.90
Lhca4	1.06	0.05	0.08	0.07	0.09	0.01
Lhca1/4 contaminant	50%	4.6%	6.9%	6.3%	7.8%	0.90%

SI2 Absorption properties of the red forms

In order to get more details about the red forms, the Q_y region of the absorption spectra was described as a sum of Gaussians. A problem often encountered in this kind of analysis is that due to a lack of spectral structure in the red tail, more than one combination of Gaussians can describe the data. However, for the Lhca1/4 dimer the position of the maximum of the red-most form can be discerned by second-derivative analysis (~706nm). Furthermore, only one form should absorb above 705nm as was shown in a site-selected and anisotropy fluorescence study on LHCI (Ihalainen *et. al.* 2000). The Gaussian fit meeting this requirement is presented in figure SI2A. The red-most form shows its maximum at 706nm and a FWHM of 25nm. In the absorption spectrum of the Lhca2/3 dimer no clear maximum of the red-most form was observed by second-derivative analysis, giving rise to a larger uncertainty of the fit. The best result was obtained with the maximum of the red-most form at 706-707nm with a FWHM of 25nm (fig SI2B). The red-most Gaussian band represents 8.5% and 8.9% of the total oscillator strength in the Q_y region (630-750nm) for Lhca1/4 and Lhca2/3, respectively.

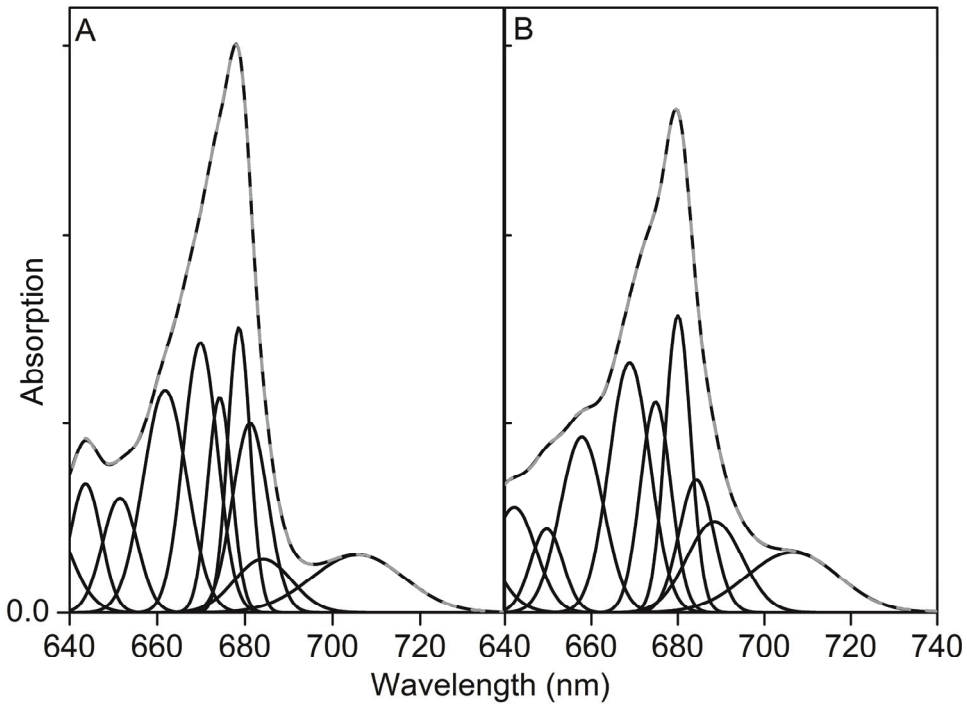

Fig SI2 Gaussian analysis. The Q_y region of the LT absorption spectra (grey dash) of Lhca1/4 (A) and Lhca2/3 (B) described by Gaussian bands (black). Note that the fitting is only meant to extract the characteristics of the red bands, using the restrictions as explained in the text.

SI3 Reconstituted vs Native complexes

Due to the difficulties in purification of the individual native Lhca antennas, a large part of our Lhca knowledge stems from the study of *in vitro* reconstituted complexes. However, based on the analysis of a PSI preparation depleted in the individual complexes, it has been suggested that the native complexes could have different properties (Klimmek *et. al.* 2005). To check this suggestion we directly compared the properties of the reconstituted complexes with those of the native antennas.

Pigment composition

In table SI3 the pigment composition of the native dimers is compared to the sum of the pigments in the reconstituted monomers (Croce *et. al.* 2007b). Based on the properties of the monomers identical Chl *a*/*b* and Chl/Car ratios are expected for the two dimers. This is indeed the case. The difference in the absolute value of the Chl *a*/*b* ratio (3.7 vs. 3.1) can be due to the absence of some Chls in the reconstituted complexes or to a too low Chl *a*/*b* ratio used in the reconstitution. Indeed, it has been suggested that the reconstituted complexes only coordinates 10 Chl molecules (Croce *et. al.* 2002b), while in the crystal structure 13-14 Chls are associated to each complex (Amunts *et. al.* 2007). We have tentatively normalized the number of Chls per native dimer to 24, taking into account that some of the Chls observed in the structure are located at the periphery of the complexes, and do not seem to belong to a specific protein. They are probably stabilized by protein-protein interaction, and are thus most likely lost during purification.

Although neoxanthin was present in the pigment mixture used for the reconstitution, the rLhca do not coordinate this Car, thus indicating that the Car binding of the reconstituted complexes is specific. The amount of violaxanthin is very similar in the sum of the monomers when compared to the native dimer. Lutein is in both cases the most abundant Car, but in the native dimers the amount is smaller than in the sum of the monomers, while the opposite is true for β-carotene. The data thus suggest that ~1 lutein is replaced by a β-carotene in both native dimers, as compared to the monomers. Interestingly, also the reconstituted Lhca1/4 dimer was shown to be able to coordinate β-carotene, although the two monomers were not (Croce *et. al.* 2002b). This suggests that dimerization stabilises the coordination of β-carotene, or that the binding of β-carotene is required for dimerization.

In conclusion, the comparison of the pigment composition of native and reconstituted complexes show very high similarity, the differences could be associated with the effect of the dimerization.

Table SI3 Pigment-binding properties of Lhca complexes. Cars in reconstituted Lhca, taken from (Croce *et. al.* 2002b; Croce *et. al.* 2007b), nd = not detected; r = reconstituted; n= native

	Chl *a*/*b*	Chl/Car	Vio	Lut	β-car	Total Chls
rLhca1	4.0	3.3	1.0	1.8	nd	10
rLhca2	1.9	5.0	0.5	1.5	nd	10
rLhca3	6.0	3.5	0.7	1.6	0.5	10
rLhca4	2.4	4.8	0.4	1.7	nd	10
rLhca1/4	3.0	4.0	1.6	2.4	0.8	20
rLhca1+rLhca4	3.1	3.9	1.4	3.5	nd	20
rLhca2+rLhca3	3.1	4.1	1.2	3.1	0.5	20
nLhca1/4	3.7	4.8	1.3	2.7	1.0	24
nLhca2/3	3.7	4.7	1.0	2.5	1.6	24

Lhca1/4 – In figure SI3.1 the Q_y region of the LT absorption spectra of native and reconstituted Lhca1/4 dimers are compared. In general there is good agreement between the two spectra. However, rLhca1/4 shows less absorption at 706nm and more around 673nm. The second-derivative spectrum demonstrates that the band at 673nm is only present in rLhca1/4. It has been suggested that Chl 603 and Chl 609, which are responsible for the red forms when they are in excitonic interaction, absorb around 675nm in the absence of such interaction (Morosinotto *et. al.* 2003). Therefore, it can be proposed that a fraction of the rLhca1/4 is lacking the strong excitonic Chl *a* interaction. However, although the oscillator strength of the red most form is smaller in the reconstituted dimer as compared to the native one, the other properties of the band (maximum, FWHM) are similar in the two preparations (SI4 and Croce *et. al.* 2007a).

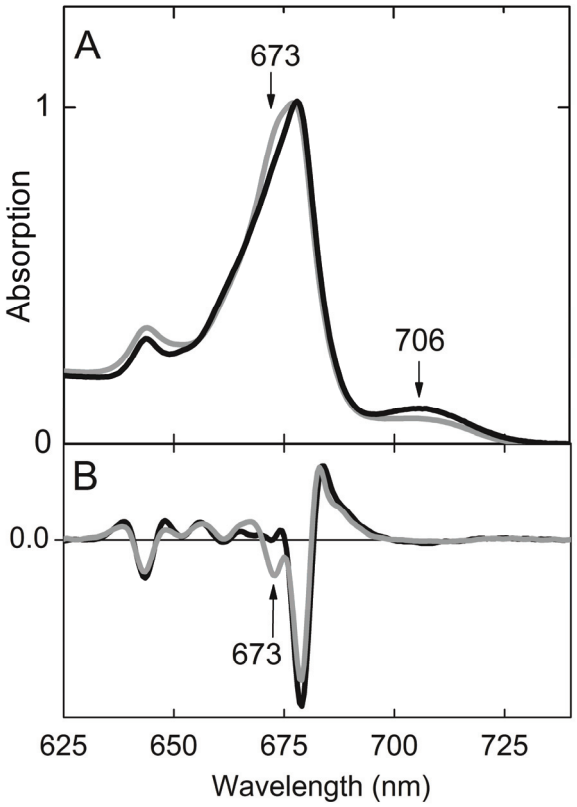

Fig SI3.1 Absorption spectra at 77K of native and reconstituted Lhca1/4. Absorption (A) and second derivative thereof (B) for native (black) and reconstituted (grey) Lhca1/4. Absorption spectra are normalized to the area.

Lhca2 and Lhca3 – Unfortunately, it has not been possible so far to obtain a reconstituted Lhca2/3 dimer (Schmid *et. al.* 2002). This is probably due to the fact that this dimer is far less stable than the Lhca1/4 dimer, as also the present data indicate, and therefore cannot endure the quite harsh detergent treatment during the reconstitution procedure. Moreover, it has been demonstrated in the case of the Lhca1/4 dimer, that dimerization induces changes in the spectroscopic properties of some of the chromophores (Croce *et. al.* 2002b), making it difficult to compare these properties for monomers and dimers. However, high-light treatment induced the monomerization of Lhca2/3 dimer without addition of detergent, giving the opportunity to compare the complexes in their monomeric aggregation state. In figure SI3.2 the absorption and CD spectra of the monomeric Lhca2 and Lhca3 fractions, as obtained after light treatment of the native Lhca2/3 dimer (Fig 8), are compared with the sum of the spectra of the reconstituted Lhca2 and Lhca3 complexes. It should be noted that the normalized CD (Fig 9) and absorption (data not shown) spectra of the dimeric Lhca2/3 complex before and after light-treatment were very similar. Therefore, the spectra of the monomeric complexes are also not expected to be strongly affected by the light. The striking similarity of the spectra shows that the pigment organization in the reconstituted complexes is virtually identical to that of the native ones.

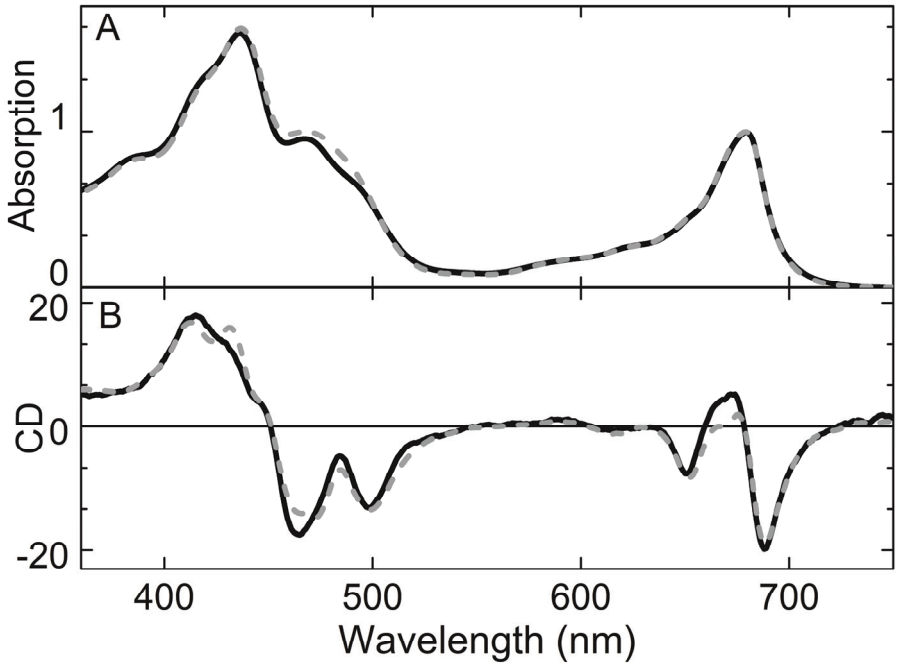

Fig SI3.2 Native and recombinant Lhca2 and Lhca3. Absorption (A) and CD (B) spectra of a mixture of native Lhca2 and Lhca3 (black), obtained by light-induced monomerization of the Lhca2/3 dimer, and the sum of rLhca2 and rLhca3 spectra (grey dash). Spectra are normalized to the Chl content.

SI4 Spectroscopic properties of the red forms

Table SI4 shows the main properties of the red forms of the two dimers obtained from the steady-state measurements. The properties are very similar, and apart from the relative area, also comparable to those found for the refolded complexes (Croce *et. al.* 2007a).

Table SI4. Spectroscopic properties of the red forms.

	Abs nm	Area %	Em (nm)	Su cm^{-1}	$FWHM_{tot}$ cm^{-1}	$FWHM_{hom}$ cm^{-1}	$FWHM_{inh}$ cm^{-1}
Lhca1/4	706	8.5	731.5	247	502	383	325
Lhca2/3	707	8.9	728.5	209	501	352	357

Reported are: absorption wavelength, the relative contribution to the absorption on cm^{-1} scale in the Q_y region, fluorescence emission wavelength, optical reorganization energy (Su) obtained from the Stokes shift (= 2Su), the $FWHM_{tot}$ of the absorption band described with a Gaussian shape, $FWHM_{hom}^2 = 7.7SuT$ (Zucchelli *et. al.* 1996) and $FWHM_{tot}^2 = FWHM_{hom}^2 + FWHM_{inh}^2$.

Chapter 4

Excitation energy transfer dynamics of higher plant Photosystem I light-harvesting complexes

Emilie Wientjes, Ivo H.M. van Stokkum, Herbert van Amerongen and Roberta Croce

This chapter is based on:

Biophysical Journal (2011) 100:1372-1380.

Abstract

Photosystem I (PSI) plays a major role in the light reactions of photosynthesis. In higher plants PSI is composed of a core complex and four outer antennas which are assembled as two dimers: Lhca1/4 and Lhca2/3. Time-resolved fluorescence measurements on the isolated dimers show very similar kinetics. The inter-monomer transfer processes are resolved using target analysis. They occur with similar rates as transfer to the PSI core, suggesting competition between both transfer pathways. It appears that each dimer is adopting various conformations that correspond to different lifetimes and emission spectra. A special feature of the Lhca complexes is the presence of an absorption band at low energy, originating from an excitonic state of a chlorophyll dimer, mixed with a charge-transfer state. These low-energy bands have high oscillator strengths and they are superradiant in both Lhca1/4 and Lhca2/3. This challenges the view that the low-energy charge-transfer state always functions as a quencher in plant Lhcs and it also challenges previous interpretations of the PSI kinetics. The very similar properties of the low-energy states of both dimers indicate that the organization of the involved chlorophylls should also be similar, in disagreement with the available structural data.

Introduction

The driving force of photosynthesis is light, which is harvested by membrane embedded photosystems (PSs). In oxygen-evolving photosynthesis, two photosystems, PSII and PSI, work in series to drive electrons from water to $NADP^+$. The PSs are pigment-protein supercomplexes, consisting of a core complex and a peripheral light-harvesting system. The core complex of PSI harbors the reaction centre, the electron-transport chain, ~100 chlorophylls *a* (Chls *a*) and ~20 β-carotene pigments (Jordan *et. al.* 2001; Amunts *et. al.* 2007). In higher plants another ~70 Chls *a* and *b* and ~15 carotenoids are coordinated by the peripheral light harvesting complex of PSI (LHCI) (Croce *et. al.* 2006; Amunts *et. al.* 2007). Their function is to absorb light and transfer the excitation energy to the core complex where it can be used for photochemistry by the reaction centre.

LHCI is composed of four Lhca complexes, located at one side of the core and assembled as two hetero-dimers: Lhca1/4 and Lhca2/3 (Boekema *et. al.* 2001; Amunts *et. al.* 2007; Wientjes and Croce 2011, Chapter 3). Lhca proteins are encoded by nuclear genes belonging to the Lhc multigene family, which also encodes the Lhcb proteins of Photosystem II (PSII) (Jansson 1999). A special feature of the Lhca complexes is the presence of “red forms”: Chls with extremely

red-shifted and broad absorption and fluorescence spectra. It was found that the red forms of LHCI have absorption bands around 705-712nm (Ihalainen *et. al.* 2000; Croce *et. al.* 2007). This is ~30nm red shifted, and thus about 3kT lower in energy, compared to bulk Lhc Chls *a.*

Red forms are conserved in plants, algae and bacteria. Still, their function is not fully understood. It has been suggested that they: (i) focus the energy to the primary electron donor, (ii) have a role in protection against light-stress, or (iii) absorb light efficiently in a dense vegetation system where light is enriched in wavelengths above 690 nm (Rivadossi *et. al.* 1999).

In higher plants the red forms are only responsible for a small part of the absorption of PSI, but due to their low energy they have a strong effect on excitation energy transfer and trapping of the whole PSI complex (Croce *et. al.* 1996; Croce *et. al.* 2000; Gobets *et. al.* 2001b; Jennings *et. al.* 2003b; Ihalainen *et. al.* 2005b; Engelmann *et. al.* 2006). It has been shown that at room temperature (RT) excitations reside 80% of the time on the red forms (Croce *et. al.* 1996). These excitations must thus be transferred energetically up-hill, from the red forms to P700, in order to be used for photochemistry (Jennings *et. al.* 2003b).

For a long time it has been believed that LHCI is composed of two fractions: LHCI-680 and LHCI-730, named after their 77K fluorescence emission maxima. The first fraction mainly consisted of monomeric Lhca2 and Lhca3, while the second was highly enriched in the Lhca1/4 heterodimer (Knoetzel *et. al.* 1992; Tjus *et. al.* 1995; Schmid *et. al.* 2002). Therefore, it was assumed that only the Lhca1/4 dimer possesses red forms, but recently we have shown that Lhca2 and Lhca3 also form a red-emitting heterodimer, and that LHCI-680 is not a native state of LHCI (Wientjes and Croce 2011, Chapter 3).

Due to the dimeric nature and the similar biochemical properties of the native Lhca complexes it has so far been impossible to purify the individual Lhcas. Therefore it was difficult to acquire information about their properties. This problem was partially solved by the use of *in vitro* reconstituted Lhca complexes (Schmid *et. al.* 1997; Croce *et. al.* 2002; Schmid *et. al.* 2002; Castelletti *et. al.* 2003). It was found that the low temperature (LT) fluorescence emission maxima were located at: 690nm (Lhca1), 702nm (Lhca2), 725nm (Lhca3), and 733nm (Lhca4) (Schmid *et. al.* 1997; Croce *et. al.* 2002; Schmid *et. al.* 2002; Castelletti *et. al.* 2003). Furthermore, using *in vitro* reconstitution it has been shown that the red forms in the Lhca complexes originate from a strongly excitonically coupled Chl dimer, involving Chl603 and Chl609 (nomenclature as in Liu *et. al.* 2004) (Morosinotto *et. al.* 2002; Morosinotto *et. al.* 2003; Croce *et. al.* 2004; Morosinotto *et. al.* 2005; Mozzo *et. al.* 2006). To account for the extremely broad and red-shifted spectra, it was proposed that the lowest exciton state of the

dimer mixes with a charge-transfer (CT) state (Ihalainen *et. al.* 2003); this was recently proven to be indeed the case for the Lhca4 monomer (Romero *et. al.* 2009). It has been suggested that this CT state is responsible for the low fluorescence quantum yield and emitting dipole strength of Lhca3 and Lhca4 (Ihalainen *et. al.* 2005a), but a recent study has shown that the fluorescence quenching of Lhca4 is not related to the presence of the red forms and thus the CT state (Passarini *et. al.* 2010).

Although several studies have analyzed the energy transfer and trapping kinetics in PSI of higher plants, no general agreement has been reached about their kinetics (Ihalainen *et. al.* 2005b; Slavov *et. al.* 2008; van Oort *et. al.* 2008). This is mainly due to the fact that PSI is a large and complex system. To be able to disentangle the contribution of the individual complexes from the analysis of the whole system, information on the excitation energy transfer in, and the spectroscopic properties of the PSI building blocks (Lhca1/4, Lhca2/3 and PSI core) is needed.

The steady-state spectroscopic properties of the Lhca1/4 complex have been thoroughly investigated, both by studying the reconstituted complex (Schmid *et. al.* 1997; Croce *et. al.* 2002; Schmid *et. al.* 2002; Castelletti *et. al.* 2003) and the LHCI-730 fraction (Knoetzel *et. al.* 1992; Tjus *et. al.* 1995; Schmid *et. al.* 2002). Time-resolved fluorescence studies were also performed. The reconstituted Lhca1/4 complex showed two main decay components of 0.7 and 2.9ns at RT (Ihalainen *et. al.* 2005a) and of 3.2 and 7ns at 77K (Melkozernov *et. al.* 2000). Time-resolved studies have also been reported for the LHCI-730 fraction (Palsson *et. al.* 1995; Melkozernov *et. al.* 1998), but the measured fluorescence decay lifetimes were very short, on the sub-ns time-scale. This can be explained by the absence of detergent in the sample which is known to induce aggregation and a shortening of the lifetimes (Horton *et. al.* 1996).

The Lhca2/3 dimer could not be obtained either by reconstitution or purification from WT PSI. Therefore, only a mixture of native Lhca1/4 and Lhca2/3 (in the following named: LHCI) could be studied, giving information averaged over the two dimers (Ihalainen *et. al.* 2000; Gobets *et. al.* 2001a; Engelmann *et. al.* 2006). Time resolved fluorescence studies on this preparation have revealed that the fluorescence decay is multi-exponential, with a 2.7-3.0ns lifetime being the major decay component (Gobets *et. al.* 2001a; Engelmann *et. al.* 2006).

So far, accurate information about the excitation energy decay pathways of the native Lhca1/4 and Lhca2/3 dimers is lacking. Recently, the use of Lhca lacking mutant *A.thaliana* plants, allowed us to purify both native dimers: Lhca1/4 and Lhca2/3 (Wientjes and Croce 2011, Chapter 3). In this work we study the dimers by time-resolved fluorescence. We elucidate the inter-monomer energy transfer

rates and show that the fluorescence decays multi-exponentially for both dimers. The emitting dipole strengths of the dimers are determined in order to answer the question whether the CT state is indeed responsible for the low fluorescence quantum yield, as was proposed earlier (Ihalainen *et. al.* 2005a).

Materials & Methods

Lhca1/4 and Lhca2/3 isolation – Samples were isolated and characterized as in (Wientjes and Croce 2011, Chapter 3). In short: PSI from Lhca2 and Lhca1 lacking *A.thaliana* plants that only contained the Lhca1/4 or Lhca2/3 dimer, respectively (Wientjes *et. al.* 2009, Chapter 2) were solubilised and fractionated by sucrose density ultra-centrifugation. Using this method Lhca1/4 was obtained without any Lhca2/3 contamination, while the Lhca2/3 dimer was contaminated with only ~5% Lhca1/4 (Wientjes and Croce 2011, Chapter 3).

Steady-state spectroscopy – Absorption spectra were recorded on a Varian Cary 4000UV-Vis-spectrophotometer, Varian, Palo Alto, CA. For 77K measurements a home-built liquid N_2 cooled low-temperature device was used. Fluorescence spectra were recorded at 77K and 283K on a Fluorolog 3.22 spectrofluorimeter (HORIBA Jobin Yvon, Longjumeau, France). Samples were diluted to an OD of 0.04cm^{-1} at the Q_y maximum. All measurements were performed in 10mM tricine pH 7.8, 0.03% α-DM and 0.5M sucrose (room temperature (RT) and 283K) or 67% (w/v) glycerol for 77K measurements.

Streak camera measurements and data analysis – Streak-camera fluorescence measurements were performed with a set of lasers and a synchroscan streak-camera detection system as described in (van Oort *et. al.* 2009). In short, vertically polarized excitation pulses (475nm wavelength, 200fs duration, 0.2mW of power) with a repetition rate of 253kHz were focussed to a 150µm diameter spot in a static cuvette of 4 x 10mm at RT. The sample (absorption of 0.2cm^{-1} at Q_y maximum) was pumped through the cuvette with a flow rate of 4ml/min. Fluorescence light was collected at 90^o with respect to the excitation direction through a 630nm long-pass filter and a polarizer set at magic-angle orientation, and dispersed as a function of wavelength and time, using respectively a spectrograph and a synchroscan streak camera. Streak images were recorded on a CCD camera, the detection wavelength ranged from 560 to 810nm. Time windows of 160ps and 2.1ns were used. Images were corrected for background signal and sensitivity non-linearities of the detection system. The experimental data were

globally analyzed using the R package TIMP (Mullen and van Stokkum 2007), from 650 to 780 nm, with a spectral resolution of 5 nm, and the decay associated spectra (DAS) were estimated. The instrument response function was modeled as a Gaussian, the location in the time window and the full width at half maximum (FWHM) were free fit parameters. FWHM values of about 3 and 13ps were found for the 160ps and 2.1ns time window, respectively.

Target analysis yielded the Species Associated Spectra (SAS) of the individual Lhcas and the excitation energy transfer rates between the Lhcas. To be able to solve the model it was needed to constrain the spectra of the Lhca1 and Lhca2 compartment to zero for λ>760 where they are known to have little emission (Schmid *et. al.* 1997; Castelletti *et. al.* 2003). The ratio of forward and backward energy transfer between the monomers was estimated by requiring reasonable relative amplitudes of the SAS. For details on target analysis see (Stokkum *et. al.* 2004).

For the Lhca1/4 data the 160ps and 2.1ns time-window were linked in the analysis. For the Lhca2/3 data there was some difference in the kinetics obtained with the two time-windows, therefore the data-sets were analyzed separately. The results obtained on the 2.1ns data-set are shown (Fig. 3 and 4). It should be noted that the transfer component, which is the important part to solve the inter-monomer energy transfer, is nearly the same for the two time-windows. The difference is found in the spectrum of the ns component.

TCSPC – Time-correlated single-photon counting (TCSPC) of fluorescence was performed with a homebuilt setup, as described previously (Somsen *et. al.* 2005). The samples were diluted to an OD of 0.1cm^{-1} at the Q_y maximum, stirred in a 3.5ml cuvette with a path length of 1cm, and kept at 283K. Excitation was performed with a light pulse at 475nm and a repetition rate of 3.8MHz. Pulse energies of sub-pJ were used with a pulse duration of 0.2ps and a spot diameter of ~1mm. The instrument response function (~60ps FWHM) was obtained with pinacyanol iodide in methanol, with a 6 ps fluorescence lifetime (van Oort *et. al.* 2008). Fluorescence was collected at 90^{o} with respect to the excitation direction through a long-pass (530nm) and interference filter with FWHM of 10-15nm and transmission maxima as indicated in Fig. 4*C* and *D* (Schott, Mainz, Germany or Balzer B-40, Rolyn Optics, Covina, CA, USA). Individual photons were detected with magic angle polarisation by a microchannel plate photomultiplier, and arrival times were stored in 4096 channels of a multichannel analyzer, the channel time spacing of which was 5ps, resulting in a 20ns time window. Excitation intensity was reduced to obtain count rates of 30 000 s^{-1}, and care was taken to minimize data distortion.

The experimental data were globally analysed using homebuilt software (Digris *et. al.* 1999). The fit quality was evaluated from the χ^2, and from plots of the weighted residuals and the autocorrelation thereof. The steady-state fluorescence emission spectra were used to calculate the DAS.

Results

Steady state absorption and fluorescence – The RT absorption properties of Lhca1/4 and Lhca2/3 are similar (Fig. 1*A*), in agreement with the presence of red forms in both dimers, and the similar pigment composition (Wientjes and Croce 2011, Chapter 3). The red forms have a large effect on the fluorescence spectra, as apparent from the strong emission at wavelengths >700nm for both dimers (Fig. 1*B*).

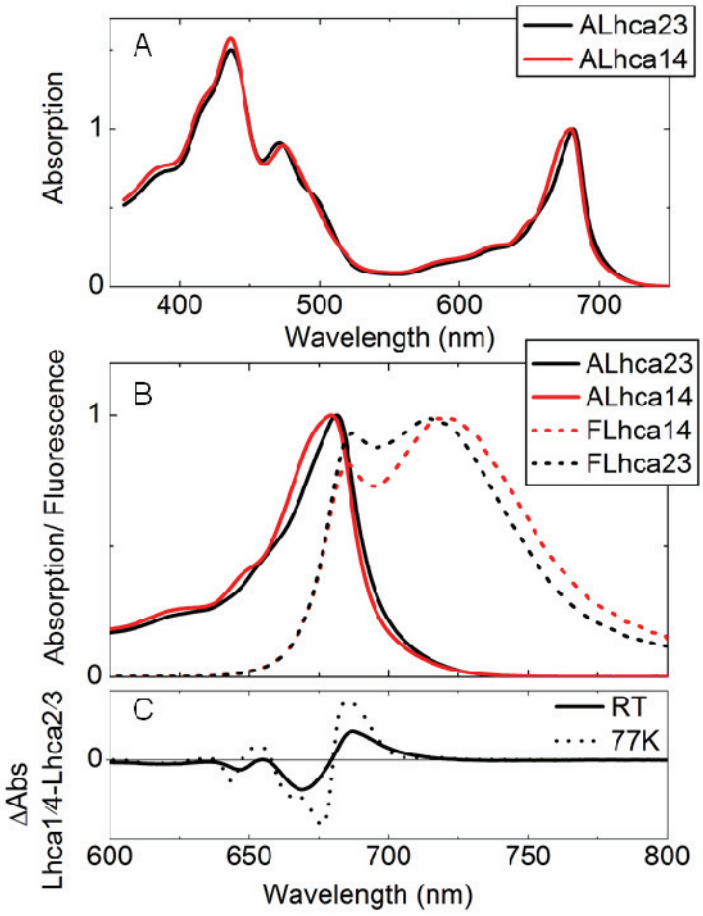

Figure 1: Steady-state absorption and fluorescence of Lhca1/4 and Lhca2/3. (*A*) RT absorption. (*B*) RT absorption and 283K fluorescence. (*C*) Difference between absorption spectra of Lhca1/4 minus Lhca2/3 (normalized to the same area in the Q_y region) at RT and 77K.

By zooming in on the Q_y region of the absorption spectra, clear differences can also be appreciated (Fig. 1*B*). Lhca1/4 shows stronger absorption at wavelengths shorter than 680nm, while Lhca2/3 absorbs stronger at longer wavelengths (Fig1. *B* and *C*). However, at wavelengths > 705nm where the red forms are mainly responsible for the absorption, the difference is small, especially at 77K (Fig. 1*C*). In order to get more detailed information about the absorption of the Q_y region, which in principle also defines the fluorescence emission, the spectra were described in terms of Gaussians. At 77K

the red most bands show maxima at 706-707nm and a FWHM of 25nm and they represent 8.5% and 8.9% of the total oscillator strength in the Q_y region (630-750nm) for Lhca1/4 and Lhca2/3, respectively (Fig. 2). A second red band with maximum at 689nm for Lhca2/3 and 684 nm for Lhca1/4 is needed to describe the spectra. Although the uncertainty is large due to the lack of structure in this spectral region, it is clear that the oscillator strength around 690nm is far stronger for Lhca2/3 than for Lhca1/4. This additional absorption can be assigned to Lhca2, which was shown to have a band around 690nm (Croce *et. al.* 2004), while Lhca1 has almost no absorption at this wavelength (Morosinotto *et. al.* 2002). The stronger absorption around 690nm is reflected in an increased fluorescence emission at this wavelength for the Lhca2/3 dimer, as compared to the Lhca1/4 dimer (Fig. 1*B*), and this can thus be assigned to a relatively stronger excitation population of Lhca2 as compared to Lhca1.

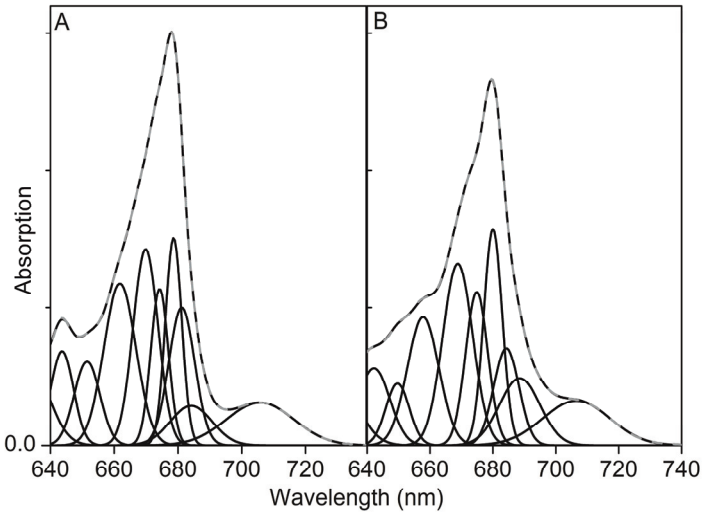

Figure 2: Gaussian description of LT absorption. The Q_y region of the LT absorption spectra (*grey dash*) of Lhca1/4 (*A*) and Lhca2/3 (*B*) described by Gaussian bands (*black*). Note that the fitting is meant to extract the characteristics of the red bands, using the restrictions as explained in the text.

Time-Resolved Fluorescence – To get a better insight in the excitation energy transfer dynamics of the two dimers, their fluorescence dynamics was studied by streak-camera and TCSPC measurements. Due to its narrow instrument response function (3ps fwhm) the streak-camera has a high time-resolution, whereas one measurement provides information over a broad spectral-range of 570-830nm. However, due to the short time window (2.1ns for the longest time range), the method is not very accurate for discriminating between fluorescence lifetimes on the ns time-scale. To better cover the entire decay process we also performed TCSPC measurements with a 20ns time window.

Lhca1/4 and Lhca2/3 show similar fluorescence kinetics – Fig. 3*A* shows examples of the spectral evolution from the Lhca1/4 and Lhca2/3 dimers measured with the streak-camera at RT. On the 160ps time-range (Fig. 3*A left*) a rapid decrease of fluorescence at ~690 nm can be observed, while there is a concomitant increase

of fluorescence at longer wavelengths, thus reflecting energy transfer. On the 2.1ns time-range (Fig. *3A right*) the overall fluorescence decay can be observed.

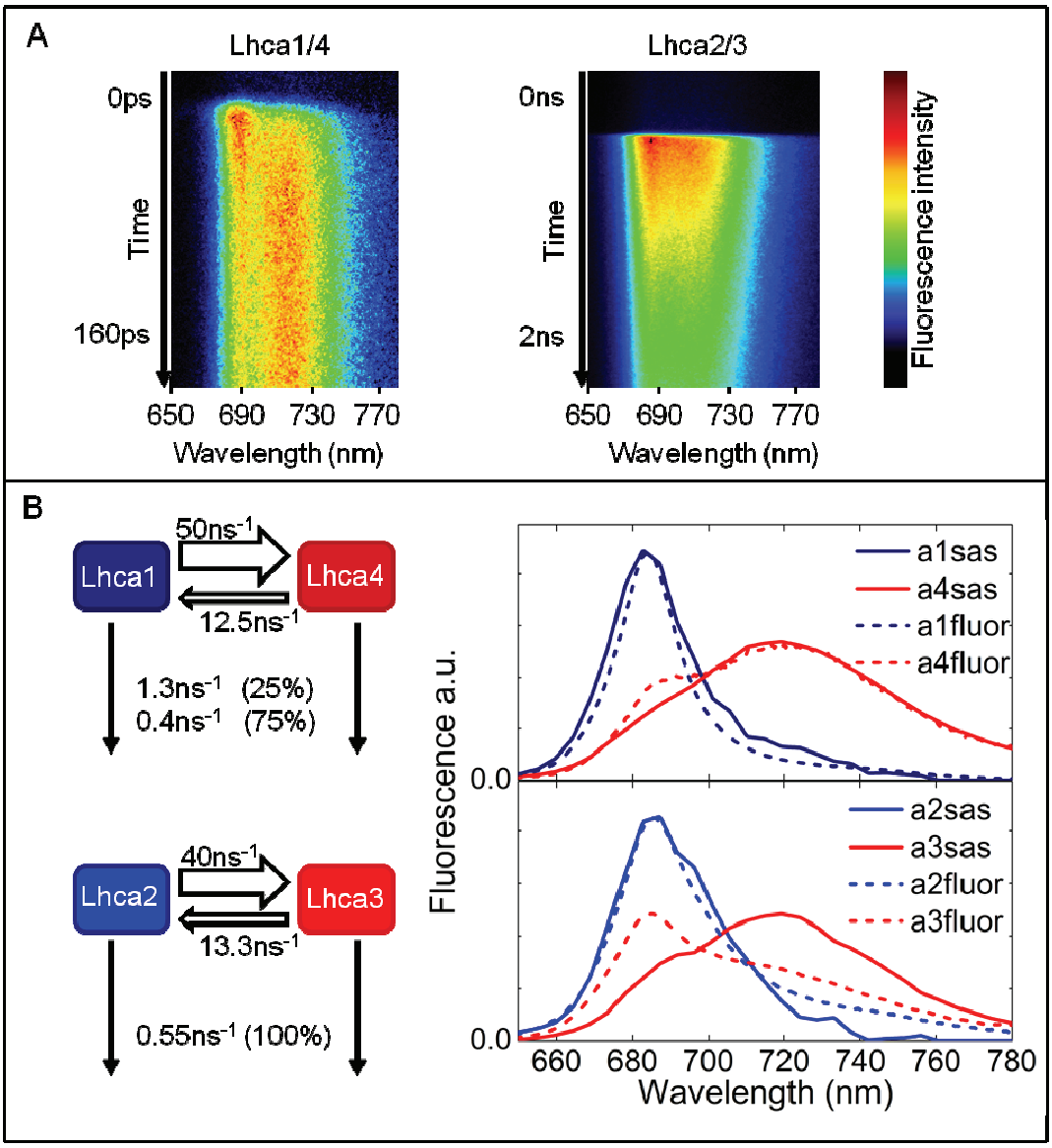

Figure 3: Streak camera measurements. (*A*) Example of streak images for the 160ps and 2.1ns time-window of Lhca1/4 and Lhca2/3 respectively, recorded at RT. (*B*) Excitation energy transfer and decay model (*left*), with rates (*left*) and SAS (*right*) obtained by target analysis. Fluorescence spectra of reconstituted Lhcas are also reported. Spectra of Lhca1-Lhca3 were recorded at RT, spectra of Lhca4 was recorded at 283K, which can slightly enhance the red emission due to a higher population of the red forms at lower temperature. Initial excitations at 475nm were estimated, for the Lhca1/4 dimer Lhca1 (56%) and Lhca4 (44%), and in Lhca2/3 Lhca2 (60%) and Lhca3 (40%). These values are in good agreement with the expected initial excitations based on the absorption and excitation spectra of the reconstituted Lhcas.

To solve in detail the fluorescence kinetics on the ps to ns range, global analysis was performed (see M&M) providing the decay associated spectra (DAS). The DAS (Fig. 4*A* and *B*) of both dimers are very similar. The spectra associated with a lifetime of 13-15ps have a positive amplitude peaking around 685nm and negative amplitude in the red, thus representing energy equilibration between bulk and low-energy Chls. It has been shown that in monomeric (m)Lhca4 bulk-red equilibration occurs in less than 5ps (Gibasiewicz *et. al.* 2005). This indicates that the 13-15ps component observed in the dimers mainly represents excited-state energy equilibration between Lhca1 and Lhca2, which do not have low-energy Chls, and Lhca4 and Lhca3, respectively. The fluorescence decay is largely described with a 2ns lifetime, but a second sub-ns component is also resolved.

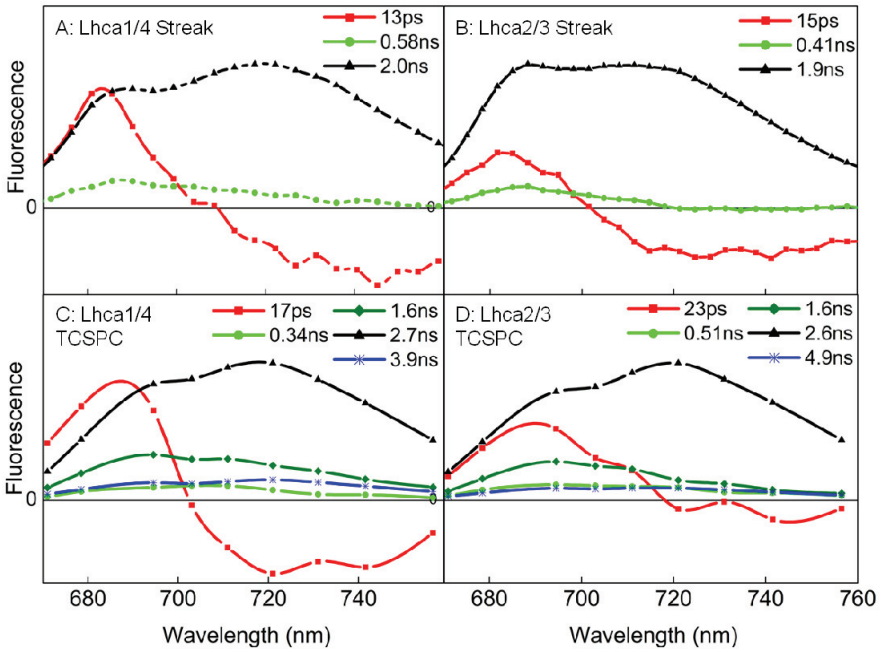

Figure 4: DAS of dimers. DAS of Lhca1/4 (*AC*) and Lhca2/3 (*BD*) estimated from streak- (*AB*) and TCSPC measurements (*CD*). Streak measurements were performed at RT, TCSPC at 283K, excitation was at 475nm.

Resolving the inter monomer energy transfer – The DAS are a mathematical description of the fluorescence decay, and they do not necessarily represent a physical part (for instance a pigment pool) of the sample. To extract more information about the "physical origin" of the observed fluorescence kinetics, target-analysis was performed. In this analysis the data is fitted to a compartmental model were the compartments represent the different physical parts of the system, see Stokkum et al. (2004) for a detailed description. Our model (Fig. 3*B left*) aims to resolve the excitation energy transfer rates between the individual Lhca complexes of each dimer. Solving such a model also gives the emission spectra of the different compartments (the SAS). It should be noted that the aim of the model is to solve the inter-monomer transfer rates. For details on the constraints that were used to solve the model, see M&M.

Fig. 3*B* shows the result of the fit. In this case the SAS are the emission spectra of Lhca1-4, which should thus be similar to the steady-state spectra of the reconstituted Lhcas. This is indeed the case for Lhca1, Lhca2 and Lhca4 (Fig. 3*B right*), only for Lhca3 the spectrum of the reconstituted complex shows less ~720nm emission than the SAS. This is probably related to the lower stability of reconstituted Lhca3 as compared to the other Lhcas, as is for instance apparent from its lower denaturation temperature (Morosinotto *et. al.* 2003).

In the Lhca1/4 dimer, energy transfer from Lhca1 to Lhca4 occurs with a rate of $50ns^{-1}$, whereas the backward transfer is four times slower (Fig. 3*B*). In the Lhca2/3 dimer the rate of transfer from Lhca2 to Lhca3 is $40ns^{-1}$ while the backward rate is 3 times slower (Fig. 3*B*). Thus, after equilibration only 25% of the emission arises from Lhca1 in Lhca1/4, while this is 33% for Lhca2 in the Lhca2/3 dimer. This is in agreement with the analysis of the steady-state spectra, which show stronger Lhca2 fluorescence emission as compared to Lhca1 emission (Fig. 1). The high excitation probability of Lhca3 and Lhca4 clearly shows the large effect of the low-energy Chls present in these complexes on the energy-transfer kinetics.

Table 1: Relative area of the DAS obtained by TCSPC. Relative Areas (A) of DAS (fig 5CD) are presented, as well as the averaged lifetime given by $\langle\tau\rangle = \Sigma A_i\tau_i$.

Lhca2/3		Lhca1/4	
0.5ns	8%	0.3ns	6%
1.6ns	16%	1.6ns	20%
2.6ns	70%	2.7ns	65%
4.9ns	7%	3.9ns	10%
<τ>	2.45ns		2.45ns

Multi-exponential decay – The fluorescence kinetics of Lhca1/4 and Lhca2/3 measured with the streak-camera shows a bi-exponential decay with time constants of around 0.5 and 2 ns. This is puzzling because from an equilibrated system the fluorescence decay is in principle expected to be mono-exponential. To study this in more detail TCSPC measurements were performed, which allow to estimate the longer lifetimes more accurately. Fluorescence decay traces were recorded at 9 emission wavelengths and were globally analyzed. The calculated DAS are presented in Fig. 4*C* and *D*. The streak and TCSCP measurements gave qualitatively similar results, but the TCSPC allowed to resolve five components: one transfer component and four decay components in the (sub-)ns range, thus confirming the multi-exponential fluorescence decay. The main component has a lifetime of 2.6-2.7ns for both dimers, in agreement with previous studies on LHCI (Gobets *et. al.* 2001a; Engelmann *et. al.* 2006). The DAS obtained by TCSPC allow for an accurate calculation of the average fluorescence lifetimes (table 1), which are 2.45ns for

both dimers. This value is far lower than that of Chl in solution (5.9ns table 2) and of LHCII (3.9ns, table 2), supporting the idea of partially quenched states of the dimers.

Are the red forms superradiant? – The analysis of the LT absorption spectrum of the dimeric Lhca complexes indicates that the red-most bands account for 8.5% and 8.9% of the LT absorption in Lhca1/4 and Lhca2/3, respectively. Assuming a number of 24 Chls per dimer (Wientjes and Croce 2011, Chapter 3), the absorption of the red forms corresponds to a dipole strength of ~2 Chls per dimer. It was shown that the red forms represent the lowest-energy state of a dimer of two excitonically coupled Chls *a* (603-609) in both Lhca3 and Lhca4 (Morosinotto *et. al.* 2003; Mozzo *et. al.* 2006). Taken together, this indicates that most of the oscillator strength of the exciton state of the coupled Chl dimer corresponds to the low-energy band. Because the low-energy state is heavily populated, it can be expected that the Lhca dimers have relatively large emitting dipole strengths and are thus superradiant. In agreement with this, we found that the area under the SAS (on a wavenumber scale), which correlates with the emitting dipole strength, is 1.7 times higher for Lhca4 than for Lhca1. However, it has also been proposed that the CT state quenches the fluorescence in LHCII aggregates (Miloslavina *et. al.* 2008) and Lhcas (Ihalainen *et. al.* 2005a). To investigate this further, the emitting dipole strengths were calculated according to equations 1 and 2 (Table 2).

$$k_{rad} = \frac{\Phi_{Fl}}{<\tau_F>} \qquad (1)$$

$$|\vec{\mu}|^2 = k_{rad} \frac{3\varepsilon_0 hc^3}{n16\pi^3 \nu^3} \qquad (2)$$

where k_{rad} is the radiative rate (in s^{-1}), Φ_{Fl} is the fluorescence quantum yield (taken from Wientjes and Croce 2011, Chapter 3) $<\tau_F>$ is the average fluorescence lifetime, $|\mu|^2$ is the emitting dipole strength (in C^2m^2), ε_0 is the vacuum dielectric constant (in C^2/Jm), *h* is Planck's constant (in Js), *c* is the speed of light in vacuum in (m/s), ν is the emission frequency in (s^{-1}) and *n* is the refractive index. Formula 2 was taken from (Palacios *et. al.* 2002).

The emitting dipole strengths of both dimers are higher than that of LHCII and 1.4-1.5 times that of Chl *a* in solution, meaning that both dimers are indeed superradiant. One should realize that this value of 1.5 is (even) a lower limit for the red band because of the contribution of "non-dimeric" Chl bands to the fluorescence. It has been suggested that in Lhca3 and Lhca4 mixing of the excitonic state with a dark CT state reduces the emitting dipole moment to a

value smaller than 1.0 (Ihalainen *et. al.* 2005a). Clearly, our present data are in disagreement with this finding.

Table 2: Fluorescence quantum yield, average lifetimes and calculated "average" emitting dipole strength.

Sample	Φ_F	$\langle\tau\rangle$ (ns)	$\langle\nu^3\rangle$* in cm^{-3}	Rad rate (ns^{-1}) †	Refractive index	Emitting dipole strength (relative to Chl a‡)
Chl a	0.30¶	5.9‖	3.19e12	0.051	1.36	1.00
Lhca1/4	0.14§	2.5‖	2.73e12	0.057	1.33	1.37
Lhca2/3	0.15§	2.5‖	2.76e12	0.061	1.33	1.46
LHCII	0.21§	3.9‖	3.05e12	0.054	1.33	1.16

*The average value $\langle\nu^3\rangle$ is obtained as described in (Palacios et al. 2002). †The radiative rate is calculated according: $k_{rad} = \Phi_F / \tau_{fl}$. ‡The emitting dipole moment is calculated according to $k_{rad} = (16n\pi^3\nu^3/3\varepsilon_0 hc^3)|\mu|^2$, the emitting dipole moment of Chl *a* is corrected for the somewhat different value of the refractive index (1.36 vs 1.33) according to the empirical relation: $D = 20.2 + 23.6(n-1)$ (D^2) (Knox 2003). ¶Taken from (Weber and Teale 1957). §Fluorescence quantum yields were obtained as reported in (Wientjes and Croce 2010). ‖Fluorescence lifetimes were obtained by TCSPC. For further details see (Palacios et al. 2002).

Discussion

The domain harbouring the Chl responsible for the red forms is conserved in the two dimers – A remarkable feature of the antenna complexes of PSI is the presence of Chls that absorb above 700 nm and which are associated with Lhca3 and Lhca4 (Croce *et. al.* 2007). The red forms represent the lowest-energy state of a dimer of two excitonically coupled Chls *a* (Morosinotto *et. al.* 2003; Mozzo *et. al.* 2006). In an excitonically coupled dimer the sum of the electronic oscillator strengths is identical to the sum of the oscillator strengths of the isolated molecules, but the oscillator strengths can be redistributed over the two transitions. The redistribution depends on the energy levels of the involved Chls, the distance between them, and the geometric arrangement of their transition dipoles (van Amerongen *et. al.* 2000).

The analysis of the absorption spectra of Lhca1/4 and Lhca2/3 indicates that the oscillator strength of the lowest-energy band corresponds to approximately 2 Chls, indicating that most of the oscillator strength corresponds to this low-energy band of the excitonically coupled Chl *a* dimer. This means that the transition dipole moments of the two interacting Chls must be more or less parallel and in

line (van Amerongen *et. al.* 2000). At the moment there are no Lhca structures available where the orientation of the transition dipole moments are assigned, thus a comparison is not possible. However the relative geometric organization of the transition dipole moments is expected to be similar as for those in LH1 and the special pair of purple bacteria (thus parallel and in line) (Roszak *et. al.* 2003; Koepke *et. al.* 2007), where indeed almost all the oscillator strength is on the low-energy bands of excitonically coupled bacteriochlrophyll dimers (Knapp *et. al.* 1985; Visschers *et. al.* 1991).

The red forms have nearly identical spectroscopic properties in both dimers (Fig. 1C and Wientjes and Croce 2011, Chapter 3), suggesting that their environment and organization must be very similar. This is at variance with the present structural data of PSI-LHCI (Amunts *et. al.* 2007; Amunts *et. al.* 2010), which show a very different pigment organization (both orientation and distance) of the domains responsible for the red forms in the two complexes, thus indicating that there is room for improvement in the LHCI structure.

Multi-exponential fluorescence decay of the Lhca dimers – The fluorescence decay of a homogeneous preparation of a light-harvesting antenna, where the excitation equilibration has been reached, is expected to be mono-exponential. However, in the case of the dimeric Lhca complexes, four rates are needed to get a satisfactory description of the TCSPC decay traces. Heterogeneity in the fluorescence decay of Lhca dimers was observed previously (Mukerji and Sauer 1993; Melkozernov *et. al.* 1998; Gobets *et. al.* 2001a; Ihalainen *et. al.* 2005a; Engelmann *et. al.* 2006). Several explanations were provided: i. the presence of three different dimeric Lhca complexes in the sample (Gobets *et. al.* 2001a), ii. the presence of four Lhca complexes in the native LHCI preparation (Engelmann *et. al.* 2006), iii. slow excitation equilibration between the bulk and low-energy pigments (Jennings *et. al.* 2004), and iv. a structural rearrangement in the excited state (Ihalainen *et. al.* 2005a). The first two explanations can be discarded because we analyzed one dimer at a time and still observed mutiexponential decay kinetics. The third option would require both slow downhill and uphill energy transfer, i.e. from the bulk pigments to the low-energy red forms and vice versa. The authors suggest (Jennings *et. al.* 2004) that the uphill energy transfer is slow due to the large energy difference. However, according to the detailed balance relationship, the downhill energy transfer should still be fast, which would mean that the equilibration rate is even faster. Therefore, slow uphill energy transfer cannot explain the multiple slow decay components. Ihalainen et al. (30) propose a structural rearrangement in the excited state of the Lhca complexes, to account for the 45-190ps DAS which deviates from a typical Chl *a* emission spectrum in the

sense that it lacks the vibronic wing. However, in our TCSPC experiments such a "deformed" spectrum could not be observed. Thus none of the proposed explanations can account for our observations.

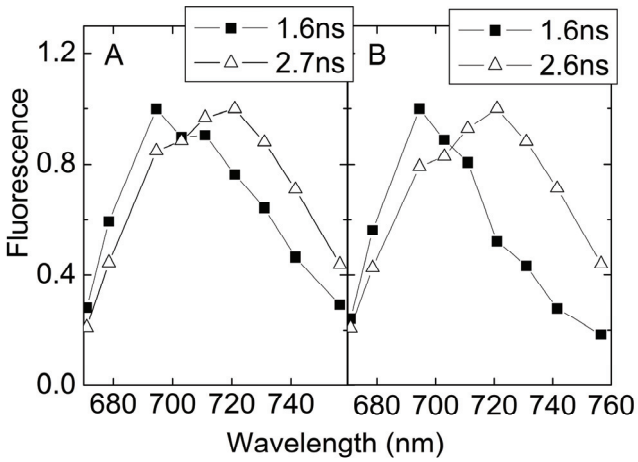

Figure 5: Red and blue DAS. Spectra estimated from TCSPC data of Lhca1/4 (A) and Lhca2/3 (B) associated with a lifetime of 1.6ns and 2.6-2.7ns. Spectra are normalized to each other in their maxima.

Lhca dimers adopt different conformations – The occurrence of a multi-exponential fluorescence decay was also found for the antenna of PSII, especially for the minor Lhcb complexes (Moya *et. al.* 2001) and for monomeric LHCII (van Oort *et. al.* 2007) and it has been proposed that it arises from the presence of various distinct conformations of the pigment-protein complex (Moya *et. al.* 2001). The fluorescence lifetime can be affected by pigment-pigment and pigment-protein interactions (Naqvi 1998; van Amerongen and van Grondelle 2001). Because these interactions are strongly dependent on the distances between the chromophores and molecular groups in their direct environment, small conformational variations can have a substantial effect on the fluorescence decay (see e.g. van Oort *et. al.* 2007). In addition, in Lhca complexes small conformational differences can have a strong effect on the emission spectra, because the red forms, which are the low-energy states of the system, originate from interactions (excitonic and charge transfer) which are strongly distance and orientation dependent. The spectra associated with the two main decay components of both dimers differ substantially (Fig. 5), with the 2.6-2.7ns component emitting more to the red than the 1.6ns (and 0.34-0.51ns) component. Similar observations were made for reconstituted Lhca4 (Passarini *et. al.* 2010). This can be explained by different conformations having different emission spectra and lifetimes. It should be noted that a protein is not a static scaffold, but a rather dynamic system. Spontaneous switching between conformations with different emission spectra has for example been observed for the homologous major light-harvesting antenna of PSII in a single molecule study (Kruger *et. al.* 2010). It can be concluded that the possibility to assume different

conformations and to exist in different quenching states is a property of all Lhc family members. Interestingly, in the case of the Lhcas, the different quenching states have different emission spectra. The redder spectra observed for the longer lifetimes indicate that the quenched conformation and the red conformation are mutually exclusive, as is also the case for reconstituted Lhca4 (Passarini *et. al.* 2010).

The presence of various emitting states can also explain why the RT fluorescence emission spectra of LHCI are different upon excitation of the bulk pigments as compared to excitation of the red band (720nm) (Jennings *et. al.* 2003a). In the first case both "red" and "non-red" conformations are excited, while upon 720nm only the "red" conformations are excited, thus resulting in a relative stronger red emission.

Energy transfer in PSI – The study of excitation energy transfer and trapping in PSI is extremely complex because the system is composed of ~170 Chl molecules, making the modeling of the fluorescence kinetics very challenging. The system is usually described using compartmental models in which the major building blocks (Lhca complexes, core complex, and reaction centre) are considered. Knowledge about the spectroscopic properties of the compartments is required for the evaluation of these models (Slavov *et. al.* 2008). Until now this information was not available for the native Lhca dimers. Modeling of time-resolved fluorescence data of PSI complexes led to the assignment of two spectra with very different fluorescence quantum yield and emission maxima to the red states of Lhca3 and Lhca4 (Slavov *et. al.* 2008). However, our experimental work shows that the fluorescence quantum yield of both dimers (Wientjes and Croce 2011, Chapter 3) and the emission maxima of Lhca3 and Lhca4 are very similar, thus suggesting that the model of Slavov *et al*. (2008) can be improved taking these new constraints into account.

The complete excitation energy transfer of PSI can be described by transfer between Lhcas, between Lhcas and the core, and trapping of excitation energy by the reaction centre. In this study we were able to resolve the inter-monomer energy transfer rates for both dimers. Transfer from Lhca1 and Lhca2 to, respectively, Lhca4 and Lhca3, occurs with a rate of 40-50 /ns. The backward transfer is 3-4 times slower, resulting in an equilibration time of 16-18ps. From time-resolved fluorescence measurements on PSI-LHCI it was concluded that the average excited-state lifetime is 10 $\pm$ 5ps longer when LHCI is excited than when PSI core is excited (van Oort *et. al.* 2008). This difference was mainly ascribed to the extra time that is needed to reach the reaction center when LHCI instead of the core is excited. This implies that the time of transfer from LHCI to core is in

the same order of magnitude as the equilibration time within the Lhca1/4 and Lhca2/3 dimer, meaning that Lhca1 and Lhca2 transfer a considerable part of their absorbed energy directly to the core and not to their dimeric partner.

Based on the highly similar absorption spectra and fluorescence kinetics it can be concluded that the basic light-harvesting properties are practically identical for both dimers, and thus the difference in energy transfer to the PSI core, if any, would be mainly determined by the connections between the Lhca dimers and the core complex.

The information of the isolated dimers will thus be helpful to finally understand the energy-transfer pathways in the complete PSI complex, which is with a quantum yield close to 100% the most-efficiently operating photo-electric nano-machine known to date (Nelson and Yocum 2006).

Acknowledgements

We thank Arie van Hoek and Rob Koehorst for technical support with the time-resolved fluorescence measurements, and Sergey Laptenok for help with the use of TIMP for the streak-data analysis. This work was supported by ‘‘De Nederlandse Organisatie voor Wetenschappelijk Onderzoek (NWO), Earth and Life Science (ALW)’’, through a Vidi grant (to R.C.).

Chapter 5

Conformational switching explains the intrinsic multifunctionality of plant-light harvesting complexes

Tjaart P.J. Krüger*, Emilie Wientjes*, Roberta Croce, and Rienk van Grondelle

*Equal contributions

This chapter is based on:

Proc Natl Acad Sci U S A (2011) 108:13516-13521.

Abstract

The light-harvesting complexes of photosystem I and II (Lhcas and Lhcbs) of plants display a high structural homology and similar pigment content and organization. Yet the spectroscopic properties of these complexes, and accordingly their functionality, differ substantially. This difference is primarily due to the charge-transfer (CT) character of a chlorophyll dimer in all Lhcas, which mixes with the excitonic states of these complexes, while this CT character is generally absent in Lhcbs. By means of single-molecule spectroscopy near room temperature we demonstrate that the presence or absence of such a CT state in Lhcas and Lhcbs can occasionally be reversed, i.e., these complexes are able to interconvert conformationally to quasi-stable spectral states that resemble the Lhcs of the other photosystem. The high structural similarity of all the Lhca and Lhcb proteins suggests that the stable conformational states that give rise to the mixed CT-excitonic state are similar for all these proteins, and similarly for the conformations that involve no CT state. This indicates that the specific functions related to Lhca and Lhcb complexes are realized by different stable conformations of a single generic protein structure. We propose that this functionality is modulated and controlled by the protein environment.

Introduction

Although conformational changes are essential for the function of proteins, little is known about their complex structural dynamics. Protein motions can partially be described by dynamic disorder in the crystalline, glasslike, or liquid states of matter (Weber 1975; Frauenfelder *et. al.* 1991; Lindorff-Larsen *et. al.* 2005). A feasible conceptual framework has been developed to visualize these dynamics as transitions between hierarchically ordered minima in the high-dimensional energy landscape of the protein (Frauenfelder *et. al.* 1979; Miyashita *et. al.* 2003). Such a landscape represents all possible energy states as a function of the protein's conformation. The local minima, which signify conformational substates (CSs), are divided by energy barriers into different tiers. The order of a tier is characterized by an average barrier height, a higher barrier of which corresponds to a lower rate of conformational transitions (Hofmann *et. al.* 2003). Protein-embedded pigments often serve as effective probes of conformational changes. In particular, strong intra-pigment interactions in pigment aggregates can considerably increase the sensitivity of the pigments to the local environment (Novoderezhkin *et. al.* 2007). As a result, transitions between CSs are reflected as changes in the pigment electronic states and can be observed as distinct shifts in their absorption and

emission energies. In conventional spectroscopy on large ensembles of proteins, energy equilibration after an excitation perturbation is monitored as the average of a very large number of possible trajectories on the energy landscapes of many similar proteins. In contrast, in single-molecule spectroscopy (SMS), the energy landscape of a single protein can be probed. For various pigment-protein complexes this technique has proven successful to identify conformational changes that occur at rates of 1–10 s^{-1} and which correspond to energy fluctuations of ~10–2500 cm^{-1} (van Oijen *et. al.* 1999; Jelezko *et. al.* 2000; Rutkauskas *et. al.* 2004; Rutkauskas *et. al.* 2006; Brecht *et. al.* 2008; Brecht *et. al.* 2009; Kruger *et. al.* 2010), dynamics that were irresolvable by ensemble techniques.

In this study, similar conformational fluctuations are examined for the photosynthetic pigment-protein complexes that constitute the light-harvesting antennae of plants. These light-harvesting complexes (Lhcs) are associated with two photosystems (PS), known as PSI and PSII. Upon absorption of a photon, the Lhcs are capable to transfer the excitation energy rapidly and very efficiently to the PSI or PSII core complexes, which are responsible for the primary photochemistry. The outer antenna of PSI comprises the four complexes Lhca1–4, which naturally assemble into the heterodimers Lhca1/4 and Lhca2/3 (Croce *et. al.* 2002; Ben-Shem *et. al.* 2003; Wientjes and Croce 2011, Chapter 3). The major outer antenna of PSII, often referred to as LHCII, is a trimer of any combination of the three very similar complexes Lhcb1–3, while the minor antenna consists of the three monomers Lhcb4–6, also known as CP29, CP26, and CP24, respectively. The proteins of all these complexes show a high structural homology (Jansson 1999; Liu *et. al.* 2004; Amunts *et. al.* 2007; Pan *et. al.* 2011) and coordinate the same pigments, viz., chlorophyll (Chl) *a* and *b* molecules and a few carotenoids in a comparable organization. Despite their structural and compositional similarities, Lhcas exhibit considerably red-shifted and broadened fluorescence emission with respect to Lhcbs. In Lhcas this property originates from a Chl dimer, Chls 603 and 609 (nomenclature as in Liu *et. al.* 2004) (Morosinotto *et. al.* 2003; Morosinotto *et. al.* 2005; Mozzo *et. al.* 2006), often called “red Chls”, which possesses a charge-transfer (CT) state that strongly mixes with the lower exciton states of the complex (Ihalainen *et. al.* 2003; Morosinotto *et. al.* 2003; Vaitekonis *et. al.* 2005; Croce *et. al.* 2007a; Romero *et. al.* 2009). The resulting low-energy states are often referred to as “red forms”. The degree of mixing and accordingly the emission maximum strongly depend on the local protein environment and in particular on the nature of the ligand of Chl 603 (Morosinotto *et. al.* 2003). Lhca1 and Lhca2, which contain the ligand histidine (H), have low-temperature emission maxima at 690 nm and 701 nm, respectively, while the ligand asparagine (N) in

Lhca3 and Lhca4 assists in shifting the maxima to 725 nm and 732 nm, respectively (Schmid *et. al.* 1997; Castelletti *et. al.* 2003). Changing in Lhca4 the ligand of Chl 603 from an N into an H, thus producing the mutant Lhca4-NH, shifts the low-temperature emission maximum to 686 nm, while an additional emission band is present at ~702 nm (Morosinotto *et. al.* 2003). When the CT character is absent, as in the case of all Lhcbs under normal conditions, the room-temperature emission peaks at ~682 nm. However, by applying SMS on LHCII trimers at room temperature we found that sometimes these complexes switch reversibly to emissive states that are reminiscent of Lhca (Kruger *et. al.* 2010). Moreover, it was suggested that the red emission exhibited by LHCII oligomers can be explained by a similar mixed electronic-CT state (Miloslavina *et. al.* 2008).

It is well established that Lhcb complexes have a dual function: apart from efficient light harvesting, they also participate in photoprotection by dissipating excess absorbed energy in high-light conditions. In LHCII trimers it has been proposed that this is accomplished by conformational switching between a light-harvesting and a dissipating state (Pascal *et. al.* 2005; Ruban *et. al.* 2007), while in the minor antennae formation of a carotenoid radical cation was suggested to be involved (Ahn *et. al.* 2008; Avenson *et. al.* 2008). Although a photoprotective role has been suggested for Lhca complexes as well (Alboresi *et. al.* 2009), little is known about the nature of this process in Lhcas, in particular whether the red Chls play an active role. Participation of the red Chls in singlet quenching has been disputed (Passarini *et. al.* 2010); however, these pigments may be involved in enhanced triplet quenching (Carbonera *et. al.* 2005; Croce *et. al.* 2007b). The general consensus is that the red states serve primarily or solely to significantly enlarge the absorption energy window (Rivadossi *et. al.* 1999).

This study particularly focuses on the energy fluctuations of the red Chls in dimeric and monomeric units of Lhca, and compares the spectral dynamics with those of Lhcbs obtained before (Kruger *et. al.* 2010). This is the first time, to the best of our knowledge, that individual Lhca complexes are investigated spectroscopically.

Materials & Methods

Sample Isolation – The Lhca1/4 and Lhca2/3 complexes were purified from *A. thaliana* plants as described before (Wientjes and Croce 2011, Chapter 3). The recombinant Lhca4-WT and Lhca4-NH complexes were obtained by overexpression of the *A.thaliana* (WT or NH mutant sequence) apoprotein in *E. coli* and subsequent refolding *in vitro* with spinach pigments as described in Ref. (Passarini *et. al.* 2010). The Lhca4-NH mutant was obtained by site-directed

mutagenesis, replacing the Chl-603 binding residue (N47) with a Histidine (Morosinotto *et. al.* 2003).

Experimental Conditions – A home-built confocal microscope was used to observe the fluorescence emission from single complexes. The experimental setup and data acquisition are described in detail in (Rutkauskas *et. al.* 2005; Kruger *et. al.* 2010). In short, pulsed excitation light at 630 nm from a Ti:Al_2O_3 laser source (Mira 900, Coherent) coupled to an optical parametric oscillator (OPO, Coherent) was used. A near-circular polarization was obtained by using a Berek polarization compensator (5540M, New Focus). Complexes were solubilized in 10 mM Tricine at pH 7.8 and 0.03% n-dodecyl-α-D-maltoside and diluted to a few pM. An immobilization substrate of 3-aminopropyltriethoxisilane (APTES, Sigma) or poly-L-lysine (PLL, Sigma) was used. For the Lhca1/4 dimers, excitation intensities of 40–240 W/cm^2 (equivalently 167–1000 nW) were used. Lhca4 complexes were irradiated with 0.3 μW and the other complexes with 1.0 μW. After immobilization, the sample cell was washed to remove freely diffusing complexes and was deoxygenated by means of the enzymes glucose oxidase and catalase in combination with glucose (all from Sigma). Measurements were performed at 7°C. Under the utilized conditions, single Lhca1/4 dimeric complexes could be illuminated continuously for tens of seconds and sometimes even a couple of minutes before irreversible photobleaching. Fluorescence emission spectra from large ensembles of complexes were recorded with a Fluorolog 3.22 spectrofluorimeter (Jobin Yvon-Spex).

Data Screening – A single quantum-coupled subunit of PSI was identified by the simultaneous fluctuation of the blue and red spectral bands as the result of fluorescence intermittency. A common irreversible spectral anomaly of complexes in the Lhc family is spectral bluing, characterized by spectra peaking between 650 nm and 670 nm (Kruger *et. al.* 2010). The fraction of complexes exhibiting spectral bluing was inversely related to the stability of the complex. Complexes displaying this behavior were disregarded. Spectral profiles consisting of two main spectral components were fitted with a double skewed Gaussian function.

Results

Emission Properties of Single Lhca1/4 Dimers – The fluorescence spectrum of a large ensemble of Lhca1/4 dimers in solution near room temperature is characterized by a broad, structureless, red band at ~720 nm, and a considerably narrower blue band at ~685 nm. Fig. S1 shows that the room-temperature ensemble-averaged spectra acquired from our SM setup and from a spectrofluorimeter were almost identical, suggesting that the single-molecule environment did not notably affect the average spectroscopic behavior of the complexes as compared to solubilized complexes. However, the spectral shape varied considerably from one complex to the next, in particular the spectral peak position and the relative contribution of the blue and red spectral components. We investigated the time dependence of these spectral properties by resolving the emission spectra on a timescale of 1 s. Large energy fluctuations were observed for the red band, exhibiting peak maxima between ~710 nm and ~735 nm, while the maximum of the blue band was confined to ~685 ± 3 nm (Fig. 1). Nearly 10% of the complexes exhibited large, resolvable spectral shifts of the red band, frequently covering a range of >10 nm (Figs. S2 and S3). These two figures suggest signs of correlated behavior between the peak position and intensity of the red bands. Indeed, considering that the blue and red spectral components originate from different Chl pools in the Lhca1/4 dimer, the intensity of the blue band is expected to scale positively with the energetic position of the red band after complete energy equilibration. Further investigation provided evidence that most complexes displayed such a correlation (Fig. 2*A*), with the exception of <1% of the investigated complexes (Fig. 2*B*).

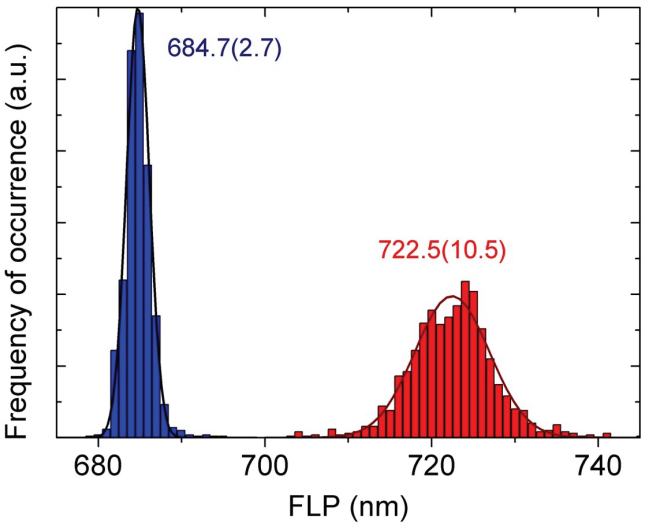

Figure 1: Distribution of fluorescence peak (FLP) of 66 individually measured Lhca1/4 dimers. An average of ~30 spectra was resolved from every complex. The left and right distributions correspond to the maxima of the blue and red bands of a double skewed Gaussian fit, respectively. Gaussian fits of the distributions are shown; values denote the maxima of these fits, with the FWHM indicated in parentheses.

Occasionally, a single Lhca1/4 dimer entered an emission state that was almost identical to the typical emission from Lhca1, as demonstrated in Fig. 3.

After a few seconds such a dimeric complex usually switched back to a state with emission properties identical to those of the original state (Fig. 3 and Fig. S4), or

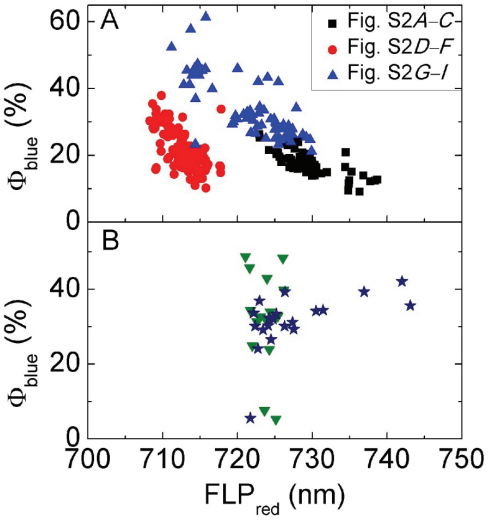

Figure 2: Relationship between the relative yield of the blue spectral component (Φ_{blue}) and the fluorescence peak of the red spectral component (FLP_{red}) of five single Lhca1/4 complexes. (*A*) Properties of the three complexes in Figs. S2 and S3. (*B*) Two examples of uncorrelated behavior.

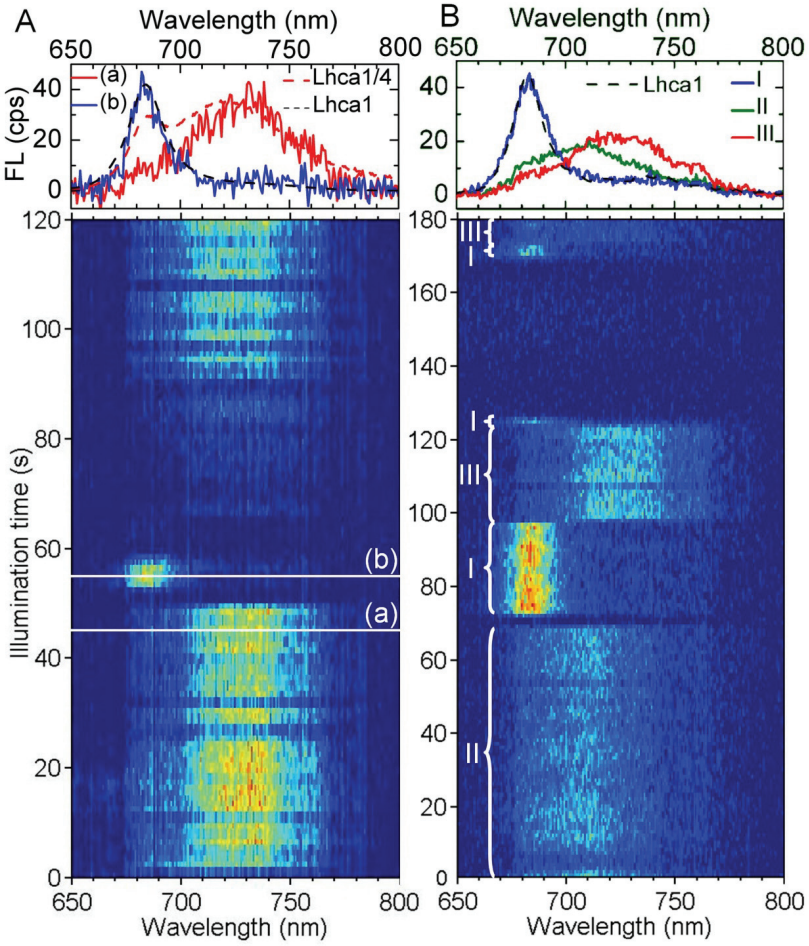

Figure 3: Representative examples of time-resolved fluorescence spectra from a single Lhca1/4 dimer which switched off its entire red spectral component. Spectra on top represent the spectra at the white, horizontal lines (*A*) or the averages of the fluorescence during the time indicated by I, II, or III (*B*). Black, dashed spectra and red, dashed spectrum (*A*) represent the normalized bulk spectrum at 10°C of an Lhca1 monomer and an Lhca1/4 dimer, respectively.

sometimes to a different low-energy state (Fig. 3*B*). Although the recovery of the emission was at times delayed by an excursion to a completely quenched state (Fig. 3*A*), the observed switches occurred within a single time step. This rate is noticeably faster than the energy fluctuations displayed in Fig. S2.

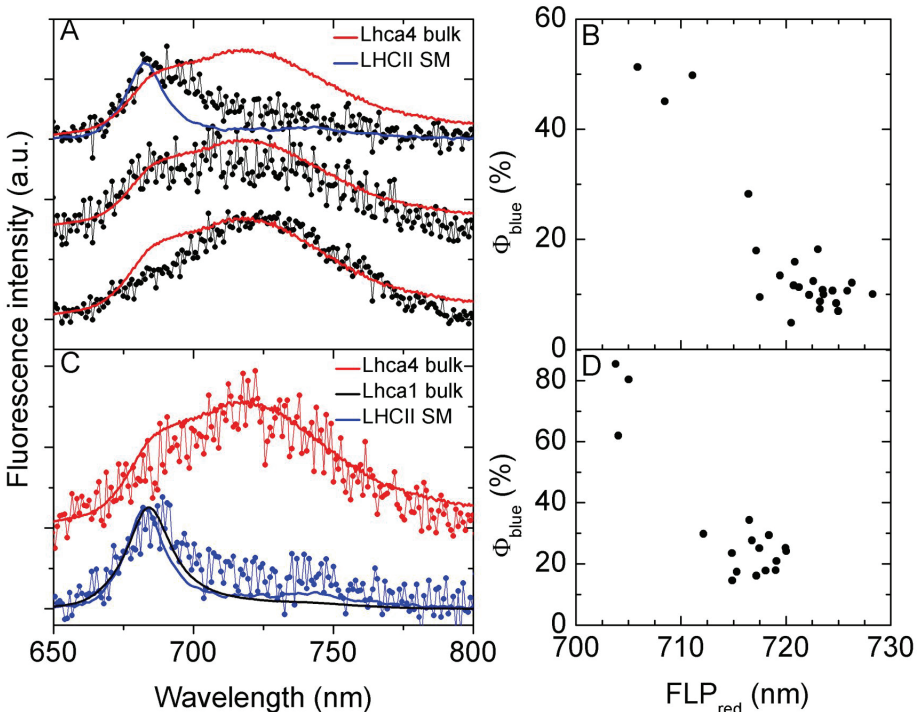

Figure 4: Time-resolved fluorescence spectra from two individually measured Lhca4 complexes. (*A*) Three different stages of spectral evolution from bottom to top, where averages were taken over spectra with similar profiles. The bottom two spectra were inter-reversible and the top spectrum represents the end state before photobleaching. Colored lines denote normalized spectra of bulk Lhca4 in solution at 10°C (red) and an LHCII trimer measured on the same single-molecule (SM) setup (blue). For clarity, spectra were shifted upward by constant factors. (*C*) Spectral profiles between which a single Lhca4 complex fluctuated reversibly. Thick, blue and red lines are defined as in (*A*). Black spectrum represents bulk Lhca1 in solution at 10°C. (*B,D*) Relationship between the relative yield of the blue spectral component (Φ_{blue}) and the fluorescence peak of the red spectral component (FLP_{red}) of the complexes in (*A*) and (*C*), respectively.

Emission Properties of Single Lhca4 Monomers – The low-energy emission of the Lhca1/4 dimer is known to originate from the red Chls of the Lhca4 monomeric subunit (Schmid *et. al.* 1997). It was of interest what the role is of Lhca1 in the observed spectral dynamics of Lhca1/4, and whether similar dynamics are exhibited when Lhca1 is absent. To this end, we investigated single Lhca4 complexes under the same conditions. Fig. 4 indicates that these complexes were also capable to exhibit significantly varying spectral shapes on timescales of >1 s. The dynamics were such that the fraction of blue emission correlated inversely

with the peak position of the red emission (see Fig. S5 for another example of strong correlation between these two spectral properties). Absence of such a correlation was not observed for this complex. Notably, the blue spectral profiles in Fig. 4*A* and *C* compare well with the blue emission profile of Lhca1/4 in Fig. S2*I*, all of which are characterized by a small red shift and pronounced red tail as compared to an Lhca1 bulk spectrum and a typical LHCII single-molecule spectrum.

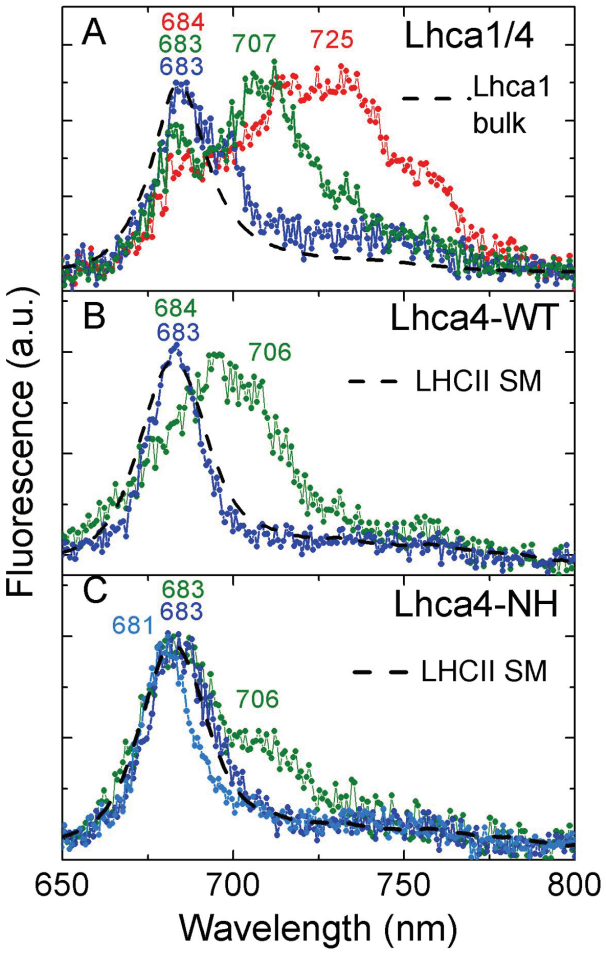

Figure 5: Different stages of spectral evolution of the emission from three individually measured complexes. Averages were taken over spectra with similar profiles. Maxima of fitted spectral components are indicated on top, with the colors corresponding to the spectra. (*A*) Spectra from a single Lhca1/4 dimer and compared to the normalized spectrum of bulk Lhca1 in solution at 10°C (black, dashed line). Red spectrum disappeared irreversibly and fluctuations continued between other two spectra. (*B*) Spectra from a single Lhca4 wildtype (WT) complex as compared to a single LHCII trimer under similar conditions (black, dashed line). (*C*) Spectra from a single Lhca4-NH mutated complex as compared to a single LHCII trimer under similar conditions (black, dashed line). Spectrum in light blue originates from a different single complex.

Figs. 4*A* and *C* suggest that Lhca4 is able to perform a transition from a state with emission at 720–730 nm to a state involving an emission band near 705 nm. Although no clearly reversible occurrence of such a transition was observed, a ~705-nm band is characteristically emitted by Lhca4 complexes and in particular by the Lhca4-NH mutant (Croce *et. al.* 2007a), and thus encouraged further investigation. Fig. 5 shows that not only single Lhca4 and Lhca4-NH complexes were capable to exhibit a ~705-nm band, but occasionally the broad ~720-nm band of a single Lhca1/4 dimer was replaced by a band at ~705 nm (Fig. 5*A*). For Lhca4 complexes, the ~705-nm emission appeared mostly since the onset of illumination. Remarkably, this band could be switched off and back on by each of

the complexes Lhca1/4, Lhca4, and Lhca4-NH under continuous illumination, where the switching occurred within a single time step. For the monomeric complexes, the spectral states lacking the 705-nm band were almost identical to the typical emission spectra of single Lhcb complexes, while for Lhca1/4 this state resembled emission from Lhca1.

Lhca4 complexes were significantly less stable than Lhca1/4 under the utilized conditions, surviving typically 2–3 times shorter before irreversible photobleaching and exhibiting a considerable fraction of spectral bluing (see M&M). Less than 10% of the measured Lhca4 complexes exhibited spectra that could be considered useful for our investigation. The fluorescence spectrum of a large ensemble of Lhca4 complexes in solution (Fig. S6) suggests that conformations with blue-shifted emission were favored under the utilized conditions. The Lhca4-NH mutant was even less stable under single-molecule conditions, with only ~5% of the investigated complexes which exhibited useful spectral information. Spectral states that resemble a typical Lhcb spectrum were most stable, and spectra that were typically ~20% narrower and ~2 nm blue-shifted as compared to an Lhcb spectrum were also observed frequently (Fig. 5*C*), though the irreversibility of the latter state points to an unnatural conformation.

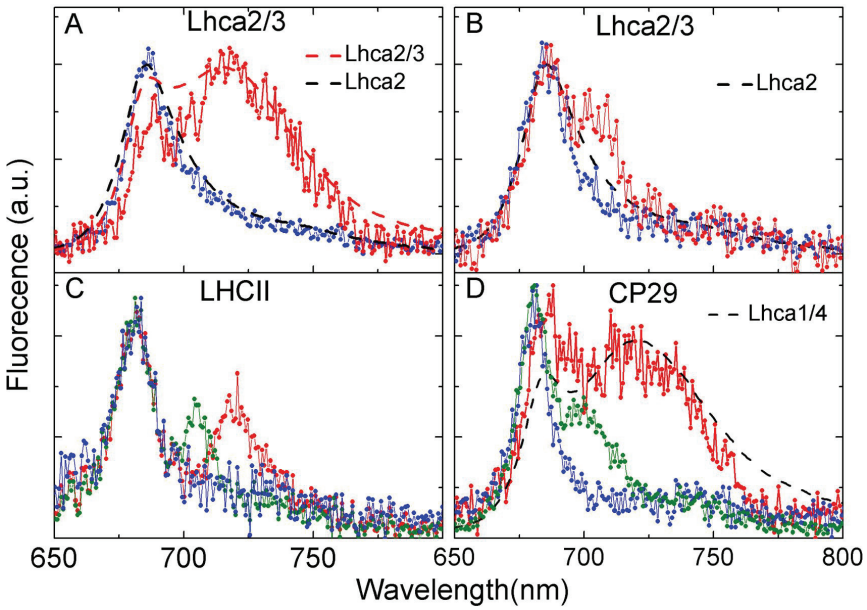

Figure 6: Representative spectra from individually measured Lhca and Lhcb complexes which switched reversibly between single- and double-band spectral profiles. Averages were taken over spectra with similar profiles. (*A,B*) Reversible disappearance of the ~720-nm band (*A*) or ~705-nm band (*B*) from an Lhca2/3 complex as compared to the bulk spectrum at 10°C of an Lhca2/3 dimer (red) and an Lhca2 monomer (black). (*C,D*) Spectral profiles from a single LHCII trimer (*C*) and two CP29 complexes (*D*) as compared to the bulk spectrum at 10°C of an Lhca1/4 dimer (black). Red and green profiles in (*D*) originate from different complexes.

Emission Properties of Single Lhca2/3 Dimers – In the utilized single-molecule environment, Lhca2/3 dimers exhibited a similar weak stability as the Lhca4-NH mutant. Nonetheless, the spectral dynamics showed much resemblance with those of Lhca1/4: the amount of blue emission correlated positively with the energy of the red emission band, and instances were observed where the ~720-nm band or a ~705-nm band disappeared reversibly within a single time step (Fig. 6*A,B*). The single, blue-band spectra now corresponded well to the emission from Lhca2 complexes.

Emission Properties of Single Lhcbs – Remarkably, Lhcb complexes have shown the exact opposite switching behavior between single- and double-band spectra as compared to Lhca complexes: occasionally, a strongly red-shifted emission band appeared temporarily in addition to the characteristic band at ~682 nm (Kruger *et. al.* 2010). In addition, similar to Lhca complexes, the spectral profile of the double-band state most frequently remained constant in time, but when it was altered, the energy of the red band correlated well with the intensity of the blue emission band. Fig. 6*C* and *D* show examples of double- and single-band emission spectra between which single Lhcb complexes switched reversibly. The red bands of Lhcbs were generally narrower than those originating from Lhca1/4 (Fig. 6*C*), but occasionally the widths were comparable (Fig. 6*D*).

Discussion

Spectral behaviour of single Lhcas – The measured fluorescence spectra are a direct reflection of the energy distribution within the complex at the time of photon emission, averaged over 1 s. Of particular interest are those spectral states that originate from the red Chls, i.e., the excitonic states that are coupled to the CT state of the Chl *a* dimer 603-609 (Morosinotto *et. al.* 2003; Romero *et. al.* 2009). Due to their admixed CT character these states have acquired the lowest energy (Ihalainen *et. al.* 2003; Novoderezhkin *et. al.* 2007) and thus contribute to the emission with the highest probability. In the Lhca1/4 dimer, most fluorescence originates from the red Chls of the Lhca4 subunit, and similarly for the red Chls of Lhca3 in the Lhca2/3 dimer.

The spectral behavior of the Lhca1/4 dimer, which was the most stable complex, will be considered first. The behavior exhibited by the Lhca2/3 dimer can be explained in an identical manner. The presented spectral dynamics can be classified into four categories: (i) A correlated relationship between the energy variations of the red emission and the relative yield of blue emission; (ii) Absence

of such a correlation; (iii) Disappearance of the red band within one experimental time step; (iv) Occasional shift of the red band from ~720 nm to ~705 nm within one time step.

For type (i) behavior, energy variations of the red band between 710 nm and 740 nm were observed, while the spectral fluctuations of the blue band were one order of magnitude smaller. The energy of the red states depends critically on the degree of mixing between the excitonic states and the CT state, which in turn is related to the energetic position of the CT state. Due to the nature of the CT states involving charges, these states interact strongly with their local environment. This strong environmental sensitivity is reflected by the large Huang-Rhys factors that have been estimated for the red emission on the basis of energy selective fluorescence experiments (Gobets *et. al.* 1994; Ihalainen *et. al.* 2003; Croce *et. al.* 2007a). The energy of the CT state is strongly affected by the distance between the red Chls, their relative orientation, and the local charge distribution. As such, subtle changes in the local protein environment can induce sizable shifts in the energy of this state. Indeed, it was shown previously that substitution of Asn, the natural ligand of Chl 603 in Lhca4, with a His, leaded to the loss of the red-most form due to a small increase in the distance between Chls 603 and 609 (Morosinotto *et. al.* 2003).

The protein energy landscape model provides an explicable framework to describe the observed energy fluctuations. The considerable amount of energy variations is a clear indication that these systems cannot be considered as rigid entities but that substantial underlying conformational disorder is involved and that the proteins are thus capable to traverse large extents of their energy landscapes. The considerable spectral heterogeneity can be explained by a large number of accessible quasi-stable CSs with different emission properties and differing energies in the energy landscape of the Lhca4 subunit. The large spectral heterogeneity suggests that either the transition frequency between different CSs was often irresolvable on our experimental timescale or that a quasi-continuum of possible energies exists, or a combination thereof. All cases involve relatively low energy barriers between the CSs, reflecting again the sensitivity of the red Chls to their local environment.

It is important to consider the intensity fluctuations of the spectral components in relation to fluorescence intermittency, a property shared by a large range of fluorescing systems and which denotes rapid intensity variations at irregular time intervals (Kulzer and Orrit 2004). Fluorescence intermittency originates from temporal energy dissipation via an energy trap which is intrinsic or coupled to the fluorescing system. Upon excitation of a pigment in Lhca1/4, the energy is equilibrated over the whole complex within ~15 ps (Wientjes *et. al.*

2011, Chapter 4). Due to this energy equilibration, an energy quencher at any site within the complex inevitably leads to energy dissipation. Fluorescence intermittency therefore affects all spectral components equally and is thus distinct from type (i) behavior.

According to the Boltzmann distribution, type (i) behavior is expected for a system in which the excitation energy is fully equilibrated. This is the case for the majority of Lhca1/4 complexes, considering that the main fluorescence lifetime component of ~2.5 ns (Wientjes *et. al.* 2011, Chapter 4) is two orders of magnitude larger than the timescale of energy equilibration (~15 ps). However, these values represent the averages of a broad distribution, thus allowing the possibility that the energy in a small fraction of complexes may not be equilibrated. Type (ii) behavior is expected only for such a non-equilibrated system and indicates that the rate of excitation energy transfer (EET) to the red Chls of Lhca4 is significantly reduced, probably due to some variation in the inter-monomeric distance. As expected, type (ii) behavior was not observed for isolated Lhca4 complexes.

Type (iii) behavior, reversible disappearance of the red band, is a particularly interesting property, and most likely involves a change in the nature of the red forms in Lhca4 such that the CT character was completely abolished. Such a conformation would involve that the inter-molecular distance of the red Chls is too large and/or their relative orientation is such that no partial charge transfer takes place, a similar situation as for Lhcbs. In addition, the low frequency of this transition and the quasi-stable emission states before and after the transition signify that the corresponding CSs are separated by relatively high energy barriers.

Type (iv) behavior, occasional shifts of the red band from ~720 nm to ~705 nm, will be considered with the aid of the Lhca monomers. Absence of the 705-nm band in Lhca4 mutants lacking either Chl 603 or Chl 609 (Morosinotto *et. al.* 2005) strongly suggests that this band originates from the red Chls of monomeric Lhca4 complexes. Indeed, there is a strong indication that all low-energy emission from Lhca complexes originates from the Chl dimer 603-609 (Morosinotto *et. al.* 2002; Morosinotto *et. al.* 2003; Croce *et. al.* 2004). The 705-nm species of wildtype Lhca4 and Lhca4-NH can thus be explained in a similar way as the low-emission state of Lhca4, viz., excitonic-CT mixing (Romero *et. al.* 2009), but corresponding to a different stable conformation that permits a smaller degree of mixing. For the Lhca1/4 dimer, type (iv) behavior can be explained by the Lhca4 subunit adopting a very similar conformation. This behavior could be considered a special case of type (i) behavior. The reversible disappearance of the 705-nm band within one experimental time step can therefore be explained in a similar way as type (iii) behavior. Consequently, the ability of an isolated Lhca4 complex to

reversibly switch off its 705-nm emission suggests that it should also be capable to reversibly switch off its emission at lower energies (type (iii) behavior). The natural arrangement of Lhca4 in the Lhca1/4 dimer possibly increases the probability of this behavior.

Conformational Switching Model – All the investigated dimeric and monomeric complexes of the Lhca family have shown the intrinsic ability (or very likely the possibility) to reversibly switch off their red emission. The most plausible explanation is a conformational switch of the Lhca4 complex or subunit between quasi-stable states with and without a CT character, and similarly for the Lhca3 complex or subunit. The reversibility of these switches strongly suggests that these states represent natural states that can be populated in vivo. The nearly identical structures of Lhca1 and -2 suggest an identical behavior of these complexes. This idea is supported by the observation that the Lhca4-NH mutant, which contains the same Chl 603-binding residue as Lhca1 and -2, showed a similar switching on and off of its red emission.

Based on the observed spectral dynamics, we propose in Fig. 7 a simplified protein energy landscape model of all Lhca monomeric complexes. The x-axis depicts the variable or set of variables that determines the emission wavelength of the complex. Tiers of three orders are shown. The highest tier consists of two CSs, one involving a mixed CT-exciton-state character and one without this property. These two CSs are separated by the highest depicted energy barrier, which has a very low probability to be crossed. The intermediate tier is shown only for states exhibiting a CT character and comprises six CSs in this cartoon. Transitions between these CSs are observed as spectral jumps of 1–15 nm. The conformation that corresponds to a ~705-nm emission band can be regarded as one of the relatively stable CSs in this tier. The lowest illustrated tier contains the smallest energy fluctuations. Transitions between the CSs in this tier occurred too fast (<1 s) and involved spectral shifts (typically <1 nm) that were too small to be resolved.

The spectral behavior of single, Lhcb complexes suggests that the energy landscapes of these complexes are conceptually similar to those of Lhcas, as demonstrated in Fig. 7. First, the spectral signature of Lhca in a blue conformation is almost identical to a typical Lhcb spectrum (Fig. 5). Second, the time-dependent properties of the red emission from Lhcb complexes display much resemblance with the emission from Lhcas. Third, for LHCII it was shown that all emission states above ~695 nm very likely involve a CT character and can be explained in an identical manner as for Lhcas (Kruger *et. al.* 2010). Fourth, upon switching into a red conformation, Lhcb complexes often remained in this state for tens of

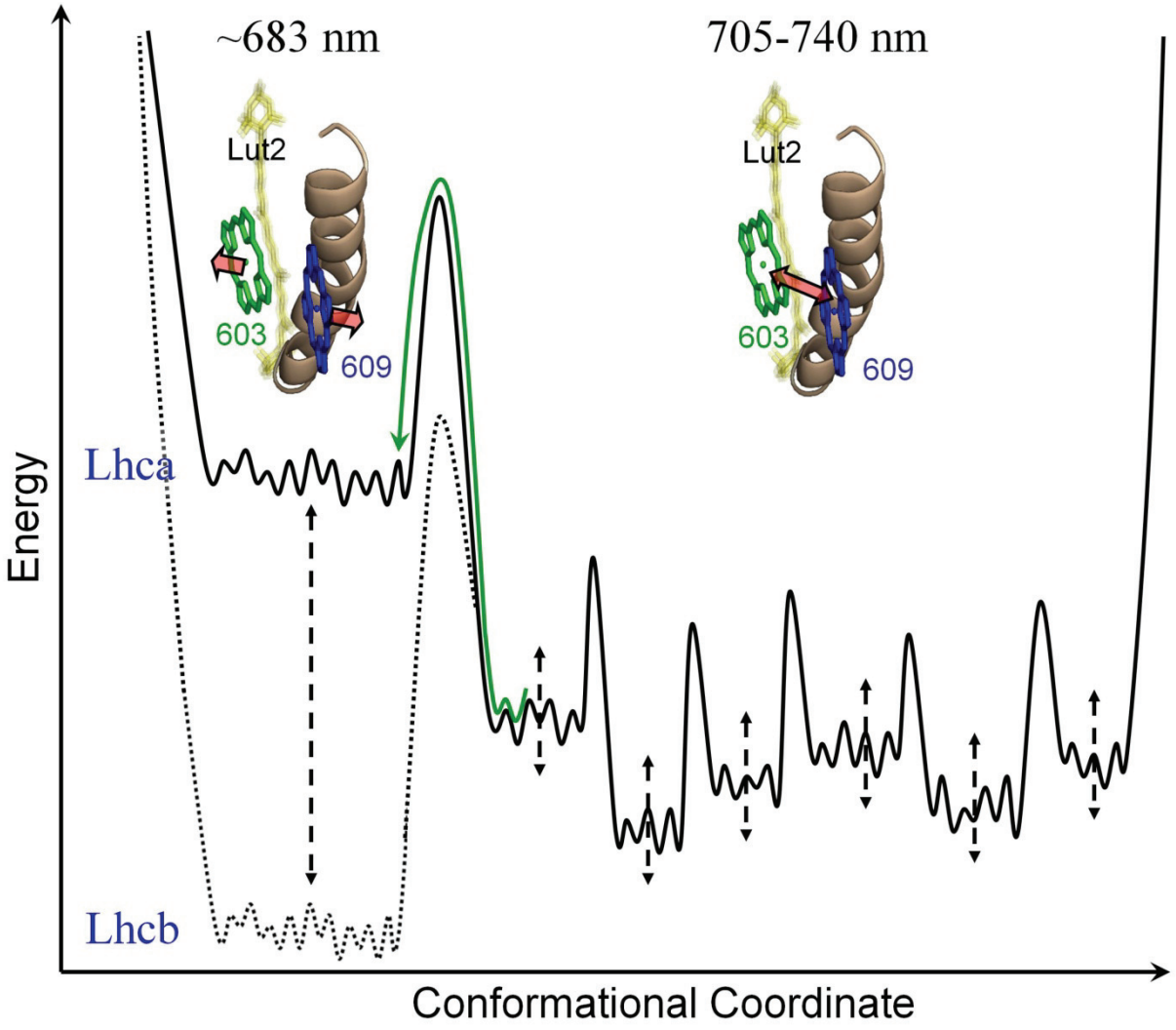

Figure 7: Cartoon of the energy landscape of a generic protein structure, representing the Lhc proteins of plants. The highest tier contains two quasi-stable conformational states, one of which involves no CT state (left) and the other which does (right). Tiers of lower order are explained in the text. The energy differences between the landscape of Lhca (solid line) and Lhcb (dotted line) are indicated only on the left. The dashed arrows indicate the energy differences induced by the local protein environment. A structural model (Ben-Shem *et. al.* 2003) of the protein domain in the vicinity of the red Chls of Lhca4 is shown. The position of the carotenoid lutein 2 (Lut2, blurred, yellow) is not resolved in this structure and was taken from Ref. (Liu *et. al.* 2004). The red arrows indicate interactions between red Chls, suggesting a negligible amount of mixing between the CT and exciton states when pointing away from each other. The values of the expected emission maxima associated with the different conformations are shown on top. The green arrow, which partially follows the curvature of the landscape, denotes a possible pathway of a conformational change during which the red emission is switched off. See text for details.

seconds, indicating stable red CSs, similar to the stable blue states of Lhcas. The major difference between the landscapes of Lhca and Lhcb can be regarded the relative energy difference between the CSs with and without a CT character.

In Fig. 7 the same conformational coordinates have been assumed for all Lhc complexes. Indeed, the property that all these structurally highly homologous complexes are capable of exhibiting very similar spectral dynamics suggests that the corresponding quasi-stable CSs are similar and that their entire energy landscapes are likely very comparable. A single protein structure thus suffices to describe to a high degree all the proteins in the Lhc family. Such a generic protein structure has the intrinsic ability to fluctuate among a large number of possible quasi-stable CSs of its energy landscape. We propose that the subtle structural differences of Lhcb proteins as compared to Lhca proteins are responsible for the former favoring the blue conformation and the latter favoring the red conformations. We also suggest that the equilibrium between the two conformations can be shifted by the local environment of a complex, altering the relative energy of the blue and red conformations, the extent of which is indicated by the vertical, dashed arrows in Fig. 7. In this way, the low-energy emission exhibited by Lhcb complexes under stress conditions and by oligomers of LHCII (Horton *et. al.* 1996; Niyogi 1999) is probably related to a small shift of the equilibrium to a red CS. Similarly, an Lhca complex can behave like an Lhcb complex when its blue conformation is favored.

Summary

We have illustrated that monomeric and dimeric Lhcs of plant PSI exhibit considerable spectral dynamics near room temperature, in particular their low-energy spectral components. PSI and II Lhcs can switch reversibly to spectral states that resemble the complexes of the other PS, strongly suggesting fluctuations between conformations with and without red forms. The remarkable similarity in structure and spectroscopic dynamics of these complexes suggests that a single protein structure can represent very well the protein of each of the complexes in the Lhc family. We propose that a subtle perturbation in the physico-chemical environment can shift the equilibrium to favor either the blue or the red conformational state, and that this generic protein structure is stabilized in particular conformational states to exhibit the specific functionalities related to Lhca and Lhcb proteins. More generally, the results of this study show that the multifunctionality of a protein can be realized via the control that the environment exhibits over the intrinsic disorder of the protein.

Acknowledgments

The authors express their gratitude to Francesca Passarini for reconstituting Lhca4-WT and Lhca-NH. This work was supported by grants from: EU FP6 Marie Curie Early Stage Training Network via the Advanced Training in Laser Sciences (ATLAS) project (T.P.J.K.); the Netherlands Organisation for Scientific Research (NWO) via the Foundations of Chemical Sciences (T.P.J.K. and R.v.G.); Earth and Life Sciences via a Vidi grant (E.W. and R.C.); Laserlab Europe.

Supporting Information

Figure S1: Fluorescence spectra of ensembles of Lhca1/4 complexes measured in different ways upon 630-nm excitation. A bulk solution measured at room temperature with a spectrofluorimeter (black), and with the single-molecule apparatus (grey).

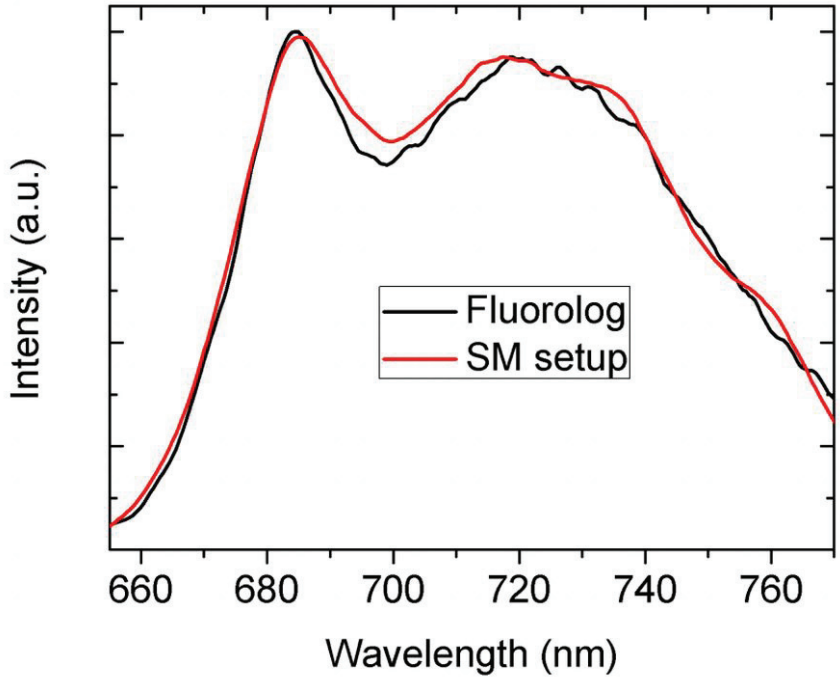

Figure S2: Three representative examples of time-resolved fluorescence spectra from a single Lhca1/4 dimer under continuous illumination. Each of *A-C, D-F*, and *G-I* corresponds to one complex. Fluorescence spectral peak (FLP) (*A,D,G*) and intensity (*B,E,H*) of the red and blue spectral components (red and black circles, respectively). Intensity is expressed in 1000 counts per second (kcps) and is integrated over all wavelengths. Correlated fluctuations in the intensity of the blue and red spectral components are indicated by black arrows. The presence of such correlations signifies that the emission originated from a single coupled system. Apart from this behavior, the wavelength of the red spectral component often correlates with its intensity and anti-correlates with the intensity of the blue spectral component. (*C,F,I*) 1-s resolved fluorescence spectra which correspond to the dashed lines in the upper panels with the corresponding color. Black spectra represent a normalized bulk spectrum of Lhca1/4 at 10°C, or of Lhca1 in (*I*) (dashed line). Green spectra and corresponding bulk spectra are shifted by 15 cps for clarity.

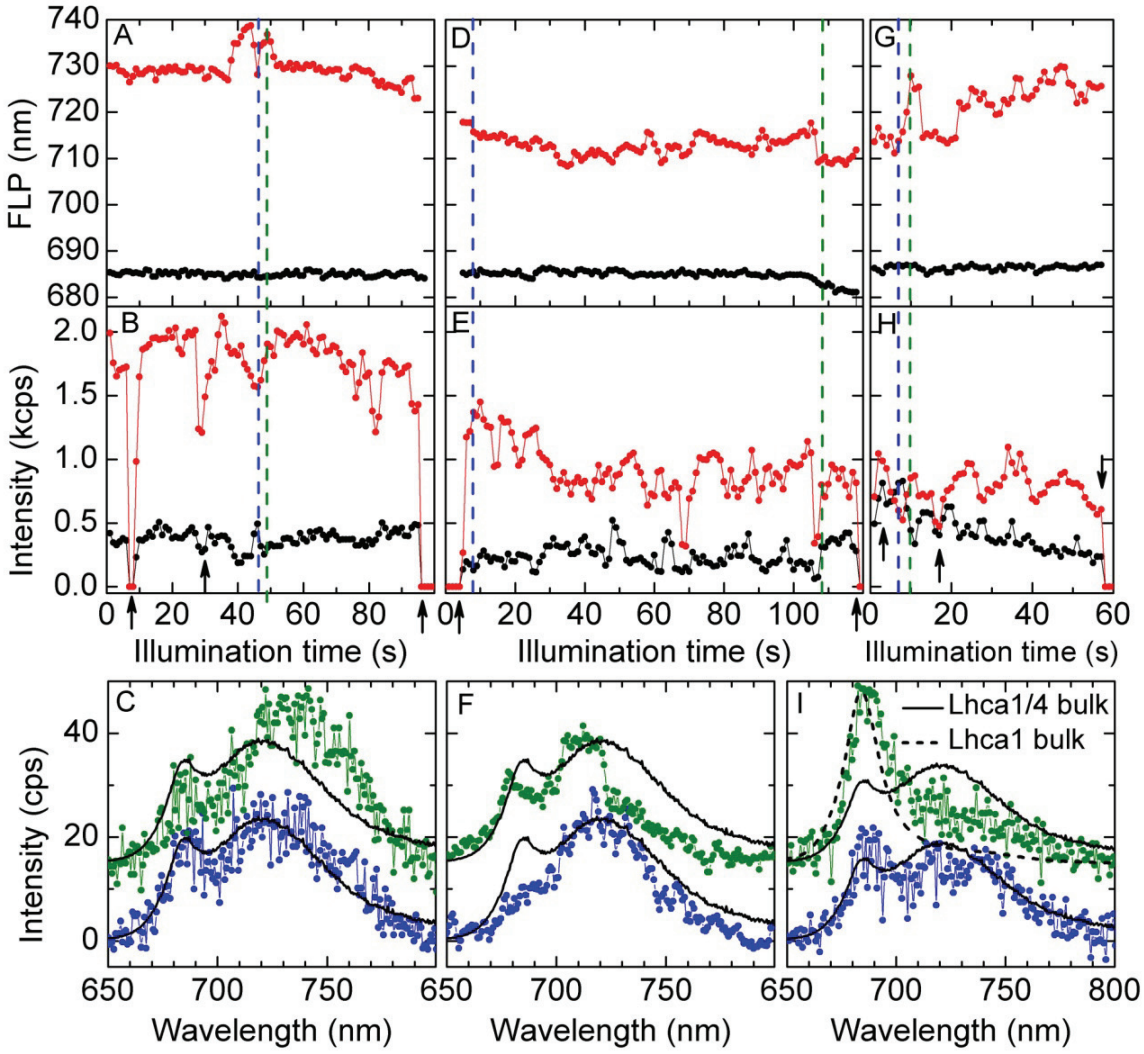

Figure S3: Time-dependent alterations of the fluorescence spectral profiles of the same complexes used in Fig. S2, indicating strong fluctuations of the spectral shapes. (*A,B*), (*C,D*) and (*E,F*) correspond to Fig. S2*A-C, D-F, G-I*, respectively. (*A,C,E*) Spectral time traces, with the peak positions denoted by black circles and the extents of the peak variations by the black dashed lines. Spectra on top represent the fluorescence intensity (FL) in counts per second (cps) at the horizontal dashed line with the corresponding color. The black spectra represent a normalized bulk spectrum of Lhca1/4 at 10°C, or a bulk spectrum of Lhca1 (dashed line in *E*). Red spectrum in (*A*) is shifted by 10 cps for clarity. (*B,D,F*) Full width at half maximum (FWHM) (black) and skewness (a measure of the asymmetry of the spectrum) (green) of the red spectral bands in (*A,C,E*). The FWHM of the red band is often correlated with its emission peak (Fig. S2*A,D,G*), while the largely fluctuating skewness exhibits a more complex behavior.

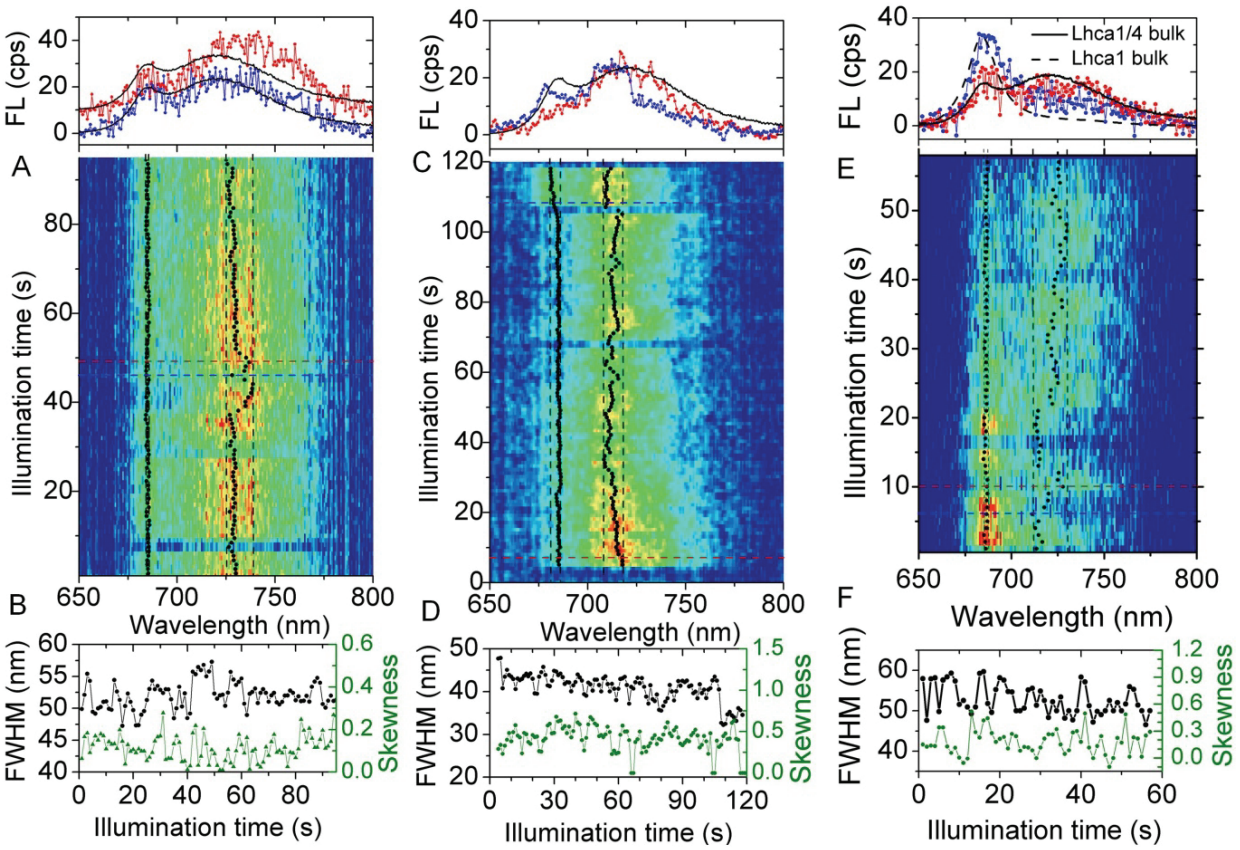

Figure S4: Representative example of time-resolved fluorescence spectra from a single Lhca1/4 dimer which switched off its entire red spectral component. Spectra on top represent the spectra at the white, horizontal, dashed lines. Black, dashed spectrum and red, dashed spectrum represent a bulk spectrum at 10°C of an Lhca1 monomer and an Lhca1/4 dimer, respectively.

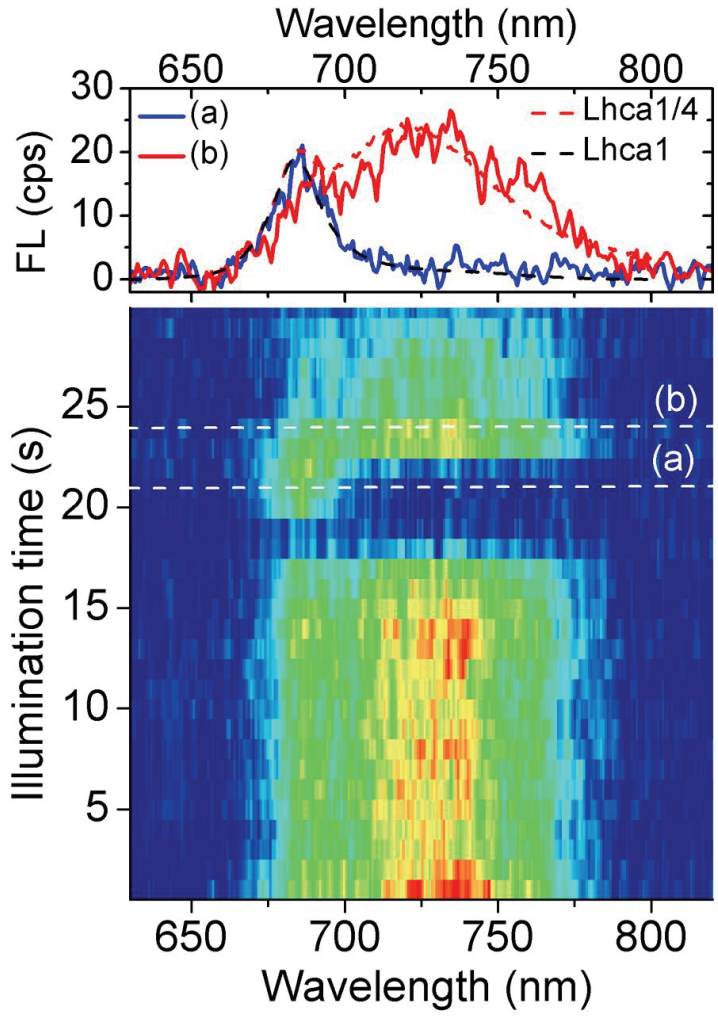

Figure S5: Relationship between the relative yield of the blue spectral component (Φ_{blue}) and the fluorescence peak of the red spectral component (FLP_{red}) of a single wildtype Lhca4 complex.

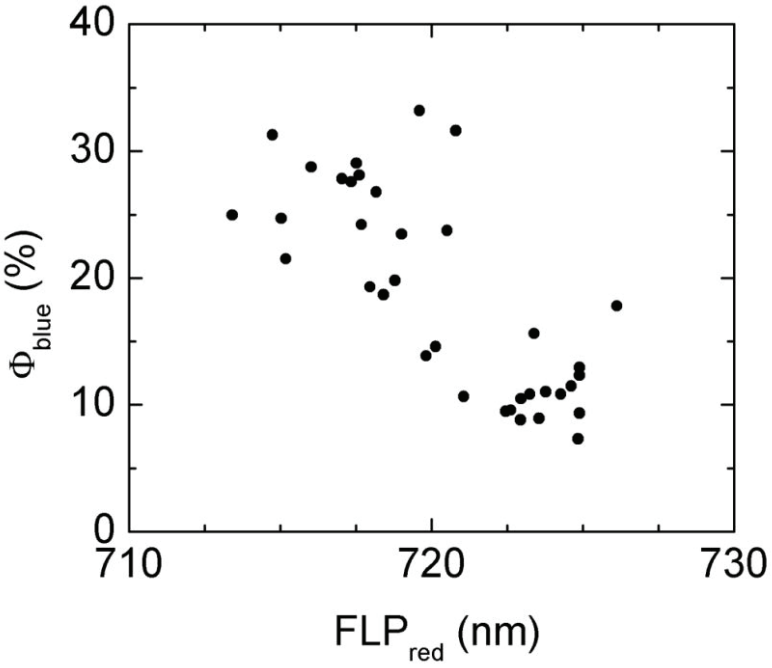

Figure S6: Fluorescence spectra of large ensembles of Lhca4 wildtype (WT) complexes measured in different ways upon 630-nm excitation. A bulk solution measured at 10°C with a spectrofluorimeter (black), and with the single-molecule apparatus (gray).

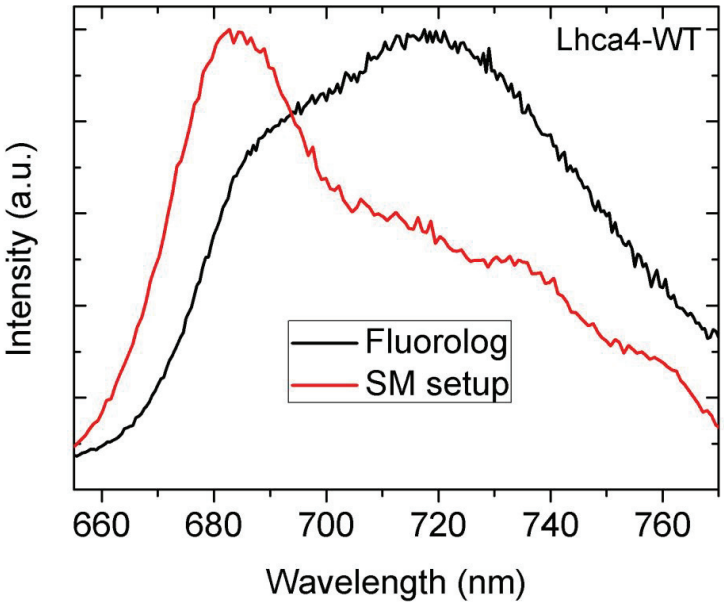

Chapter 6

From red to blue/far-red: how does the protein modulate the spectral properties of the pigments?

Emilie Wientjes, Gemma Roest and Roberta Croce

Abstract

Photosynthesis is driven by light energy which is absorbed by photosynthetic pigments, the majority of which is coordinated to light-harvesting complexes (Lhcs). The Lhcas are associated with Photosystem I and the Lhcbs with Photosystem II. The role of the protein is to organize the pigments and to tune their spectroscopic properties in terms of site energy and excited state lifetime, as such regulating light harvesting. In this work we investigate how the protein environment modulates the spectroscopic properties of the pigments by using a single-point-mutation approach. We monitor changes in the properties of the low-energy absorption/emission band typical of Lhca4, which is well separated from the bulk absorption and thus represents a perfect model system. Moreover, it was recently shown that Lhca4 exists in at least two different conformations, a dominating one with emission at 720nm and a second one with emission at 685nm, which strongly resembles that of Lhcb complexes. Here we show that the substitution of the asparagine which coordinates Chl 603 for a glutamine, moves the equilibrium almost completely towards the 685nm-conformation. This indicates that even very small changes in the protein can have a large effect on the properties of the pigments. We also show that making single amino acid substitutions allows to tune the emission spectrum of the pigments over a wide range of wavelengths. Implications of these findings for the improvement of the efficiency of photosynthesis are discussed.

Introduction

Photosynthesis is the process in which light energy is used to convert CO_2 into organic compounds. It occurs in plants, algae and photosynthetic bacteria. In the first steps light is absorbed by pigments, which transfer the excitation energy to the reaction centre (RC), where charge separation occurs. The pigments are phycobilins, carotenoids and chlorophylls (Chls) (e.g. Blankenship 1992). The pigments are generally coordinated by proteins, which keep them at appropriate orientation and distance with respect to each other and with respect to the protein itself, and hence determine the pigment environment. The environment influences the excited-state energy level of the pigments leading to blue/red shifts and broadening of their absorption spectra (e.g. Fowler *et. al.* 1992; van Amerongen *et. al.* 2000). In this way a small variety of pigments can be used to absorb light over a broad spectral range.

Pigment selection and tuning can improve the match between the absorption spectrum of the photosynthetic complexes and the irradiation spectrum, as is

nicely demonstrated for photosynthetic micro-organisms living in different spectral niches (Stomp *et. al.* 2007). Furthermore, tuning of the Chl excited-state-energy level is important for the efficiency of excitation-energy transfer to the RC. For instance, in purple photosynthetic bacteria chemically identical bacteriochlorophylls *a* can absorb light at very different wavelengths, which ensures that light energy absorbed by external antennas is efficiently funneled "down-hill" to the inner antenna, and onto the RC (e.g. Cogdell and Gardiner 2001).

In higher plants Chl *a*, Chl *b* and carotenoids (Cars) are coordinated by light-harvesting complexes (Lhcs). Upon absorption of a photon by an Lhc, excitation energy is efficiently transferred to the RC located in the core complex of Photosystem I (PSI) or Photosystem II (PSII). There are four PSI antennas (Lhca1-4), which are organized as two hetero-dimers: Lhca1/4 and Lhca2/3 (Knoetzel *et. al.* 1992; Croce *et. al.* 2002b; Ben-Shem *et. al.* 2003; Wientjes and Croce 2011, Chapter 3). The six PSII antennas are named Lhcb1-6. Lhcb1-3 form the major trimeric antenna, called LHCII. Lhcb4-6 are the minor monomeric Lhcs, also named CP29, CP26 and CP24, respectively (Jansson *et. al.* 1992).

All Lhcs are encoded by the Lhc gene family (Jansson 1999). Based on the available Lhca and Lhcb crystal structures, it can be inferred that they share their protein fold and have a similar Chl organization (Kühlbrandt *et. al.* 1994; Ben-Shem *et. al.* 2003; Liu *et. al.* 2004; Amunts *et. al.* 2010; Pan *et. al.* 2011). In Lhcbs the Chls *a* Q_y transitions show a maximum in the 660-680nm range (Jennings *et. al.* 1993; Nussberger *et. al.* 1994). For Lhcas this range is extended to the red. The most red-shifted absorption band is found in Lhca4, at 708nm (Croce *et. al.* 2007a). Absorption at long wavelengths can be important under a canopy where light is enriched in λ > 700nm (Rivadossi *et. al.* 1999). Furthermore, these low-energy Chls have a high probability to be populated upon excited-state equilibration and can thus play an important role in photoprotection (Karapetyan *et. al.* 1999; Carbonera *et. al.* 2005; Alboresi *et. al.* 2009).

In the past decade it was discovered that the low-energy Chls, also called red forms, of all Lhcas originate from the low-energy band of the excitonically coupled Chl *a* 603-609 dimer (nomenclature as in Liu *et. al.* 2004) (Morosinotto *et. al.* 2003; Morosinotto *et. al.* 2005; Mozzo *et. al.* 2006), mixed with a charge-transfer (CT) state (Ihalainen *et. al.* 2003; Romero *et. al.* 2009). Mixing with the CT state explains the large change of dipole moment in the excited state, which leads to: (i) a large contribution of optical transitions into higher vibronic sub-states, (ii) a large Stokes shift, and (iii) a large homogeneous broadening by strong coupling of the electronic transition to the phonons of the protein (van Amerongen *et. al.* 2000; Croce *et. al.* 2007a). Because both, excitonic interactions and CT states, are

strongly dependent on inter-pigment distance and orientation, the red forms are very sensitive to conformational variations in the protein, which give rise to large inhomogeneous broadening of the absorption and emission spectra.

The red forms give a strong contribution to the fluorescence emission spectra. For all Lhcbs the emission maxima are found at ~680nm, while for Lhca4 the emission maximum is observed at 720nm at 283K (Passarini *et. al.* 2010) and shifts to 732nm at 77K (Schmid *et. al.* 1997). Based on time-resolved fluorescence measurements it was proposed that Lhca4 can occur in different conformations: a "blue" (maximum at 680-690nm) conformation with a relatively short excited state lifetime and a "red" (720nm) one with a long lifetime (Passarini *et. al.* 2010). The existence of different emission states was recently confirmed by single molecule fluorescence spectroscopy, that showed that the "red" emission from an Lhca complex can occasionally switch to a typical "blue" Lhcb spectrum, while a "blue" Lhcb complex can switch to a typical "red" Lhca emitting state (Kruger *et. al.* 2011). The reversible disappearance of the red band was explained by a conformational change of the protein, involving an increase of the inter-pigment distance and/or a change of the orientation of the Chls responsible for the red forms such that the CT-exciton state is lost. The red emission from Lhcb complexes can be explained in an identical manner, with a conformational change bringing Chls 603 and 609 closer together. For Lhca complexes the equilibrium lies at the red-emitting side, while for Lhcb complexes it lies at the blue-emitting one (Kruger *et. al.* 2010; Kruger *et. al.* 2011).

In this work we investigate how the protein environment influences the excited-state energy levels of Chls. The focus is on the red Chls of Lhca4, for which potential changes are easy to observe as their absorption and emission bands are well separated from those of the bulk Chls. Site-directed mutagenesis and *in vitro* reconstitution were used to obtain Lhca4 complexes with single amino acid substitutions in the vicinity of the red Chls and different effects that can influence the Chl excited-state-energy level have been investigated:

(i) Influence of changes in the pigment organization. We investigate how large the change in pigment organization must be to lose the red forms of Lhca4 and thus to convert a typical Lhca complex into a typical Lhcb complex. This will provide information about the extent that the protein conformation is changing when it spontaneously switches between the "blue" and the "red" emitting states, and thus about the flexibility of these proteins. The flexibility of Lhc complexes is a matter of discussion. On the one hand quenching of Lhc complexes is assumed to be caused by a conformational change which switches the complex from a light-harvesting into a quenched state (Moya *et. al.* 2001; Ruban *et. al.* 2007). On the other hand, based on the low crystallographic temperature factor

and the high similarity of LHCII structural models obtained from crystals grown under different conditions and originating from different organisms, it was argued that LHCII is very rigid and therefore unlikely to undergo conformational changes (Barros *et. al.* 2009).

(ii) Influence of putative neighboring pigments. It has been proposed that an additional Chl, located in close proximity to Chl 603-609, is involved in the red-shifted absorption and emission of these pigments (Melkozernov and Blankenship 2003). If this is indeed the case, mutation at the putative ligand of this Chl - histidine (H) 99 - into a residue which cannot coordinate a Chl, would induce a blue shift of the red absorption and emission bands.

(iii) Direct influence of the protein environment. We study the effect of the presumably negatively charged glutamic acid (E) 94 residue, located near Chl609, by changing it into the neutral glutamine (Q). Due to their CT character red forms are sensitive to the presence of charges in their environment and might thus be influenced by such a mutation. Furthermore, in LHCII a Q in this position stabilizes Chls *b* in site 607 and 609, through H-bonds to their formyl groups (Liu *et. al.* 2004). Occupation of the 609 site with a Chl *b* could have interesting effects, because it would form a Chl *a* 603-Chl *b* 609 heterodimer. Due to the larger difference in the excited-state energy, the excitonic splitting will be smaller, whereas the chemical differences of the two Chls might lead to an increased CT character.

The results show that we can tune the absorption and emission properties of the red forms over a wide spectral range. Implications for the optimization of photosynthesis are discussed.

Materials & Methods

Mutagenesis and reconstitution of Lhca4 complexes – A modified pET-28a (+) vector containing the sequence coding for the mature protein of *A. thaliana* Lhca4 has been mutated by site directed mutagenesis using the Stratagene QuikChange Site Directed Mutagenisis Kit. The following mutations were introduced: in N47Q the Chl603 ligand (N47) was substituted for another Chl ligand Q, in E94Q the acidic water mediated Chl-606 ligand E is mutated into the neutral water mediated Chl-606 ligand Q, in H99A the putative Chl binding residue H is mutated into Alanine (A) a residue that cannot coordinate a Chl. WT and mutant apoproteins were overexpressed in Rosetta2(DH3) strain of *E. coli*. The proteins were purified as inclusion bodies, as described in (Paulsen *et. al.* 1990). Reconstitution was done as described in (Giuffra *et. al.* 1996). The reconstituted complexes were purified by His-tag Ni-affinity chromatography and sucrose

density ultracentrifugation, on a 0.1-1M sucrose gradient (with 0.06% n-dodecyl-α-D-maltoside, 10mM Hepes pH 7.6) at 41.000 rpm (Beckman Coulter, SW41 rotor) at 4 ^{o}C for at least 18h.

Steady state spectroscopy and pigment analysis – Absorption spectra were recorded on a Varian Cary 4000 UV–visible spectrophotometer (Varian, Palo Alto, CA). For 77K measurements, a homebuilt liquid-nitrogen cooled low-temperature device was used. Fluorescence spectra were recorded at 77K and 283K on a Fluorolog 3.22 spectrofluorimeter (HORIBA Jobin Yvon-Spex, Longumeau, France). Samples were diluted to an absorbance of 0.04 cm^{-1} at 680 nm. The fluorescence quantum yield (Φ_{Fl}) was determined as described in (Wientjes and Croce 2011, Chapter 3), based on spectral integration from 640nm to 850nm. CD spectra were recorded at 283 K on an AVIV 62ADS spectropolarimeter (Aviv Associates, Lakewood, NJ). All measurements were performed in 10 mM Tricine, pH 7.8, 0.03% α-DM and 0-0.5 M sucrose (283K) or 67% (w/v) glycerol (77K).

Pigment analysis was based on fitting of the absorption spectra of the acetone-extracted pigments with the spectra of the individual pigments, as described in (Croce *et. al.* 2002a).

Results

Introduced mutations – Figure 1 shows the mutations introduced in Lhca4. All mutations are targeting residues located nearby Chl 603 and Chl 609, which are the pigments responsible for the red-shifted absorption and emission of Lhca4. In the H99A mutant the putative Chl binding site H99 (proposed by Melkozernov and Blankenship 2003) was substituted for A, which cannot coordinate the central Mg of a Chl. The second mutation is directed to asparagine N47, the ligand of Chl 603. It has been shown previously that substitution of N47 for H induces a strong blue-shift of the red forms (Morosinotto *et. al.* 2003). This was explained by the larger dimensions of H as compared to N, which increases the Chl 603-609 distance and thus lowers the interaction energy between these pigments. Here, we substitute N47 for glutamine (Q), thus increasing the side-chain lengths of the Chl ligand by one C-C bond, but without further changes in the amino acid characteristics. The last mutation is E94Q, this mutation is expected to change the Chl *a*/*b* occupancy of a neighboring Chl-binding site (607 or 609) and remove a negative charge.

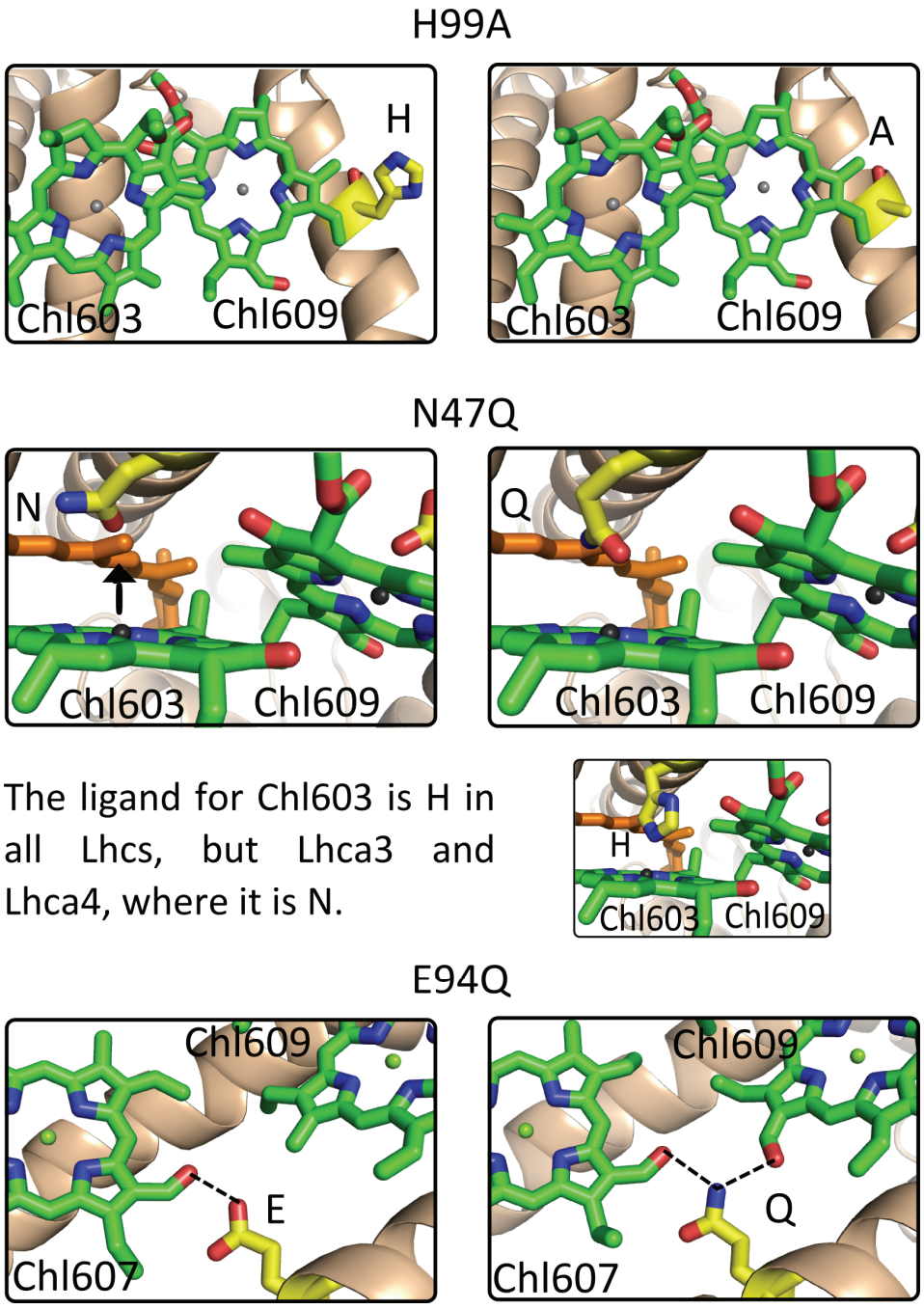

Figure 1: Molecular models of the introduced mutations – Models are based on the structure of LHCII (Liu *et. al.* 2004) or for the left lower panel of CP29 (Pan *et. al.* 2011). The LHCII and CP29 structures are used because they were solved to higher resolution than the one of Lhca4 (in the higher plant PSI structure, Amunts *et. al.* 2010). Note that the Chl *a*/*b* occupancy in Lhca4 can be different from that in LHCII and CP29. Only pigments nearby the mutated site are shown, the phytol chains of the Chls are omitted. The Chls and the mutated residue are colored by element: nitrogen (blue), oxygen (red) and carbon (green/yellow). In the middle panel a Car is shown in orange, and the black arrow indicates that in Lhca4 Chl603 is located closer to its ligand (N) compared to the figure, which is based on the LHCII model where the Chl603 ligand is an H (small cartoon). The dashed lines in the lower panel show hydrogen bonds. Figures were prepared with PyMOL (DeLano, WL. The PyMOL Molecular Graphics System, 2002).

Pigments composition – The Chl *a*/*b* and Chl/Car ratios of the Lhca4 samples are reported in Table 1. In Lhca4-WT the Chl/Car ratio indicates that ~2 Cars are present per Lhca4 complex assuming a total of 10Chls, in agreement with previous results (Croce *et. al.* 2007b). The Chl/Car ratio of H99A is similar to that of WT, while a decrease to 4.5 would be expected if one Chl was lost. This suggests that H99 is not a Chl-binding residue. The Chl/Car ratio of E94Q is also similar to that of WT, while for N47Q this ratio is higher, suggesting that 1.7 Cars are present per Lhca4. Most likely the Car binding in the 621 (L2) site, nearby Chl 603 and 47Q (fig 1), is slightly destabilized by the mutation. It can be concluded that none of the mutations lead to loss of Chls.

The difference in Chl *a*/*b* ratio between WT and E94Q indicates that in the mutant 0.3 Chls *a* are replaced by Chls *b*. In the other two mutant complexes the number of Chls *a* per complex is the same that in the WT (the difference is +/- 0.1, which is smaller than the error of the measurement) and it can thus be concluded that these mutations do not affect the affinity of the binding sites for Chl *a* or *b*.

Sample	Chl/Car	Chl *a*/*b*
WT	4.9	1.9
H99A	4.8	2.0
N47Q	5.8	1.8
E94Q	5.2	1.7

Table 1 Pigment composition. Chl *a*/*b* and Chl/Car ratio of Lhca4 samples, based on two repetitions, the standard deviation (SD) is <0.15.

Absorption properties – Figure 2 shows the 77K absorption spectra of the Lhca4 complexes and their second derivatives. In the Soret region the main spectral features are not affected by the mutations, however in the Q-region large differences can be appreciated. In the N47Q mutant the absorption above 700nm is strongly decreased, while it increases at 674nm. The 674nm band can be attributed to the absorption of “monomeric” Chl 603 and Chl 609, i.e. in absence of the strong excitonic interaction, in agreement with previous results (Morosinotto *et. al.* 2003). The absorption spectrum of E94Q shows, compared to that of the WT, a decrease in the amplitude at λ < 722nm, but an increase at longer wavelengths (fig 2, inset), thus suggesting that the red forms band is broadened in the mutant. The H99A mutant has an absorption spectrum that is almost indistinguishable from that of WT (only in the red a slight increase in absorption is observed).

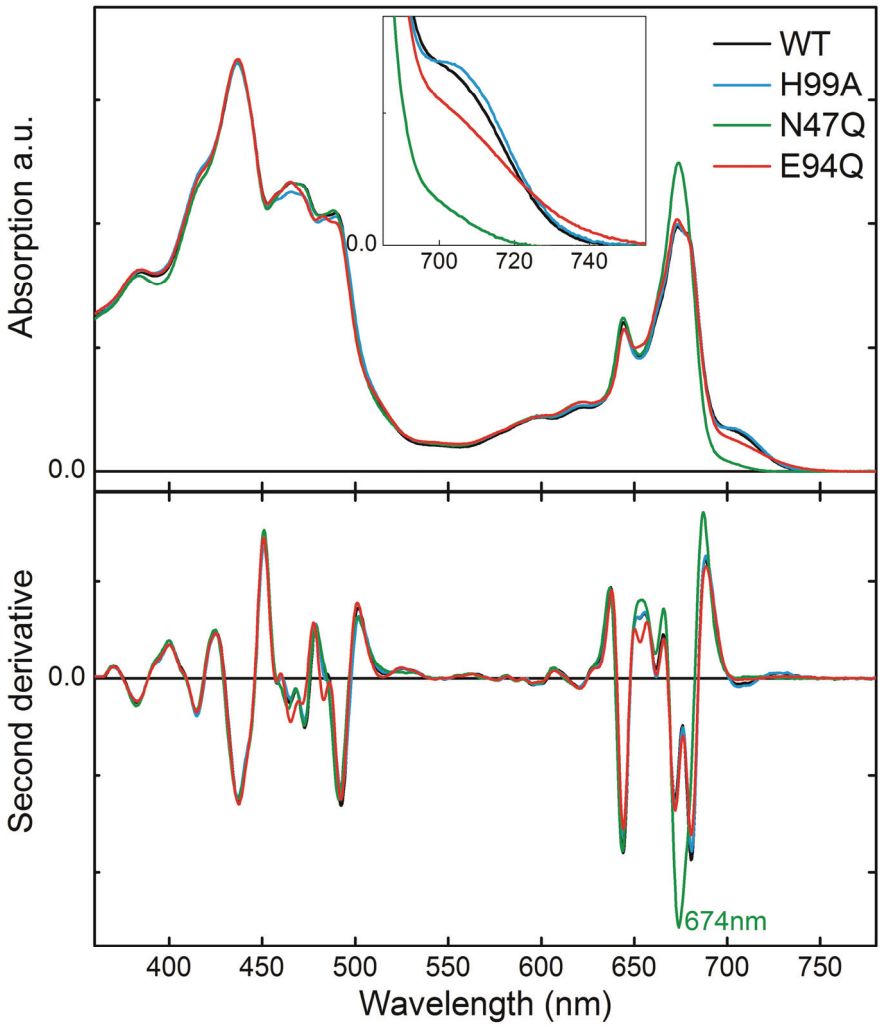

Figure 2: 77K absorption spectra of Lhca4 complexes. Upper panel: absorption spectra normalized to same area in the Q_y region. Lower panel: second derivative of the absorption spectra.

Fluorescence emission – Because the red forms have a high probability to be populated, they strongly contribute to the fluorescence emission, with the result that the effect of the mutations on the red forms can be better appreciated in fluorescence. Figure 3 shows the emission spectra of the complexes at 283K and 77K. For H99A the properties of the red forms (emission maximum and band-width) are not different from those of the WT. The only difference is a small change in the ratio between the "blue" (685 nm) and the "red" (720 nm) emission, which suggests that the H99A mutant favors the red conformation slightly more than the WT complex. Similarly, the emission spectra of the N47Q mutant show that this complex favors the "blue" emitting Lhcb-like conformation. However, the emission in the red is stronger than for real Lhcb complexes, suggesting that part of the complexes can still form an excitonic-CT state. The red

band of the E94Q emission spectrum is red-shifted and broadened compared to the WT, in agreement with the broader red absorption band.

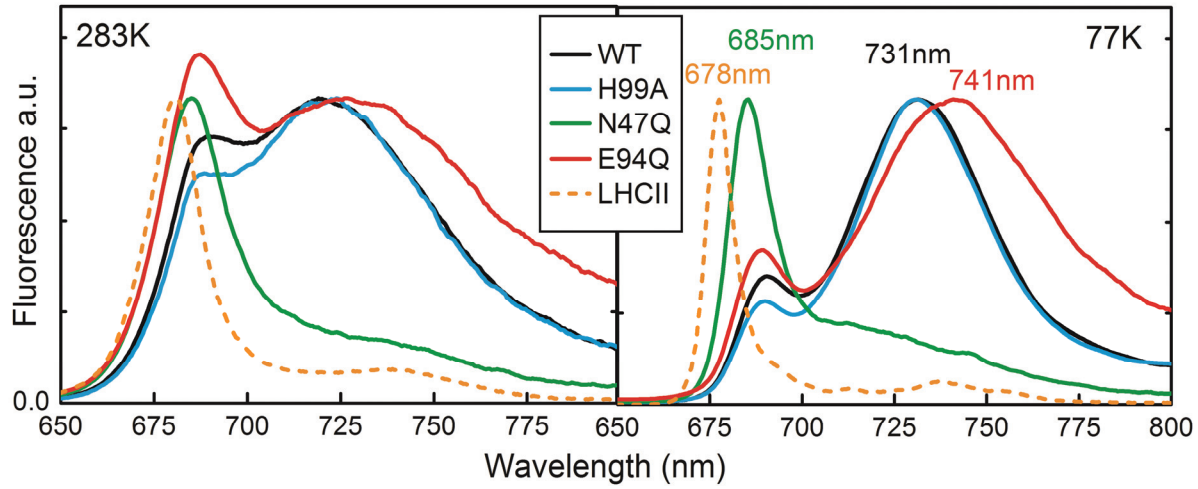

Figure 3 Fluorescence emission spectra of Lhca4 complexes. Emission spectra recorded at 283K and 77K after excitation at 500nm. Spectra were normalized to their maximum.

Table 2 shows the fluorescence quantum yields (Φ_{Fl}) of the Lhca4 complexes. The Φ_{Fl} of H99A is higher than that of WT. This is in agreement with the observation that this mutation seems to stabilize the red-conformation, which has longer fluorescence lifetimes (Passarini *et. al.* 2010). The Φ_{Fl} of N47Q is strongly decreased, but we can exclude that this is related to the loss of red forms, because the N47H mutant, which also has a reduced red form content (Morosinotto *et. al.* 2003), shows a Φ_{Fl} comparable to that of WT. Also the E94Q mutant shows a decreased Φ_{Fl}.

Table 2 Fluorescence quantum yield of Lhca4 complexes. Φ_{Fl} determined for two independent reconstitutions, average and SD is given. The Φ_{Fl} of LHCII and Lhca4-N47H were also determined.

Sample	WT	H99A	N47Q	E94Q	N47H	LHCII
Φ_{Fl} (SD)	7.8 (0.4)	10.4 (0.1)	4.3 (0.5)	4.2 (1)	7.1	22

Circular dichroism – The CD spectrum (Fig 4) of the E94Q mutant shows, compared to the WT, an increase in the amplitudes in the Soret region. The difference spectrum (E94Q – WT, not shown) has maxima at 443nm (+) and 473nm (-), suggesting that a new Chl *a*/*b* interaction has been created in the mutant. The spectrum of the N47Q mutant is similar to that of the WT in the Soret region, indicating that the mutation does not change the overall pigment organization of the complex. The slight decrease of amplitude in the Car region is probably related to the small loss of Cars. Large differences are observed in the

red part (λ > 700nm) of the spectrum, where the mutant clearly lacks the strong excitonic interaction responsible for the red absorption. The CD spectra of the H99A mutant and the WT complex are nearly indistinguishable.

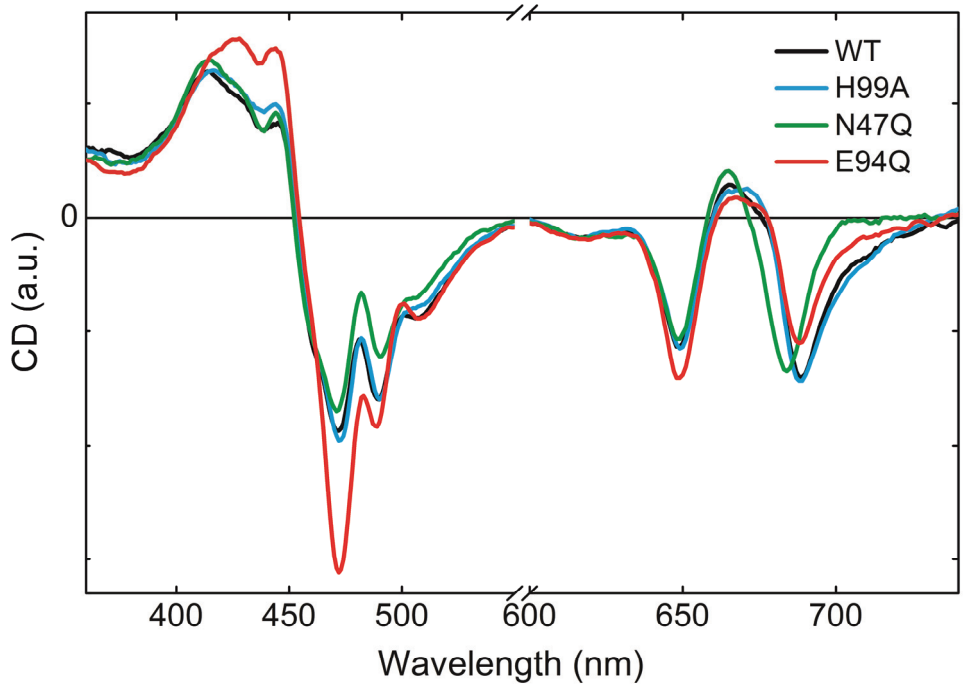

Figure 4 CD spectra of Lhca4 complexes. Spectra are normalized to the same absorption in the Q_y region.

Discussion

Proteins have the intriguing ability to alter the optical properties of pigments. This modulation is caused by changes in pigment-pigment and pigment-protein interactions. This ability of the protein to tune the properties of the pigments lies at the basis of the efficient functioning of the light-harvesting process and allows its regulation.

It has been shown that both Lhca and Lhcb complexes can occasionally switch between states that are characterized by differences in emission maxima as large as 50nm, suggesting that the Chl excited-state energy levels can be strongly modified by spontaneous changes of the protein conformation (Kruger *et. al.* 2011). Considering that the protein can alter the Chl energy levels by small changes in its conformation, it should also be possible to alter the energy levels by making small changes in the protein. It has indeed been observed that the single amino acid N47H substitution in Lhca4 can blue shift the red emission maximum by 30nm, while the number of coordinated Chls remains the same (Morosinotto

et. al. 2003). In this work we extend the study on how the red forms of Lhca4 can be modified. Different hypotheses are tested with the aim to improve the understanding of how Lhcs regulate the excited-state energy levels of Chls.

H99 is not a Chl binding residue – It was proposed that H99, which is unique for Lhca4, coordinates a Chl to form a pigment cluster with the nearby located Chls 603 and 609 (Melkozernov and Blankenship 2003). These three Chls were proposed to strongly interact and to be responsible for the low-energy band. If this were indeed the case the energy level of the red forms would change in the absence of this Chl. Our analysis shows that substitution of H into a residue that cannot coordinate a Chl does not induce a Chl loss, leading to the conclusion that H99 is not a Chl ligand in monomeric Lhca4. In addition, the data show that the substitution of the polar H with a unipolar residue does not substantially change the properties of the red form, thereby demonstrating that this residue is also not involved in the modulation of the energy level of Chl 603 and 609

From Lhca to Lhcb… how flexible are Lhcs? – It has been observed, with single-molecule fluorescence spectroscopy, that an Lhca4 complex can occasionally switch off its entire red emission band (Kruger *et. al.* 2011). This is explained by a conformational change. The red forms can be lost by a combination of the following factors: (i) an increase in inter-pigment distance, (ii) a decrease of the pigment orientation factor, and (iii) the lost capability to form a CT state. But, how large should the change be to lose the red forms? To the best of our knowledge there are no structure-based calculations available that can correctly predict the excited-state energy levels of the red forms and therefore their tuning. To answer this question we have thus tried to move the equilibrium between the conformations towards the blue by mutating residues in the protein located close to the Chls responsible for the red forms. It is shown that increasing the side chain length of the Chl603 ligand by one carbon-carbon bond (1.54Å) is enough to lose the red forms in the major part of the complexes. In fact, the mutant shows characteristics that resemble more that of a typical Lhcb complex than that of an Lhca complex. First, its emission maximum is located at 685nm, only 5nm red-shifted as compared to the Lhcbs (and 45 nm blue shifted compared to Lhca4 WT). Second, the width of the main fluorescence emission band is more similar to that of Lhcbs than to that of Lhcas (fig 5). Third, the mutant shows only little absorption and CD signal for $\lambda > 700$ nm. The increase in distance, between the backbone C_α and the oxygen that coordinate the central Mg of the Chl, depends on the side-chain conformation; for the models shown in figure 1 it is 0.74Å. This

suggests that a rather small change in the protein scaffold can have a very large effect on the spectroscopic properties of the pigments.

A likewise small change in the other direction can explain the sporadic occurrence of red emitting LHCII complexes (Kruger *et. al.* 2011). In our opinion the possibility of Lhcs to undergo conformational changes is not necessarily in contrast with the low-temperature factor of the LHCII structure (Barros *et. al.* 2009). The spectral changes occur rarely, suggesting a high-energy barrier between the different states, and once a complex is switched it is stable in the other state. Thus both states can be considered to be rather rigid.

Red, redder, reddest… - the E94Q mutant – The emission of the E94Q mutant is strongly red-shifted and broadened as compared to the WT. This can be explained by an increased CT character and thus a stronger electron-phonon coupling. There are a few possibilities how this mutation could increase the CT character. (i) The effect can be due to the removal of a negative charge in the surrounding of Chl 609. For *in vitro* reconstituted CP29 it has been shown that this E, at the same position as E94 in Lhca4, is a DCCD binding site and thus a protonable residue (Pesaresi *et. al.* 1997). Given the pKa of 4.2 for the E side chain, it is most likely negatively charged under the used experimental conditions. For Q the side chain is an amide and as such always neutral. For the red forms charges are especially important, because they can make the environment of Chl603-609 asymmetric and as such increase the CT character. Thus, if the red shift in E94Q is due to the elimination of the negative charge, it would mean that this change increases the asymmetry of the Chl dimer environment. (ii) The substitution of E, which can at most stabilize the binding of one Chl *b*, into Q which can stabilize two Chls *b*, slightly increased the amount of Chl *b* in the complex (Table 1). This additional Chl *b* can in principle be located in sites 609 or 607. If it is located in the 609 site, the excitonic Chl 603 - Chl 609 pair becomes a Chl *a*-Chl *b* dimer, which could in theory favor the CT state by enhancing the asymmetric character of the pair. However, the large difference between the excited-state energy of these pigments will result in a smaller exciton splitting than in the WT complex. Thus, mixing of the exciton state with the CT state should strongly lower the energy to be able to explain the 10nm red shift. (iii) If the extra Chl *b* is located in the 607 site it might also influence the red forms. It has been suggested that Chl *b* is involved in (Schmid *et. al.* 2001) or required for the stabilization of (Castelletti *et. al.* 2003) the red forms of Lhca4, and coordination of Chl *b* in this site has been proposed to stabilize the red Lhca4 conformation (Passarini *et. al.* 2010).

Keeping the Φ_{Fl} high, the precision of Nature – In two of the mutants the Φ_{Fl} was strongly decreased as compared to the WT complex (table 2). For N47Q the quenching might be explained by the higher flexibility (compared to N and H) of the long Q side-chain which can bring Chl 603 close enough to the Car in the L2 site for Chl Q_y – Car S_1 mixing to take place. As the lifetime of Cars is short, even a small degree of mixing will seriously shorten the Chl excited-state lifetime (van Amerongen and van Grondelle 2001). Such interactions were recently proposed to lie at the basis of non-photochemical quenching, which protects plants from high-light damage (Lampoura *et. al.* 2002; Bode *et. al.* 2009).

The E94Q seems to have an increased CT character. It has been proposed that mixing with a dark CT state can shorten the singlet excited state lifetime of Lhcs (Ihalainen *et. al.* 2005; Miloslavina *et. al.* 2008). For the native Lhca1/4 dimer such quenching was not observed (Wientjes *et. al.* 2011, Chapter 4), however the E94Q mutant is clearly quenched. It can therefore be suggested that Nature has selected for a red absorbing antenna, which still has a rather high Φ_{Fl} and thus proper light-harvesting characteristics. The large decrease of Φ_{Fl} caused by single amino acid substitutions shows how finely tuned the system is.

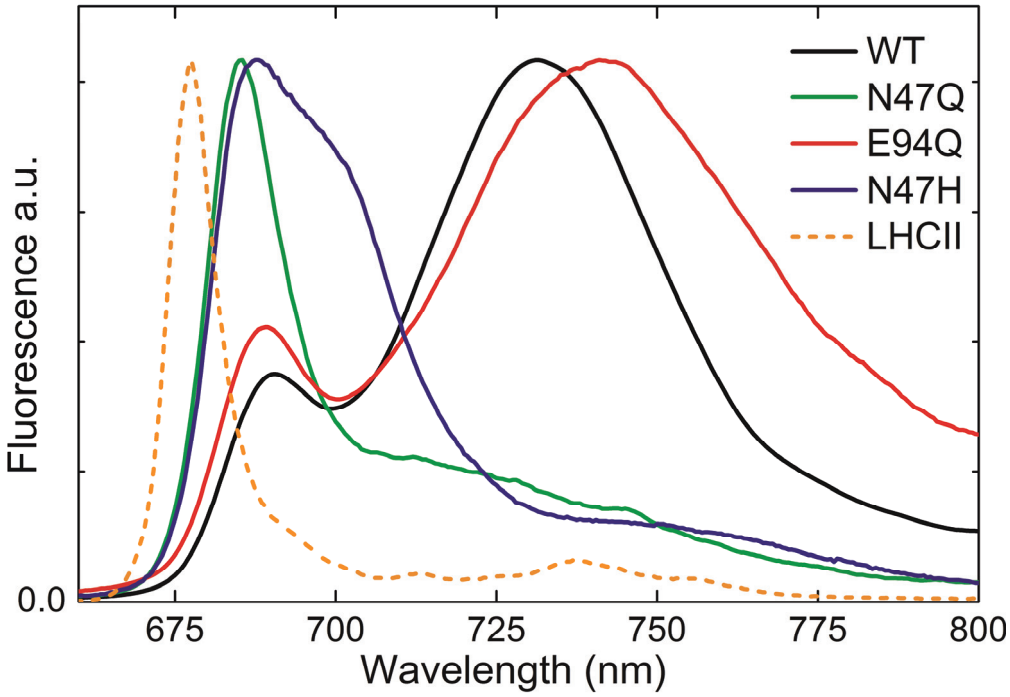

Figure 5 77K fluorescence emission spectra of Lhca4 complexes and LHCII. Spectra are normalized to their emission maxima, excitation was at 500nm.

Improving photosynthesis – This study shows the feasibility to adjust the spectral properties of Chls by making small changes in the protein (fig 5). An interesting application would be to use directed evolution with (semi) high-throughput

screening to obtain Lhcs which are more suitable to harvest light of a specific spectrum. It would be possible to produce plants with improved light harvesting for a high-pressure sodium lamp (λ_{max} around 600nm) used as supplemental light source in green houses. Another possibility would be to harvest more of the solar spectrum by extending the absorption into the red (Blankenship and Chen 2011). In plants PSI has significant absorption at wavelengths > 700nm, but the absorption of PSII in this spectra region is negligible. It has long been believed that low-energy photons (λ > 700nm) would fail to drive water splitting. However, the isolation of a cyanobacterium with Chl *d* (λ_{MAX} = 700-710nm) as main light-harvesting pigment has indicated that the actual energy threshold must be at lower energy (Miyashita *et. al.* 1996; Kuhl *et. al.* 2005). This is further supported by the recent observation that light up to 780nm can drive water splitting in PSII of spinach (Thapper *et. al.* 2009). Thus, expanding the light absorption of Lhcbs into the red could help to improve the efficiency of photosynthesis by harvesting a larger fraction of the available solar spectrum, especially under a canopy where the light is enriched in the long wavelengths (Rivadossi *et. al.* 1999). As the low-energy Chls might decrease the PSII efficiency, it can be considered to use differential expression; expressing the far red absorbing Lhcbs only under the canopy where the benefit from the increased absorption is larger than the disadvantage of the decreased PSII efficiency.

Acknowledgements

This work was supported by De Nederlandse Organisatie voor Wetenschappelijk Onderzoek (NWO), Earth and Life Sciences (ALW), through a Vidi grant (to R.C.).

Chapter 7

The role of the individual Lhcas in Photosystem I excitation energy trapping

Emilie Wientjes, Ivo H.M. van Stokkum, Herbert van Amerongen and Roberta Croce

This chapter is based on:

Biophysical Journal (2011) 101:745-754.

Abstract

In this work we have investigated the role of the individual antenna complexes and of the low-energy forms in excitation energy transfer and trapping in higher plants Photosystem I. To this aim, a series of Photosystem I (sub)complexes with different antenna size/composition/absorption have been studied by picosecond fluorescence spectroscopy. The data show that Lhca3 and Lhca4, that harbor the most red forms, have similar emission spectra (λ_{max}=715-720nm) and transfer excitation energy to the core with a relative slow rate of ~25/ns. Differently, the energy transfer from Lhca1 and Lhca2, the "blue" antenna complexes, occurs about four times faster. In contrast to what is often assumed, it is shown that energy transfer from the Lhca1/4 and Lhca2/3 dimer to the core occurs on a faster time scale than energy equilibration within these dimers. Furthermore, it is shown that all four monomers contribute almost equally to the transfer to the core and that the red forms slow down the overall trapping rate by about two times. Combining all the data allows the construction of a comprehensive picture of the excitation-energy transfer routes and rates in PSI.

Introduction

Photosystem I (PSI) is a plastocyanin: ferredoxin oxidoreductase which plays a major role in the photosynthetic light reactions in cyanobacteria, algae and higher plants. Although cyanobacteria and plants have diverged in evolution one billion years ago, they have a highly conserved PSI core complex (Jordan *et. al.* 2001; Ben-Shem *et. al.* 2003). This pigment-protein complex coordinates about 100 chlorophylls *a* (Chls *a*), β-carotene molecules, the reaction centre (RC), and all the electron transport cofactors (Jordan *et. al.* 2001). Light is harvested by the pigments and the excitation energy is transferred to the RC where it is used for charge separation. In algae and higher plants additional light-harvesting complexes (Lhcs) are present to increase the absorption cross-section of PSI. In higher plants these Lhcs are composed of two heterodimers: Lhca1/4 and Lhca2/3, which are organized as a crescent shape around the core (Boekema *et. al.* 2001; Croce *et. al.* 2002; Ben-Shem *et. al.* 2003; Wientjes and Croce 2011a, Chapter 3). A fifth complex, Lhca5 is present in sub-stoichiometric amounts (Jansson 1999; Ganeteg *et. al.* 2004a). Gap pigments are located in between the core and the Lhcas and presumably facilitate excitation-energy transfer (EET) between the different parts of the system (Ben-Shem *et. al.* 2003). The supercomplex composed of PSI core and all four Lhcs (PSI-LHCI) coordinates ~170

Chls *a* and *b*, and carotenoids: β-carotene, violaxanthin, lutein (Schmid *et. al.* 1997; Croce and Bassi 1998; Amunts *et. al.* 2010).

A special feature of almost all PSI complexes is the presence of the red forms: Chls that absorb at longer wavelengths than the RC (Gobets and van Grondelle 2001; Melkozernov 2001). Thus, EET from these Chls to the RC is energetically up-hill and needs to be thermally activated (Jennings *et. al.* 2003). Even though up-hill EET slows down the trapping rate, the quantum efficiency of PSI is still extremely high (Gobets and van Grondelle 2001; Nelson and Yocum 2006). In higher plant PSI some red forms are located in the core, and are responsible for the 720nm low-temperature (LT) fluorescence emission, but most red forms are coordinated by LHCI (Croce *et. al.* 1998; Ihalainen *et. al.* 2003). In vitro reconstitution studies have shown that Lhca3 and Lhca4 coordinate Chls that absorb at 705-710nm and emit at 725-735nm (Schmid *et. al.* 1997; Castelletti *et. al.* 2003; Croce *et. al.* 2007a). Also Lhca2 shows a red-shifted LT emission maximum (compared to 680nm observed for PSII antenna) at 701nm (Castelletti *et. al.* 2003), which arises from an absorption band at 690nm (Croce *et. al.* 2004). Lhca1 has its emission maximum at 690nm and a shoulder at 701nm (Morosinotto *et. al.* 2002). It has been shown that the red-shifted absorption of Lhca complexes arises from two strongly coupled Chls *a,* named 603 and 609 (nomenclature as in Liu *et. al.* 2004) (Morosinotto *et. al.* 2002; Morosinotto *et. al.* 2003; Croce *et. al.* 2004; Morosinotto *et. al.* 2005b; Mozzo *et. al.* 2006) forming a CT state (Romero *et. al.* 2009).

The presence of red forms in the native Lhca1/4 dimer has been known for a long time (Schmid *et. al.* 1997), in contrast to the presence of red forms in Lhca2/3 which was more controversial and could only recently be confirmed (Wientjes and Croce 2011a, Chapter 3). It was shown that the red form content in Lhca1/4 and Lhca2/3 is practically identical, and that they show 77K emission maxima at 731.5nm and 728.5nm, respectively (Wientjes and Croce 2011a, Chapter 3; Wientjes *et. al.* 2011, Chapter 4). Due to their low excited-state energy, red forms have an important effect on EET and trapping in PSI. Indeed, at room temperature they give rise to 80% of the fluorescence emission of higher plant PSI (Croce *et. al.* 1996).

The function of the red forms is not fully understood, it has been proposed that they play a role in photoprotection, concentrate the excitation energy and/or strongly contribute to the PSI absorption under specific light conditions (Trissl 1993; Karapetyan *et. al.* 1999; Rivadossi *et. al.* 1999; Carbonera *et. al.* 2005).

The EET and trapping processes in PSI have been studied extensively by time-resolved techniques: transient absorption, fluorescence upconversion, synchroscan streak camera and time correlated single photon counting (TCSPC).

Gobets et al. (2001b) studied a range of PSI complexes from cyanobacteria with different red form content and found that the excitation energy trapping of all complexes could be described with a lifetime of 18ps and an additional slower component. The lifetime and amplitude of the slower component correlate with the amount and energy of the red forms. Also the fluorescence decay time of the higher plant PSI cores is ~18ps (Engelmann *et. al.* 2006; Slavov *et. al.* 2008), while it is still unknown whether a second slower lifetime is needed to describe the red form decay kinetics.

Time-resolved fluorescence studies on PSI-LHCI from higher plants have shown that, compared to the purified core, additionally red-shifted decay-associated spectra (DAS) are needed to describe the data (Croce *et. al.* 2000b; Jennings *et. al.* 2003; Ihalainen *et. al.* 2005b; Engelmann *et. al.* 2006; Slavov *et. al.* 2008; van Oort *et. al.* 2008). The exact lifetimes and DAS differ from study to study, probably reflecting a high sensitivity of PSI to handling and measuring conditions, but most studies show a similar trend: a fast ~5-10ps bulk/red energy equilibration component, a ~20ps trapping component with a PSI core-like spectrum, and at least one red-shifted DAS with lifetimes ≥ 55ps. In some studies a smaller number of components is used to describe the data (Croce *et. al.* 2000b; Engelmann *et. al.* 2006), but most likely these DAS represent an average of components that are resolved in the other reports.

In the past decade it has become clear that the slow phase in the PSI-LHCI fluorescence decay is related to the low-energy Chls in LHCI (Croce *et. al.* 2000b; Ihalainen *et. al.* 2002; Jennings *et. al.* 2003; Ihalainen *et. al.* 2005a; Ihalainen *et. al.* 2005b; Engelmann *et. al.* 2006), in particular of Lhca3 and Lhca4 (Slavov *et. al.* 2008). So far, however, there is no agreement about the spectra and decay kinetics of the individual Lhcas when associated with the core (Ihalainen *et. al.* 2002; Ihalainen *et. al.* 2005b; Ihalainen *et. al.* 2005c; Slavov *et. al.* 2008; van Oort *et. al.* 2008). This is mainly because PSI is a very large and complex system, making it difficult to extract the details from the decay kinetics. To tackle this problem and to improve the understanding of EET in PSI-LHCI we have chosen a systematic approach. First, to reduce the complexity, we purified the major PSI building blocks: Lhca1/4, Lhca2/3, and core and studied their time-resolved fluorescence dynamics. Then we gradually increased the complexity, by “rebuilding” the system, making use of PSI from a mutant plant which consists of a PSI core, only coordinating the Lhca1/4 dimer (Klimmek *et. al.* 2005; Morosinotto *et. al.* 2005a; Wientjes *et. al.* 2009, Chapter 2), and finally studying the WT complex. In addition, to specifically investigate the role of the red forms we studied a complex in which Lhca4 (with red forms) is substituted by Lhca5 (without red forms) (Wientjes *et. al.* 2009, Chapter 2).

Materials & Methods

Isolation of PSI complexes – All complexes were obtained from *A.thaliana* plants. Lhca1/4 and Lhca2/3 were isolated as described in (Wientjes and Croce 2011a, Chapter 3) and the PSI core was obtained as in (Croce *et. al.* 1998). PSI complexes were obtained from WT, Lhca2 anti-sense and Lhca4 knock-out plants (Ganeteg *et. al.* 2001; Ganeteg *et. al.* 2004b) as described before (Wientjes *et. al.* 2009, Chapter 2). All complexes were separated by sucrose density ultracentrifugation, on a 0.1-1M sucrose gradient with 0.03% n-dodecyl-α-D-maltoside (α-DDM) and 10mM tricine, pH 7.8. PSI complexes were further purified by one (PSI-WT, PSI Lhca2 anti-sense) or two (PSI Lhca4 knock-out) subsequent sucrose gradients. After harvesting the complexes were snap frozen in N_2 (l) and stored at 193K.

All spectroscopic measurements were performed in 0.5M sucrose, 0.03% α-DDM and 10mM tricine pH 7.8.

Steady-state spectroscopy – Absorption spectra were recorded on a Cary 4000 UV-Vis spectrophotometer (Varian, Palo Alto, CA). Fluorescence spectra were recorded on a Fluorolog 3.22 spectrofluorimeter (HORIBA Jobin Yvon, Longjumeau, France). Intactness of the sample was checked by recording the steady state emission spectra before and after time-resolved fluorescence measurements. No significant changes were observed.

TCSPC – TCSPC was performed at 283K with a homebuilt setup, as described previously (Somsen *et. al.* 2005). Excitation was performed with a light pulse at 440 or 475nm and a repetition rate of 3.8MHz. Pulse energies of (sub)-picojoules were used with pulse duration of 0.2ps and a spot diameter of 2mm. The instrument response function (~80ps at full width halve maximum) was obtained with pinacyanol iodide in methanol, with a 6-ps fluorescence lifetime (van Oort *et. al.* 2008). A channel time spacing of 2ps was used, resulting in an 8-ns time window. Further experimental settings were as in (Wientjes *et. al.* 2011, Chapter 4). The steady-state fluorescence emission spectra were used to calculate the DAS.

Calculation of LHCI to core migration time – Based on the fractions of PSI core and LHCI excitation at two different excitation wavelengths (see, SI. 2) and the respective average fluorescence lifetimes, the fluorescence lifetime upon selective excitation of only LHCI ($\bar{\tau}_{\mathrm{L}}$) or only PSI core ($\bar{\tau}_{\mathrm{C}}$) can be calculated (van Oort *et. al.* 2008). The average fluorescence lifetime is the sum of the trapping time, which is independent of the location of the initial excitation, and the migration time. Thus the difference between $\bar{\tau}_{\mathrm{L}}$ and $\bar{\tau}_{\mathrm{C}}$, given by Eq. 1, can be

attributed to the extra migration time from LHCI to the core (van Oort *et. al.* 2008).

$$\bar{\tau}_{\mathrm{L-C}} = \frac{<\tau>_{475} - <\tau>_{440}}{ExLHCI_{475} - ExLHCI_{440}} \quad (1)$$

With $\bar{\tau}_{\mathrm{L-C}}$ being the difference in average lifetime after excitation of LHCI or core. $< \tau >_{\#\#\#}$ is the average fluorescence lifetime after excitation at ###nm. And $ExLHCI_{\#\#\#}$ is the fraction of excitation that is created on LHCI upon ###nm excitation.

Synchroscan streak-camera measurement and modeling – Streak-camera fluorescence measurements were performed (at 295K) with a set of lasers and a synchroscan streak-camera detection system, as described in (van Oort *et. al.* 2009). Excitation was at 475nm and a time window of 160ps was used. Further experimental settings and data analysis were as in (Wientjes *et. al.* 2011, Chapter 4). Target analysis yielded the species associated spectra (SAS) of and the transfer rates between the *red* Lhca, *blue* Lhca, core bulk and core red compartment; for details on target analysis see (Stokkum *et. al.* 2004). To reduce the number of free fit parameters the spectrum of *blue* antenna is taken to be the same as the bulk core spectrum, the *red* antenna emission is 0 for λ <680nm, the red core emission is 0 for λ <695nm. For PSI-WT the initial excitation fraction of the core was fixed at 35% as obtained from the absorption spectra (Table 1). LHCI excitation was 65%, the fractions of *red* vs *blue* antenna excitation were estimated at 0.22 and 0.78, indicating that the *red* Lhca compartment represents the red forms and the Chls nearby. The dissipative rate of purified Lhca1/4 was 0.47/ns, this loss rate was used for all compartments.

Results

Red forms of PSI complexes studied with LT fluorescence – Fig1 shows the LT emission of Lhca1/4, PSI core, PSI-Lhca1/4 and PSI-Lhca1/4-Lhca2/3 (further called PSI-WT) (the absorption spectra are reported in SI. 1). The emission maximum of PSI-Lhca1/4 is a few nm blue-shifted as compared to PSI-WT indicating that in the case of PSI-Lhca1/4 relatively more emission is coming from the core (Klimmek *et. al.* 2005). Since contamination of the PSI-Lhca1/4 preparation with PSI-core can be excluded (Wientjes *et. al.* 2009, Chapter 2), the data indicates that the EET between the core and Lhca1/4 in PSI-Lhca1/4 is not as good as in the WT complex.

The low fluorescence intensity in the 680nm region observed for all complexes, shows that most pigments transfer their excitation energy to the red forms, meaning that the samples are virtually free of PSII contaminations and/or uncoupled Chls.

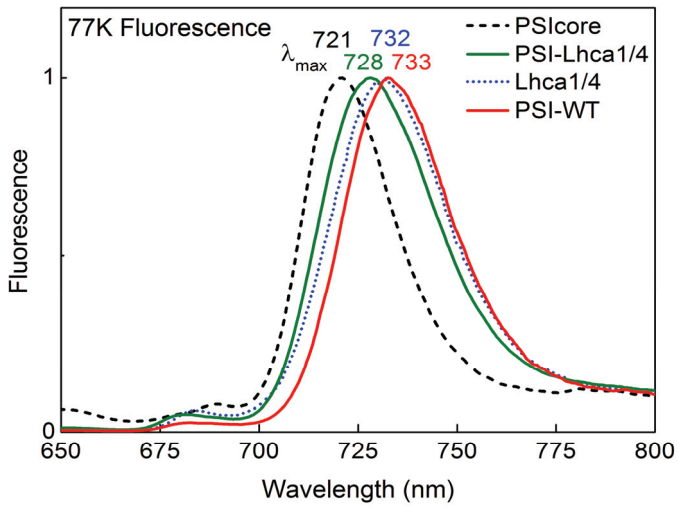

Figure 1: 77K fluorescence emission of PSI (sub)complexes upon 475nm excitation.

Fluorescence decay dynamics: Streak camera measurements – The fluorescence dynamics of the complexes (Fig. 2 *A*) were studied at room temperature with the synchroscan streak camera, after excitation at 475nm. It is immediately clear from the streak images that the fluorescence of the Lhca1/4 dimer shows hardly any decay on the 140ps time scale, only energy equilibration between the bulk pigments and the red forms can be observed (Fig. 2 *B*). The PSI core on the other hand decays extremely fast (Fig. 2 *B*). When the Lhca1/4 dimer is associated with the core (PSI-Lhca1/4) the fluorescence decay is still fast, although slightly slower than for the PSI core and it shows stronger emission at the longer wavelengths (~720nm) (Fig. 2 *B*). If also the Lhca2/3 dimer is associated with the core (PSI-WT) an additional increase in the longer wavelengths emission is observed (Fig. 2 *B*). The fast decay of PSI-Lhca1/4 and PSI-WT as compared to Lhca1/4 indicates that in these complexes the excitation energy is efficiently transferred from Lhcas to the core and subsequently used for charge separation.

To investigate the effect of the LHCI antenna on the fluorescence decay in a quantitative way the DAS were estimated (Fig. 2 *C*). The DAS associated with the shortest lifetimes (3-13ps) have spectra with a positive contribution around ~680nm and a negative one around ~720nm for all complexes. This is typical for PSI complexes and represents energy equilibration between the bulk pigments and the low-energy forms. In Lhca1/4 the main fluorescence decay occurs with a 2ns lifetime and the DAS shows a maximum around 720nm due to emission from the low-energy Chls. A fraction of Lhca1/4 decays faster (0.58ns), which presumably arises from complexes in a quenched conformation (Wientjes *et. al.* 2011, Chapter 4). The PSI core decays mainly with a 18ps lifetime, as observed previously (Engelmann *et. al.* 2006; Slavov *et. al.* 2008). In addition, a small

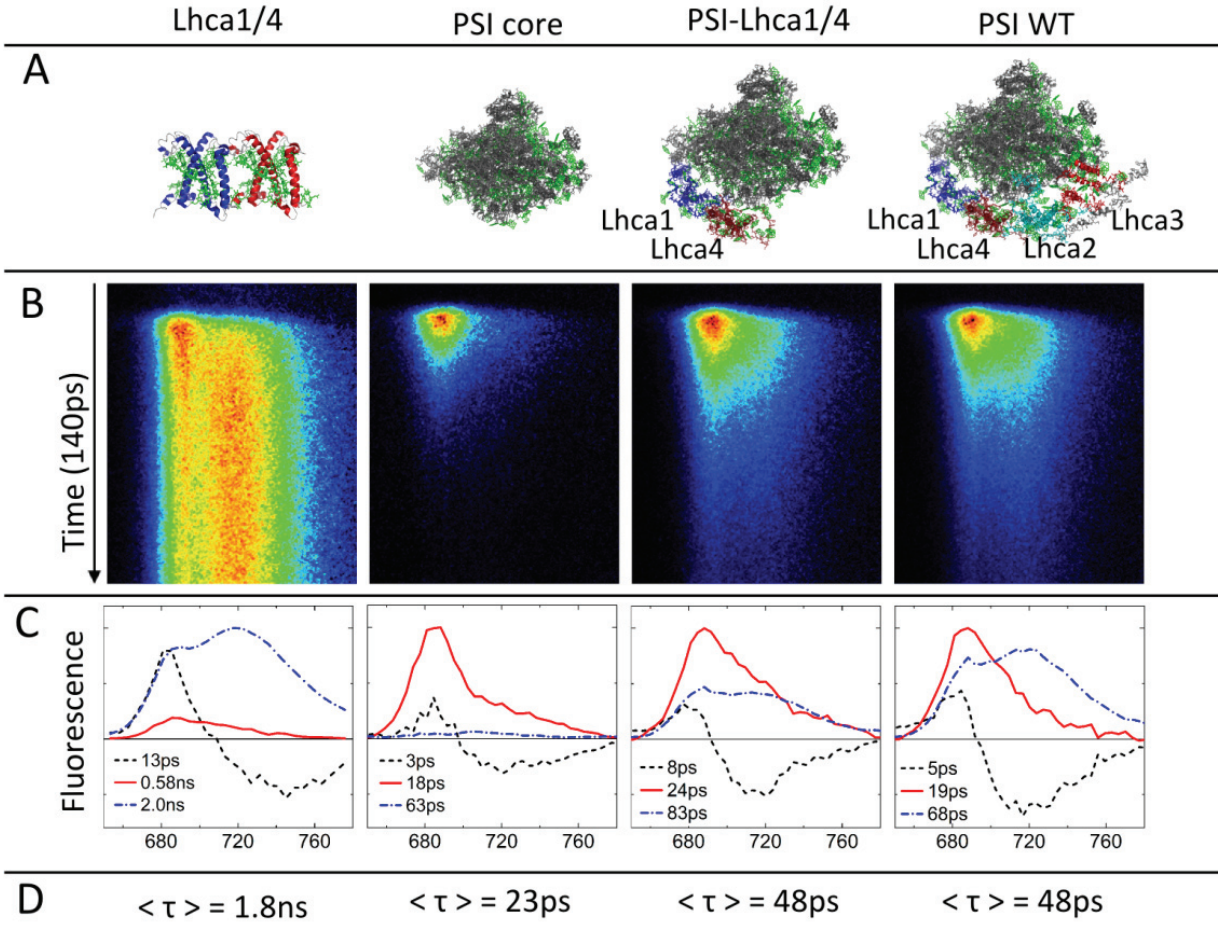

Figure 2: Streak-camera time-resolved fluorescence measurements. A: Cartoons of the investigated complexes were prepared with PyMOL (DeLano, W.L. The PyMOL Molecular Graphics System (2002) on http://www.pymol.org) from the structural data of PSI-LHCI (Amunts *et. al.* 2007) (and LHCII (Liu *et. al.* 2004) for Lhca1/4) (Pdb codes: 2O01 and 1RWT). B: streak images showing 140ps along the y-axis and 650-780nm along the x-axis. Color represents fluorescence intensity with black no fluorescence, red highest intensity. Excitation was at 475nm. C: DAS estimated from the streak data, shown in B. D average lifetime calculated according to $\tau_{av}=\Sigma A_i*\tau_i$, with A the relative area under the DAS and τ the corresponding lifetime, the transfer component was not taken into account.

contribution of a 63ps component with red emission is observed due to the presence of red forms in the core (see LT emission (Fig. 1) and (Croce *et. al.* 1998; Gobets and van Grondelle 2001)). For PSI-Lhca1/4 a 24-ps component with a similar spectrum as the 18 ps core DAS is present together with a 83 ps DAS resembling the 2ns DAS of Lhca1/4. In PSI-WT similar DAS as in PSI-Lhca1/4 were observed, but the amplitude of the Lhca1/4-like DAS increased, while its lifetime was somewhat shorter (68ps). It can thus be concluded that both Lhca2/3 and Lhca1/4 contribute to the amplitude of the red-shifted DAS. The average lifetime of the complexes (Fig. 2 *D*) increases from 20ps for PSI core, to 48ps for PSI-WT.

PSI-Lhca1/4 also has an average lifetime of 48ps, which is surprising considering the smaller number of Chls and red forms in PSI-Lhca1/4.

TCSPC after preferential core and antenna excitation – The fluorescence decay of the complexes was also investigated by TCSPC (at 283K). This technique is more sensitive than the streak camera allowing for a more accurate estimation of the fluorescence lifetimes. A disadvantage is the broader instrument response function that results in a lower time resolution, hampering the resolution of the blue to red EET component (3-8ps in the PSI complexes, Fig. 2).

TCSPC measurements were performed after excitation at 440nm (exciting mainly Chl *a* and Cars) and 475nm (exciting Chl *b* and Cars). Because Chl *b* is only present in LHCI, 475nm excitation is more selective for the antenna, while 440nm is preferentially exciting the core complex, see SI2.

Fig. 3 shows the DAS estimated from the TCSPC measurements of: PSI-core, PSI-Lhca1/4 and PSI-WT complexes. Due to the rather broad global fit minimum (Engelmann *et. al.* 2006) various combinations of amplitude and lifetimes can describe the data; to be able to compare the relative amplitudes, the two sets of measurements (440 and 475nm excitation) were fitted simultaneously. For all complexes five lifetimes were needed to describe the data; the fastest three (ps to sub-ns) were attributed to PSI, while two long lifetime components (ns) with very small amplitudes were ascribed to PSII contaminations/free Chls.

The decay of the core is mainly described with an 18ps lifetime (Fig. 3 *A*, table1). In addition two red DAS, with lifetimes 44ps (amplitude 11% for 440nm excitation) and 0.28ns (amplitude 0.3%) are needed to describe the data (Table 1). The 44ps component are ascribed to red forms in the core (Fig. 1), because the sample is not notably contaminated with PSI-LHCI, as can be judged from LT emission (Fig. 1) and protein analysis (see fig4 in Wientjes *et. al.* 2009, Chapter 2). Interestingly, upon excitation at 475nm the contribution of the red component increased as compared to excitation at 440nm (Table 1). This suggests that some β-carotenes (the only pigments excited in the core complex at 475nm) are located close to the red forms to which they transfer energy. As the red Chls have a higher probability to be excited and thus, to generate potentially harmful triplets, a carotenoid, in van der Waals contact would be effective in protecting the complex by quenching Chl triplets. By analogy, in LHCI the red forms (Chls603 and 609) are protected by a carotenoid located in the nearby 621 site (Carbonera *et. al.* 2005; Croce *et. al.* 2007b).

Analysis of PSI-Lhca1/4 and PSI-WT data reveals two main components: a ~20ps one with a core-like spectrum, and an 80-90ps component with an Lhca-like spectrum (720-730nm). A small additional component associated with a longer

PSI core			PSI-Lhca1/4			PSI-WT		
τ	A $_{440}$	A $_{475}$	τ	A $_{440}$	A $_{475}$	τ	A $_{440}$	A $_{475}$
18ps	88%	84%	23ps	69%	59%	20ps	54%	45%
44ps	11%	16%	89ps	25%	35%	83ps	43%	51%
0.28ns	0.3%	0.4%	0.29ns	2.3%	3.0%	0.23ns	2.7%	2.9%
2.4ns	0.1%	0.2%	2.3ns	1.6%	2.4%	1.7ns	0.2%	0.2%
5.2ns	0.4%	0.1%	5.5ns	1.8%	0.8%	5.3ns	0.3%	0.1%
$<\tau>^*$ (ps)	21.3	22.9		46.6	55.5		52.9	58.4
$\tau_{475\text{-}440}$ (ps)		1.6			8.9			5.5
Ex core	100%	100%		76%	47%		62%	35%
$\bar{\tau}_{\mathrm{C}}$ (ps)					39.0			45.5
$\bar{\tau}_{\mathrm{L}}$ (ps)					70.3			65.1
$\bar{\tau}_{\mathrm{L-C}}$ (ps)					31			20

PSI-Lhca5		
τ	A $_{440}$	A $_{475}$
26ps	67%	65%
78ps	29%	32%
0.47ns	2.2%	1.3%
3.1ns	1.7%	1.9%
8.9ns	0.4%	0.3%
$<\tau>^*$ (ps)	41.4	42.7
$\tau_{475\text{-}440}$ (ps)		1.3
Ex core	61%	38%
$\bar{\tau}_{\mathrm{C}}$ (ps)		39.2
$\bar{\tau}_{\mathrm{L}}$ (ps)		44.9
$\bar{\tau}_{\mathrm{L-C}}$ (ps)		6

Table 1: TCSPC Fluorescence decay parameters of PSI complexes. $A_{440,475}$ is the relative contribution to fluorescence decay based on area under DAS after excitation at 440 or 475nm. The underlined lifetimes are used to calculate the average lifetimes: $<\tau>^* = \sum_{i=1}^{3} A_i * \tau_i$. Fraction of core excitation is indicated, see SI2 for details. $\bar{\tau}_{\mathrm{C}}$ is the calculated lifetime for hypothetical selective excitation of the core, and $\bar{\tau}_{\mathrm{L}}$ for selective excitation of LHCI, $\bar{\tau}_{\mathrm{L-C}}$ is the migration time from LHCI to the core.

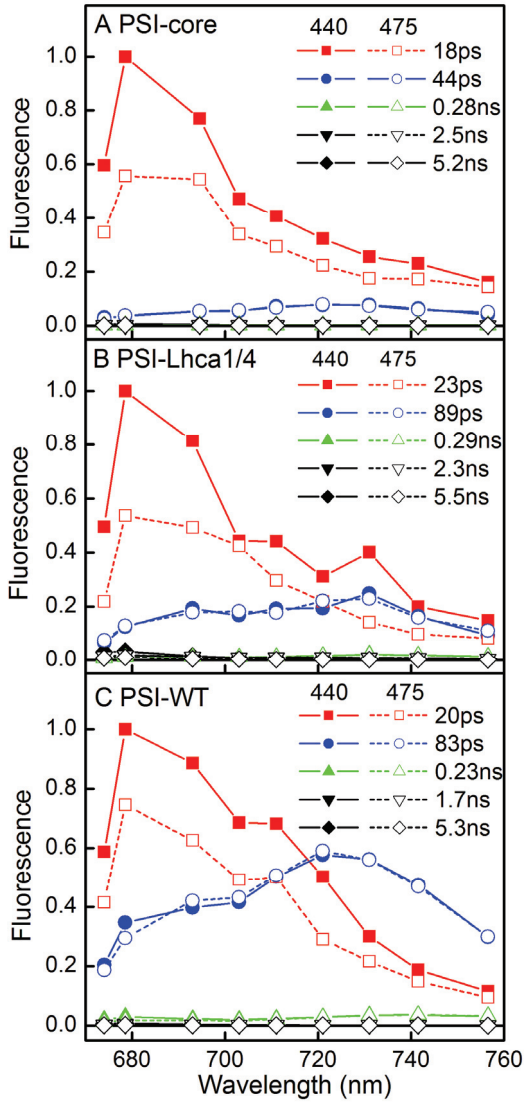

Figure 3: TCSPC. TCSPC DAS of PSI core (A), PSI-Lhca1/4 (B) and PSI-WT (C), excitation was at 440 (solid) and 475nm (dashed). DAS are normalized to each other based on the area under the red-shifted DAS.

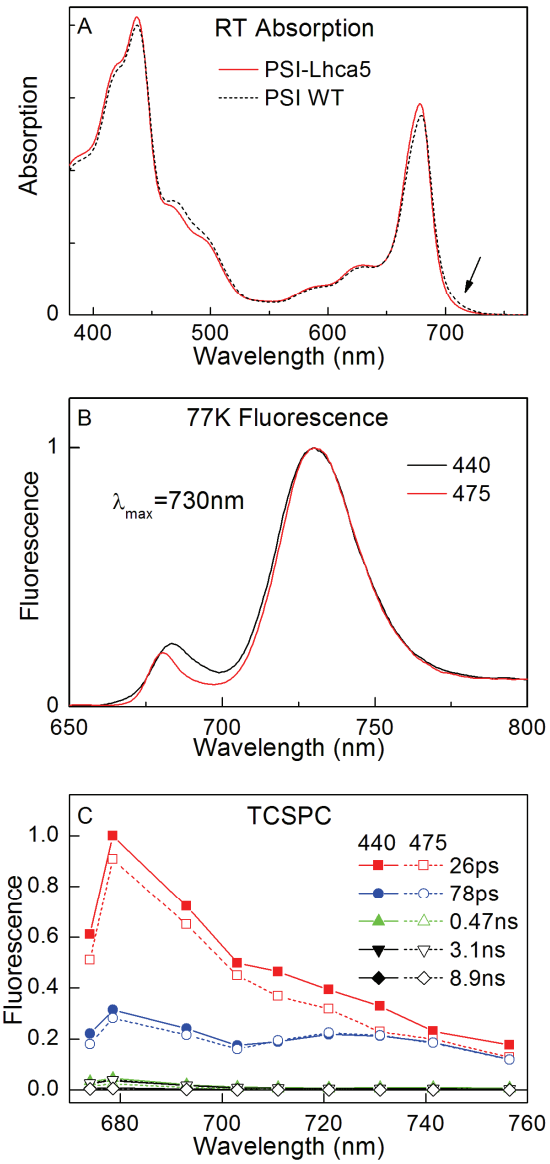

Figure 4: PSI-Lhca5. RT absorption (A), 77K emission (B) and TCSPC DAS (C) of PSI-Lhca5. For comparison the absorption spectrum of PSI-WT is also shown (A). Spectra are normalized to the number of Chls in the Q_y region (A), or the red maximum (B,C).

lifetime (0.23 -0.29ns) and a red-shifted maximum at ~740nm is also present. Similar observations were reported for PSI-WT (Slavov *et. al.* 2008; van Oort *et. al.* 2008). The average lifetimes after 475nm excitation are 55.5ps for PSI-Lhca1/4 and 58.4ps for PSI-WT (Table 1), somewhat longer than the 48ps found with the streak. If the 0.23-0.29ns lifetime, which was not resolved in the streak experiment, is not taken into account, more similar values of 48ps and 53ps are obtained for PSI-Lhca1/4 and PSI-WT,

respectively. Upon more selective excitation of the core (440nm) the contribution of the ~20ps decay component increases (Fig. 3 *BC*, Table 1). This results in a decrease of the average lifetime to 46.6ps for PSI-Lhca1/4 and 52.9ps for PSI-WT (Table 1). Using the average lifetimes obtained after 440 and 475nm excitation and the relative fraction of core excitation (Table 1 and SI. 2), the lifetimes upon excitation of the core complex ($\bar{\tau}_{\mathrm{C}}$) or LHCI only ($\bar{\tau}_{\mathrm{L}}$) can be calculated (see M&M and (van Oort *et. al.* 2008), Table 1). For PSI-Lhca1/4 $\bar{\tau}_{\mathrm{C}}$ is shorter than for PSI-WT, in agreement with the lower content of (red) Chls. However, upon hypothetical excitation of the antenna system the average lifetime ($\bar{\tau}_{\mathrm{L}}$) of PSI-Lhca1/4 becomes somewhat longer than for PSI-WT, indicating that the average EET from LHCI to core ($\bar{\tau}_{\mathrm{L-C}}$) takes longer for PSI-Lhca1/4 (31ps) than for PSI-WT (20ps). Further analysis (SI. 3) shows that EET from Lhca1/4 to the core is slower in PSI-Lhca1/4 than in intact PSI complexes.

The 20ps $\bar{\tau}_{\mathrm{L-C}}$ for PSI-WT is longer than the 9.4±4.9ps reported previously for dissolved PSI crystals (van Oort *et. al.* 2008). This difference can be explained by three factors. 1) The lower contribution of red emission for the PSI crystals (van Oort *et. al.* 2008) as compared to PSI-WT described here (Fig. 3), 2) the different values used for the carotenoid to Chl transfer efficiency (SI2B), and, 3) the different method used to calculate the average lifetimes; in (van Oort *et. al.* 2008) this was based on the average of the lifetimes obtained independently for each detection wavelengths, while in this study the average lifetimes were based on the relative area under the DAS. The latter method takes into account that some wavelengths contribute stronger to the fluorescence decay than others.

*The PSI-Lhca1/**5**-Lhca2/3 supercomplex* – To investigate the effect of the presence/absence of red forms in the intact system, we analyzed a PSI complex in which Lhca4 is substituted by Lhca5. The PSI-Lhca1/5-Lhca2/3 complex has the same supra-molecular organization as PSI-WT (Wientjes *et. al.* 2009, Chapter 2), but a reduced amount of red forms, because Lhca5 does not coordinate them (Storf *et. al.* 2005).

The absorption spectrum of PSI-Lhca5 is similar to that of PSI-WT (Fig. 4 *A*), but the absorption above 700nm is less intense. The LT fluorescence emission spectrum of PSI-Lhca5 shows a maximum at 730nm (Fig. 4 *B*). Because Lhca4 is not present in this sample the 730nm emission can be entirely attributed to Lhca3, which now contains the lowest energy excited state of the system.

The fluorescence decay was studied with TCSPC after excitation at 440nm and 475nm. The DAS are presented in Fig. 4 *C*: The core-like DAS is associated with a lifetime of 26ps, somewhat longer than the 20ps found for PSI-WT. The 78ps

spectrum shows red-shifted emission like the 83ps component in PSI-WT, but with smaller amplitude (Table 1). This indicates that most of the excitation energy from the Lhca1/5 dimer is rapidly transferred to the core, and thus hardly contributes to the 78ps spectrum. This results in an average lifetime of only 42.7ps for PSI-Lhca5, as compared to 58.4ps in PSI-WT. Upon excitation at 440nm the average lifetime decreases only with 1.3ps, giving a $\bar{\tau}_{\mathrm{L-C}}$ of 6ps.

Discussion

In this study we have investigated the effect of individual Lhcas on the EET dynamics of higher plant PSI by analyzing a series of complexes with different antenna size/composition/absorption.

Lhca1/4 and Lhca2/3 have similar effect on PSI decay kinetics – The effect of individual Lhcas on the PSI decay kinetics is discussed in a contradictory way in literature. Based on a comparison of the decay kinetics of intact PSI-LHCI and of PSI largely missing Lhca1/4, it was suggested that EET from Lhca1/4 and Lhca2/3 to the core occurs in a parallel way with similar spectra and kinetics (Ihalainen *et. al.* 2005b). Conversely, in a study on PSI lacking 20-30% of Lhca2/3 it was suggested that this dimer mainly contributes to a red 50ps DAS, while the Lhca1/4 dimer contributes to a stronger red-shifted 120ps DAS (Ihalainen *et. al.* 2002). Similarly, based on target analysis of PSI-LHCI fluorescence decay kinetics two red Chl compartments with RT emission maxima at ~720 and ~740nm (decay lifetimes of 33 and 95ps) were assigned to Lhca3 and Lhca4, respectively (Slavov *et. al.* 2008). In both studies the amplitude of the "Lhca4" related DAS was far lower than that of the "Lhca3" related DAS, which was explained by Slavov et al. (Slavov *et. al.* 2008) by a low emitting dipole strength for Lhca4 as is apparent from the small area of the Lhca4 species associated spectrum (SAS).

Our collection of PSI particles with different antenna composition is well suited to investigate the effect of the individual Lhcas on the PSI decay kinetics. If the spectra and kinetics of Lhca3 and Lhca4 would indeed differ strongly as proposed (Slavov *et. al.* 2008), then in PSI-Lhca5, where only Lhca3 contributes to the red emission, the lifetime and emission maximum of the red DAS should be considerably shorter than in PSI-Lhca1/4. However, this is not the case: all investigated PSI-Lhca complexes show two main decay components of 20-26ps (blue spectrum) and 78-89ps (red spectrum, see SI. 4). The relative amplitude of the red DAS correlates with the presence of the red antennae: PSI-WT> PSI-Lhca1/4> PSI-Lhca5. This relation qualitatively shows that Lhca3 and Lhca4 contribute about equally to the ~80ps DAS, consistent with the similar absorption

and emission properties of Lhca3 and Lhca4 (Wientjes and Croce 2011a, Chapter 3; Wientjes *et. al.* 2011, Chapter 4). The data disprove the assignments in (Ihalainen *et. al.* 2002; Slavov *et. al.* 2008) in which spectra with very different amplitude, emission maxima and lifetimes were assigned to Lhca3 and Lhca4.

Nevertheless, as observed previously (Croce *et. al.* 2000b; Ihalainen *et. al.* 2002; Slavov *et. al.* 2008; van Oort *et. al.* 2008), a small second red DAS was resolved for PSI-WT and PSI-Lhca1/4 (SI. 4, Fig. 3, Table 1). As our data show that this heterogeneity of the fluorescence decay cannot be explained by a very different coupling of Lhca3 and Lhca4 to the core, we propose that it might be attributed to the large inhomogeneous broadening of the red forms (Gobets *et. al.* 1994; Ihalainen *et. al.* 2003; Croce *et. al.* 2007a).

Fast energy transfer from the blue antenna to the core – To study in more detail the effect of the red forms, we have used PSI-Lhca5, with the same antenna size and organization as WT, but with reduced red forms content. EET from the antenna to the core occurs substantially faster than in PSI-WT. Since the only difference is the replacement of *red*-Lhca4 by *blue*-Lhca5, it can be concluded that the *blue* antennae, namely Lhca1, Lhca2 and Lhca5, are responsible for fast EET to the core. Thus, the main barrier for EET between LHCI and core are the low-energy Chls, as was suggested based on a temperature dependence (Jennings *et. al.* 2003) and modeling (Slavov *et. al.* 2008) of PSI excitation energy trapping kinetics. At variance with a previous suggestion (Ihalainen *et. al.* 2005b) the data show that EET from Lhca5 to the core is very efficient.

Impact of the red forms on the effective trapping rate – To investigate the effect of LHCI on the average fluorescence lifetime, we compare <τ> = ~22 ps of PSI-core to $\bar{\tau}_{\mathrm{L}}$ = ~65 ps of PSI-WT upon selective LHCI excitation. This shows that LHCI slows down the effective trapping rate by a factor of three, in agreement with previous results (Engelmann *et. al.* 2006; Slavov *et. al.* 2008). Because PSI-WT coordinates ~1.5 times more Chls *a* than the core (40, 50), for well coupled iso-energetic Chls *a* it can be assumed that $\bar{\tau}_{\mathrm{L}}$ increases with the same factor (from 22 to 33ps). The additional 2x increase to 65ps can be ascribed to the slow energetically uphill EET from the red forms to the trap. Treating the data of Engelman et al (Engelmann *et. al.* 2006) in the same way also gives a 2x increase of the trapping time due to the red forms, and a similar increase of 2.3x was reported by Slavov et al (Slavov *et. al.* 2008) based on their kinetic modeling results.

Comparing the effect of the red forms on $\bar{\tau}_{\mathrm{L}}$ of PSI-Lhca5, which only contains the red forms of Lhca3 (Castelletti *et. al.* 2003; Wientjes *et. al.* 2009,

Chapter 2), and PSI-WT, allows to disentangle the effect of Lhca3 and Lhca4. The effective trapping time of PSI-Lhca5 is increased by a factor of 1.4 (from 33 to 45ps) compared to the case of iso-energetic pigments. This suggests that about 40% of the increase in trapping time in PSI-WT can be ascribed to the red form of Lhca3, and 60% to that of Lhca4.

If a dissipative rate of 0.4/ns (as found for LHCI Wientjes *et. al.* 2011, Chapter 4) is assumed for PSI in the absence of charge separation, it follows that the trapping efficiencies of core, PSI-WT, PSI-Lhca5 are 99.1, 97.4 and 98.2%, respectively. Thus, even though Lhca3 and Lhca4 severely slow down the trapping rate, the effect on trapping efficiency is limited. It can be speculated that Nature has searched for an optimal PSI light harvesting, using as much of the solar spectrum as possible while remaining to work at an extremely high efficiency. It is should be noted that, while the red-forms are only responsible for a small fraction (4-5%) of light-absorption under a normal daylight environment, they may be responsible for up to 40% of the light absorption under deep shade-light conditions (Rivadossi *et. al.* 1999). Thus, especially under shade conditions the small drop in PSI efficiency is negligible compared to the advantage of the increased absorption.

All Lhcas contribute equally to EET to the core – The association of LHCI to the core gives rise to a long trapping lifetime (Fig. 2,3), reflecting slow EET between (part of) LHCI and the core. This has been explained by (i) difficulties in EET between the complexes and/or (ii) by the red forms of LHCI (Croce *et. al.* 2000b; Ihalainen *et. al.* 2002; Jennings *et. al.* 2003; Ihalainen *et. al.* 2005b; Ihalainen *et. al.* 2005c; Engelmann *et. al.* 2006; Slavov *et. al.* 2008). If inter-monomer EET within Lhca1/4 and Lhca2/3 takes place on a faster time scale than transfer to the core, which can occur if (i) is dominating, than the EET occurs from an equilibrated system and can be described by a single rate constant for each dimer, as assumed in (Ihalainen *et. al.* 2002; Ihalainen *et. al.* 2005b; van Oort *et. al.* 2008). However, if (ii) has the most important contribution, then EET from LHCI to the core is slower for the complexes with more red-shifted emission (Slavov *et. al.* 2008), thus $k_{Lhca4} < k_{Lhca3} << k_{Lhca2} < k_{Lhca1}$ (Schmid *et. al.* 1997; Castelletti *et. al.* 2003). The experimental evidence for fast EET from the *blue* Lhcas to the core (discussed above) indicates that (i) does not play a significant role, and that (ii) mainly contributes to the slow trapping in PSI-LHCI.

This means that the rates of transfer from the individual Lhcas to the core can be estimated based on energetic considerations. If it is assumed that (a) energy equilibration within Lhca is faster than EET between Lhca and core, and (b) EET from the core to all Lhcas occurs with the same rate, then the ratio of the EET

rates from individual Lhcas to the core (formula 2) can be derived from the detailed balance equation (see SI. 5 *A*). The validity of assumption (a) will be discussed below. The second assumption is justified because the Förster overlap integral between the emission of a bulk Chl and the absorption of a red-shifted Chl (with an oscillator strength of 2 Chls (Wientjes *et. al.* 2011, Chapter 4), see SI. 5 *B*) is similar to the overlap with a bulk-Chl; furthermore in absorption the red forms do not play such an important role (as compared to fluorescence).

$$\frac{k_{a4C}}{k_{a1C}} = \frac{k_{a4a1}}{k_{a1a4}} \quad \text{and} \quad \frac{k_{a3C}}{k_{a2C}} = \frac{k_{a3a2}}{k_{a2a3}} \qquad (2)$$

Where: $k_{a\#C}$ is the rate of transfer from Lhca# to the core, and $k_{a\#a*}$ is the rate of transfer from Lhca# to Lhca*, and $k_{a*a\#}$ is the backward rate.

The inter-monomer EET rates of Lhca1/4 and Lhca2/3 in solution have been resolved in (Wientjes *et. al.* 2011, Chapter 4). Similar ratios of transfer rates are expected when the dimers are coordinated to the core complex; it thus follows that k_{a1C} is four times k_{a4C} and k_{a2C} is three times k_{a3C} (Wientjes *et. al.* 2011, Chapter 4). For PSI-WT we obtained an antenna-core migration rate of 50/ns from the analysis of the TCSPC experiments. Assuming equal average rates for both dimers and equal initial excitation of the Lhcas (which is reasonable based on the similar absorption properties of the dimers (Wientjes and Croce 2011a, Chapter 3) we obtain k_{a1C} and k_{a2C} 80 and 75/ns, and k_{a3C} and k_{a4C} 25 and 20/ns, respectively (Fig. 6). The faster transfer from Lhca3 compared to Lhca4 might explain the slightly shorter lifetime (78ps) of the red DAS found for PSI-Lhca5, and slightly longer lifetime for PSI-Lhca1/4 (89ps), compared to PSI-WT (83ps). The fastest transfer occurs with a rate of 80/ns, a factor of ~2.5 slower than the slowest equilibration process in Lhca4 and Lhcbs (Croce *et. al.* 2003; Gibasiewicz *et. al.* 2005), indicating that assumption (a) is reasonable. However, it cannot be excluded that a fraction of the excitation energy is transferred to the core before energy equilibration within the Lhcas is completed. In this case the effective average transfer time from the high-energy forms would be somewhat faster and that of the red forms somewhat slower than found with our current model. This might explain the faster transfer obtained for PSI-Lhca5 as compared to the transfer from blue Lhca in PSI-WT.

The EET from the *blue* Lhca to the core and to the *red* Lhca in the dimer is fast, while both transfer rates are slow for the *red* Lhcas (see above and (Wientjes *et. al.* 2011, Chapter 4)). Therefore, upon equal excitation, both *blue* and *red*

Lhcas transfer the same fraction of their absorbed energy (>60%) directly to the core, while the rest (<40%) is transferred to the other Lhca in the dimer (Fig. 6).

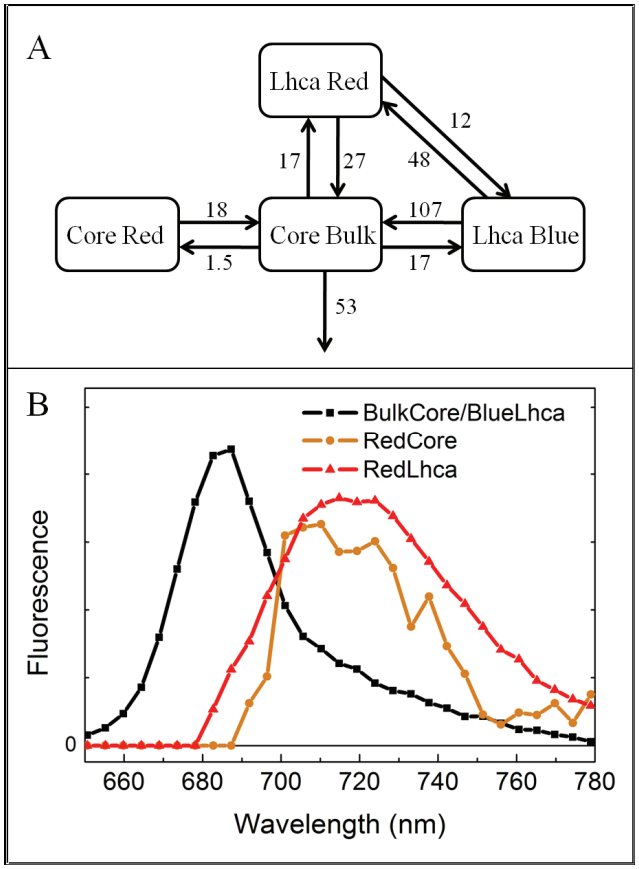

Figure 5: Target analysis of PSI-LHCI kinetics. A: Compartmental model of PSI-LHCI, with EET rates in /ns. B: SAS of the compartments.

Target analysis: Photosystem I model – To obtain a complete picture of the transfer and trapping kinetics of PSI-LHCI, target analysis was performed on the streak-camera data. The data were fitted to a compartmental model where the compartments represent a simplified picture of the different parts of the system. This provides the spectra of, and the transfer rates between the different compartments (see (Stokkum *et. al.* 2004) for details).

First the decay of the PSI core was modeled. Its detailed trapping kinetics is discussed controversially in literature (see e.g. (Holzwarth *et. al.* 2006) versus (Shelaev *et. al.* 2010)), and is beyond the scope of this paper. We describe the kinetics with a simple two compartment model: one for bulk Chls from which trapping occurs and one for red Chls (Fig. 5 *A*). An apparent trapping rate of 53/ns was obtained, in good agreement with 56/ns which was proposed as general trapping rate for bulk Chls in PSI core particles (Gobets *et. al.* 2001b). In the second step PSI-WT is modeled, assuming that the core kinetics remain the same. Because the emission spectra at RT of Lhca1 and Lhca2 and of Lhca3 and Lhca4 (Schmid *et. al.* 1997; Castelletti *et. al.* 2003; Wientjes *et. al.* 2011, Chapter 4) are similar, we introduce only one *blue* (Lhca1,2) and one *red* (Lhca3,4) compartment in the model. The ratio of EET from the *blue* antenna to the core is forced to be four times faster than that of the *red* antenna, similar to the ratios used for the analysis of the TCSPC data. The transfer rates between *blue* and *red* antenna were obtained from the analysis of the Lhca1/4 dimer (Wientjes *et. al.* 2011, Chapter 4). Although the modeling is coarse grained, it provides a satisfactory description of the data (Fig.

5, SI. 6). The emission maximum of the *red* Lhcas is found at 720nm, in good agreement with our previous work on isolated LHCI dimers (see Lhca3 and Lhca4 spectra (Wientjes *et. al.* 2011, Chapter 4)). The evolution of the excitation concentrations on the different compartments are shown in SI. 7. The rates of transfer from antenna to core (*blue* 107/ns, *red* 27/ns) are similar but somewhat faster than the ones based on the analysis of TCSPC data (*blue* 75-80/ns, *red* 20-25/ns).

Target analysis was also performed for PSI-Lhca1/4 (SI. 8). The rate of transfer from antenna to core was estimated to be 75% of that in PSI-WT, in agreement with the larger $\bar{\tau}_{\mathrm{L-C}}$ obtained from the TCSPC data. The ratio between forward and backward transfer between core and Lhcas is half in PSI-Lhca1/4 as compared to PSI-WT, which is expected when the Lhca antenna size is reduced by a factor of two.

Two previous studies have addressed the rates of transfer from Lhca3 and Lhca4 to the core. In Ihalainen et al. (Ihalainen *et. al.* 2005c) a 7/ns *red* Lhca to core rate was reported, thus ~3 times slower than the 23/ns obtained from our analysis. However, an unusual large LHCI loss channel of 7/ns was also needed to describe the data, while the isolated dimers decay with a lifetime of 0.4/ns (Gobets *et. al.* 2001a; Wientjes *et. al.* 2011, Chapter 4), thus suggesting that the model does not give a realistic description of the kinetics. In the study of Slavov et al. (Slavov *et. al.* 2008) the reported values of 14 and 36/ns for *red* Lhca to core are comparable to the 27/ns obtained here but the decay of Lhca3 and Lhca4 was described with very different spectra and kinetics, while our data indicate that this cannot be the case.

Summarizing conclusion

Combining streak-camera and TCSPC measurements we investigated excitation energy transfer and trapping kinetics of higher plant PSI-LHCI, taking into account the transfer rates from, to and between individual Lhcas. Fig. 6 summarizes the results:

- Transfer from Lhca1 and Lhca2 to the core occurs very fast (~100/ns) and faster than energy equilibration between the Lhcas.
- Excitation energy can only “slowly” (~25/ns) escape from Lhca3 and Lhca4 to the core.
- Each Lhca contributes about equally to the transfer to the core.
- The spectra of Lhca3 and Lhca4 are similar, with a red-emission maximum at 715-720nm.

- The red forms of Lhca3 and Lhca4 slow down the effective PSI trapping rate in a comparable manner, and together by about 2 times.

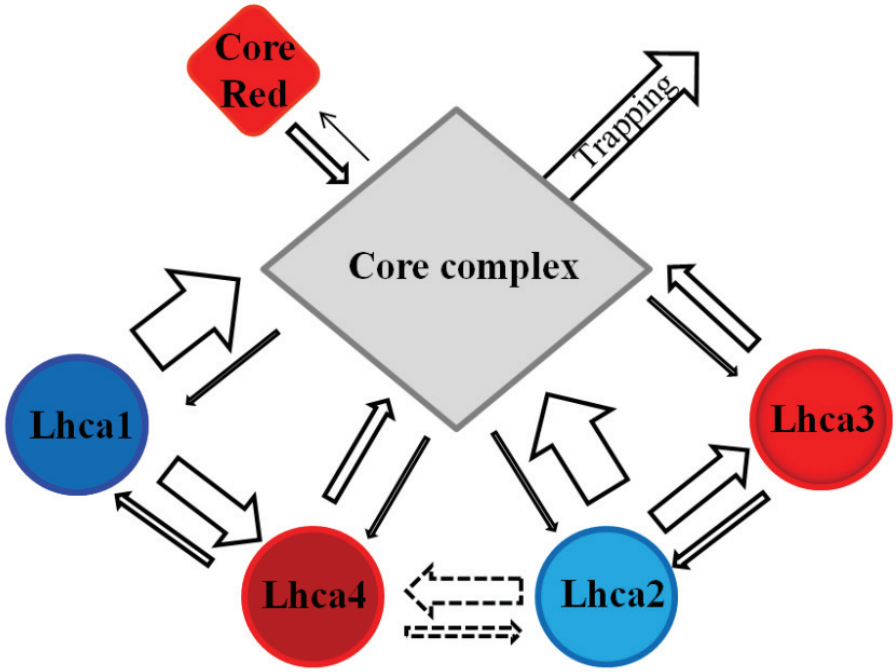

Figure 6: Schematic presentation of energy transfer and trapping in PSI-LHCI. Thickness of the arrows indicates the rates. The transfer rate between Lhca2 and Lhca4 could not be estimated from our target analysis, but, based on structural data, it has been suggested to be similar to the intra-dimer transfer rates (Ben-Shem *et. al.* 2003; Sener *et. al.* 2005).

Acknowledgements

The authors thank Arie van Hoek and Rob Koehorst for excellent technical support and Stefan Jansson for providing the Lhca mutant lines. This work was supported by De Nederlandse Organisatie voor Wetenschappelijk Onderzoek (NWO), Earth and Life Sciences (ALW), through a Vidi grant (to R.C.).

Supplementary information

SI1 Absorption spectra of PSI complexes

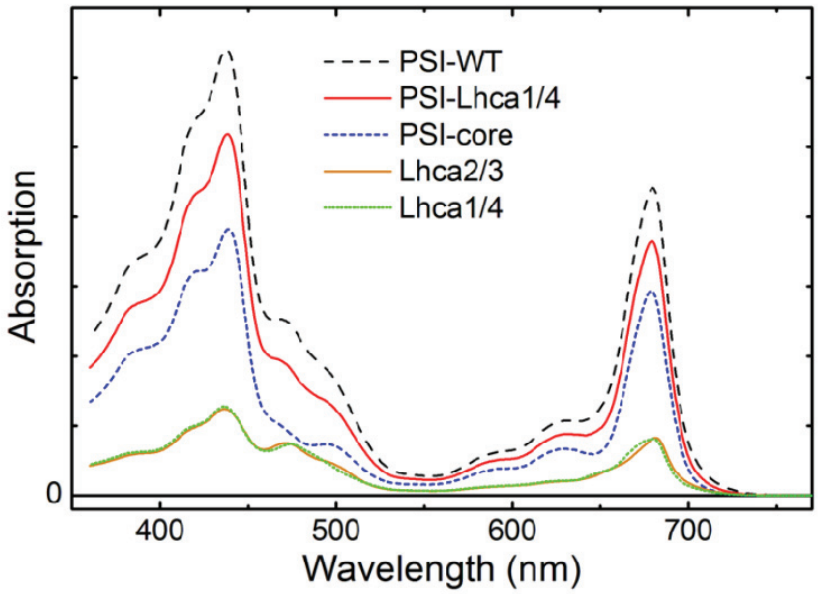

Figure SI1: RT absorption spectra of PSI-complexes. Spectra are normalized in the Q_y region based on 170 Chls for PSI-WT, 135 Chls for PSI-Lhca1/4, 100 Chls for PSI-core and 35 Chls (see SI. 2 *A*) for both Lhca1/4 and Lhca2/3. The oscillator strengths of Chl *b* is assumed to be 0.7 times that of Chl *a* in the Q_y region (630-750nm).

SI2A Fraction of PSI core excitation

In order to obtain the fraction of core and LHCI excitation at specific wavelengths a few factors have to be taken in account. First, the efficiency of energy transfer from the carotenoids (Car) to the Chls. For the Lhca1/4 and Lhca2/3 dimers we obtained these efficiencies by comparing the absorption and excitation spectra. The absorption spectra were fitted with the spectra of all pigments in a protein environment (Croce *et. al.* 2000a). The excitation spectra are fitted with the same spectral forms, allowing the carotenoids to contribute less as compared to the absorption spectra see figure SI2.1. In this way Car to Chl transfer efficiencies of 70% for Lhca1/4 and 64% for Lhca2/3 were obtained. For the PSI core a 70% Car to Chl efficiency was used (de Weerd *et. al.* 2003). The absorption spectrum of PSI-LHCI needs to be described with the spectra of the core and LHCI. This was done in two ways. Method I: the core was normalized to 100 Chls *a* in the Q_y region, and each dimer to 35 Chls, which gives the spectra shown in Fig SI2.2. A disadvantage of this method is that there is a small difference between the absorption spectrum of the whole complex and the sum of its parts. Therefore, in

Method 2 all absorption of the complex that is not due to the core is ascribed to LHCI, and these values are used in this study. In both methods the gap-pigments are counted as LHCI pigments, and the Car to Chl transfer efficiency is assumed to be the same as obtained for LHCI.

Table SI2.1 shows the effective excitation of the core compartment after correction for the Car to Chl transfer efficiency.

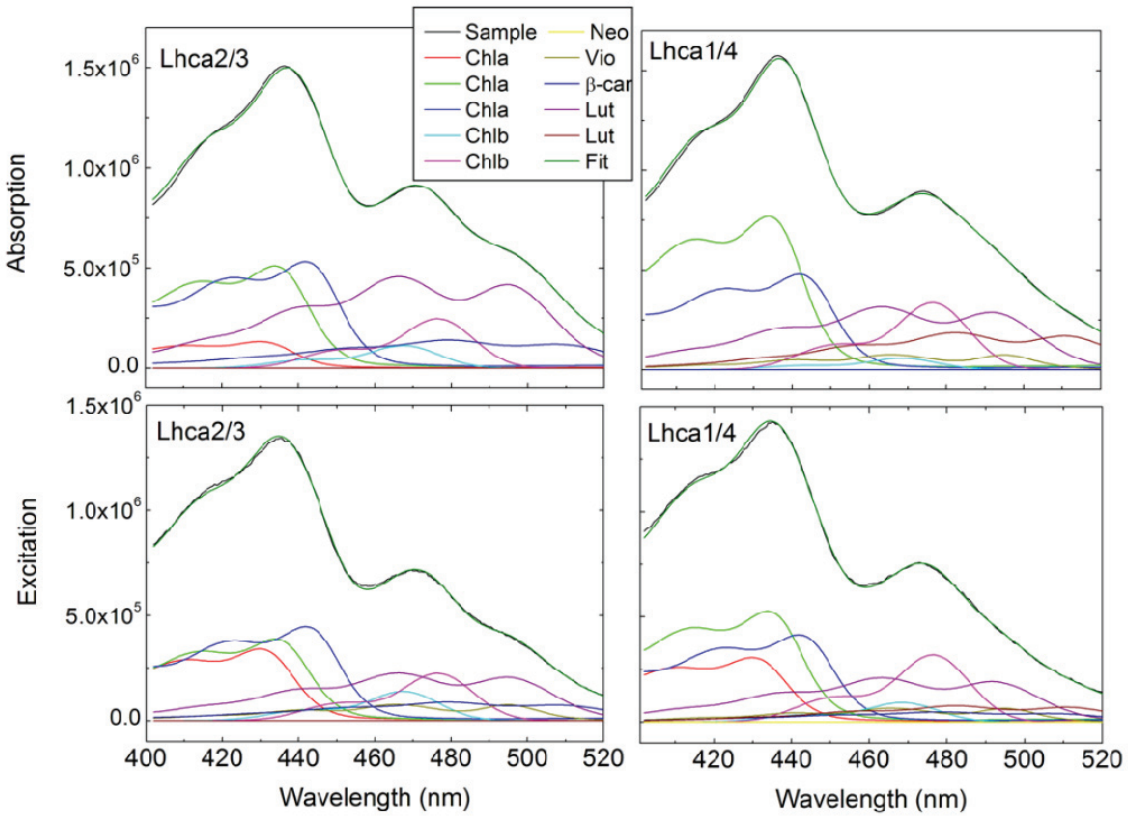

Figure SI2.1: Decomposition of the Soret region. Decomposition of the Soret region of the absorption (*top*) and excitation (*bottem*) spectra of the dimers in terms of the individual pigments: Chl *a*, Chl *b,* neoxanthin (Neo), violaxanthin (Vio), β-carotene (β-car) and lutein (Lut). The sum of the individual pigments is also shown (Fit).

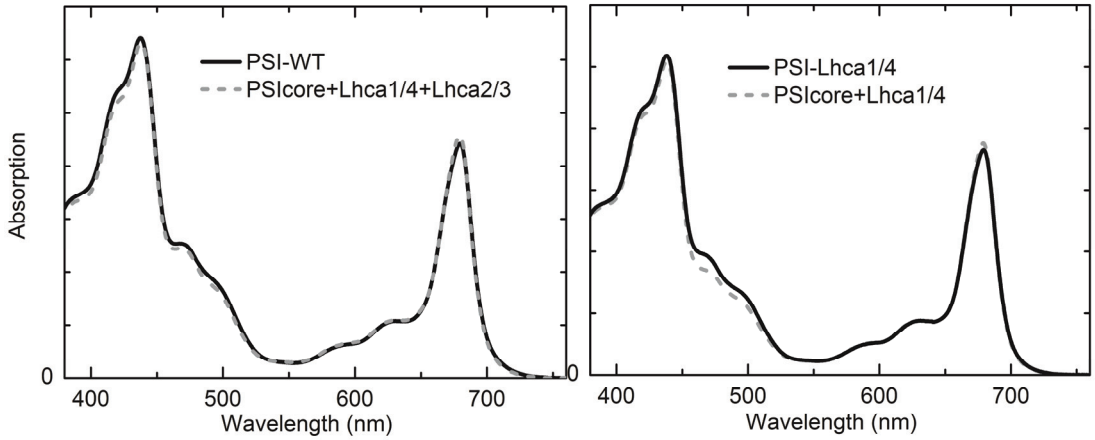

Figure SI2.2: Absorption spectra of PSI-Lhca complexes compared to the sum of PSI core and Lhca dimer(s).

Table SI2.1: Fraction of core excitation. Values are reported obtained with the two methods described above as Method1/Method2. For PSI-Lhca5 the absorption spectrum of Lhca1/5 is not known, thus only Method 2 is used where the LHCI Car to Chl efficiency is supposed to be the same as for WT LHCI.

	PSI-WT	PSI-Lhca1/4	PSI-Lhca5
Core excitation 440nm	0.63/0.62	0.77/0.76	/0.61
Core excitation 475nm	0.36/0.35	0.53/0.47	/0.38

SI2B Possible errors in the estimation on the core excitation fraction and the effect on LHCI to core transfer times

To estimate the core excitation fraction a few assumptions have to be made, possibly giving rise to an error. The main uncertainties are the Car to Chl energy transfer efficiencies. The effects of assuming different transfer efficiencies for PSI-WT are reported in Table SI2.2. In column A the assumptions described in SI2A were used. In column B a Car to Chl transfer efficiency of 90% is used for the core as reported in (Kennis *et. al.* 2001). In C the absorption of the few Chls *b*, always present in the PSI core preparation of higher plants (Chla/b=33), are not taken into account. This means that at 475nm only Cars are excited (which are assumed to transfer 70%), while in A 20% of Chl excitation (transferring 100%) was assumed, see Fig SI2.3. In D a higher Car to Chl transfer efficiency was assumed, comparable to values found for Lhcb complexes, e.g. (Gradinaru *et. al.* 2000). It should be noted that LHCI in this case also includes the gap pigments of which the transfer efficiency is unknown. In E the assumptions used in C and D are combined, these assumptions were used in van Oort et al. (van Oort *et. al.* 2008). The range of obtained $\bar{\tau}_{\mathrm{L-C}}$ values (Table SI2.2) provides an indication of the possible inaccuracy of this value.

Table SI2.2: Core excitation fraction of PSI-WT. See text for explanation.

	A See SI2A	B 90% Car trans Core	C Chl *b* Core not considered	D 85% Car trans LHCI	E = C+D
Ex Core 440	0.62	0.63	0.62	0.60	0.62
Ex core 475	0.35	0.39	0.33	0.31	0.30
Diff	0.28	0.24	0.30	0.29	0.32
$\bar{\tau}_{L-C}$ (ps)	19.6	22.8	18.5	19.0	17.1

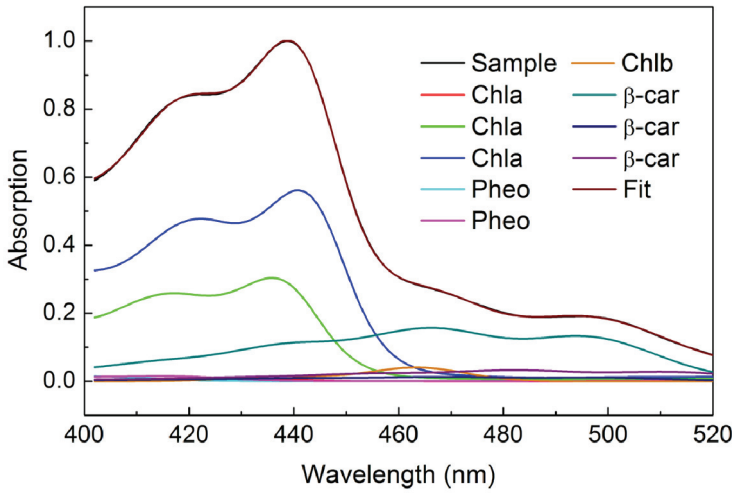

Figure SI2.3: Description of PSI core absorption. Description of PSI core absorption spectrum with Chl *a*, β-carotene and a low amount of Chl *b*, furthermore a very small contribution of Pheophytin (Pheo) was needed to describe the absorption. Note that the absorption of the sample overlaps perfectly with the sum of the individual pigments.

SI3 PSI-Lhca1/4 is working less efficiently than the intact system

Based on the TCSPC study with two excitation wavelengths it was estimated that excitation energy transfer from LHCI to the core occurs with an average rate of 50/ns in PSI-WT, and only with a rate of 32/ns in PSI-Lhca1/4. This would thus imply about 2 times faster energy transfer from Lhca2/3 to the core, than from Lhca1/4. To investigate this in more detail the average fluorescence lifetimes of PSI-WT and PSI-Lhca1/4 are plotted as a function of the emission wavelengths (Fig SI3). After 475nm excitation PSI-Lhca1/4 has a longer average lifetime than PSI-WT for the red-shifted wavelengths. This means that the excitation energy transfer from Lhca1/4 to the core is slower in PSI-Lhca1/4 than in WT, otherwise the lifetime would always be shorter for a complex harboring less (red) Chls. Shorter lifetimes are indeed observed for PSI-Lhca1/4 after more selective core excitation (440nm) (Fig SI3). It can thus be concluded that the connectivity between Lhca1/4 and the core is better in intact PSI-WT, than in the sub-complex lacking Lhca2/3, in agreement with the LT fluorescence results (Fig 1). This also

means that the difference in transfer rates from both dimers to the core in PSI-WT is smaller than a factor two, and thus that the rates are rather similar. More efficient energy transfer in intact photosynthetic supercomplexes, compared to complexes lacking some Lhc antennae, might be a general PS feature, as it has also been observed for PSII (Caffarri *et. al.* 2011).

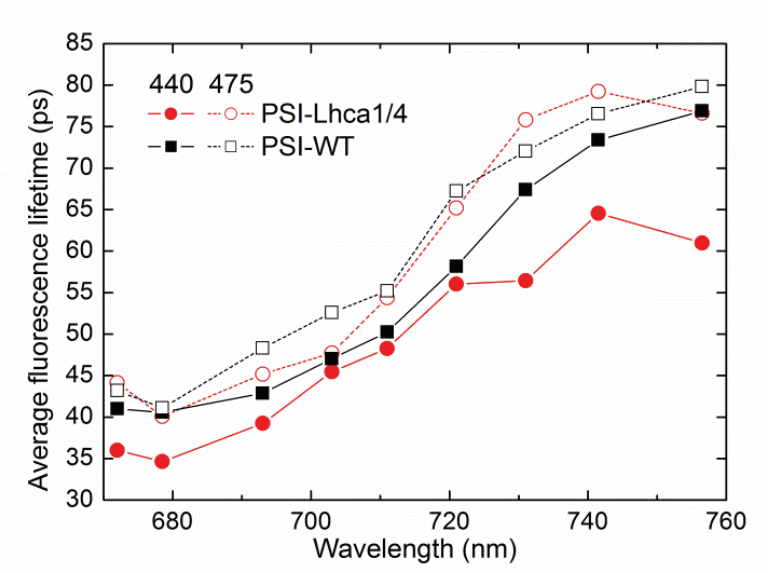

Figure SI3: Wavelength dependence of average fluorescence lifetime. Average fluorescence lifetime of PSI-Lhca1/4 and PSI-WT calculated from the three shortest lifetimes as found with TCSPC after 440nm and 475nm excitation (Fig 3).

SI4 Comparing the DAS from different PSI complexes

Fig SI4 *A* shows that the ~80ps DAS of PSI-WT, PSI-Lhca1/4 and PSI-Lhca5 have similar red emission maxima. Fig SI4 *B* shows the strongly red-shifted sub-ns DAS of PSI-WT and PSI-Lhca1/4.

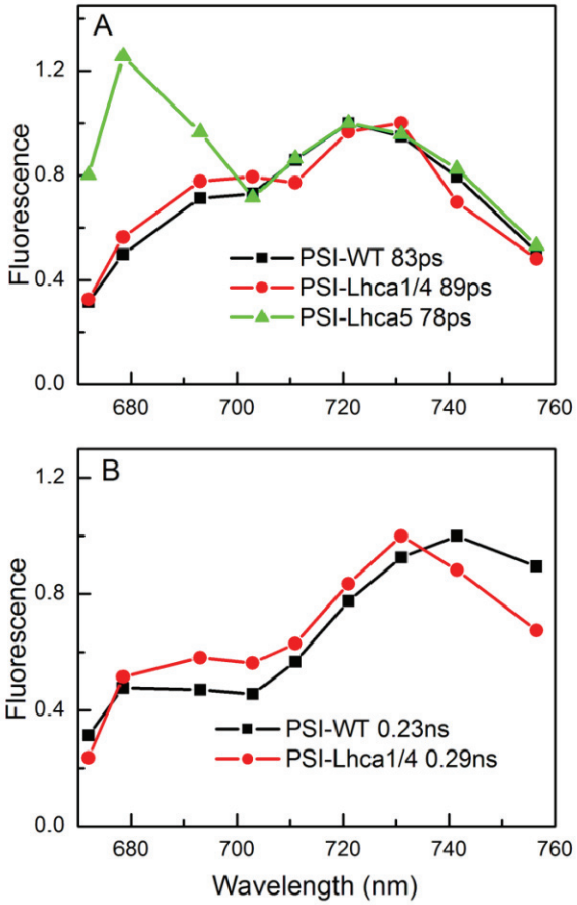

Figure SI4: Comparing PSIs DASs. A: decay associated spectra with ~80ps lifetime of PSI-WT, PSI-Lhca1/4 and PSI-Lhca5. B: The sub-ns DAS of PSI-WT and PSI-Lhca1/4. DAS have been normalized on the maximum of the red emission.

SI5A Determination of the Lhca to core transfer rates

In case energy equilibration within Lhca is fast compared to the energy transfer to the core, then the rates $k_{a\#C}$ (rate of energy transfer from Lhca# to core) and $k_{Ca\#}$ (rate of energy transfer from core to Lhca#) should follow the detailed balance equation. It is assumed that the core to Lhca transfer rate is equal for Lhca1 and Lhca4 (See below), thus $k_{Ca1} = k_{Ca4} = A$.

Thus for energy transfer between Lhca1 and Lhca4 and the core:

(1) $$\frac{k_{Ca1}}{k_{a1C}} = \frac{n_{a1}}{n_C} * e^{-(E_{a1}-E_C)/kT} = \frac{A}{k_{a1C}}$$ and

(2) $$\frac{k_{Ca4}}{k_{a4C}} = \frac{n_{a4}}{n_C} * e^{-(E_{a4}-E_C)/kT} = \frac{A}{k_{a4C}}$$

with n the number of pigments and E the excited state energy of the Lhca and the core. It follows that:

$$\frac{(Eq.1)}{(Eq.2)} = \frac{k_{a4C}}{k_{a1C}} = \frac{n_{a1}}{n_{a4}} * e^{-(E_{a1}-E_{a4})/kT} = \frac{k_{a4a1}}{k_{a1a4}}$$

where k_{a4a1} and k_{a1a4} are the rates of energy transfer from Lhca4 to Lhca1 and from Lhca1 to Lhca4, respectively. These rates have been obtained in (Wientjes *et. al.* 2011).

SI5B Förster overlap integral with red forms

The Förster overlap integral J depends on the emission properties of the donor and the absorption properties of the acceptor, according to:

$$J = \int_0^\infty f_D(\lambda) * \varepsilon_A(\lambda) * \lambda^4 d\lambda$$

The spectra in Fig SI5B were used to compare the overlap integral between bulk Chl *a* donor and bulk Chl *a* acceptor, or a high red Chl *a* acceptor. Taking these spectra $J_{bulk\text{-}red}/J_{bulk\text{-}bulk}$ is 0.83. When the emission spectrum of the donor is 4nm red-shifted (λ_{max} 685nm) this ratio increases to 1.14. This indicates that the energy transfer from bulk Chls to bulk or red Chls are similar, under the assumption that the dipole orientation factor (κ^2) is the same.

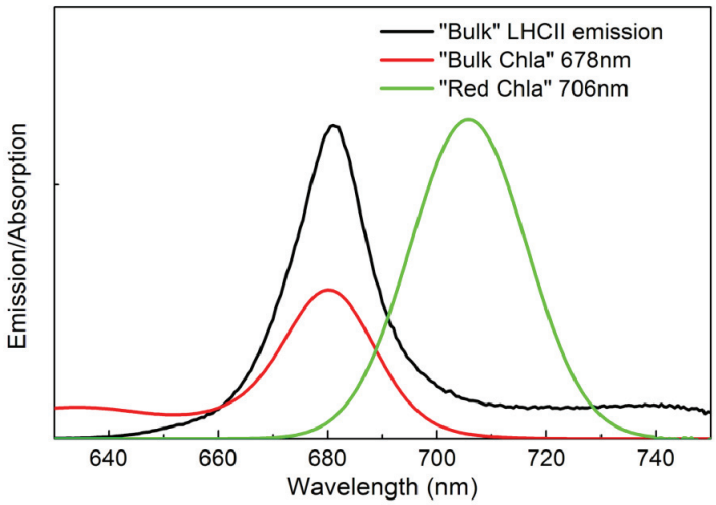

Figure SI5B: Chl absorption and emission. Emission spectrum of LHCII (*black*), absorption band of Chl *a* in protein environment (Cinque *et. al.* 2000) with maximum at 678nm (*red*), Gaussian band-shape with maximum at 706nm and full width at half maximum (*green*) represents the red Chls of Lhca3 and Lhca4 (Wientjes and Croce 2011b). Oscillator strength in Q_y region is two times larger for the red Chls compared to the bulk Chl *a,* as was observed in (Wientjes *et. al.* 2011).

SI6 Synchroscan streak camera data and target analysis description

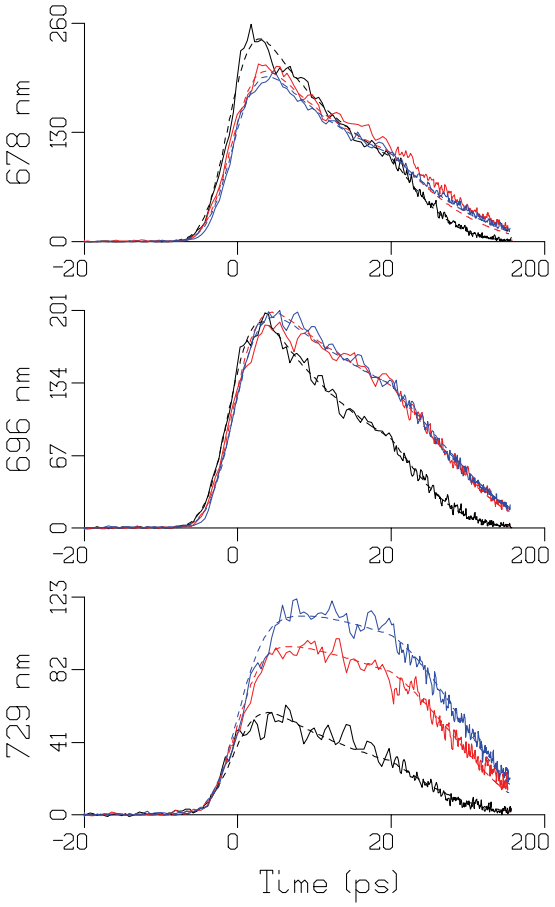

Figure SI6: Synchroscan streak camera data and fit. Synchroscan streak camera decay traces (*solid*) and fit based on target analysis (*dashed*) at three detection wavelengths for PSI core (*black*), PSI-Lhca1/4 (*red*) and PSI-WT (*blue*). Note that the time axis is linear until 20 ps, and logarithmic thereafter.

SI7 Transient excitation concentration of PSI-WT compartments

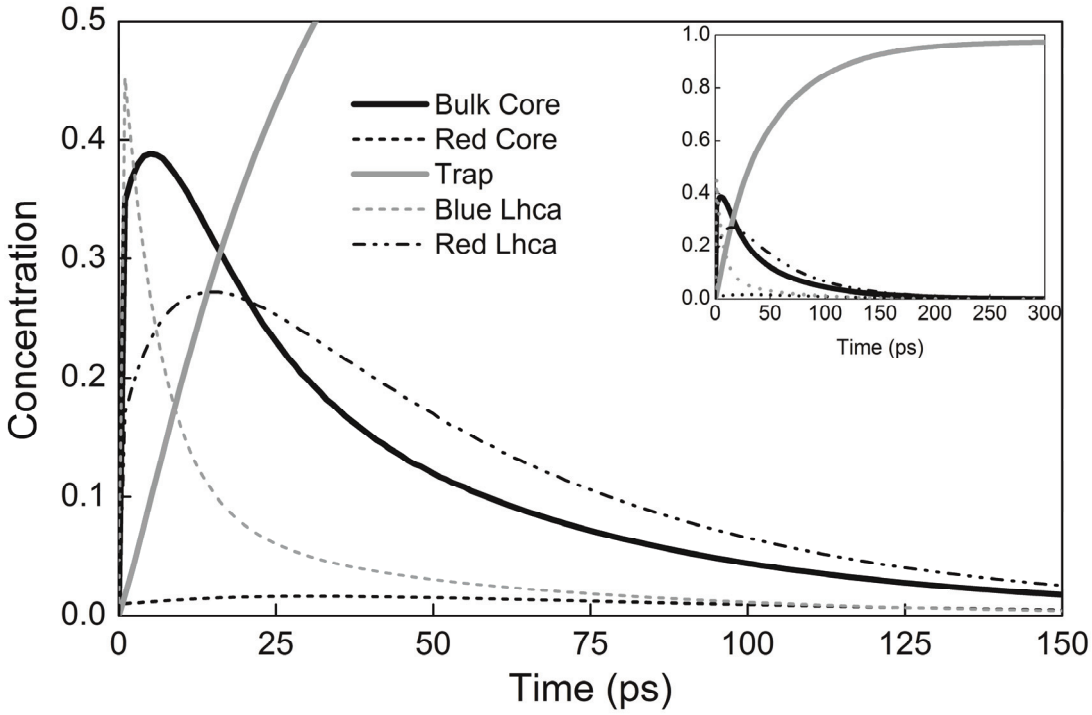

Figure SI7: Evolution of the excitation population of each compartment of PSI-WT.

SI8 Target analysis PSI-Lhca1/4

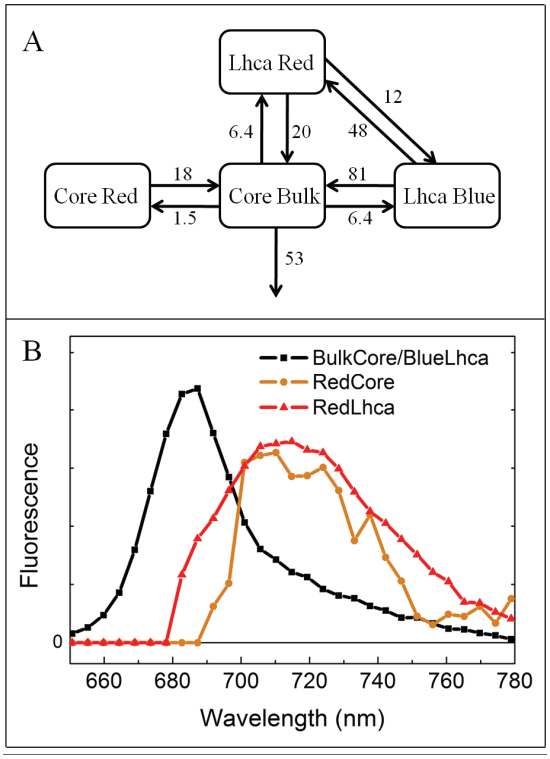

Figure SI8: Target analysis of PSI-Lhca1/4 kinetics. A: Compartment model of PSI-Lhca1/4, with EET rates in /ns. B: SAS of the compartments. Initial excitation fraction of the core was fixed at a value of 53% as obtained from the absorption spectra (Table 1 main text). LHCI excitation was 65%, the fractions of *red* vs *blue* antenna excitation were estimated at 0.25 and 0.75.

Chapter 8

PMS: Photosystem I electron donor or fluorescence quencher?

Emilie Wientjes and Roberta Croce

Photosynthesis research, in press.

Abstract

Light energy harvested by the pigments in Photosystem I (PSI) is used for charge separation in the reaction centre (RC), after which the positive charge resides on a special chlorophyll dimer called P700. In studies on the PSI trapping kinetics, $P700^+$ is usually chemically reduced to re-open the RCs. So far, the information available about the reduction rate of these reducing agents is limited, even though this information is indispensible to estimate the fraction of open RCs under known experimental conditions. Moreover, it would be important to understand if these reagents have a chlorophyll fluorescence quenching effect to avoid the introduction of exogenous singlet excitation quenching in the measurements. In this study we investigated the effect of the commonly used reducing agent phenazine methosulfate (PMS) on the RC and fluorescence emission of higher plant PSI-LHCI. We measured the $P700^+$ reduction rate for different PMS concentrations, and show that a reliable estimation on the fraction of closed RCs can be given based on these rates. In addition, the data show that PMS is quenching chlorophyll fluorescence emission. Finally, we determined that the fluorescence quantum yield of PSI with closed RCs is 4% higher than with open RCs.

Introduction

Photosystem I (PSI) plays a major role in the light harvesting reactions of photosynthesis. The structure of the cyanobacterial PSI core complex has been solved at 2.5Å resolution, it consists of at least 12 proteins, which coordinate 96 Chlorophylls (Chls) *a,* 22 β-carotenes, 2 phylloquinones and 3 Fe_4S_4 clusters (Jordan *et. al.* 2001). Higher plant PSI has a very similar structure as the complex of cyanobacteria (Ben-Shem *et. al.* 2003), but in addition it contains four light harvesting antenna's (Lhca) (Boekema *et. al.* 2001; Ben-Shem *et. al.* 2003). These Lhcas bind carotenoids, Chls *a* and *b* and serve to increase the absorption cross section (Schmid *et. al.* 1997; Croce *et. al.* 2002). In green algae the antenna system is even larger. The PSI complex of *Chlamydomonas reinthardtii* is believed to coordinate up to 14 Lhca antennas (Germano *et. al.* 2002; Busch *et. al.* 2010) which would mean that it can bind more than 300 Chls. In the higher plant PSI-LHCI structure173 Chls were assigned (Amunts *et. al.* 2010).

Light energy harvested by this large number of pigments is efficiently transferred to the reaction centre (RC), located in the core complex, where primary charge separation occurs. The common view is that a Chl *a* dimer called P700 is the primary electron donor; after charge separation the released electron

is transferred along the electron transport chain: A_0 (Chl *a*), A_1 (phylloquinone) and the Fe_4S_4 clusters F_X, F_A and F_B, reviewed in Brettel *et al.* (1997). Alternatively, it has been proposed that the accessory Chl(s), located in the proximity of P700, are the primary electron donor, while P700 only gets oxidized in the secondary electron transfer step (Holzwarth *et. al.* 2006; Di Donato *et. al.* 2011).

If PSI is in its natural environment, i.e. associated with the thylakoid membrane in cyanobacteria or chloroplasts, the electron from F_B is donated to ferredoxin (or flavodoxin), while the hole on $P700^+$ is filled by an electron coming from plastocyanin (or cytochrome c_6). To understand the trapping kinetics of PSI, its excited state decay has been extensively investigated with different time-resolved techniques: transient absorption, emission measured by a synchroscan streak camera, time correlated single photon counting (TCSPC) or fluorescence up-conversion. Under generally applied experimental conditions the endogenous oxidizing and reducing agents are not present. In absence of electron donors and acceptors charge recombination occurs on the µs to ms time-scale, e.g. (Brettel 1997; Vassiliev *et. al.* 1997). However, electrons can also escape from the Fe_4S_4 cluster to other electron acceptors, such as oxygen (Rousseau *et. al.* 1993). Therefore, in absence of electron donors and in the presence of light all P700s are soon blocked in their oxidized (closed /$P700^+$) state (Savikhin 2006). To study the kinetics of PSI with open RCs, reducing agents are added to the buffer. Most often phenazine methosulfate (PMS) reduced by sodium ascorbate (NaAsc) is used for this purpose. PMS is supplied at different concentrations: 10µM e.g. (Turconi *et. al.* 1993; Gobets *et. al.* 2001; Ihalainen *et. al.* 2005), 20µM (Nuijs *et. al.* 1986; Karapetyan *et. al.* 1997; Engelmann *et. al.* 2006; Giera *et. al.* 2010), 60µM (Slavov *et. al.* 2008) or 150µM (Byrdin *et. al.* 2000).

In this work we study how fast PMS re-reduces $P700^+$ to its neutral state, and use these rates to estimate the fraction of closed RCs under different light intensities. We show that PMS itself is quenching fluorescence of light-harvesting complexes. And we show that closing the RC of higher plant PSI increases its fluorescence quantum yield by only 4%.

Materials & Methods

Purification of photosynthetic complexes – Thylakoids were isolated from *Arabidopsis thaliana* plants as described previously (Bassi and Simpson 1987). The major light-harvesting complex of PSII (LHCII) and the PSI complex were obtained by mild solubilisation of the thylakoids followed by sucrose gradient density centrifugation, as described in (Caffarri *et. al.* 2001). For all fluorescence measurements the obtained PSI complexes were run over a second sucrose

gradient to improve the purity. Indeed, the low-temperature emission shows that the sample is very pure (Wientjes *et. al.* 2009, Chapter 2). Photosystem II membranes were obtained as described in (Berthold *et. al.* 1981). The PSI light-harvesting antenna Lhca1/4 was obtained as described in (Wientjes and Croce 2011, Chapter 3).

Absorption and fluorescence spectroscopy – Absorption spectra were recorded on a Cary 4000 UV-Vis spectrophotometer (Varian, Palo Alto, CA). Fluorescence spectra were recorded on a Fluorolog 3.22 spectrofluorimeter (HORIBA Jobin Yvon, Longjumeau, France); samples were diluted to an optical density of 0.05 /cm at the Q_y maximum, unless stated otherwise.

P700 and fluorescence kinetics – The P700 oxidative state and fluorescence kinetics were measured with the Dual-PAM-100 (Heinz Walz, Effeltrich, Germany). For $P700^+$ detection the 830 minus 875 nm absorption difference signal was used. The 635nm actinic light was provided by a LED array (intensity as indicated). The fluorescence measuring light was operated at 40 μmol/m^2/s with a frequency of 10 (in the PAM software), emission was detected through a RG9 filter (Schott). One ml of PSI solution was contained in a 1x1x3 cm cuvette, at an optical density of 3.3 /cm in the Q_y maximum.

All measurements were performed at room temperature in 10 mM tricine, pH 7.8, 0.03% dodecyl-α-D-maltoside and between 0 and 1 M sucrose.

Results

P700 reduction rate – We tested the P700 reduction rate for commonly used PMS/NaAsc concentrations on higher plant PSI. The broad 800-840 nm absorption band of oxidized P700 was used to monitor the oxidation state during the reduction of P700 after a strong light pulse (fig. 1). The traces were fitted with a mono-exponential decay function. The obtained reduction rate constants were 36, 204 and 412 /s for respectively 10, 60 and 150 μM PMS, with a standard deviation of ≤ 5% from four repetitions. The rates are similar to those reported previously for PSI of *Synechocystis sp. PCC* 6803 (Gourovskaya *et. al.* 1997) and *Synechococcus elongatus* (Byrdin *et. al.* 2000). If only 10mM NaAsc was supplied as reducing agent, the rate constant was 0.053 /s. This is six times faster than what was reported previously (Savikhin *et. al.* 2001). The mono-exponential decay and the decay constant of ~20 s for NaAsc indicates that charge recombination, which takes place on the μs to ms time-scale, does not play a role in the $P700^+$ reduction reported here.

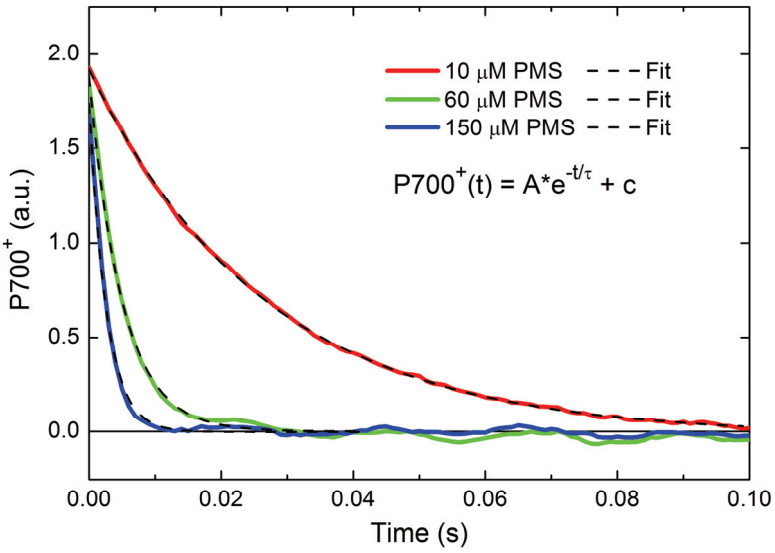

Figure 1: Rate of photo-oxidized P700 reduction by PMS. The 830 minus 875 nm absorption signal is monitored after P700 is oxidized by a 20 mmol/m^2/s light pulse with a duration of 0.2 s. PMS/ NaAsc concentrations were as in previous reports: 10μM /10mM e.g. (Ihalainen *et. al.* 2005), 60μM/ 40mM (Slavov *et. al.* 2008) and 150μM/ 5mM (Byrdin *et. al.* 2000).

Fraction of open RCs – For spectroscopic measurements on PSI it is often claimed that the RCs are open before excitation. The fraction of open RCs can, in principle, be calculated based on the experimental conditions and the P700 reduction rate. To validate these (theoretical) calculations we measured the fraction of closed RCs under a range of different light intensities and PMS concentrations. Figure 2 shows an example of these measurements. The P700$^+$ concentration reaches 75% of the maximum (obtained after a saturating light pulse for the 10 μM PMS sample) during illumination with 531 μmol/m^2/s of light if 10 μM PMS is supplied, while it reaches only 14% for 150 μM.

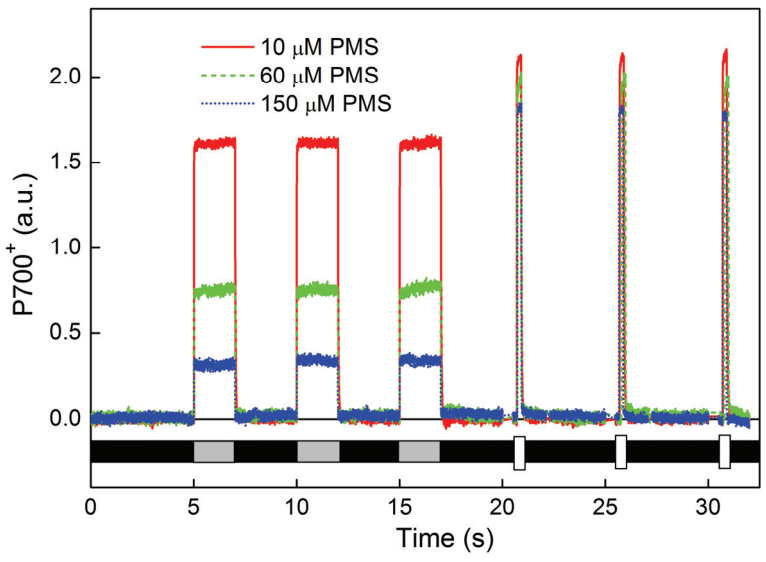

Figure 2: P700$^+$ build-up for different PMS concentrations. The P700$^+$ formation upon illumination of PSI with 531 μmol/m^2/s of actinic light (grey bar) was compared to that after a strong light pulse of 20 mmol/m^2/s (white bar), the rest of the time the light was off (black bar) to allow for full re-opening of the RCs. PMS was reduced with NaAsc, at concentrations reported in the legend of fig. 1.

The combination of the charge separation and P700$^+$ reduction rates determines the fraction of closed RCs in equilibrium, see Equation box 1. The charge separation rate depends mainly on the number of absorbed photons per

PSI per second, which can be calculated if the excitation conditions are known. In the experiment described above 531 µmol/m^2/s of light was used and the excitation area was 1cm^2, thus 5.31*10^{-8} mol photons/s are fired at the sample.

Light absorption by PSI drives charge separation in the RC, resulting in the formation of P700+. PMS reduces P700+ to P700. The forward reaction rate depends on the light quantity, while the backward rate depends on the PMS

$$P700 \underset{PMS}{\overset{h\upsilon}{\rightleftarrows}} P700^+$$

At equilibrium the ratio between the P700+ and P700 concentrations are determined by the forward (k_f) and backward (k_b) reaction rates (/s).

$$\frac{k_f}{k_b} = \frac{[P700^+]}{[P700]}$$

Thus, in equilibrium the fraction of closed RCs ($P700^+$) is given by:

$$\frac{[P700^+]}{[P700]+[P700^+]} = \frac{k_f}{k_f + k_b}$$

Equation box 1.

The optical density was 0.85 /cm at the excitation wavelength (635nm), with a cuvette path length of 1 cm; this means that 14% ($10^{-0.85}$) of the light is transmitted, thus the absorptance is 86%, meaning that 4.56*10^{-8} mol photons/s are absorbed by PSI. Considering the extinction coefficient of Chl *a* and *b* being approximately the same at 635 nm and around 14000 /M/cm, the extinction coefficient of a higher plant PSI complex (containing ~170 Chls, Amunts *et. al.* 2010) is 2.38*10^6 /M/cm for PSI. This means that in the measured volume of one cubic centimeter (10^{-3} L) the number of PSI complexes is 0.85/2.38*10^6/10^3 is 3.57*10^{-10} mol. Thus on average each PSI absorbs 4.56*10^{-8}/3.57*10^{-10} that is 128 photon/s. We assume that PSI operates with an efficiency close to 100%, thus roughly each absorbed photon results in charge separation. With a P700 reduction rate of 36/s as found in the presence of 10 µM PMS, this means that k_f /(k_f+k_b) = 128/(36+128) = 78% of the RCs is expected to be closed (Equation box 1), while for a reduction rate of 412/s (150 µM PMS) 24% of the RCs is expected to be closed.

Figure 3 shows the calculated fraction of closed RCs against the measured values (obtained from measurements as shown in figure 2). The almost perfect correlation for the 10 µM PMS data points show that the calculation indeed gives meaningful information. For 60 µM PMS the measured fraction of closed RCs is somewhat lower than the calculated one and this difference is more pronounced

for 150 µM PMS. These differences can be explained by the actual PSI efficiency being smaller than ~100%. A considerable lower efficiency is indeed expected for the 60 and 150 µM data, because PMS is a strong Chls fluorescence quencher (see below).

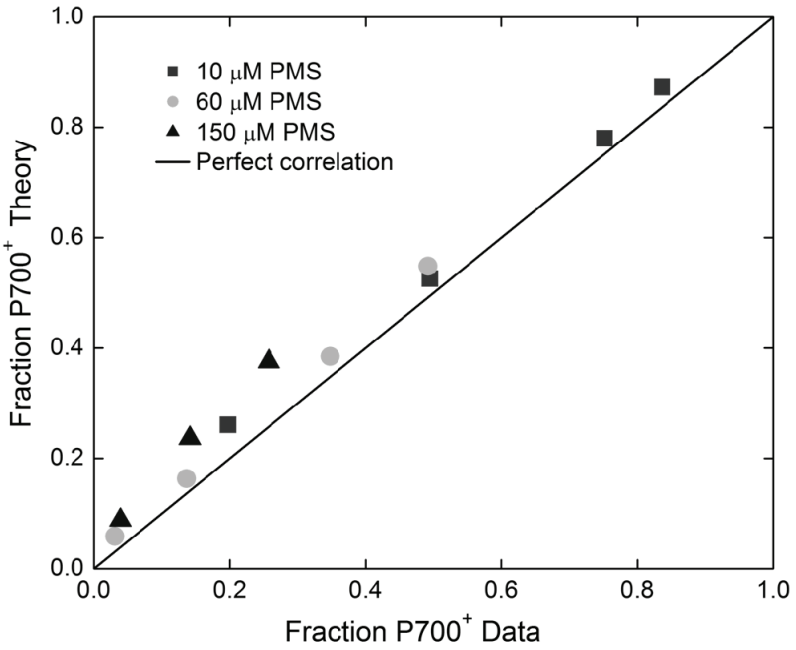

Figure 3: Theoretical and empirical fraction of closed RCs. PMS concentrations were 10, 60 and 150 µM, light intensities were 53, 166, 531 and 1028 µmol/m^2/s. For 150 µM of PMS the lowest light intensity gave a $P700^+$ fraction which was too low to quantify, therefore this data point is not reported.

PMS is a fluorescence quencher – To avoid introduction of artifacts in the measurements, the reducing agent used to re-open the PSI RC should not by itself have an effect on the fluorescence. To investigate if this is the case for PMS we added it to an LHCII solution. Figure 4 shows the result. Addition of oxidized PMS did not affect the fluorescence intensity, however as soon as PMS was reduced by NaAsc the intensity rapidly dropped. This effect was independent of the light intensity used. NaAsc itself did not reduce the fluorescence yield. Adding NaAsc first followed by PMS initially gave a similar result, however for the higher PMS concentrations the solution rapidly became turbid. This turbidity was also observed in absence of Lhc complexes, and can possibly be explained by the aggregation of PMS. The addition of PMS followed by NaAsc reduced the fluorescence intensity by a factor of 2 for 10 µM, 18 for 60 µM, up to a factor of 64 for the highest concentration. The absorption of reduced PMS at these concentrations is below 0.05 /cm for wavelengths longer than 500 nm, thus direct absorption of either excitation or emission light by PMS cannot explain the results. Therefore it has to be concluded that PMS is quenching the chlorophyll emission. To investigate whether this is a general property, 60 µM of PMS and 40 mM of NaAsc were added to PSII membranes (BBY's, Berthold *et. al.* 1981) and to the PSI antenna complex Lhca1/4. In both cases the fluorescence was strongly

quenched, by 11 and 15 times, respectively. We also tested if also *N,N,N',N'*-tetramethyl-p-phenylenediamine (TMPD) is quenching the LHCII emission. This is another reducing agent, which we found capable of reducing $P700^+$ with a rate of

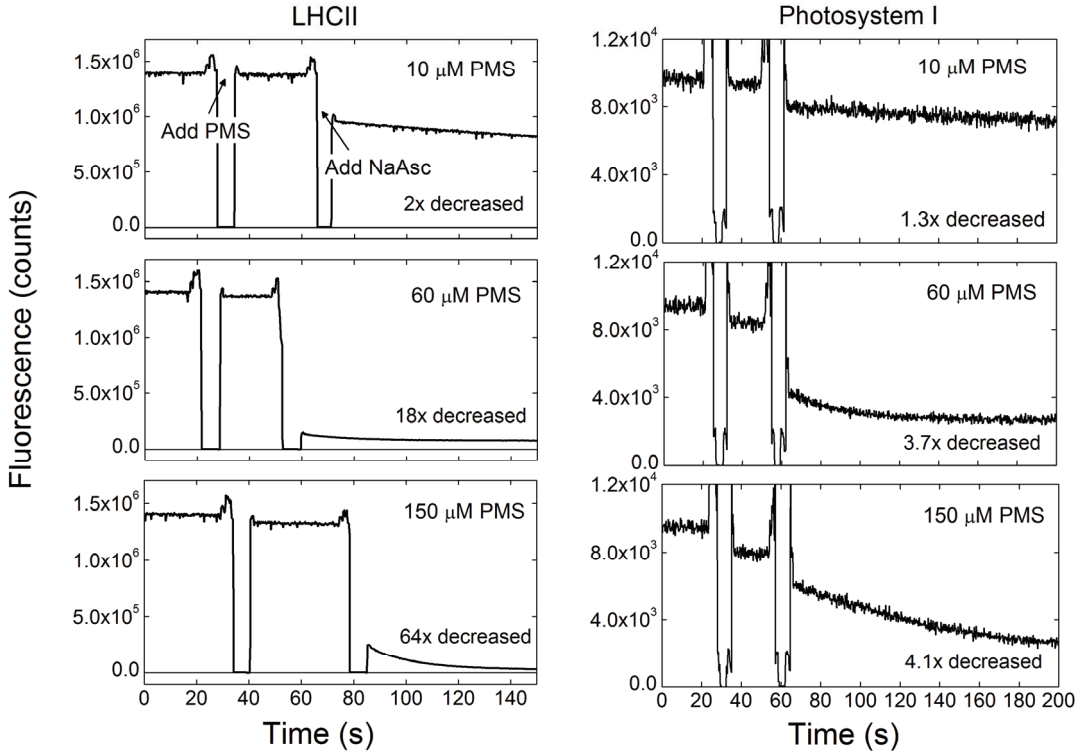

Figure 4: Fluorescence emission of LHCII and PSI followed in time during the addition of PMS and NaAsc. For LHCII the excitation was at 630nm and the emission was detected at 680nm, for PSI the excitation was at 500nm and the emission was detected at 725nm. Excitation of PSI at 630nm gave similar results.

33/s at 2mM concentration. Unfortunately, also TMPD was found to quench the LHCII emission.

We proceeded to investigate the effect of PMS on the emission of PSI. Addition of 10 μM reduced PMS decreased the fluorescence intensity by 23%. Based on the excitation power of ~250 μmol/m^2/s (at 500nm), the 1.5 times larger PSI extinction coefficient at 500nm compared to 635nm, and the reduction rate of 36/s, it was estimated that ~80% of the RCs were still closed under these conditions, indicating that the drop in fluorescence is due to the PMS quenching effect and not to a different trapping efficiency of P700 versus $P700^+$. The quenching effect was more pronounced for the higher PMS concentrations. The emission intensity dropped more than 3 times. The combination of 150μM PMS and 5mM NaAsc alone, also showed some emission under the measuring conditions, meaning that the actual quenching was even greater. For the combination of 60μM PMS and 40mM NaAsc we tested if the extent of quenching was dependent on the PSI concentration. Increasing the PSI concentration six

times, did not alter the level of PMS quenching, thus indicating that the level of quenching is only dependent on the PMS and not on the PSI concentration. Addition of NaAsc alone (40 mM) did not affect the fluorescence intensity.

Closing of PSI RCs slightly increases the fluorescence quantum yield – An interesting aspect of PSI excitation energy trapping is that the overall trapping lifetime of PSI with open or closed RCs is usually found to be very similar (Nuijs *et. al.* 1986; Owens *et. al.* 1988; Turconi *et. al.* 1993; Savikhin *et. al.* 2000), although for the cyanobacterium *Synechococcus elongatus* a notable difference of 10% has been found (Byrdin *et. al.* 2000). To get quantitative data on higher plant PSI, we investigated if there is a change in the fluorescence quantum yield (and thus in the trapping efficiency) upon closing the RCs. The possibility, of the Dual-PAM-100, to simultaneously detect the P700 oxidation state and the chlorophyll fluorescence, was used. The fluorescence signal is recorded by a pulse modulated measuring light which is operated at a low frequency. This allows to record the PSI emission while most of the RCs remain open. The fluorescence excited by the much stronger actinic or saturating light is not detected. In our experiment the fluorescence measuring light closed approximately 5% of the RCs (fig. 5). Switching on the actinic light closed > 95% of the RCs. This resulted on average (from 15 repetitions) in a 3.6% increase of the fluorescence emission. As this is caused by closing of >90% of the RCs this means that the closing of all RCs increases the fluorescence emission by 4% (with a standard deviation of 0.7%). Note that the increase/decrease of PSI emission in the light/dark follows the $P700^+$ reduction kinetics, thus showing that the P700 oxidative state is indeed responsible for the change of the fluorescence quantum yield.

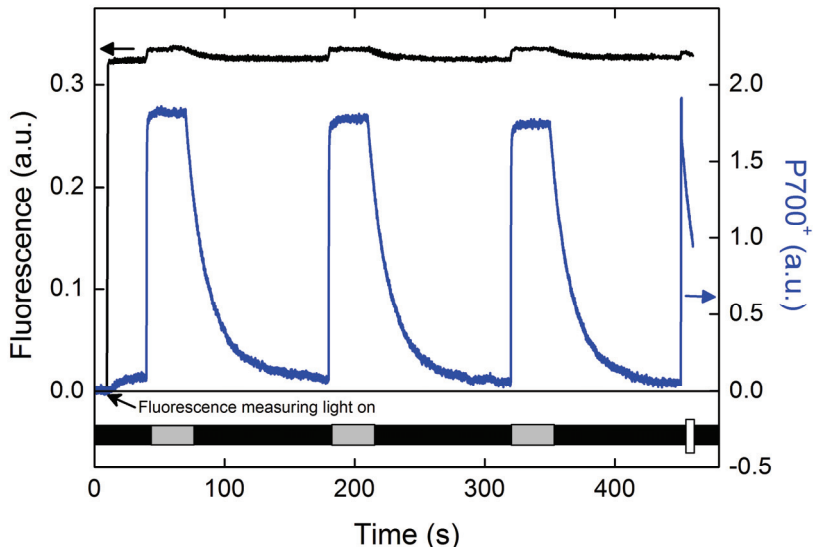

Figure 5: Simultaneous detection of fluorescence emission and $P700^+$ absorption of PSI. The fluorescence emission of PSI was followed during the photo-oxidation of P700 with 70 µmol/m^2/s of actinic light (grey bar) and the re-opening of the RCs in the dark by 10 mM NaAsc (black bar). The maximum level of $P700^+$ was determined by a 500 ms saturating light pulse of 8000 µmol/m^2/s (white bar).

Discussion

Although in virtually all studies investigating the PSI trapping kinetics, reducing agents are added to re-open the RCs, there are very few reports on the effect of these reagents. To our knowledge, there is just one study of the P700 reduction rate as function of the PMS concentration (Gourovskaya *et. al.* 1997), while Byrdin *et al.* (2000) reported the reduction rate for the specific concentration used in their study. Further, we found one comment by Bulychev and Vredenberg (2001) that PMS at concentrations ≥ 5μM is a light dependent quencher for chlorophyll fluorescence of thylakoids. In this study we investigated (i) the $P700^+$ reduction rate in presence of different PMS concentrations in order to estimate which fraction of RCs is closed at specific light intensities, (ii) the chlorophyll fluorescence quenching effect of PMS and (iii) the difference in fluorescence quantum yield of PSI with open and closed RCs.

RC: open or closed? – While in most of the experiments reported in the literature it is claimed that the RCs are open, quantitative data are usually not presented. In a typical synchroscan streak-camera experiment on PSI the excitation light intensity is ~100 μW, the repetition rate is 150 kHz, the path length is 2mm and the spot diameter is 150 μm e.g. (Gobets *et. al.* 2001; Ihalainen *et. al.* 2005; Giera *et. al.* 2010). Taking into account the photon energy of the excitation wavelength the number of photons per second and per pulse can be obtained. And based on the absorption of the sample, the estimated extinction coefficient and the excited volume, the number of photons absorbed per PSI per second and per pulse can be calculated. In the result section we have shown that this information can be used to give a reliable estimation of the fraction of closed RCs. In the experiment of Ihalainen *et al.* (2005) the number of photons absorbed per PSI per pulse was ~0.3, thus 45000 photons/PSI/s. With a P700 reduction rate of 36/s (using 10 μM of PMS), 99.9% of the RCs would be closed. To lower the excitation pressure the sample was contained in a spinning cuvette with a diameter of 10cm and rotated at a speed of 30Hz. As there is space for ~2000 spots on the circle, the average number of absorbed photons/PSI/s/spot is lowered to 23. However, taking into account the reduction rate of 36/s, still ~40% of the RCs are expected to be closed. This number is probably even higher because the sample is hit by 2.4 pulses while passing through the excitation spot, meaning that there is a considerable probability to hit one PSI twice during the short passes time.

One solution to lower the fraction of closed RCs, under very similar experimental conditions, is to increase the PMS concentration, see e.g. (Giera *et. al.* 2010). However, this will also increase the PMS chlorophyll fluorescence quenching (fig. 4). A more elegant way to keep the RCs open is given by Müller *et*

al. (2003). They use a spinning cuvette, which also moves sideways, in this system the excitation cycle time of the same volume is ~1min (Müller *et. al.* 2003). With a rotation speed of 70 Hz (Slavov *et. al.* 2008), this would allow to have ~100% of the RCs open in the streak-camera experiment described above, even if PSI was reduced at a rate of 4/s. Such a reduction rate can be obtained with 1 µM of PMS, which will not notably quench the fluorescence (Bulychev and Vredenberg 2001). The special spinning cuvette also allows performing transient absorption (Müller *et. al.* 2003; Holzwarth *et. al.* 2006) and TCSPC (Slavov *et. al.* 2008) experiments with nearly all the PSI RCs in open state.

Another obvious solution to lower the fraction of closed RCs is to lower the excitation power. For a very sensitive technique, for example TCSPC, this can still give data with a good signal to noise ratio. However, for other techniques such as fluorescence up-conversion, this will not be possible, and one might have to settle with measuring PSI with closed RCs (Kennis *et. al.* 2001).

PMS: to add or not to add? – Our study shows that the commonly used reducing agent PMS quenches the fluorescence emission of PSI. This effect might be avoided by using very low concentrations of PMS (Bulychev and Vredenberg 2001), but under this condition the P700 reduction rate is also low. Another disadvantage of PMS is its low stability in water. Decomposition of solutions in deionized water takes only hours, while the stability is even lower in neutral buffers (Sigma Product Information sheet). Thus, during long measurements the actual PMS concentration, and thus the P700 reduction rate, will be lower than expected. The best solution would be to find a stable and fast P700 reducing agent that does not quench chlorophyll fluorescence. In the absence of such a reagent it can be preferable, depending on the goal of the experiment, to measure PSI with closed RCs as the fluorescence quantum yield and thus the trapping efficiency is only slightly dependent on the P700 oxidative state (fig. 5).

Acknowledgements

This work was supported by De Nederlandse Organisatie voor Wetenschappelijk Onderzoek (NWO), Earth and Life Sciences (ALW), through a Vidi grant (to R.C.).

Bibliography

Ahn TK, Avenson TJ, Ballottari M, Cheng YC, Niyogi KK, Bassi R, Fleming GR (2008) Architecture of a charge-transfer state regulating light harvesting in a plant antenna protein. *Science (New York, NY)* 320:794-797.

Alboresi A, Ballottari M, Hienerwadel R, Giacometti GM, Morosinotto T (2009) Antenna complexes protect Photosystem I from Photoinhibition. *Bmc Plant Biology* 9:-.

Amunts A, Drory O, Nelson N (2007) The structure of a plant photosystem I supercomplex at 3.4 angstrom resolution. *Nature* 447:58-63.

Amunts A, Nelson N (2008) Functional organization of a plant photosystem I: Evolution of a highly efficient photochemical machine. *Plant Physiology and Biochemistry* 46:228-237.

Amunts A, Toporik H, Borovikova A, Nelson N (2010) Structure determination and improved model of plant photosystem I. *Journal of Biological Chemistry* 285:3478-3486.

Andersson PO, Bachilo SM, Chen RL, Gillbro T (1995) Solvent and Temperature Effects on Dual Fluorescence in a Series of Carotenes. Energy Gap Dependence of the Internal Conversion Rate. *Journal of Physical Chemistry* 99.

Andreeva A, Abarova S, Stoitchkova K, Picorel R, Velitchkova M (2007) Selective photobleaching of chlorophylls and carotenoids in photosystem I particles under high-light treatment. *Photochemistry and Photobiology* 83:1301-1307.

ASTM Reference Solar Spectral Irradiance: Air Mass 1.5.
http://rredc.nrel.gov/solar/spectra/am1.5/.

Atkins PW (1992) Physical Chemistry. 4th edn. Oxford University Press, Oxford.

Avenson TJ, Ahn TK, Zigmantas D, Niyogi KK, Li Z, Ballottari M, Bassi R, Fleming GR (2008) Zeaxanthin radical cation formation in minor light-harvesting complexes of higher plant antenna. *The Journal of biological chemistry* 283:3550-3558.

Bailey S, Walters RG, Jansson S, Horton P (2001) Acclimation of Arabidopsis thaliana to the light environment: the existence of separate low light and high light responses. *Planta* 213:794-801.

Ballottari M, Govoni C, Caffarri S, Morosinotto T (2004) Stoichiometry of LHCI antenna polypeptides and characterization of gap and linker pigments in higher plants Photosystem I. *Eur J Biochem* 271:4659-4665.

Ballottari M, Dall'Osto L, Morosinotto T, Bassi R (2007) Contrasting behavior of higher plant photosystem I and II antenna systems during acclimation. *Journal of Biological Chemistry* 282:8947-8958.

Barros T, Royant A, Standfuss J, Dreuw A, Kuhlbrandt W (2009) Crystal structure of plant light-harvesting complex shows the active, energy-transmitting state. *Embo Journal* 28:298-306.

Bassham JA, Benson AA, Calvin M (1950) The Path of Carbon in Photosynthesis .8. The Role of Malic Acid. *Journal of Biological Chemistry* 185:781-787.

Bassi R, Simpson D (1987) Chlorophyll-Protein Complexes of Barley Photosystem-I. *Eur J Biochem* 163:221-230.

Bassi R, Pineau B, Dainese P, Marquardt J (1993) Carotenoid-binding proteins of photosystem II. *Eur J Biochem* 212:297-303.

Bassi R, Croce R, Cugini D, Sandona D (1999) Mutational analysis of a higher plant antenna protein provides identification of chromophores bound into multiple sites. *Proc Natl Acad Sci U S A* 96:10056-10061.

Ben-Shem A, Frolow F, Nelson N (2003) Crystal structure of plant photosystem I. *Nature* 426:630-635.

Bengis C, Nelson N (1975) Purification and Properties of Photosystem-I Reaction Center from Chloroplasts. *Journal of Biological Chemistry* 250:2783-2788.

Berthold DA, Babcock GT, Yocum CF (1981) A Highly Resolved, Oxygen-Evolving Photosystem-Ii Preparation from Spinach Thylakoid Membranes - Electron-Paramagnetic-Res and Electron-Transport Properties. *Febs Letters* 134:231-234.

Blankenship RE (1992) Origin and early evolution of photosynthesis. *Photosynth Res* 33:91-111.

Blankenship RE (2002) Molecular Mechanisms of Photosynthesis. Blackwell Science.

Blankenship RE, Chen M (2011) Expanding the solar spectrum used by photosynthesis. *Trends in Plant Science* 16:427-431.

Bode S, Quentmeier CC, Liao PN, Hafi N, Barros T, Wilk L, Bittner F, Walla PJ (2009) On the regulation of photosynthesis by excitonic interactions between carotenoids and chlorophylls. *Proceedings of the National Academy of Sciences of the United States of America* 106:12311-12316.

Boekema EJ, Jensen PE, Schlodder E, van Breemen JFL, van Roon H, Scheller HV, Dekker JP (2001) Green plant photosystem I binds light-harvesting complex I on one side of the complex. *Biochemistry* 40:1029-1036.

Bouvier A, Wadhwa M (2010) The age of the Solar System redefined by the oldest Pb-Pb age of a meteoritic inclusion. *Nature Geoscience* 3:637-641.

Brecht M, Nieder JB, Studier H, Schlodder E, Bittl R (2008) Red antenna states of photosystem I from Synechococcus sp. PCC 7002. *Photosynthesis Research* 95:155-162.

Brecht M, Radics V, Nieder JB, Bittl R (2009) Protein dynamics-induced variation of excitation energy transfer pathways. *Proceedings of the National Academy of Sciences of the United States of America* 106:11857-11861.

Brettel K (1997) Electron transfer and arrangement of the redox cofactors in photosystem I. *Bba-Bioenergetics* 1318:322-373.

Bulychev AA, Vredenberg WJ (2001) Modulation of photosystem II chlorophyll fluorescence by electrogenic events generated by photosystem I. *Bioelectrochemistry* 54:157-168.

Busch A, Nield J, Hippler M (2010) The composition and structure of photosystem I-associated antenna from Cyanidioschyzon merolae. *Plant Journal* 62:886-897.

Byrdin M, Rimke I, Schlodder E, Stehlik D, Roelofs TA (2000) Decay kinetics and quantum yields of fluorescence in photosystem I from Synechococcus elongatus with P700 in the reduced and oxidized state: are the kinetics of excited state decay trap-limited or transfer-limited? *Biophysical Journal* 79:992-1007.

Caffarri S, Croce R, Breton J, Bassi R (2001) The major antenna complex of photosystem II has a xanthophyll binding site not involved in light harvesting. *Journal of Biological Chemistry* 276:35924-35933.

Caffarri S, Passarini F, Bassi R, Croce R (2007) A specific binding site for neoxanthin in the monomeric antenna proteins CP26 and CP29 of Photosystem II. *Febs Letters* 581:4704-4710.

Caffarri S, Kouril R, Kereiche S, Boekema EJ, Croce R (2009) Functional architecture of higher plant photosystem II supercomplexes. *Embo Journal* 28:3052-3063.

Caffarri S, Broess K, Croce R, van Amerongen H (2011) Excitation energy transfer and trapping in higher plant Photosystem II complexes with different antenna sizes. *Biophysical Journal* 100:2094-2103.

Carbonera D, Agostini G, Morosinotto T, Bassi R (2005) Quenching of chlorophyll triplet states by carotenoids in reconstituted Lhca4 subunit of peripheral light-harvesting complex of photosystem I. *Biochemistry* 44:8337-8346.

Castelletti S, Morosinotto T, Robert B, Caffarri S, Bassi R, Croce R (2003) Recombinant Lhca2 and Lhca3 subunits of the photosystem I antenna system. *Biochemistry* 42:4226-4234.

Cinque G, Croce R, Bassi R (2000) Absorption spectra of chlorophyll a and b in Lhcb protein environment. *Photosynthesis Research* 64:233-242.

Cogdell R, Gardiner AT (2001) Light harvesting by purple bacteria: a circular argument. *Microbiology Today* 28:120-122.

Croce R, Zucchelli G, Garlaschi FM, Bassi R, Jennings RC (1996) Excited state equilibration in the Photosystem I light-harvesting I complex: P700 is almost isoenergetic with its antenna. *Biochemistry* 35:8572-8579.

Croce R, Bassi R (1998a) The light-harvesting complex of Photosystem I: pigment composition and stoichiometry. In: Garab G (ed), vol 1. Photosynthesis. Mechanisms and Effects. Kluwer Academic Publishers, Dordrecht, pp 421-424.

Croce R, Bassi R (1998b) Photosynthesis. Mechanisms and Effects, vol 1. Kluwer Academic Publishers, Dordrecht.

Croce R, Zucchelli G, Garlaschi FM, Jennings RC (1998) A thermal broadening study of the antenna chlorophylls in PSI-200, LHCI, and PSI core. *Biochemistry* 37:17355-17360.

Croce R, Weiss S, Bassi R (1999) Carotenoid-binding sites of the major light-harvesting complex II of higher plants. *Journal of Biological Chemistry* 274:29613-29623.

Croce R, Cinque G, Holzwarth AR, Bassi R (2000a) The Soret absorption properties of carotenoids and chlorophylls in antenna complexes of higher plants. *Photosynthesis Research* 64:221-231.

Croce R, Dorra D, Holzwarth AR, Jennings RC (2000b) Fluorescence decay and spectral evolution in intact photosystem I of higher plants. *Biochemistry* 39:6341-6348.

Croce R, Canino G, Ros F, Bassi R (2002a) Chromophore organization in the higher-plant photosystem II antenna protein CP26. *Biochemistry* 41:7334-7343.

Croce R, Morosinotto T, Castelletti S, Breton J, Bassi R (2002b) The Lhca antenna complexes of higher plants photosystem I. *Bba-Bioenergetics* 1556:29-40.

Croce R, Muller MG, Bassi R, Holzwarth AR (2003a) Chlorophyll b to chlorophyll a energy transfer kinetics in the CP29 antenna complex: a comparative femtosecond absorption study between native and reconstituted proteins. *Biophysical Journal* 84:2508-2516.

Croce R, Muller MG, Caffarri S, Bassi R, Holzwarth AR (2003b) Energy transfer pathways in the minor antenna complex CP29 of photosystem II: a femtosecond study of carotenoid to chlorophyll transfer on mutant and WT complexes. *Biophysical Journal* 84:2517-2532.

Croce R, Morosinotto T, Ihalainen JA, Chojnicka A, Breton J, Dekker JP, van Grondelle R, Bassi R (2004) Origin of the 701-nm fluorescence emission of the Lhca2 subunit of higher plant photosystem I. *Journal of Biological Chemistry* 279:48543-48549.

Croce R, Morosinotto T, Bassi R (2006) Photosystem I: the light-driven plastocyanin : ferredoxin oxidoreductase, vol 24. Advances in photosynthesis and photorespiration. Springer link, Dordrecht, The Netherlands.

Croce R, Chojnicka A, Morosinotto T, Ihalainen JA, van Mourik F, Dekker JP, Bassi R, van Grondelle R (2007a) The low-energy forms of photosystem I light-harvesting complexes: Spectroscopic properties and pigment-pigment interaction characteristics. *Biophysical Journal* 93:2418-2428.

Croce R, Mozzo M, Morosinotto T, Romeo A, Hienerwadel R, Bassi R (2007b) Singlet and triplet state transitions of carotenoids in the antenna complexes of higher-plant Photosystem I. *Biochemistry* 46:3846-3855.

de Weerd FL, John TM, Jan P, van Grondelle R (2003) β-Carotene to Chlorophyll Singlet Energy Transfer in the Photosystem I Core of Synechococcus elongatus Proceeds via the β-Carotene S2 and S1 States. *Journal of Physical Chemistry B* 107:5995-6002.

Dekker JP, Boekema EJ (2005) Supramolecular organization of thylakoid membrane proteins in green plants. *Biochimica Et Biophysica Acta-Bioenergetics* 1706:12-39.

Demmig-Adams B, Adams WW (1996) The role of xanthophyll cycle carotenoids in the protection of photosynthesis. *Trends in Plant Sci* 1:21-26.

Di Donato M, Stahl AD, van Stokkum IHM, van Grondelle R, Groot ML (2011) Cofactors Involved in Light-Driven Charge Separation in Photosystem I Identified by Subpicosecond Infrared Spectroscopy. *Biochemistry* 50:480-490.

Digris AV, Skakoun VV, Novikov EG, van Hoek A, Claiborne A, Visser AJ (1999) Thermal stability of a flavoprotein assessed from associative analysis of polarized time-resolved fluorescence spectroscopy. *Eur Biophys J* 28:526-531.

Dreuw A, Fleming GR, Head-Gordon M (2003) Charge-transfer state as a possible signature of a zeaxanthin-chlorophyll dimer in the non-photochemical quenching process in green plants. *Journal of Physical Chemistry B* 107:6500-6503.

Du M, Xie XS, Jia Y, Mets L, Fleming GR (1993) Direct observation of ultrafast energy transfer in PSI core antenna. *Chemical Physics Letters* 201.

Eisenberg R, Nocera DG (2005) Preface: Overview of the forum on solar and renewable energy. *Inorganic Chemistry* 44:6799-6801.

Engelmann E, Zucchelli G, Casazza AP, Brogioli D, Garlaschi FM, Jennings RC (2006) Influence of the photosystem I - Light harvesting complex I antenna domains on fluorescence decay. *Biochemistry* 45:6947-6955.

Forster T (1946) Energiewanderung Und Fluoreszenz. *Naturwissenschaften* 33:166-175.

Forster T (1948) *Zwischenmolekulare Energiewanderung Und Fluoreszenz. *Annalen Der Physik* 2:55-75.

Fowler GJS, Visschers RW, Grief GG, Grondelle vR, Hunter CN (1992) Genetically modified photosynthetic antenna complexes with blueshifted absorbance bands. *Nature* 355:848-850.

Frank HA, Cua A, Chynwat V, Young A, Gosztola D, Wasielewski MR (1994) Photophysics of the Carotenoids Associated with the Xanthophyll Cycle in Photosynthesis. *Photosynthesis Research* 41:389-395.

Frauenfelder H, Petsko GA, Tsernoglou D (1979) Temperature-Dependent X-Ray-Diffraction as a Probe of Protein Structural Dynamics. *Nature* 280:558-563.

Frauenfelder H, Sligar SG, Wolynes PG (1991) The Energy Landscapes and Motions of Proteins. *Science* 254:1598-1603.

Fromme P, Jordan P, Krauss N (2001) Structure of photosystem I. *Biochim Biophys Acta, Bioenergetics* 1507:5-31.

Fyfe PK, Jones MR, Heathcote P (2002) Insights into the evolution of the antenna domains of Type-I and Type-II photosynthetic reaction centres through homology modelling. *Febs Letters* 530:117-123.

Ganeteg U, Strand A, Gustafsson P, Jansson S (2001) The properties of the chlorophyll a/b-binding proteins Lhca2 and Lhca3 studied in vivo using antisense inhibition. *Plant Physiology* 127:150-158.

Ganeteg U (2004) The light-harvesting antenna of higher plant photosystem I. PhD Thesis, PhD Thesis, Umea

Ganeteg U, Klimmek F, Jansson S (2004a) Lhca5 - an LHC-type protein associated with photosystem I. *Plant Molecular Biology* 54:641-651.

Ganeteg U, Kulheim C, Andersson J, Jansson S (2004b) Is each light-harvesting complex protein important for plant fitness? *Plant Physiology* 134:502-509.

Garab G, Cseh Z, Kovacs L, Rajagopal S, Varkonyi Z, Wentworth M, Mustardy L, Der A, Ruban AV, Papp E, Holzenburg A, Horton P (2002) Light-induced trimer to monomer transition in the main light-harvesting antenna complex of plants: thermo-optic mechanism. *Biochemistry* 41:15121-15129.

Germano M, Yakushevska AE, Keegstra W, van Gorkom HJ, Dekker JP, Boekema EJ (2002) Supramolecular organization of photosystem I and light- harvesting complex I in Chlamydomonas reinhardtii. *Febs Letters* 525:121-125.

Gibasiewicz K, Croce R, Morosinotto T, Ihalainen JA, van Stokkum IHM, Dekker JP, Bassi R, van Grondelle R (2005) Excitation energy transfer pathways in Lhca4. *Biophysical Journal* 88:1959-1969.

Giera W, Ramesh VM, Webber AN, van Stokkum I, van Grondelle R, Gibasiewicz K (2010) Effect of the P700 pre-oxidation and point mutations near A0 on the reversibility of the primary charge separation in Photosystem I from Chlamydomonas reinhardtii. *Bba-Bioenergetics* 1797:106-112.

Gillbro T, Cogdell RJ (1989) Carotenoid Fluorescence. *Chemical Physics Letters* 158.

Giuffra E, Cugini D, Croce R, Bassi R (1996) Reconstitution and pigment-binding properties of recombinant CP29. *Eur J Biochem* 238:112-120.

Glazer AN (1983) Comparative biochemistry of photosynthetic light-harvesting systems. *Annu Rev Biochem* 52:125-157.

Gobets B, van Amerongen H, Monshouwer R, Kruip J, Rogner M, van Grondelle R, Dekker JP (1994) Polarized Site-Selected Fluorescence Spectroscopy of Isolated Photosystem-I Particles. *Biochim Biophys Acta, Bioenergetics* 1188:75-85.

Gobets B, Kennis JTM, Ihalainen JA, Brazzoli M, Croce R, van Stokkum LHM, Bassi R, Dekker JP, van Amerongen H, Fleming GR, van Grondelle R (2001a) Excitation energy transfer in dimeric light harvesting complex I: A combined streak-camera/fluorescence upconversion study. *Journal of Physical Chemistry B* 105:10132-10139.

Gobets B, van Grondelle R (2001) Energy transfer and trapping in photosystem I. *Biochim Biophys Acta, Bioenerg* 1507:80-99.

Gobets B, van Stokkum IHM, Rogner M, Kruip J, Schlodder E, Karapetyan NV, Dekker JP, van Grondelle R (2001b) Time-resolved fluorescence emission measurements of photosystem I particles of various cyanobacteria: A unified compartmental model. *Biophys J* 81:407-424.

Gourovskaya KN, Mamedov MD, Vassiliev IR, Golbeck JH, Semenov AY (1997) Electrogenic reduction of the primary electron donor P700(+) in photosystem I by redox dyes. *Febs Letters* 414:193-196.

Gouterman M (1961) Spectra of Porphyrins. *Journal of molecular Spectroscopy* 6.

Govindjee, Krogmann D (2004) Discoveries in oxygenic photosynthesis (1727-2003): a perspective. *Photosynthesis Research* 80:15-57.

Gradinaru CC, van Stokkum IHM, Pascal AA, van Grondelle R, van Amerongen H (2000) Identifying the pathways of energy transfer between carotenoids and chlorophylls in LHCII and CP29. A multicolor, femtosecond pump-probe study. *Journal of Physical Chemistry B* 104:9330-9342.

Grondelle vR, Dekker JP, Gillbro T, Sundstrom V (1994) Energy-Transfer and Trapping in Photosynthesis. *Biochimica Et Biophysica Acta-Bioenergetics* 1187:1-65.

Groot ML, Pawlowicz NP, van Wilderen LJGW, Breton J, van Stokkum IHM, van Grondelle R (2005) Initial electron donor and acceptor in isolated Photosystem II reaction centers identified with femtosecond mid-IR spectroscopy. *Proceedings of the National Academy of Sciences of the United States of America* 102:13087-13092.

Haworth P, Watson JL, Arntzen CJ (1983) The Detection, Isolation and Characterization of a Light-Harvesting Complex Which Is Specifically Associated with Photosystem-I. *Biochimica Et Biophysica Acta* 724:151-158.

Heathcote P, Fyfe PK, Jones MR (2002) Reaction centres: the structure and evolution of biological solar power. *Trends in Biochemical Sciences* 27:79-87.

Heathcote P, Jones MR, Fyfe PK (2003) Type I photosynthetic reaction centres: structure and function. *Philosophical Transactions of the Royal Society of London Series B-Biological Sciences* 358:231-243.

Hemelrijk PW, Kwa SLS, Vangrondelle R, Dekker JP (1992) Spectroscopic Properties of Lhc-Ii, the Main Light-Harvesting Chlorophyll-a/B Protein Complex from Chloroplast Membranes. *Biochimica Et Biophysica Acta* 1098:159-166.

Hoffmann M, Schmidt K, Fritz T, Hasche T, Agranovich VM, Leo K (2000) The lowest energy Frenkel and charge-transfer excitons in quasi-one-dimensional structures: application to MePTCDI and PTCDA crystals. *Chemical Physics* 258:73-96.

Hofmann C, Aartsma TJ, Michel H, Kohler J (2003) Direct observation of tiers in the energy landscape of a chromoprotein: A single-molecule study. *Proceedings of the National Academy of Sciences of the United States of America* 100:15534-15538.

Holt NE, Zigmantas D, Valkunas L, Li XP, Niyogi KK, Fleming GR (2005) Carotenoid cation formation and the regulation of photosynthetic light harvesting. *Science (New York, NY)* 307:433-436.

Holzwarth AR, Müller MG, Niklas J, Lubitz W (2006a) Ultrafast transient absorption studies on Photosystem I reaction centers from Chlamydomonas reinhardtii. 2: mutations near the P700 reaction center chlorophylls provide new insight into the nature of the primary electron donor. *Biophysical Journal* 90:552-565.

Holzwarth AR, Muller MG, Reus M, Nowaczyk M, Sander J, Rogner M (2006b) Kinetics and mechanism of electron transfer in intact photosystem II and in the isolated reaction center: Pheophytin is the primary electron acceptor. *Proceedings of the National Academy of Sciences of the United States of America* 103:6895-6900.

Horton P, Ruban AV, Walters RG (1996) Regulation Of Light Harvesting In Green Plants. *Annu Rev Plant Physiol Plant Mol Biol* 47:655-684.

Hui Y, Jie W, Carpentier R (2000) Degradation of the photosystem I complex during photoinhibition. *Photochemistry and Photobiology* 72:508-512.

Ihalainen JA, Gobets B, Sznee K, Brazzoli M, Croce R, Bassi R, van Grondelle R, Korppi-Tommola JEI, Dekker JP (2000) Evidence for two spectroscopically different dimers of light-harvesting complex I from green plants. *Biochemistry* 39:8625-8631.

Ihalainen JA, Jensen PE, Haldrup A, van Stokkum IHM, van Grondelle R, Scheller HV, Dekker JP (2002) Pigment organization and energy transfer dynamics in isolated, photosystem I (PSI) complexes from Arabidopsis thaliana depleted of the PSI-G, PSI-K, PSI-L, or PSI-N subunit. *Biophysical Journal* 83:2190-2201.

Ihalainen JA, Ratsep M, Jensen PE, Scheller HV, Croce R, Bassi R, Korppi-Tommola JEI, Freiberg A (2003) Red spectral forms of chlorophylls in green plant PSI - a site-selective and high-pressure spectroscopy study. *Journal of Physical Chemistry B* 107:9086-9093.

Ihalainen JA, Croce R, Morosinotto T, van Stokkum IHM, Bassi R, Dekker JP, van Grondelle R (2005a) Excitation decay pathways of Lhca proteins: A time-resolved fluorescence study. *Journal of Physical Chemistry B* 109:21150-21158.

Ihalainen JA, Klimmek F, Ganeteg U, van Stokkum IHM, van Grondelle R, Jansson S, Dekker JP (2005b) Excitation energy trapping in photosystem I complexes depleted in Lhca1 and Lhca4. *Febs Letters* 579:4787-4791.

Ihalainen JA, van Stokkum IHM, Gibasiewicz K, Germano M, van Grondelle R, Dekker JP (2005c) Kinetics of excitation trapping in intact Photosystem I of Chlamydomonas reinhardtii and Arabidopsis thaliana. *Biochim Biophys Acta-Bioenergetics* 1706:267-275.

Jansson S, Pichersky E, Bassi R, Green RB, Ikeuchi M, Melis A, Simpson DJ, Spanfort M, Staehelin LA, Thornber JP (1992) A Nomenclature for the Genes Encoding the Chlorophyll a/b-Binding Proteins of Higher Plants. *Plant Molecular Biology Reporter* 10:242-253.

Jansson S (1994) The light-harvesting chlorophyll a/b-binding proteins. *Biochim Biophys Acta* 1184:1-19.

Jansson S (1999) A guide to the Lhc genes and their relatives in Arabidopsis. *Trends in Plant Sci* 4:236-240.

Jelezko F, Tietz C, Gerken U, Wrachtrup J, Bittl R (2000) Single-molecule spectroscopy on photosystem I pigment-protein complexes. *The Journal of Physical Chemistry B* 104:8093-8096.

Jennings RC, Bassi R, Garlaschi FM, Dainese P, Zucchelli G (1993) Distribution of the chlorophyll spectral forms in the chlorophyll-protein complexes of photosystem II antenna. *Biochemistry* 32:3203-3210.

Jennings RC, Garlaschi FM, Morosinotto T, Engelmann E, Zucchelli G (2003a) The room temperature emission band shape of the lowest energy chlorophyll spectral form of LHCI (vol 547, pg 107, 2003). *Febs Letters* 549:181-181.

Jennings RC, Zucchelli G, Croce R, Garlaschi FM (2003b) The photochemical trapping rate from red spectral states in PSI-LHCI is determined by thermal activation of energy transfer to bulk chlorophylls. *Biochim Biophys Acta, Bioenerg* 1557:91-98.

Jennings RC, Zucchelli G, Engelmann E, Garlaschi FM (2004) The long-wavelength chlorophyll states of plant LHCI at room temperature: A comparison with PSI-LHCI. *Biophysical Journal* 87:488-497.

Jensen PE, Gilpin M, Knoetzel J, Scheller HV (2000) The PSI-K subunit of photosystem I is involved in the interaction between light-harvesting complex I and the photosystem I reaction center core. *Journal of Biological Chemistry* 275:24701-24708.

Jensen PE, Rosgaard L, Knoetzel J, Scheller HV (2002) Photosystem I activity is increased in the absence of the PSI-G subunit. *Journal of Biological Chemistry* 277:2798-2803.

Jensen PE, Bassi R, Boekema EJ, Dekker JP, Jansson S, Leister D, Robinson C, Scheller HV (2007) Structure, function and regulation of plant photosystem I. *Biochimica Et Biophysica Acta-Bioenergetics* 1767:335-352.

Johnson GN (2011) Physiology of PSI cyclic electron transport in higher plants. *Biochimica Et Biophysica Acta-Bioenergetics* 1807:384-389.

Jordan P, Fromme P, Witt HT, Klukas O, Saenger W, Krauss N (2001) Three-dimensional structure of cyanobacterial photosystem I at 2.5 angstrom resolution. *Nature* 411:909-917.

Karapetyan NV, Dorra D, Schweitzer G, Bezsmertnaya IN, Holzwarth AR (1997) Fluorescence spectroscopy of the longwave chlorophylls in trimeric and monomeric photosystem I core complexes from the cyanobacterium Spirulina platensis. *Biochemistry* 36:13830-13837.

Karapetyan NV, Holzwarth AR, Rogner M (1999) The photosystem I trimer of cyanobacteria: molecular organization, excitation dynamics and physiological significance. *Febs Letters* 460:395-400.

Kennis JTM, Gobets B, van Stokkum IHM, Dekker JP, van Grondelle R, Fleming GR (2001) Light harvesting by chlorophylls and carotenoids in the photosystem I core complex of Synechococcus elongatus: A fluorescence upconversion study. *Journal of Physical Chemistry B* 105:4485-4494.

Khrouchtchova A, Hansson M, Paakkarinen V, Vainonen JP, Zhang SP, Jensen PE, Scheller HV, Vener AV, Aro EM, Haldrup A (2005) A previously found thylakoid membrane protein of 14 kDa (TMP14) is a novel subunit of plant photosystem I and is designated PSI-P. *Febs Letters* 579:4808-4812.

Klimmek F, Ganeteg U, Ihalainen JA, van Roon H, Jensen PE, Scheller HV, Dekker JP, Jansson S (2005) Structure of the higher plant light harvesting complex I: In vivo characterization and structural interdependence of the Lhca proteins. *Biochemistry* 44:3065-3073.

Knapp EW, Fischer SF, Zinth W, Sander M, Kaiser W, Deisenhofer J, Michel H (1985) Analysis of optical spectra from single crystals of Rhodopseudomonas viridis reaction centers. *Proc Natl Acad Sci U S A* 82:8463-8467.

Knoetzel J, Svendsen I, Simpson DJ (1992) Identification of the Photosystem-I Antenna Polypeptides in Barley - Isolation of 3 Pigment-Binding Antenna Complexes. *Eur J Biochem* 206:209-215.

Knox RS (2003) Dipole and oscillator strengths of chromophores in solution. *Photochemistry and Photobiology* 77:492-496.

Koepke J, Krammer EM, Klingen AR, Sebban P, Ullmann GM, Fritzsch G (2007) pH modulates the quinone position in the photosynthetic reaction center from Rhodobacter sphaeroides in the neutral and charge separated states. *Journal of Molecular Biology* 371:396-409.

Kouril R, Arteni AA, Lax J, Yeremenko N, D'Haene S, Rogner M, Matthijs HCP, Dekker JP, Boekema EJ (2005) Structure and functional role of supercomplexes of IsiA and Photosystem I in cyanobacterial photosynthesis. *Febs Letters* 579:3253-3257.

Krinsky NO (1979) CAROTENOID PROTECTION AGAINST OXIDATION. *Pure & Applied Chemistry* 51.

Kruger TP, Novoderezhkin VI, Ilioaia C, van Grondelle R (2010) Fluorescence spectral dynamics of single LHCII trimers. *Biophys J* 98:3093-3101.

Kruger TP, Wientjes E, Croce R, van Grondelle R (2011) Conformational switching explains the intrinsic multifunctionality of plant light-harvesting complexes. *Proc Natl Acad Sci U S A* 108:13516-13521.

Kuhl M, Chen M, Ralph PJ, Schreiber U, Larkum AWD (2005) A niche for cyanobacteria containing chlorophyll d. *Nature* 433:820-820.

Kühlbrandt W, Wang DN, Fujiyoshi Y (1994) Atomic Model of Plant Light-Harvesting Complex by Electron Crystallography. *Nature* 367:614-621.

Kulzer F, Orrit M (2004) Single-molecule optics. *Annual Review of Physical Chemistry* 55:585-611.

Laemmli UK (1970) Cleavage of Structural Proteins during Assembly of Head of Bacteriophage-T4. *Nature* 227:680-685.

Lam E, Ortiz W, Malkin R (1984) Chlorophyll a-B Proteins of Photosystem-I. *Febs Letters* 168:10-14.

Lampoura SS, Barzda V, Owen GM, Hoff AJ, van Amerongen H (2002) Aggregation of LHCII leads to a redistribution of the triplets over the central xanthophylls in LHCII. *Biochemistry* 41:9139-9144.

Lindorff-Larsen K, Best RB, DePristo MA, Dobson CM, Vendruscolo M (2005) Simultaneous determination of protein structure and dynamics. *Nature* 433:128-132.

Liu Z, Yan H, Wang K, Kuang T, Zhang J, Gui L, An X, Chang W (2004) Crystal structure of spinach major light-harvesting complex at 2.72 A resolution. *Nature* 428:287-292.

Lucinski R, Schmid VHR, Jansson S, Klimmek F (2006) Lhca5 interaction with plant photosystem I. *Febs Letters* 580:6485-6488.

Manhes G, Allegre CJ, Dupre B, Hamelin B (1980) Lead Isotope Study of Basic-Ultrabasic Layered Complexes - Speculations About the Age of the Earth and Primitive Mantle Characteristics. *Earth and Planetary Science Letters* 47:370-382.

Melkozernov AN, Schmid VHR, Schmidt GW, Blankenship RE (1998) Energy redistribution in heterodimeric light-harvesting complex LHCI-730 of photosystem I. *Journal of Physical Chemistry B* 102:8183-8189.

Melkozernov AN, Lin S, Schmid VHR, Paulsen H, Schmidt GW, Blankenship RE (2000) Ultrafast excitation dynamics of low energy pigments in reconstituted peripheral light-harvesting complexes of photosystem I. *Febs Letters* 471:89-92.

Melkozernov AN (2001) Excitation energy transfer in Photosystem I from oxygenic organisms. *Photosynth Res* 70:129-153.

Melkozernov AN, Blankenship RE (2003) Structural modeling of the Lhca4 subunit of LHCI-730 peripheral antenna in photosystem I based on similarity with LHCII. *Journal of Biological Chemistry* 278:44542-44551.

Miloslavina Y, Wehner A, Lambrev PH, Wientjes E, Reus M, Garab G, Croce R, Holzwarth AR (2008) Far-red fluorescence: A direct spectroscopic marker for LHCII oligomer formation in non-photochemical quenching. *Febs Letters* 582:3625-3631.

Miyashita H, Ikemoto H, Kurano N, Adachi K, Chihara M, Miyachi S (1996) Chlorophyll d as a major pigment. *Nature* 383:402-402.

Miyashita O, Onuchic JN, Wolynes PG (2003) Nonlinear elasticity, proteinquakes, and the energy landscapes of functional transitions in proteins. *Proceedings of the National Academy of Sciences of the United States of America* 100:12570-12575.

Morosinotto T, Castelletti S, Breton J, Bassi R, Croce R (2002) Mutation analysis of Lhca1 antenna complex - Low energy absorption forms originate from pigment-pigment interactions. *Journal of Biological Chemistry* 277:36253-36261.

Morosinotto T, Breton J, Bassi R, Croce R (2003) The nature of a chlorophyll ligand in Lhca proteins determines the far red fluorescence emission typical of photosystem I. *Journal of Biological Chemistry* 278:49223-49229.

Morosinotto T, Ballottari M, Klimmek F, Jansson S, Bassi R (2005a) The association of the antenna system to photosystem I in higher plants. *Journal of Biological Chemistry* 280:31050-31058.

Morosinotto T, Mozzo M, Bassi R, Croce R (2005b) Pigment-pigment interactions in Lhca4 antenna complex of higher plants photosystem I. *Journal of Biological Chemistry* 280:20612-20619.

Moya I, Silvestri M, Vallon O, Cinque G, Bassi R (2001) Time-resolved fluorescence analysis of the photosystem II antenna proteins in detergent micelles and liposomes. *Biochemistry* 40:12552-12561.

Mozzo M, Morosinotto T, Bassi R, Croce R (2006) Probing the structure of Lhca3 by mutation analysis. *Biochim Biophys Acta, Bioenerg* 1757:1607-1613.

Mozzo M, Passarini F, Bassi R, van Amerongen H, Croce R (2008) Photoprotection in higher plants: The putative quenching site is conserved in all outer light-harvesting complexes of Photosystem II. *Biochimica Et Biophysica Acta-Bioenergetics* 1777:1263-1267.

Mozzo M, Mantelli M, Passarini F, Caffarri S, Bassi R, Croce R (2010) Functional analysis of Photosystem I light-harvesting complexes (Lhca) gene products of Chlamydomonas reinhardtii. *Biochimica Et Biophysica Acta-Bioenergetics* 1797:212-221.

Mukerji I, Sauer K (1993) Energy-Transfer Dynamics of an Isolated Light-Harvesting Complex of Photosystem-I from Spinach - Time-Resolved Fluorescence Measurements at 295-K and 77-K. *Biochimica Et Biophysica Acta* 1142:311-320.

Mullen KM, van Stokkum IHM (2007) TIMP: An R package for modeling multi-way spectroscopic measurements. *Journal of Statistical Software* 18:-.

Müller MG, Niklas J, Lubitz W, Holzwarth AR (2003) Ultrafast transient absorption studies on photosystem I reaction centers from Chlamydomonas reinhardtii. 1. A new interpretation of the energy trapping and early electron transfer steps in photosystem I. *Biophysical Journal* 85:3899-3922.

Mullet JE, Burke JJ, Arntzen CJ (1980) Chlorophyll Proteins of Photosystem-I. *Plant Physiology* 65:814-822.

Munekaga Y, Hashimoto M, Miyaka C, Tomizawa KI, Endo T, Tasaka M, Shikanai T (2004) Cyclic electron flow around photosystem I is essential for photosynthesis. *Nature* 429:579-582.

Naqvi R (1998) Photosynthesis Mechanisms and Effects, vol 1. Kluwer Academic Publisher, Dordrecht.

Nelson N, Yocum CF (2006) Structure and function of photosystems I and II. *Annual Review Plant Biology* 57:521-565.

Nisbet EG, Sleep NH (2001) The habitat and nature of early life. *Nature* 409:1083-1091.

Niyogi KK, Grossman AR, Bjorkman O (1998) Arabidopsis mutants define a central role for the xanthophyll cycle in the regulation of photosynthetic energy conversion. *Plant Cell* 10:1121-1134.

Niyogi KK (1999) Photoprotection revisited: Genetic and molecular approaches. *Annual Review of Plant Physiology and Plant Molecular Biology* 50:333-359.

Novoderezhkin VI, Dekker JP, Van Grondelle R (2007) Mixing of exciton and charge-transfer states in photosystem II reaction centers: modeling of stark spectra with modified Redfield theory. *Biophysical Journal* 93:1293-1311.

Novoderezhkin VI, van Grondelle R (2010) Physical origins and models of energy transfer in photosynthetic light-harvesting. *Physical Chemistry Chemical Physics* 12:7352-7365.

Nuijs AM, Shuvalov VA, Vangorkom HJ, Plijter JJ, Duysens LNM (1986) Picosecond Absorbency Difference Spectroscopy on the Primary Reactions and the Antenna-Excited States in Photosystem-I Particles. *Biochim Biophys Acta* 850:310-318.

Nussberger S, Dekker JP, Kuhlbrandt W, Vanbolhuis BM, Vangrondelle R, Vanamerongen H (1994) Spectroscopic Characterization of 3 Different Monomeric Forms of the Main Chlorophyll a/B Binding-Protein from Chloroplast Membranes. *Biochemistry* 33:14775-14783.

Oesterhelt D (1998) The structure and mechanism of the family of retinal proteins from halophilic archaea. *Current Opinion in Structural Biology* 8:489-500.

Oostergetel GT, Keegstra W, Brisson A (1998) Automation of specimen selection and data acquisition for protein electron crystallography. *Ultramicroscopy* 74:47-59.

Owens TG, Webb SP, Alberte RS, Mets L, Fleming GR (1988) Antenna Structure and Excitation Dynamics in Photosystem-I .1. Studies of Detergent-Isolated Photosystem-I Preparations Using Time-Resolved Fluorescence Analysis. *Biophysical Journal* 53:733-745.

Palacios MA, de Weerd FL, Ihalainen JA, van Grondelle R, van Amerongen H (2002) Superradiance and exciton (de)localization in light-harvesting complex II from green plants? *Journal of Physical Chemistry B* 106:5782-5787.

Palsson LO, Tjus SE, Andersson B, Gillbro T (1995) Ultrafast Energy-Transfer Dynamics Resolved in Isolated Spinach Light-Harvesting Complex-I and the Lhc-I-730 Subpopulation. *Biochimica Et Biophysica Acta-Bioenergetics* 1230:1-9.

Pan X, Li M, Wan T, Wang L, Jia C, Hou Z, Zhao X, Zhang J, Chang W (2011) Structural insights into energy regulation of light-harvesting complex CP29 from spinach. *Nature Structural & Molecular Biology* 18:309-315.

Pascal AA, Liu ZF, Broess K, van Oort B, van Amerongen H, Wang C, Horton P, Robert B, Chang WR, Ruban A (2005) Molecular basis of photoprotection and control of photosynthetic light-harvesting. *Nature* 436:134-137.

Passarini F, Wientjes E, van Amerongen H, Croce R (2010) Photosystem I light-harvesting complex Lhca4 adopts multiple conformations: Red forms and excited-state quenching are mutually exclusive. *Biochim Biophys Acta* 1797:501-508.

Paulsen H, Rumler U, Rudiger W (1990) Reconstitution of Pigment-Containing Complexes from Light-Harvesting Chlorophyll-a/B-Binding Protein Overexpressed in Escherichia-Coli. *Planta* 181:204-211.

Peng LW, Fukao Y, Fujiwara M, Takami T, Shikanai T (2009) Efficient Operation of NAD(P)H Dehydrogenase Requires Supercomplex Formation with Photosystem I via Minor LHCI in Arabidopsis. *Plant Cell* 21:3623-3640.

Pesaresi P, Sandona D, Giuffra E, Bassi R (1997) A single point mutation (E166Q) prevents dicyclohexylcarbodiimide binding to the photosystem II subunit CP29. *Febs Letters* 402:151-156.

Peter GF, Thornber JP (1991) Biochemical-Composition and Organization of Higher-Plant Photosystem-Ii Light-Harvesting Pigment-Proteins. *Journal of Biological Chemistry* 266:16745-16754.

Photosynthesis - History Of Research. http://science.jrank.org/pages/5189/Photosynthesis-History-research.html.

Plumley FG, Schmidt GW (1987) Reconstitution of Chlorophyll a/B Light-Harvesting Complexes - Xanthophyll-Dependent Assembly and Energy-Transfer. *Proceedings of the National Academy of Sciences of the United States of America* 84:146-150.

Polivka T, Sundstrom V (2004) Ultrafast dynamics of carotenoid excited States-from solution to natural and artificial systems. *Chem Rev* 104:2021-2071.

Polivka T, Frank HA (2010) Molecular factors controlling photosynthetic light harvesting by carotenoids. *Accounts of Chemical Research* 43:1125-1134.

Rajagopal S, Joly D, Gauthier A, Beauregard M, Carpentier R (2005) Protective effect of active oxygen scavengers on protein degradation and photochemical function in photosystern I submembrane fractions during light stress. *Febs Journal* 272:892-902.

Rivadossi A, Zucchelli G, Garlaschi FM, Jennings RC (1999) The importance of PSI chlorophyll red forms in light-harvesting by leaves. *Photosynth Res* 60:209-215.

Romero E, Mozzo M, van Stokkum IHM, Dekker JP, van Grondelle R, Croce R (2009) The Origin of the Low-Energy Form of Photosystem I Light-Harvesting Complex Lhca4: Mixing of the Lowest Exciton with a Charge-Transfer State. *Biophys J* 96:L35-L37.

Romero E, van Stokkum IHM, Novoderezhkin VI, Dekker JP, van Grondelle R (2010) Two Different Charge Separation Pathways in Photosystem II. *Biochemistry* 49:4300-4307.

Roszak AW, Howard TD, Southall J, Gardiner AT, Law CJ, Isaacs NW, Cogdell RJ (2003) Crystal structure of the RC-LH1 core complex from Rhodopseudomonas palustris. *Science* 302:1969-1972.

Rousseau F, Setif P, Lagoutte B (1993) Evidence for the Involvement of Psi-E Subunit in the Reduction of Ferredoxin by Photosystem-I. *Embo Journal* 12:1755-1765.

Ruban AV, Lee PJ, Wentworth M, Young AJ, Horton P (1999) Determination of the stoichiometry and strength of binding of xanthophylls to the photosystem II light harvesting complexes. *J Biol Chem* 274:10458-10465.

Ruban AV, Wentworth M, Yakushevska AE, Andersson J, Lee PJ, Keegstra W, Dekker JP, Boekema EJ, Jansson S, Horton P (2003) Plants lacking the main light-harvesting complex retain photosystem II macro-organization. *Nature* 421:648-652.

Ruban AV, Berera R, Ilioaia C, van Stokkum IHM, Kennis JTM, Pascal AA, van Amerongen H, Robert B, Horton P, van Grondelle R (2007) Identification of a mechanism of photoprotective energy dissipation in higher plants. *Nature* 450:575-U522.

Rutkauskas D, Novoderezkhin V, Cogdell RJ, van Grondelle R (2004) Fluorescence spectral fluctuations of single LH2 complexes from Rhodopseudomonas acidophila strain 10050. *Biochemistry* 43:4431-4438.

Rutkauskas D, Novoderezhkin V, Cogdell RJ, van Grondelle R (2005) Fluorescence spectroscopy of conformational changes of single LH2 complexes. *Biophysical Journal* 88:422-435.

Rutkauskas D, Cogdell RJ, van Grondelle R (2006) Conformational relaxation of single bacterial light-harvesting complexes. *Biochemistry* 45:1082-1086.

Savikhin S, Xu W, Chitnis PR, Struve WS (2000) Ultrafast primary processes in PS I from Synechocystis so. PCC 6803: Roles of P700 and A(o). *Biophys J* 79:1573-1586.

Savikhin S, Xu W, Martinsson P, Chitnis PR, Struve WS (2001) Kinetics of charge separation and A(0)(-)-> A(1) electron transfer in photosystem reaction centers. *Biochemistry* 40:9282-9290.

Savikhin S (2006) Ultrafast Optical Spectroscopy of Photosystem I. In: Golbeck J (ed) Photosystem I: the light-driven plastocyanin : ferredoxin oxidoreductase, vol 24. Springer, Dordrecht, pp 155-175.

Schmid VHR, Cammarata KV, Bruns BU, Schmidt GW (1997) In vitro reconstitution of the photosystem I light-harvesting complex LHCI-730: Heterodimerization is required for antenna pigment organization. *Proc Natl Acad Sci U S A* 94:7667-7672.

Schmid VHR, Thome P, Ruhle W, Paulsen H, Kuhlbrandt W, Rogl H (2001) Chlorophyll b is involved in long-wavelength spectral properties of light-harvesting complexes LHC I and LHC II. *Febs Letters* 499:27-31.

Schmid VHR, Potthast S, Wiener M, Bergauer V, Paulsen H, Storf S (2002) Pigment binding of photosystem I light-harvesting proteins. *Journal of Biological Chemistry* 277:37307-37314.

Schubert WD, Klukas O, Krauss N, Saenger W, Fromme P, Witt HT (1997) Photosystem I of Synechococcus elongatus at 4 angstrom resolution: Comprehensive structure analysis. *Journal of Molecular Biology* 272:741-769.

Sener MK, Jolley C, Ben-Shem A, Fromme P, Nelson N, Croce R, Schulten K (2005) Comparison of the light-harvesting networks of plant and cyanobacterial photosystem I. *Biophys J* 89:1630-1642.

Shelaev IV, Gostev FE, Mamedov MD, Sarkisov OM, Nadtochenko VA, Shuvalov VA, Semenov AY (2010) Femtosecond primary charge separation in Synechocystis sp. PCC 6803 photosystem I. *Biochim Biophys Acta, Bioenerg* 1797:1410-1420.

Slavov C, Ballottari M, Morosinotto T, Bassi R, Holzwarth AR (2008) Trap-limited charge separation kinetics in higher plant photosystem I complexes. *Biophys J* 94:3601-3612.

Somsen OJ, Keukens LB, de Keijzer MN, van Hoek A, van Amerongen H (2005) Structural heterogeneity in DNA: temperature dependence of 2-aminopurine fluorescence in dinucleotides. *Chemphyschem* 6:1622-1627.

Stokkum vIHM, Larsen DS, Grondelle vR (2004) Global and target analysis of time-resolved spectra. *Biochim Biophys Acta, Bioenerg* 1657:82-104.

Stomp M, Huisman J, Stal LJ, Matthijs HC (2007) Colorful niches of phototrophic microorganisms shaped by vibrations of the water molecule. *ISME J* 1:271-282.

Storf S, Stauber EJ, Hippler M, Schmid VHR (2004) Proteomic analysis of the photosystem I light-harvesting antenna in tomato (Lycopersicon esculentum). *Biochemistry* 43:9214-9224.

Storf S, Jansson S, Schmid VHR (2005) Pigment binding, fluorescence properties, and oligomerization behavior of Lhca5, a novel light-harvesting protein. *J Biol Chem* 280:5163-5168.

Thapper A, Mamedov F, Mokvist F, Hammarstrom L, Styring S (2009) Defining the far-red limit of photosystem II in spinach. *Plant Cell* 21:2391-2401.

Tikkanen M, Piippo M, Suorsa M, Sirpio S, Mulo P, Vainonen J, Vener AV, Allahverdiyeva Y, Aro EM (2006) State transitions revisited - a buffering system for dynamic low light acclimation of Arabidopsis (vol 62, pg 795, 2006). *Plant Molecular Biology* 62:795-795.

Tjus SE, Roobolboza M, Palsson LO, Andersson B (1995) Rapid Isolation of Photosystem-I Chlorophyll-Binding Proteins by Anion-Exchange Perfusion Chromatography. *Photosynthesis Research* 45:41-49.

Trissl HW (1993) Long-Wavelength Absorbing Antenna Pigments and Heterogeneous Absorption-Bands Concentrate Excitons and Increase Absorption Cross-Section. *Photosynth Res* 35:247-263.

Turconi S, Schweitzer G, Holzwarth AR (1993) Temperature-Dependence of Picosecond Fluorescence Kinetics of a Cyanobacterial Photosystem-I Particle. *Photochemistry and Photobiology* 57:113-119.

Umena Y, Kawakami K, Kamiya N, Shen JR (2011) Crystal structure of oxygen-evolving photosystem II at a resolution of 1.9 angstrom. *Nature* 473:55-U65.

Vaitekonis S, Trinkunas G, Valkunas L (2005) Red chlorophylls in the exciton model of photosystem I. *Photosynthesis Research* 86:185-201.

van Amerongen H, Valkunas L, van Grondelle R (2000) Photosynthetic Excitons. World Scientific Publishing.

van Amerongen H, van Grondelle R (2001) Understanding the energy transfer function of LHCII, the major light-harvesting complex of green plants. *Journal of Physical Chemistry B* 105:604-617.

van Oijen AM, Ketelaars M, Kohler J, Aartsma TJ, Schmidt J (1999) Unraveling the electronic structure of individual photosynthetic pigment-protein complexes. *Science (New York, NY)* 285:400-402.

van Oort B, van Hoek A, Ruban AV, van Amerongen H (2007) Aggregation of Light-Harvesting Complex II leads to formation of efficient excitation energy traps in monomeric and trimeric complexes. *Febs Letters* 581:3528-3532.

van Oort B, Amunts A, Borst JW, van Hoek A, Nelson N, van Amerongen H, Croce R (2008) Picosecond Fluorescence of Intact and Dissolved PSI-LHCI Crystals. *Biophys J* 95:5851-5861.

van Oort B, Murali S, Wientjes E, Koehorst RBM, Spruijt RB, van Hoek A, Croce R, Amerongen van H (2009) Ultrafast resonance energy transfer from a site-specifically

attached fluorescent chromophore reveals the folding of the N-terminal domain of CP29. *Chem Phys* 357:113-119.

Vanselow C, Weber APM, Krause K, Fromme P (2009) Genetic analysis of the Photosystem I subunits from the red alga, Galdieria sulphuraria. *Biochimica Et Biophysica Acta-Bioenergetics* 1787:46-59.

Varotto C, Pesaresi P, Jahns P, Lessnick A, Tizzano M, Schiavon F, Salamini F, Leister D (2002) Single and double knockouts of the genes for photosystem I subunits G, K, and H of Arabidopsis. Effects on photosystem I composition, photosynthetic electron flow, and state transitions. *Plant Physiology* 129:616-624.

Vassiliev IR, Jung YS, Mamedov MD, Semenov AY, Golbeck JH (1997) Near-IR absorbance changes and electrogenic reactions in the microsecond-to-second time domain in photosystem I. *Biophys J* 72:301-315.

Visschers RW, Chang MC, van Mourik F, Parkes-Loach PS, Heller BA, Loach PA, van Grondelle R (1991) Fluorescence polarization and low-temperature absorption spectroscopy of a subunit form of light-harvesting complex I from purple photosynthetic bacteria. *Biochemistry* 30:5734-5742.

Walla PJ Two-Photon Excitation of Photosynthetic Carotenoids. http://www.pci.tu-bs.de/agwalla/Photosynthesis.htm.

Weber G, Teale FWJ (1957) Determination of the Absolute Quantum Yield of Fluorescent Solutions. *Transactions of the Faraday Society* 53:646-655.

Weber G (1975) Energetics of ligand binding to proteins. *Adv Protein Chem* 29:1-83.

Wehner A, Storf S, Jahns P, Schmid VH (2004) De-epoxidation of violaxanthin in light-harvesting complex I proteins. *J Biol Chem* 279:26823-26829.

Wei J, Yu H, Li LB, Kuang TY, Wang JS, Gong YD, Zhao NM (2001) The photodamage process of pigments and proteins of PSI complexes from Spinacia Oleracea L. *Chinese Science Bulletin* 46:1812-1816.

Wientjes E, Oostergetel GT, Jansson S, Boekema EJ, Croce R (2009) The role of Lhca complexes in the supramolecular organization of higher plant photosystem I. *Journal of Biological Chemistry* 284:7803-7810.

Wientjes E, Croce R (2011) The light-harvesting complexes of higher-plant Photosystem I: Lhca1/4 and Lhca2/3 form two red-emitting heterodimers. *Biochemical Journal* 433:477-485.

Wientjes E, van Stokkum IH, van Amerongen H, Croce R (2011a) The role of the individual lhcas in photosystem I excitation energy trapping. *Biophys J* 101:745-754.

Wientjes E, van Stokkum IHM, van Amerongen H, Croce R (2011b) Excitation-energy transfer dynamics of higher plant photosystem I light-harvesting complexes. *Biophys J* 100:1372-1380.

Zucchelli G, Garlaschi FM, Jennings RC (1996) Thermal broadening analysis of the light harvesting complex II absorption spectrum. *Biochemistry* 35:16247-16254.

Summary

Introduction

Photosynthesis is the process in which light energy is used to convert carbon dioxide into carbohydrates. In the light reaction of oxygenic photosynthesis, photosystem II (PSII) and photosystem I (PSI) work in concert with cytochrome b_6f and ATP-synthase to oxidize water, reduce $NADP^+$ and produce ATP. In the subsequent light independent reaction, NADPH and ATP are used to convert carbon dioxide and water into carbohydrates.

In this thesis I study PSI of higher plants. This pigment-protein supercomplex can be divided in two moieties: the core complex and the peripheral light harvesting complex (LHCI). The core complex harbors about 100 chlorophylls *a* (Chls), ~20 β-carotenes, the reaction centre (RC) - where primary charge separation takes place - and all the electron transport cofactors. LHCI is composed of four light-harvesting pigment-protein complexes (Lhcs), named Lhca1-4, which form the Lhca1/4 and Lhca2/3 heterodimers. They coordinate Chls *a* and *b*, and the carotenoids lutein, violaxanthin and β-carotene. Their main function is to increase the absorption cross section of the complex and in addition they might play a role in photoprotection. A special feature of the Lhcas is that they coordinate red forms i.e. Chls with extremely broad and red-shifted absorption and emission bands. The red forms are believed to be important for harvesting light under a canopy where the light is strongly enriched in the long wavelengths. The reddest Chls are found in Lhca3 and Lhca4; because their energy levels are lower than that of the RC, these forms have a large effect on the excitation-energy transfer and trapping processed in PSI.

This thesis

The aim of this thesis is to understand the functioning of higher plant PSI, i.e. light harvesting and the use of excitation energy for charge separation. PSI is, with at least 19 proteins, 170 Chls and ~35 carotenoids, a very large and complex system. Therefore, to obtain a thorough understanding of the entire PSI supercomplex, we first studied in detail the properties of its "building-blocks": Lhca1/4, Lhca2/3 and the PSI core. Subsequently, we gradually increased the complexity by investigating PSI supercomplexes with reduced antenna size or altered antenna composition, and finally the wild type PSI supercomplex. By combining all the obtained information we were able to provide a comprehensive picture of the light-harvesting properties and of the excitation energy transfer and trapping routes and rates in the entire PSI supercomplex. Further, we investigate how the Lhc protein environment modulates the spectroscopic properties of its pigments. To

this end we did not only study the native Lhc complexes purified from plants, but also used recombinant and *in vitro* refolded Lhca complexes.

In **chapter 2** we studied the role of Lhcas in the structural organization of PSI by analyzing PSI complexes from Lhca-lacking *A.thaliana* plants. We used biochemical techniques and electron microscopy to determine their Lhca composition, stability and supra-molecular organization. The data show that both Lhca1/4 and Lhca2/3 dimer can be associated with the core in absence of the other dimer and that Lhca2 and Lhca4 can be associated with the core in absence of their dimeric partner. The absence of an Lhca leaves a "hole" in the structure which is not filled by another Lhca, indicating that each Lhca has a highly specific docking site. There is one exception however, Lhca5 can replace Lhca4, yielding a stable supercomplex with a supramolecular organization identical to that of the wild-type complex.

In the past LHCI was often separated in two fractions, which were named LHCI-680 and LHCI-730, after their low temperature emission maxima. LHCI-680 was mainly composed of Lhca2 and Lhca3, while LHCI-730 mainly contained Lhca1 and Lhca4. Therefore, it was assumed that Lhca2 and Lhca3 do not coordinate red forms. The lower mobility of the LHCI-680 fraction on a sucrose density gradient compared to LHCI-730, indicated that the former were monomers, while the latter were in a dimeric state. However, more recent data suggest that Lhca2 and Lhca3 also form a (hetero/homo) dimer, but this could not be verified, neither by purification of the complex nor by *in vitro* reconstitution. In **chapter 3** we used a Lhca-lacking PSI complex (described in chapter 2) to purify Lhca2 and Lhca3. We showed that they form a functional heterodimer. We revealed the biochemical and spectroscopic properties of Lhca2/3 and compared them with those of Lhca1/4. The Lhca2/3 and Lhca1/4 dimer have very similar functional properties, such as absorption, fluorescence emission and fluorescence quantum yield. The low temperature emission maxima of both dimers were found around 730nm, similar to that of the intact PSI complex. This indicates that both dimers are in their native state and that LHCI-680 is not a natural component of the PSI antenna complex.

In **chapter 4** the Lhca1/4 and Lhca2/3 dimer were studied with picosecond fluorescence spectroscopy. The inter-monomer transfer rates were resolved using target analysis. The fluorescence decay of both dimers was heterogeneous, regarding the lifetimes and the spectra. We proposed that this is due to the ability of each dimer to adopt various conformations that correspond to different lifetimes and emission spectra. We also investigated the characteristics of the red forms. The red forms in Lhca complexes originate from the low-energy band of an excitonically coupled Chl dimer mixed with a charge-transfer state. In an

excitonically coupled dimer the sum of the electronic oscillator strengths is identical to the sum of the oscillator strengths of the isolated molecules, but it can be differently distributed over the two transitions. For the red forms in Lhca3 and Lhca4 we found that the lowest-energy transition gets all the oscillator strengths. Because the low-energy bands are highly populated at equilibrium it can be expected that the Lhca dimers are superradiant. Our measurements show that this is indeed the case. This challenges the view that the low-energy charge-transfer state always functions as a quencher in plant Lhcs.

In the previous chapter heterogeneity in the decay associated spectra was observed for both dimers. This can be explained by the presence of the dimers in different conformations with different spectroscopic properties or by heterogeneity in the sample. To investigate if a single Lhca complex can switch between states with different emission spectra, the complexes were studied by Single-Molecule fluorescence spectroscopy (**chapter 5**).The data show that Lhca complexes have the ability to reversibly switch off their typical red emission, and acquire an Lhcb-like emission spectrum. For Lhcb complexes the opposite behavior has been observed. We proposed that one protein can switch between different functions by a conformational change.

If a conformational change of the Lhca4 protein can induce a large change in the fluorescence emission spectra, then a small change in the protein might have the same effect. In **chapter 6** we investigate how the protein modulates the energy level of the red forms in Lhca4. To this end single amino acid substitutions were introduced nearby the two Chls which are responsible for the red-shifted absorption and emission. We show that extending the ligand of one of these Chls with one carbon-carbon bond almost completely abolishes the red forms. In fact, the spectroscopic properties (absorption, emission, circular dichroism) of the Lhca4 mutant resemble that of a typical Lhcb complex. Further, we show that we can tune the emission spectra of Lhca4 over a wide spectral range, indicating that it is feasible to adjust the absorption of Lhc Chls to desired wavelengths. We suggest that plants could be produced that are more suitable to harvest specific light spectra, such as 600nm rich light of a high-pressure sodium lamp or far-red enriched light under a canopy.

The aim of **chapter 7** is to resolve the energy-transfer routes and rates in the intact PSI-LHCI complex. For a long time it has been virtually impossible to disentangle the role of the individual Lhcas in excitation-energy transfer from time-resolved spectroscopic data. This is caused by the complex trapping kinetics of PSI-LHCI and by a lack of knowledge of the spectral properties of the Lhcas. To overcome these problems we have first isolated and studied the native dimers (chapter 3 and 4) and PSI core complex with picosecond fluorescence

spectroscopy, subsequently we have studied a larger PSI complex with only the Lhca1/4 dimer associated, and finally the intact PSI-LHCI complex. In addition we studied a mutant PSI complex, with the same supra-molecular organization as the WT complex, but with Lhca4 substituted for Lhca5 and thus with a reduced red form content. The results show that Lhca3 and Lhca4 transfer the excitation energy relatively slowly to the core, while Lhca1 and Lhca2 transfer the energy about four times faster. The excitation energy transfer from the dimers to the core occurs on a faster time scale than energy equilibration within the dimers, therefore each Lhca contributes about equally to energy transfer to the core. The red forms in Lhca3 and Lhca4 slow down the trapping rate by about two times, however the calculated trapping efficiency is still >97%. It can thus be suggested that the increase in light harvesting, especially under shade conditions, easily compensates for the small loss in efficiency.

Phenazine methosulfate is a chemical that is often used during spectroscopic measurements to re-reduce the PSI RC after charge separation. In **chapter 8** we show that this chemical is quenching the excited state of Chls and could thus lead to artifacts in the measurements. Further we show that we can give a reliable estimation of the fraction of closed PSI RCs under specified experimental conditions. And our data reveal that the fluorescence intensity of higher plant PSI with closed RCs is 4% higher than in the open state.

This thesis is a nutshell

In this thesis we make a detailed analysis of the light-harvesting properties of higher plant PSI. We study the system at various levels of complexity, from individual antennas to supercomplexes. In the most detailed level, the level of the monomers, we investigated how the spectroscopic properties of the red forms of Lhca4 are modulated by the protein environment. At the next level we studied the light-harvesting properties of the Lhca1/4 and the Lhca2/3 dimer. Using assemble experiments we revealed the absorption and emission properties as well as the inter-monomer transfer rates. We also studied the emission properties of the Lhca complexes at the single-molecule level. The results showed that the Lhca complexes can reversible switch off their entire red-emission band by a conformational change, meaning that it is essential to consider the flexibility of the Lhc proteins in order to understand their spectroscopic properties. At the following level we have studied PSI complexes with reduced antenna size or altered antenna composition. Finally, we have presented a comprehensive picture of the excitation energy transfer routes and rates in the entire PSI supercomplex.

Samenvatting

Inleiding

Fotosynthese is een proces waarbij lichtenergie gebruikt wordt om koolstofdioxide om te zetten in koolhydraten, zoals glucose. In oxygene fotosynthese komt zuurstof vrij als afvalproduct. Dit proces vindt plaats in planten, algen en cyanobacteriën. De netto reactie is:

$$6\ H_2O + 6\ CO_2 + \text{fotonen} \rightarrow C_6H_{12}O_6 + 6\ O_2$$

water + koolstof dioxide + licht energie → glucose + zuurstof

Fotosynthese begint met het absorberen van een foton (lichtdeeltje) door een pigment. In het geval van oxygene fotosynthese zijn de pigmenten gebonden aan de eiwit structuren van fotosysteem I of fotosysteem II. Absorptie van een foton brengt het pigment in de aangeslagen/ geëxciteerde toestand. In andere woorden, de energie van de foton is nu opgenomen door het pigment. Als pigmenten dicht bij elkaar zitten, zoals in fotosystemen het geval is, dan kan de excitatie energie van pigment naar pigment springen. Op deze manier wordt de energie naar het reactiecentrum getransporteerd. Het reactiecentrum ligt ook in het fotosysteem en is een speciaal groepje pigmenten, dat voor een ladingsscheiding kan zorgen als het geëxciteerd wordt. Na de ladingsscheiding heeft één pigment een elektron te weinig en wordt positief geladen, terwijl een ander pigment een elektron teveel heeft en negatief geladen wordt. Het extra elektron zit vrij los en kan via de elektrontransportketen weggevoerd worden. Fotosysteem II gebruikt de energie van licht om elektronen uit water te onttrekken. Deze elektronen worden naar fotosysteem I getransporteerd. Fotosysteem I geeft de elektronen extra energie zodat ze uiteindelijk gebruikt kunnen worden bij de omzetting van CO_2 in koolhydraten.

In dit proefschrift bestudeer ik fotosysteem I uit hogere planten. Een structuurmodel van dit fotosysteem is te vinden op pagina 13. Alle groene vierkantjes zijn chlorofyllen, de pigmenten die samen met de carotenoïden voor de licht absorptie zorgen. Ze worden op hun plaats gehouden door eiwitten (de andere kleurrijke structuren). We onderscheiden twee delen: het grote kerngedeelte en de vier extra licht-oogstende pigment-eiwit complexen met de namen: Lhca1, Lhca2, Lhca3 en Lhca4 (zie figuur 2 p.13). De Lhca complexen bestaan elk uit één eiwit (een keten van aminozuren, in dit geval variërend in aantal van 197 tot 232), 10 tot 17 chlorofyllen en 2 tot 3 carotenoïden. Het is al sinds lange tijd bekend dat Lhca1 en Lhca4 samen een hetero-dimeer vormen, die we Lhca1/4 noemen. In dit proefschrift hebben we bewezen dat Lhca2 en Lhca3 ook een hetero-dimeer vormen.

Een belangrijk doel van het onderzoek is om te weten te komen hoe snel excitatie energie van de ene Lhca naar de andere en naar de kern wordt overgedragen. In de kern kan de excitatie energie worden gebruikt voor ladingsscheiding in het reactiecentrum. Als we weten hoe snel de energie gebruikt wordt voor de ladingsscheiding, en hoe snel de energie verloren gaat via andere processen, dan kunnen we uitrekenen hoe efficiënt fotosysteem I werkt. Als we een goed beeld hebben van de eigenschappen van de individuele licht-oogstende complexen, dan kunnen we ook begrijpen hoe zij de efficiëntie beïnvloeden. We zijn daarbij extra geïnteresseerd in het effect van Lhca3 en Lhca4, omdat deze licht-oogstende complexen speciale chlorofyllen binden die ver-rood licht (golflengte langer dan 700nm) kunnen absorberen. Omdat deze chlorofyllen een lage excitatie energie hebben is het moeilijk voor de excitatie om naar een ander chlorofyl over te springen. De sprong is als het ware bergopwaarts. Dit vertraagt de transportsnelheid naar het reactiecentrum en dus de fotosysteem I efficiëntie. Maar deze chlorofyllen hebben ook een sterke kant. Het zonlicht dat de aarde bereikt bestaat namelijk voor een belangrijk deel uit licht met golflengtes langer dan 700nm. Ver-rood absorberende chlorofyllen zijn extra belangrijk voor het absorberen van licht onder een bladerdak, waar de bovenliggende bladeren het meeste zichtbare licht al hebben geabsorbeerd. We proberen ook te begrijpen hoe het Lhca4 eiwit bepaalt bij welke golflengte de chlorofyllen absorberen. Als we dit weten kunnen we in principe planten maken die beter geschikt zijn om een bepaald licht spectrum te oogsten, bijvoorbeeld ver-rood licht of het licht uit hogedruk natriumlampen dat gebruikt wordt in kassen.

Fotosysteem I bekijken

De afmetingen van fotosysteem I zijn: 18 nanometer (nm) breed, 14 nm hoog en 9 nm dik. Eén nm is één miljoenste van een millimeter. Dit is veel kleiner dan de golflengte (400-700nm) van zichtbaar licht, en daarom kan fotosysteem I niet met een lichtmicroscoop bekeken worden. Echter, elektronen met een hoge snelheid hebben een veel kortere golflengte. Deze eigenschap wordt in elektronenmicroscopie gebruikt om kleine deeltjes zichtbaar te maken. In **hoofdstuk 2** bestuderen we fotosysteem I deeltjes van planten die geen Lhca1, Lhca2, Lhca3 of Lhca4 kunnen maken vanwege een genetische aanpassing. We gebruiken de elektronenmicroscoop om te bekijken hoe de deeltjes er zonder deze licht-oogstende complexen uitzien. Ook gebruiken we een gel waarop we de verschillende eiwitten van fotosysteem I kunnen scheiden. Zo is te zien welke

licht-oogstende complexen precies ontbreken. Samen met de structuur informatie kunnen we nu bepalen welk complex op welke plaats zit. Verder is het mogelijk om af te leiden of de Lhca eiwitten van elkaar afhankelijk zijn voor een stabiele associatie aan het fotosysteem I kern complex.

De licht-oogstende complexen

Om het intacte fotosysteem I beter te begrijpen is het nuttig eerst de verschillende onderdelen te bestuderen. Tot nu toe was dat goed gelukt voor de kern en de Lhca1/4 dimeer, maar de Lhca2/3 dimeer liet zich niet goed opzuiveren. Door gebruik te maken van een genetische aangepaste plant was het mogelijk de Lhca2/3 dimeer toch te isoleren (**hoofdstuk 3**). Dit gaf de mogelijkheid tot het bepalen van de optische eigenschappen, zoals het absorptie- en fluorescentiespectrum. We hebben verschillende eigenschappen van Lhca2/3 vergeleken met die van Lhca1/4 en gezien dat ze in veel opzichten overeen komen. Met name de eigenschappen van de ver-rood absorberende chlorofyllen lijken op elkaar. In **hoofdstuk 4** kijken we hoe snel de excitatie energie wordt overgedragen tussen de monomeren in Lhca1/4 en Lhca2/3. Dit doen we met behulp van tijds-opgeloste fluorescentie: het monster wordt met een korte lichtpuls beschenen waarna wordt bekeken hoe het fluorescentie emissie spectrum in de tijd verandert. Door absorptie van het licht raakt een chlorofyl in de geëxciteerde toestand. Deze chlorofyl heeft een grote kans om excitatie energie naar een ander chlorofyl binnen de dimeer over te brengen, er is ook een kleine kans dat de chlorofyl spontaan terugvalt naar de grondtoestand onder emissie van een foton. Omdat het emissiespectrum van Lhca1 sterk verschilt van dat van Lhca4 kunnen we bepalen van welk Lhca de emissie afkomstig is en zo kunnen we volgen hoe de excitatie energie zich in de tijd door het systeem verplaatst. Daarnaast kijken we of de ver-rode absorptie en emissie van één, of van meer dan één chlorofyl afkomstig is. Dit omdat we weten dat twee chlorofyllen die een sterke interactie hebben verantwoordelijk zijn voor de lage-energie absorptie. In het geval van zo'n sterke interactie ontstaan er in plaats van de twee energieniveaus van de aangeslagen toestand van de afzonderlijke pigmenten, twee nieuwe niveaus. De totale hoeveelheid absorptie is gelijk aan die van twee afzonderlijke chlorofyllen, maar de bijdrage aan de absorptie van de twee nieuwe overgangen hoeft niet gelijk te zijn. In het geval van Lhca3 en Lhca4 hebben we gevonden dat de laagste energetische overgang evenveel licht absorbeert als twee enkele chlorofyllen, hetgeen betekent dat de hogere energetische overgang niet plaats vindt.

In de meeste experimenten kijken we naar vele miljoenen deeltjes tegelijk. Daardoor zijn de data die we verkrijgen een gemiddelde van de eigenschappen van vele deeltjes. Echter, ook al zijn de deeltjes chemisch gelijk, ze hoeven zich niet hetzelfde te gedragen. Dit komt omdat eiwitten flexibel zijn, daardoor kan een eiwit in enigszins verschillende structuren voorkomen, die verschillende eigenschappen kunnen hebben. Om te kijken of dit voor de Lhca complexen ook het geval is hebben we in **hoofdstuk 5** naar de fluorescentie emissie van afzonderlijke complexen gekeken. Het bleek dat een enkel Lhca complex tussen zeer verschillende emissie spectra kan switchen. Voor het Lhca1/4 complex was de emissie meestal ver rood met een maximum bij 720nm. Echter, soms verdween deze ver-rode piek en verschoof het maximum naar ~683nm. Voor de licht-oogstende complexen van fotosysteem II is juist het omgekeerde gedrag waargenomen: meestal emissie bij ~680nm, maar soms rood verschoven emissie. Hieruit blijkt dat beide complexen, door een spontane verandering in de structuur, de licht-oogstende functie kunnen krijgen die normaal bij het andere fotosysteem hoort. Dit laat zien dat deze complexen structureel en functioneel flexibel zijn.

In **hoofdstuk 6** kijken we hoe we de eigenschappen van de ver-rood absorberende chlorofyllen van Lhca4 kunnen veranderen door kleine aanpassingen in het eiwit te maken. Het eiwit bepaalt namelijk de omgeving van de chlorofyllen en hoe de chlorofyllen ten opzichte van elkaar zijn gepositioneerd, en daardoor bij welke golflengte elk chlorofyl absorbeert en fluoresceert. Op deze manier kan het eiwit ervoor zorgen dat de chemisch identieke chlorofyllen zich verschillend gedragen, zodat ze over een breder spectraal gebied licht kunnen absorberen. Dit is economisch voor het organisme, omdat het zo minder verschillende pigmenten hoeft te kunnen maken. We hebben een Lhca4 complex kunnen maken dat vrijwel de hele rode absorptie- en emissieband mist, en dus meer lijkt op een licht-oogstend complex van fotosysteem II. De chlorofyllen die eerst rond 708nm absorbeerden (ver-rood licht), absorberen in het nieuwe complex rond de 674nm (rood licht). Voor deze grote spectrale verandering is het slechts nodig om één aminozuur van het eiwit te veranderen, dus voor de spontane verandering die we in hoofdstuk 5 hebben waargenomen, is waarschijnlijk ook maar een kleine verandering van de eiwitstructuur nodig. We hebben ook een Lhca4 gemaakt dat bij nog langere golflengte kan absorberen en fluoresceren dan het wild-type complex. Dit laat zien dat we goed in staat zijn om de chlorofylabsorptie eigenschappen aan te passen.

Excitatie energie overdracht in fotosysteem I

Het doel van **hoofdstuk 7** is om te ontrafelen via welke wegen en met welke snelheden de excitatie energie door fotosysteem I wordt getransporteerd om in het reactie centrum gebruikt te worden voor de lading scheiding. We doen dit door naar de fluorescentie van het complex te kijken. Zolang de excitatie tussen de pigmenten overspringt is er een kans dat het elektron vanuit de aangeslagen toestand terugvalt naar de grondtoestand onder het uitzenden van een foton; dit proces heet fluorescentie. Echter, wanneer de energie in het reactiecentrum is gebruikt voor de ladingsscheiding kan er geen fluorescentie meer plaatsvinden. Dus als de excitatie energie heel snel en dus efficiënt naar het reactie centrum wordt getransporteerd, dan zien we maar gedurende heel korte tijd fluorescentie. Omdat we weten bij welke kleuren de verschillende Lhca's en de kern van fotosysteem I fluoresceren, kunnen we ook ontrafelen van welk deel van fotosysteem I de fluorescentie afkomstig is. Door gebruik te maken van de Lhca missende fotosysteem I complexen die we in hoofdstuk 2 hebben gekarakteriseerd, en door de kennis die we in hoofdstuk 3 en 4 over de Lhca1/4 en Lhca2/3 dimeer hebben verkregen, hebben we een goed beeld kunnen geven van de rol van de individuele Lhca's in het excitatie-energie transport. We hebben gezien dat de enkele ver-rood absorberende chlorofyllen het transport naar het reactie centrum weliswaar twee keer zo langzaam maken, maar dit transport proces is nog steeds veel sneller dan de optredende verliesprocessen. De berekende efficiëntie van fotosysteem I is 97%!

Spectroscopische metingen aan fotosysteem I gebeuren meestal in een cuvet. Dit betekent dat er na de ladingscheiding geen natuurlijke elektrondonor aanwezig is om de positieve lading weer op te heffen, terwijl het elektron vaak wel opgenomen wordt door een molecuul (bijvoorbeeld zuurstof) in de oplossing. Om het fotosysteem toch weer in neutrale toestand te brengen worden daarom reducerende chemicaliën toegevoegd. In **hoofdstuk 8** hebben we laten zien hoe snel een veel gebruikte chemische stof (phenazine methosulfate) het reactie centrum van fotosysteem I kan reduceren; deze informatie is belangrijk om te weten in welke staat de reactie centra zijn tijdens het beschijnen met licht in spectroscopische experimenten. We laten zien dat phenazine methosulfate de geëxciteerde toestand van de licht-oogstende complexen verandert en daarom beter niet gebruikt kan worden.

Samenvatting

In dit proefschrift laten we voor het eerst de absorptie en emissie eigenschappen van de Lhca2/3 dimeer zien. Het blijkt dat dit complex in het ver-rode gebied sterk absorbeert, terwijl lang werd gedacht dat alleen Lhca1/4 deze eigenschap heeft. We hebben de excitatie energie overdracht in Lhca1/4, Lhca2/3 en in fotosysteem I ontrafeld. We laten zien dat een licht-oogstend complex door een spontane verandering in de structuur heel andere eigenschappen kan krijgen. Het blijkt dus dat de flexibiliteit van het eiwit belangrijk is om het gedrag van het licht-oogstende complex te verklaren. Door kleine veranderingen in het Lhca4 eiwit te maken kunnen we de licht-oogstende eigenschappen van dit complex aanpassen. Deze informatie kan gebruikt worden om planten te maken die beter geschikt zijn in het oogsten van het licht waarin ze groeien, bijvoorbeeld het licht uit hogedruk natrium lampen dat gebruikt wordt in kassen.

Publications

Miloslavina Y, Wehner A, Lambrev PH, Wientjes E, Reus M, Garab G, Croce R, Holzwarth AR (2008) Far-red fluorescence: a direct spectroscopic marker for LHCII oligomer formation in non-photochemical quenching. *FEBS Lett* 582:3625-3631.

Passarini F, Wientjes E, Hienerwadel R, Croce R (2009) Molecular basis of light harvesting and photoprotection in CP24: unique features of the most recent antenna complex. *Journal of Biological Chemistry* 284:29536-29546.

van Oort B, Murali S, Wientjes E, Koehorst R, Spruijt RB, van Hoek A, Croce R, van Amerongen H (2009) Ultrafast resonance energy transfer from a site-specifically attached fluorescent chromophore reveals the folding of the N-terminal domain of CP29. *Chemical Physics* 357:113-119.

Wientjes E, Oostergetel GT, Jansson S, Boekema EJ, Croce R (2009) The role of Lhca complexes in the supramolecular organization of higher plant photosystem I. *Journal of Biological Chemistry* 284:7803-7810.

Passarini F*, Wientjes E*, van Amerongen H, Croce R (2010) Photosystem I light-harvesting complex Lhca4 adopts multiple conformations: Red forms and excited-state quenching are mutually exclusive. *Biochim Biophys Acta* 1797:501-508.

Muller MG, Lambrev P, Reus M, Wientjes E, Croce R, Holzwarth AR (2010) Singlet energy dissipation in the photosystem II light-harvesting complex does not involve energy transfer to carotenoids. *Chemphyschem* 11:1289-1296.

Wientjes E, Croce R (2011) The light-harvesting complexes of higher-plant Photosystem I: Lhca1/4 and Lhca2/3 form two red-emitting heterodimers. *Biochemical Journal* 433:477-485.

Wientjes E, van Stokkum IH, van Amerongen H, Croce R (2011) The role of the individual lhcas in photosystem I excitation energy trapping. *Biophys J* 101:745-754.

Wientjes E, van Stokkum IHM, van Amerongen H, Croce R (2011) Excitation-energy transfer dynamics of higher plant photosystem I light-harvesting complexes. *Biophys J* 100:1372-1380.

Kruger TP*, Wientjes E*, Croce R, van Grondelle R (2011) Conformational switching explains the intrinsic multifunctionality of plant light-harvesting complexes. *Proc Natl Acad Sci U S A* 108:13516-13521.

Wientjes E, Croce R (2011) PMS: Photosystem I electron donor or fluorescence quencher? *Photosynth Res* DOI 10.1007.

*Equal contributions

Dankjulliewel!!!

Vele mensen hebben op vele manieren aan dit proefschrift bijgedragen, graag wil ik die mensen hier bedanken.

First of all I would like to thank my promotor. Roberta, thank you very much! I am grateful that your door was (literally) always open! Your enthusiasm, optimism, strong memory and super-fast correction work make you a great supervisor!

Herbert door jou ben ik begonnen aan het fotosynthese onderzoek. Aan het eind van mijn bachelor kwam ik naar je toe om te vragen wat voor afstudeervakken er bij biofysica te doen waren. Na eerst droogjes wat projecten opgenoemd te hebben, begon je over het light-harvesting complex CP29. Je vertelde over chlorofyllen, over de lange N-terminus van het eiwit en over een buitenlandse CP29 expert die naar Wageningen zou komen. Je werd zo vrolijk en enthousiast, dat ik direct besloot dit project te kiezen. Ik heb er nooit spijt van gehad! Bart, Ruud, Rob, Roberta en Herbert jullie waren een geweldig begeleidingsteam.

Tijdens mijn aio project ben ik nog vaak naar biofysica terug gekeerd voor tijds-opgeloste fluorescentie metingen. Arie en Rob, jullie zijn fantastisch! Jullie zorgden dat de apparatuur klaar was voor gebruik en voor een hoop gezelligheid! Herbert, de discussies met jou waren altijd verhelderend en je wist scherp en humoristisch commentaar te geven op mijn manuscripten, dankjewel!

All EM, x-ray and photosynthesis people, thanks for making me feel welcome, for sharing the lab and for all the fun! Especially thanks to Marcel, Niels, Jelle, Roman and other joiners of the frisbee and roof/ tree climb events and the Friday evening beer (for me) or beers (for you) fun. Francesca, it was a great pleasure to share the office and to work together with you! Stefano, I always enjoyed your visits to the lab. Egbert, dankjewel dat ik met de elektron microscoop mocht werken en voor je vertrouwen in mij. Gert, Marc, Wilco and Roman, thanks for helping me with operating the microscope and data-analysis.

Floris en Gemma, ik heb jullie master/ bachelor onderzoeksproject mogen begeleiden. Ik had geluk met zulke slimme, kritische en gezellige studenten! Floris, jij bent inmiddels ook aio geworden, veel succes! Gemma, veel succes en plezier in Denemarken!

Sander, het was goed om met iemand samen te werken die een plant als geheel ziet en niet als een verzameling van pigmenten, eiwitten, lipiden en wat andere dingen. Ik heb veel van je geleerd. Binnenkort heb ik weer tijd, zodat we het project (eindelijk) kunnen afronden! Tjaart, het was een plezier om te zien hoe jij je single-molecule opstelling nauwkeurig dresseerde en tot het uiterste dreef. Ook je enthousiasme, gedrevenheid en fascinatie voor het gedrag van de Lhc's maakte het super om met je samen te werken. Ivo, jouw target analyses waren belangrijk voor hoofdstuk 4 en 7. Vooral voor het laatste hoofdstuk heb je veel werk verzet om telkens weer een (onmogelijk) voorstel van mij uit te proberen. Dankjewel!

I would like to express my gratitude to Prof. EJ Boekema, Prof. A.R. Holzwarth and Prof. H. van Amerongen for taking place in the "beoordelingscommissie".

I like to thank Stefan Jansson for providing the seeds of the *A. thaliana* mutants, they were absolutely crucial for this thesis! And actually, I cannot end this thesis without thanking all the plants which were growing happily until I put them in the blender. Plants, I am grateful that I could study your beautiful Photosystems!

Zonder ontspanning geen inspanning! Kano vrienden, dankjulliewel dat elke woensdagavond een feestje was! Niels: fietsen, schaatsen, zwemmen of rennen afgesloten met een aflevering House, altijd een goed recept voor de dinsdagavond. Voor van alles wil ik graag bedanken: Caecilia, Ruth, Hannie, Paul, Ellen, Puck, Anke en de Mariekes. Iedereen die ik vergeten ben, ook bedankt!

Mijn gezin en familie wil ik graag bedanken voor de warmte, gezelligheid en omdat ik altijd op jullie kan rekenen!

Jannie, ik ben blij dat ik jou in Groningen gevonden heb ☺